Understanding the Molecular Mechanisms for Alleviating Boron Deficiency in Indian Mustard

A Thesis

Submitted in Partial Fulfillment of the Requirements for the Award of the Degree of

DOCTOR OF PHILOSOPHY

by

Muthuvel J

(Reg. No: 156106008)

Department of Bioscience and Bioengineering
Indian Institute of Technology Guwahati
Guwahati-781039, Assam, India

April 2022

Dedicated to My Family

Declaration

I, hereby, declare that the research embodied in this thesis entitled **"Understanding the Molecular Mechanisms for Alleviating Boron Deficiency in Indian Mustard"** is the result of investigations carried out by me under the supervision of Prof. Lingaraj Sahoo, Department of Biotechnology, Indian institute of Technology Guwahati, India for the award of Degree of Doctor of Philosophy. This work has not been submitted elsewhere for any degree, diploma, etc. of any Institute or University to the best of my knowledge and belief.

Date: April 2022 Muthuvel J

Place: IIT Guwahati Reg. No. 156106008

Indian Institute of Technology Guwahati

Department of Bioscience and Bioengineering

CERTIFICATE

This is to certify that the thesis entitled **"Understanding the Molecular Mechanisms for Alleviating Boron Deficiency in Indian Mustard"** being submitted to the Indian Institute of Technology Guwahati by Muthuvel J (Reg. No. 156106008) for the award of degree of Doctor of Philosophy in department of Bioscience and Bioengineering, is a bonafide record of research work carried out by him. The contents of this thesis have not been submitted to any other University or Institute for the award of any degree or diploma.

Date: April 2022

Place: IIT Guwahati

Prof. Lingaraj Sahoo

(Thesis Supervisor)

Acknowledgements

I want to use this opportunity to express my heartfelt gratitude and appreciation to all those who have played an important role in helping me to reach this destination and have supported me throughout my Ph.D.

I want to thank my Ph.D. supervisor Professor Lingaraj Sahoo, for choosing me to work in his laboratory and for believing in my capabilities. I am highly grateful for his support, knowledgeable advice, constructive and academic freedom; he allowed me to pursue things of my interest. Under his able guidance, I could learn scientific perspectives of the work that has helped me to implement my thesis objectives patiently. I also want to extend my sincere thanks to our collaborator Professor Junpei Takano, from Osaka Prefecture University, Japan. His guidance shaped my PhD work immeasurably.

I also would like to pay my sincerest thanks to my Doctoral Committee members Prof. Ranjan Tamuli, Prof. Vaibhav V Goud, and Dr. S Senthilkumar for evaluating my progress in time and constructive criticism throughout the course of my research work. I am also extremely grateful to the Department of Biosciences and Bioengineering, DBT Program Support Facility and Central Instrumentation Facility IIT Guwahati for providing the facility and support required to carry out my thesis work. I would also like to acknowledge IIT Guwahati for providing me research fellowship to carry out my research.

I am fortunate to have helpful senior and junior lab members. My special thanks to Dr. Sanjeev Kumar, Dr. Bedabrata Saha, Dr. Devendra Kumar Maravi, Dr. Debee Prasad Sahoo, Dr. Mohitosh Dey, Dr. Abhishek Dey, Prabin Kumar Sharma, Dr. Richa Srivastava, Mahesh Das, Kiran Dhobale, Bharatheeswaran M, Manu Shankar, Pradyut Ghosh, Ajay Roy, Sachin da and Anandha da. I want to thank all of them for providing a comfortable work environment. I am very much grateful to my friends Dr. Srirupa

Bhattacharyya, Anil Kumar D, Krishna Kumar H, Kamleshwar C, Chandrima Dey, Dr. S. Arun, and Dr. Vinoth Kumar Raja, for all their companionships and staying my side during my hardships. I am also thankful to my friends Guhan KA, Sakthi P, Prof. Anbazhagan (Annamalai University, Chidambaram), BSBE cricket team, Weekend cricket team, my school friends and IITG Tamil Sangam members.

The love for research was first instilled in me by one of my UG teacher Dr. T Eevera (Periyar Maniammai University, Thanjavur), during my college days. It was his commitment to his lectures, which inspired me to delve deep into research, which was efficiently taken over by the professional guidance of Dr. T Muthukumaran (Periyar Maniammai University, Thanjavur) after my undergraduate days. I thank both of them from the core of my heart. I also thank my uncle P Manikandan, for introducing me to the Biotechnology course.

Finally, I thank my Amma Vasanthi and Appa Jothi for giving me this life, and my sister Sindhuja and other family members for their support and love.

Muthuvel J

Table of Contents

Abstract

Boron (B) is an essential micronutrient required for the optimal growth and development of vascular plants. Globally B deficiency is the second most important micronutrient deficiency that causes significant yield reductions in crop plants. Often, seed yield and quality are compromised in plants grown under limited soil B availability without any apparent visual symptoms. B forms borate diester crosslinking with a pectic polysaccharide, rhamnogalacturonan II, during the cell wall formation and therefore, B deficiency primary affects meristem growth, vitality of the pollen grains, flower development and seed set. *Brassica juncea* is an important oilseed crop in India and other parts of the world and is extremely sensitive to B deficiency. Although the application of foliar B fertilizer improves the yield significantly in *B. juncea*, excessive application of B can be toxic due to the narrow window between its deficiency and toxicity. Molecular mechanisms of B transport have been initiated by the discovery of B transporters in *Arabidopsis thaliana*. Several aquaporins (AQP's) and borate efflux transporter (BORs) family genes have been reported to be involved in the efficient uptake and translocation of B to maintain optimal plant growth under low soil B condition and B exclusion under high soil B conditions. Soil B content in major mustard producing states of India is potentially low and hence it is important to study the B transport mechanisms in *B. juncea* for the optimal yield.

Chapter I is the Introduction and Review of Literature part, which elucidates the essential information of the primary role of B in plants and various transporter proteins involved in B transport under both deficient and excess condition in detail. The regulation of these transporter proteins is dependent on the cellular B concentration and hence B-dependent regulation of these proteins in *Arabidopsis* and crop plants were discussed. Subsequently we have mentioned the transgenic plants overexpressed with B transporter genes to alleviate the B deficiency and toxicity in

wide number of plants. Both B deficiency and toxicity are widespread agricultural problems worldwide and elucidating the molecular mechanisms of B transport should allow us to develop technology to alleviate B deficiency and toxicity problems. In addition, the importance of developing new low B tolerant genotypes were explained by discussing the effects of B deficiency in Indian mustard (*B. juncea*) and soil B content in major mustard producing states of India. We have concluded this chapter by discussing the future perspectives for the crop improvement in B deficient/toxic soils. Finally, the salient features of this thesis have been delineated.

Chapter II elaborates the genome-wide identification and characterization of the AQPs and BOR-borate efflux transporters in the *B. juncea* genome. The identified BjAQPs and BjBORs were then classified into their respective subfamilies based on *Arabidopsis* classification. The protein characteristics of BjPIPs and BjTIPs were similar to the respective *Arabidopsis* homologs, in terms of composition, structure, and substrate selectivity filters. Whereas BjNIPs showed the highest variation in their protein characteristics reflecting the complex substrate selectivity filter compositions that affect the permeation of the solutes including boric acid. Subsequent analysis of 5'UTR region revealed that BjNIP5;1 proteins consists of a signature motif required for polar localization and B dependent post-transcriptional regulation. Similarly, in clade I BjBORs, the characteristic features involved in the endocytic degradation including, tyrosine motifs, acidic di-leucine motifs, and lysine ubiquitination residue, were well conserved. In addition, all the BjBOR1s possessed WRKY binding domain which activates BOR genes under B deficiency. The expression analysis identified higher expression of NIP5;1s (BjuA02NIP5_1a, BjuA03NIP5_1b, BjuA07NIP5_1a), and BOR1 (BjuA03BOR1a) in root tissues of the cultivar mustard under deficient B condition. The induced expression of these genes implied their probable role in B uptake and mobilization under B deficiency.

The subsequent endeavor was to identify new genotypes of *B. juncea* for low B soil. In this chapter, hydroponic media experiments were conducted to screen twenty-seven

Indian mustard genotypes under different B concentrations, and performances of the genotypes were evaluated based on the taproot length. Significant alterations of physiological responses, conditioned to low B levels, have been observed at the early vegetative stages among the twenty-seven *B. juncea* genotypes. Few mustard genotypes have shown higher tolerance to B deficiency than others and among them, low B-efficient genotype Geeta was more tolerant to low B, with very mild symptoms and a higher growth rate. Also, root meristem cells in B-efficient genotype Geeta were more viable, and less reactive oxygen (ROS) activity has been observed than B-inefficient cultivar, Maya. FTIR data have demonstrated the modified composition of pectin, cellulose, and callose among contrasting genotypes under different B levels. Furthermore, the low B condition has altered the expression profile of the major B transporters among the genotypes.

In the final chapter of the thesis, we overexpressed AtBOR1, an efflux borate transporter involved in xylem loading, in mustard and attempt to validate its growth under B deficient conditions. The overexpression of AtBOR1 has enhanced the growth of various crop plants under B-deficient conditions and hence we aimed to investigate the effects of AtBOR1 overexpression in mustard under low B conditions. Three independent transgenic mustard lines were generated using *Agrobacterium*-mediated transformation. The presence and expression of AtBOR1 in successive generations of transgenic mustard plants were confirmed by polymerase chain reaction (PCR), and quantitative PCR analysis. Physiological and molecular changes were analyzed by growing transgenic mustard in hydroponic media along with the non-transgenics under B deficiency. We have observed that the transgenic plants showed a better relative growth rate than non-transgenics without any typical B deficiency symptoms in deficient B concentration. The cell wall B, uronic acid percentages were observed to be relatively higher in transgenic roots and leaves with a low degree of methylation under B-deficiency. Therefore, the stable expression of AtBOR1 improved growth in mustard under B-deficient conditions.

Conclusion and Future prospects in Chapter 5 summarizes the key findings of this current thesis. The current work bestows a lead towards B transport networks in *B. juncea* to achieve higher yield under low soil B conditions. This work provides future scope of functional characterization of mustard B transporter genes and their importance in B transport in *B. juncea*.

List of Abbreviations and Acronyms

2,7-Dichlorofluorescein Diacetate	DCF-DA
4-(2-HydroxyEthyl)-1-PiperazineEthaneSulfonic acid	HEPES
Alcohol Insoluble Residue	AIR
Aquaporins	AQPs
Aromatic/arginine selectivity filter	Ar/R SF
Asparagine-Proline-Alanine domain	NPA domain
Boron	B
Borate efflux transporters	BORs
B-polysaccharide complex	BPC
Brassica Database	BRAD
Cauliflower Mosaic Virus	CaMV
Cell Wall Materials	CWM
Centre for Application of Molecular Biology to International Agriculture	CAMBIA
Cetyltrimethyl ammonium bromide	CTAB
Cyclohexane Diamine Tetraacetic Acid	CDTA
Degree of Methylation	DM
Dulbecco's phosphate-buffered saline	DPBS
Ethidium Bromide	EtBr
Fluorescein Diacetate	FDA
Fourier Transform Infrared Attenuated Total Reflectance	FTIR ATR
Grand Average of Hydropathicity	GRAVY
Green Fluorescent Protein	GFP

Homogalacturonan	HG
Hybrid Intrinsic Proteins	HIPs
Hydrochloric acid	HCl
Hydrogen Peroxide	H_2O_2
Hygromycin phosphotransferase II	hptII
Isoelectronic Point	pI
Low Silicon1	Lsi1
Major Intrinsic Proteins	MIPs
Molecular Weight	MW
Neomycin phosphotranferase II	nptII
N-methylbenzothiazolinone-2-hydrazone	MBTH
Nodulin-26-like Intrinsic Proteins	NIPs
Plasma membrane Intrinsic Proteins	PIPs
Propidium Iodide	PI
Qingyou 10	Q10
qRTPCR	Quantitative Real-Time Polymerase Chain reaction
Reactive Oxygen Species	ROS
Rhamnogalacturonan I	RGI
Rhamnogalacturonan II	RGII
Root Growth Inhibition	RGI
Small basic Intrinsic Proteins	SIPs
Sodium Bicarbonate	Na_2CO_3
Sodium Hydroxide	NaOH
Sulfuric acid	H_2SO_4
Tonoplast Intrinsic Proteins	TIPs
Transmembrane Domains	TMDs

Uncategorized X Intrinsic Proteins	XIPs
upstream Open Reading Frames	uORF
Uronic Acid	UA
Wester 10	W10
Youngest Opened Leaves	YOL
β-glucuronidase	Gus

Units

Basepair	bp
Centimetre	cm
Degrees celcius	^{0}C
Dryweight	DW
Freshweight	FW
Gram	g
Gram per litre	g/l
hour	h
Kilo Dalton	KDa
Kilodalton	kDa
Micro molar	µM
Microgram	µg
Microgram per milliliter	µg/ml
Microlitre	µl
Micromolar	µM
Micromoles per square metre per second	µmol m^{-2} s^{-1}
Milligram	mg
Milligram per litre	mg/l
Millimetre	mm
Millimolar	mM
min	m
Molecular weight	MW
Nanometre	nm
Negative log of H^{+}	pH
Percentage	%

Revolution per minute	rpm
Seconds	sec
Unit	U
Weight per volume (concentration)	w/v

List of Figures

violet represented BOR1s, BOR2s, BOR3s, BOR4s, BOR5s, BOR6s, and BOR7s, respectively.

Figure 2.3 Phylogenetic relationship of *B. juncea* NIP5;1, NIP6;1 and NIP7;1 proteins. Phylogenetic tree derived from NIP protein sequences of *A. thaliana*, *B. rapa*, *B. nigra*, *B. juncea*, and *B. napus* using MEGA 7 with Neighbor-Joining (NJ) method, and 1,000 replicates bootstraps, and visualized by iTOL. The names colored with blue, red and green represented NIP5;1s, NIP6;1s and NIP7;1s.

Figure 2.4 Amino acid residues between the BjPIP1 proteins shows highly conserved amino acid residues.

Figure 2.5 Amino acid residues between the BjPIP2 proteins shows highly conserved amino acid residues.

Figure 2.6 Amino acid residues between the BjNIP proteins shows high variation among their amino acid residues.

Figure 2.7 Amino acid residues between the BjTIP proteins shows partially conserved amino acid residues.

Figure 2.8 Amino acid residues between the BjSIP proteins shows high variation among their amino acid residues.

Figure 2.9 Amino acid residues between the BjOR proteins shows conserved amino acid blocks between their subclass proteins.

Figure 2.10 Gene structure of BjAQPs. The exon-intron structures of the BjAQPs were determined by the alignments of coding sequences with corresponding genomic sequences, and the diagram was obtained using GSDS (Gene Structure Display Server 2.0) Web server. The purple, yellow, and black line represented the UTR regions, exons and introns, respectively.

Figure 2.11 Gene structure of BjBORs. The exon-intron structures of the BjBORs were determined by the alignments of coding sequences with

corresponding genomic sequences, and the diagram was obtained using GSDS (Gene Structure Display Server 2.0) Web server. The purple, yellow, and black line represented the UTR regions, exons and introns, respectively.

Figure 2.12 Predicted tertiary (3D) proteins structures and pore morphology of 104 BjAQPs.

Figure 2.13 Predicted tertiary (3D) proteins structures and pore morphology of 15 BjBORs.

Figure 2.14 Distribution of conserved motifs in BjAQPs. Conserved motifs of BjAQPs were analysed by MEME Web server using the protein sequences of 104 BjAQPs. Maximum twenty conserved motifs were identified, and different motifs were distinguished by different colors.

Figure 2.15 Distribution of conserved motifs in BjBORs. Conserved motifs of BjBORs were analysed by MEME Web server using the protein sequences of 15 BjBORs. Maximum twenty conserved motifs were identified, and different motifs were distinguished by different colors.

Figure 2.16 Multiple alignments of the amino acid sequences of the motifs required for substrate selectivity and regulation of BjNIP5_1s. The TPG repeats, NPA motifs, the ar/R selectivity filter and corresponding sequences in *A. thaliana*, *B. nigra*, *B. rapa*, and *B. napus* orthologs are shown. The conserved residues in the motifs are highlighted.

Figure 2.17 Multiple alignments of the amino acid sequences of the motifs required for substrate selectivity and regulation of the BjNIP6_1s. The TPG repeats, NPA motifs, the ar/R selectivity filter and TPG repeats of the corresponding sequences in *A. thaliana*, *B. nigra*, *B. rapa*, and *B.*

napus orthologs are shown. The conserved residues in the motifs are highlighted.

Figure 2.18 Multiple alignments of the amino acid sequences of the motifs required for substrate selectivity of the BjNIP7_1s. The tyrosine-81 residue, NPA motifs, and the ar/R selectivity filter of the corresponding sequences in *A. thaliana*, *B. nigra*, *B. rapa*, and *B. napus* orthologs are shown. The conserved residues in the motifs are highlighted.

Figure 2.19 Multiple alignments of the amino acid sequences of the motifs required for the polarity and vacuolar sorting. The tyrosine-based motif, the acidic di-leucine motif and the lysine residue in AtBOR1 and corresponding *A. thaliana*, *B. nigra*, and *B. napus* orthologs are shown. The conserved residues in the motifs are highlighted.

Figure 2.20 Chromosomal location of AQPs and BORs in *B. juncea*. The gene chromosome location diagram was drawn manually. There were 97 BjAQPs and 15 BjBORs located on 18 chromosomes. Seven BjAQPs were located on scaffolds and contigs.

Figure 2.21 Analysis of cis-acting elements in *B. juncea* aquaporin genes. The bars colored with blue, red, light green, and purple represented phytohormone-responsive, plant growth and developmental-responsive, light-responsive and biotic/abiotic-responsive elements, respectively. The number of cis-elements are mentioned in their respective bars.

Figure 2.22 Analysis of cis-acting elements in *B. juncea* BOR genes. The bars colored with blue, red, light green, and purple represented phytohormone-responsive, plant growth and developmental-responsive, light-responsive and biotic/abiotic-responsive elements,

B-deficient tolerant cv. Geeta can perform better under B-deficient media than others.

Figure 3.5 Difference in B content in the pectin fractions among the Indian mustard genotypes grown under varied B conditions.

The differences in B concentration in root (A, B) and leaf (C, D) pectin fractions of low B inefficient (Maya), moderately efficient (RH406) and low B efficient (Geeta) genotypes demonstrated that the B-deficient tolerant cv. Geeta can perform better under B-deficient media than others.

Figure 3.6 Difference in uronic acid (UA) percentages in root and shoot tissues among the Indian mustard genotypes grown under varied B conditions. The differences in UA% in root (A) and leaf (C) pectin fractions of low B inefficient (Maya), moderately efficient (RH406) and low B efficient (Geeta) genotypes demonstrated that the B-deficient tolerant cv. Geeta can perform better under B-deficient media than others.

Figure 3.7 Difference in degree of methylation (DM) percentages in root and shoot tissues among the Indian mustard genotypes grown under varied B conditions.

The differences in DM% in CDTA and Na_2CO_3 pectin fractions of root (A, B) and leaf (C, D) pectin fractions of low B inefficient (Maya), moderately efficient (RH406) and low B efficient (Geeta) genotypes demonstrated that the B-deficient sensitive cv. Maya have more cell wall damage under B-deficient media than others.

Figure 3.8 Effects of different B concentration on viability of root tips visualized by confocal microscopy of contrasting Indian mustard genotypes. The roots were stained with FDA-PI. Green and red fluorescence shows viable and dead cells respectively. The live and dead cell

ECORI digested plasmid for the confirmation of NOS (173bp) C. PstI and SpeI digested plasmid for the confirmation of AtBOR1 (2.8kb) D. undigested plasmid L. DNA ladder.

Figure 4.2 Stages in course of recovery of transgenic mustard plants. (a). hypocotyl explants in preculture (bar 8mm); (c). selection (bar 8mm) inset explant showing regeneration; (c). shoots in selection (bar 6mm); Transient gus assay (d), (f) transformed explants after 1 day in co-cultivation (bar 5mm) and after 7 days in selection medium (bar 3mm) showing gus activity respectively; (e), (g) untransformed controls showing no gus activity; (h). rooted shoots (bar 6mm); (i). fully grown acclimatized transgenic plant.

Figure 4.3 Establishment of transgenic mustard expressing AtBOR1. A, PCR was performed using genomic DNA as a template with primers specific to 540 bp with nptII primers, 1.6 Kb with gus primers, C. 2.8 Kb with AtBOR1. B, Total RNA was extracted from the roots of non-transgenic plants (NT) and transgenic T2 plants (T2.1.1, T2.2.1, and T2.3.1). RT-PCR was performed using primers specific to AtBOR1 or the tubulin like gene.

Figure 4.4 Overexpression of AtBOR1 in Indian mustard confers better plant growth. Low B tolerance of mustard plants overexpressing AtBOR1. 40 days old T2 plants (T2.1.1, T2.2.1, and T2.3.1) and non-transgenic (NT) were subjected to low B stress (0.46 μM B). Low B stress was given by avoiding the boron during hydroponic media preparation.

Figure 4.5 Root and shoot length, dry weights and B concentrations in transgenic mustard plants expressing AtBOR1 under B-deficiency and sufficiency. Non-transgenic (NT) and transgenic (T2.1.1, T2.2.1, and T2.3.1) plants were grown for 40 days in a hydroponic solution containing 0.46 or 46 μM boric acid. Root (A), shoot length (B) and

dry weight (C-E) differences demonstrated that the transgenic mustard performs better under B-deprived media than non-transgenics.

Figure 4.6 Difference in uronic acid (UA) percentages in root and shoot tissues of the transgenic Indian mustard genotypes grown under varied B conditions shows that transgenic mustard performs better under B-deprived media than non-transgenics.

Figure 4.7 Difference in degree of methylation (DM) percentages in root and shoot tissues among the transgenic and non-transgenic Indian mustard lines grown under varied B conditions.

The differences in DM% in CDTA and Na_2CO_3 pectin fractions of root (A, C) and leaf (B, D) pectin fractions of transgenic mustard lines demonstrated that the non-transgenics have more cell wall damage under B-deficient media than others.

Figure 4.8 AtBOR1 overexpressed mustard lines accumulates more B in the cell wall than non-transgenics. The concentration of B in cell wall material (CWM) of root (A), and leaf (B) of transgenic and non-transgenic mustards.

Figure 4.9 AtBOR1 overexpressed mustard lines accumulates more B in the CDTA cell wall fractions than non-transgenics. The concentration of B in cell wall fractions (CDTA and Na_2CO_3) of root (A and B), and leaf (C and D) of transgenic and non-transgenic mustards.

List of Tables

Chapter I

Introduction and Review of Literature

1.1 BACKGROUND

Boron (B) is an essential micronutrient required for the optimal growth and development of plants. Often, Seed yield and quality are compromised in plants grown under limited soil B availability. B consists of a narrow range between deficiency and toxicity and thus plants need to maintain their tissue B concentrations within an optimum range by regulating transport processes. The essentiality of B is mainly in the borate diester crosslinking of rhamnogalacturonan II (RGII) region of cell wall pectin. The B homeostasis in plants with respect to varied B conditions is regulated by two classes of transporter proteins: boric acid channels belonging to aquaporins (AQPs) and borate efflux transporter BORs. In this chapter we have first explained roles of various AQPs and BORs in B transport under both deficient and excess B conditions which was found in *Arabidopsis thaliana* and other plants. Secondly, various regulatory mechanisms of B transport at the cellular level were explained. Next, the recent findings in the B transport and its regulation in *Brassica napus*, *Oryza sativa*, *Hordeum vulgare*, *Triticum aestivum*, and *Zea mays* were discussed in detail. Subsequently we have mentioned the transgenic plants overexpressed with B transporter genes to alleviate the B deficiency and toxicity in wide number of plants. Elucidating the molecular mechanisms of B transport should allow us to develop technology to alleviate B deficiency and toxicity problems.

1.2 INTRODUCTION

Boron (B) is a micronutrient critical for the growth and health of all crops. B is involved in the borate-diester formation with rhamnogalacturonan II, a pectic polysaccharide, during the cell wall development. Thus, the B deficiency severely affects the structural and functional integrity of biological membranes, pollination, vitality of the pollen grains, flower development and seed set (Marschner., 2011). Adequate B is also required for active nitrogen fixation and nodulation in legume crops (Redondo-Nieto et al., 2003). Plant roots take up B mainly in the form of boric acid (H_3BO_3). Boric acid is a weak Lewis acid with a pKa of 9.14 [$B(OH)_3 + H_2O = B(OH)_4 + H^+$] and is the only essential nutrient absorbed as an uncharged form at the physiological pH (Yoshinari and Takano., 2017). Due to the high membrane permeability coefficient of boric acid, it was widely believed that B uptake would be majorly a passive process. However, the difference in membrane permeability between artificial and plant membranes due to membrane composition difference revealed that the accurate prediction of

the membrane permeability in plants is not possible by the theoretical considerations alone (Reid, 2014). Also, permeability coefficients determined using the plasma membrane of giant internodal cells of the charophyte alga (*Chara corallina*) and plasma membrane vesicles isolated from squash roots revealed boric acid has higher membrane permeability than its theoretical value (Stangoulis et al., 2001; Dordas et al., 2000). In addition to passive diffusion, plants use two other mechanisms for B transport and homeostasis: facilitated diffusion of boric acid via boric acid channels and export of borate, which is formed from boric acid in the cytoplasm, via BOR borate transporters.

Globally B deficiency is ranked as the second most crucial micronutrient constraint for crop production, and it has been reported to cause significant yield loss in many crops around the world (Rerkasem et al., 2020). Low soil B is most prevalent in high rainfall areas, which are generally calcareous, sandy, and light-textured acidic soils with low organic matter (Ahmad et al., 2012). Some of these areas are in southeast China (Wang et al., 2007), Pakistan (Rashid et al., 2009), northeast India (Singh., 2008) western Australia (Wong, 2003) and many other countries (Shorrocks 1997). Excess soil B is also toxic to plants and is mostly found in arid and semi-arid areas, including California, Chile, South Australia, and the Middle East (Nable et al., 1997). Since B is having a narrow range between deficiency and toxicity, maintaining an optimal tissue B concentration is vital for plants to grow on a wide range of soil B conditions. In this review, the various modes of B transport are examined with an emphasis on the membrane transporters.

1.3 ROLE OF B IN CELL WALL FORMATION

Boric acid and borate forms diesters with alcohols in a pH-dependent manner (Wimmer et al., 2019). The most stable borate diesters formation was observed in cis-diols on a furanoid ring, such as apiose and ribose. The majority of the plant B exists in the water-insoluble cell wall fraction in a wide range of crops when B supply is limited and cell wall deformities induced by the B deficiency was correlated with the water-insoluble B (Matoh et al., 2013). The first B-polysaccharide complex (BPC) was isolated from the radish root cell walls and subsequently the sugar moiety present in the BPC was identified as a pectic polysaccharide, rhamnogalacturonan II (RG-II) (Matoh et al 1993). Based on their research on the cell wall B-RGII complex of a wide range of plant families, including Leguminosae, Gramineae, and Brassicaceae, it was proposed that RG-II is the exclusive B binding polysaccharide in cell walls

(Matoh et al., 2013). Analysis of key enzymes for RG-II synthesis and the functions of B transporter involved in the RG-II cross linking demonstrated that the borate diester bond between B and RGII is essential for the normal growth of plants (Funakawa and Miwa., 2015).

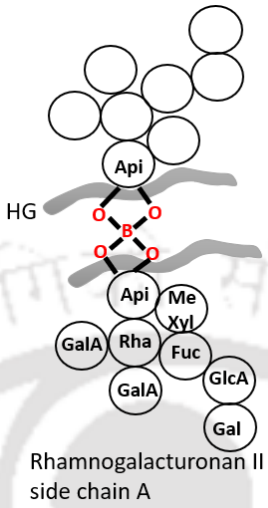

Figure 1.1 Representation of borate crosslinking with RGII. Apiosyl residue in the side chain A is covalently crosslinked by borate diester bond (Redrawn using Inkscape).

1.4 ROLE OF SOLUBLE BORON COMPLEXES IN BORON TRANSPORT

Long-distance transport of B occurs via the transpiration stream and the formation of the cis-diol esters between polyols and the B (Reid., 2014). B binds to a diverse number of biological compounds in a cell and the cell wall such as sugars and their derivatives, phenols, organic acids, and polymers (Hu et al., 1997). B influences the formation of the cis-diol complex with the organic molecules to efficiently transports them to the meristem cells via the phloem. This is supported by the presence of B-sugar alcohol complexes in phloem sap of many species (Brown and Shelp., 1997; Stangoulis et al., 2010; Du et al., 2020). Since the concentration of mannitol is very high in cell sap, B readily forms B-mannitol complexes and hence the absence of free B was observed in celery (*Apium graveolens*) (Hu et al., 1997). In sucrose-producing species, bis-sucrose borate and bis-N-acetyl-serine borate complexes were identified in wheat and canola phloem exudates, which explained the moderate phloem mobility of B (Stangoulis et al., 2010).

In species, which are all utilizing polyols (complex sugars) as a primary photosynthetic metabolite, B is transported as polyol-B-complex to the vegetative/reproductive meristems. Whereas, in species that are incapable of producing a substantial amount of polyols, B is

delivered through the transpiration stream to the leaves and shows phloem immobility. Polyols are primary photosynthesis products that occurs mainly in the source leaves. The absence of polyol synthesis in sink organs clearly suggests the long-distance transport of these compounds. Synthesis of sorbitol-6-phosphate dehydrogenase (S6PDH) under the CaMV35S promoter in tobacco supported the formation of B sorbitol complexion in the phloem. Transgenic tobacco overexpressing S6PDH resulted in markedly increased B mobility within the plant and performed well under B deficiency compared (20% greater plant weight, 10% less flower abortion, and 100% greater increase in seed yield) to non-transgenic in which the seed yield and plant growth were reduced to maximum 90% and 50%, respectively (Brown et al., 1999; Bellaloui et al., 1999). The foliar application of ^{10}B in B-deprived non-transgenic plants did not alter the abundance of ^{10}B in young tissues, flowers, and seeds in comparison with untreated plants, whereas transgenic tobacco has shown increased ^{10}B abundance in leaves and seeds. These results, together with Bellaloui et al., 2003, where the authors have studied overexpression of S6PDH in rice concerning B mobility, conclusively prove that sorbitol facilitates B mobility in plants. However, additional work is still needed to understand precisely the transport pathway for sorbitol-B complexes in plants.

1.5 BORON TRANSPORT THROUGH WATER CHANNELS

Aquaporins (AQPs) are integral membrane proteins that belong to the family of major intrinsic proteins (MIPs). The presence of AQPs is universal to all kingdoms of life and present in all subcellular membrane systems. Plant AQPs are essential transmembrane channel proteins, facilitates passive bidirectional diffusion of water and other small uncharged molecules (Bienert and Chaumont, 2014). Based on the sequence similarity and localization, plant AQPs are broadly classified into the following classes: plasma membrane intrinsic proteins (PIPs), tonoplast intrinsic proteins (TIPs), small basic intrinsic proteins (SIPs), and nodulin-26-like intrinsic proteins (NIPs), hybrid intrinsic proteins (HIPs) and the uncategorized X intrinsic proteins (XIPs) (Kong et al. 2017).

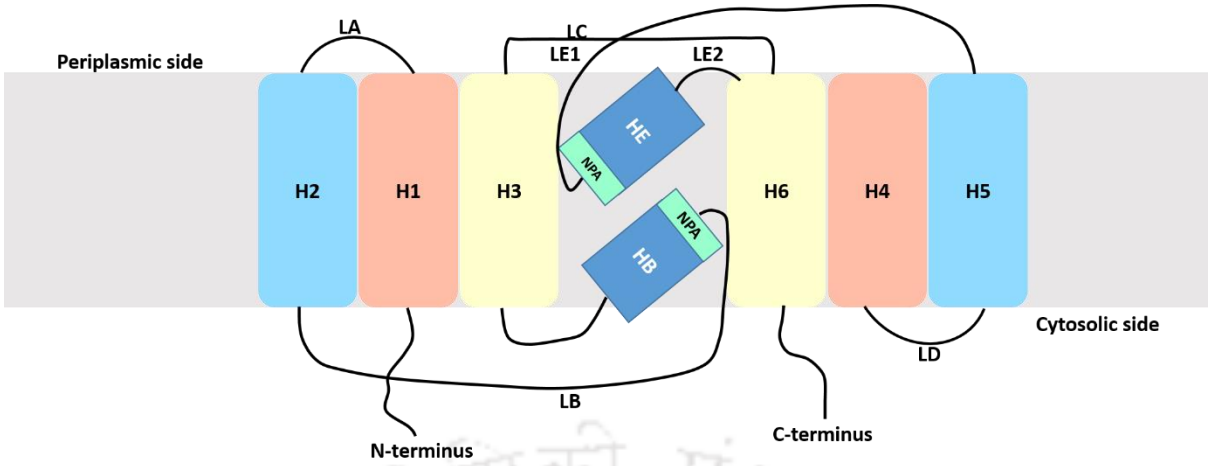

Figure 1.2 Common structural membrane diagram of aquaporins. Each aquaporin molecule consists of six transmembrane α-helices (H1–H6; light blue, light orange, pale yellow boxes) and two re-entrant HB and HE α-helices (blue). Transmembrane α-helices are inter-connected via five LA–LE loops. Two Asn-Pro-Ala (NPA) motifs HE (flanked by LE1 and LE2 loops) and HB (flanked by LB loop) (fluorescent green) are separated by ~4–5 Å. The dotted line separates bipartite structural repeats of hour-glass folded aquaporins.

1.5.1 Role of Plasma Membrane Intrinsic Proteins (PIPs) in B transport

PIPs are widely distributed plasma membrane-localized proteins involved in the transport of metalloids in addition to water (Bienert and Bienert., 2017). PIPs are broadly categorized into two subgroups, PIP1 and PIP2, based on their sequence similarity, subcellular localization, and transport properties. Unlike PIP1, PIP2 subgroup proteins have shown convincing water transport activity in a heterologous expression system.

Some PIP proteins has been shown to permeate boric acid in addition to water. In an early study, expression of maize PIP1 in *Xenopus laevis* oocytes enhanced boric acid uptake in the cell (Dordas et al., 2000). Later on, the expression of barley (*Hordeum vulgare*) PIP1;3 and PIP1;4 in yeast showed increased accumulation of B and enhahced sensitivity to high B (Fitzpatrick and Reid, 2009). Expression of rice PIP1;3, PIP2;1 and PIP2;7 in yeast also enhanced sensitivity to high B (Mosa et al., 2016; Kumar et al., 2014).The transgenic *Arabidopsis* plants over-expressing *OsPIP1;3,OsPIP2;4,OsPIP2;6* and *OsPIP2;7* showed enhanced tolerance under toxic B concentration (Kumaer et al. 2014; Mosa et al. 2016). The tracer experiments using ^{10}B-enriched boric acid at 2.5 or 5 mM showed that both B uptake and efflux from roots were increased in these transgenic

plants. Importantly, *OsPIP1;3* and *OsPIP2;6* expression was increased upon high B concentration in rice root (Mosa et al. 2016). These results suggest the function of PIPs in high-B tolerance although further studies using knocked out plants are desired.

1.5.2 Role of Tonoplast Intrinsic Proteins (TIPs) in B transport

TIPs are a distinct group of tonoplast integral proteins functions as AQPs to regulate turgor, osmo-sensing, cell growth, vacuolar differentiation and water transport across the vacuolar membrane (Maurel et al. 2016). Vacuolar subtypes have their specific TIP isoform, of highly variable sequence within ar/R selectivity filter, to transport small molecules including urea, NH_3, glycerol, H_2O_2, boric acid (Sudhakaran et al., 2021). The heterologous expression of grape TIPs (VvTnTIP1;1, VvTnTIP2;2 and VvTnTIP4;1) and maize TIPs (ZmTIP1;1 and ZmTIP1;2) in yeast showed higher sensitivities to toxic B conditions (Sabir et al. 2014; Bárzana et al. 2014). *Arabidopsis* pollen-specific *TIP5;1* gene is induced by high-B stress and overexpression of *AtTIP5;1 in planta* displayed longer hypocotyls and increased silique production under B toxicity (Pang et al., 2010). Subsequently, *AtTIP5;1* gene was found to be an essential downstream target of gibberellic acids, which activates *AtTIP5;1* by modulating the DELLA proteins to promote hypocotyl elongation. The authors suggested that the AtTIP5;1 is involved in B sequestration into the vacuoles at the toxic B concentration (Pang et al., 2010). The pollen specificity of AtTIP5;1 has been ascribed to the high demand for B during pollen germination and pollen tube growth, but the association of AtTIP5;1 in B transport inside the pollen remains to be demonstrated in detail. Transcription profiling of B deficiency-tolerant citrus rootstock revealed the upregulation of two genes *TIP2;2* and *TIP4;1*, under B deficiency with different temporal expressions (Zhou et al. 2015). However, the significance of B in vacuolar function (if any) and B sequestration capacity of different vacuolar isoforms remain obscure.

1.5.3 Role of Nodulin 26-like intrinsic proteins (NIPs) in B transport

Nodulin 26-like proteins (NIPs) were first reported to be involved in the symbiotic regulation between soybean (*Glycine max* L.) and rhizobia (Fortin et al., 1987). Though the evolutionary origin of NIPs is not yet disclosed, NIPs cluster together with a very basal lineage called aquaporin Z or glycerol uptake facilitator protein (Pommerrenig et al., 2020). The close relationship between the plant NIP and other archaeal and cyanobacterial NIP-like proteins

support horizontal gene transfer should have been occurred from these species (Pommerrenig et al., 2020).

Based on the phylogenetic relationships among the NIP family proteins, they are categorized into five or four subgroups (Abascal et al., 2014). Based on the earlier works, the plant NIPs are classified into five distinct subgroups (NIP1-NIP5) (Pommerrenig et al., 2020). These subgroups are exceptionally well conserved across the plant species. NIPs are also additionally categorized based on the similarities within the pore selectivity regions within the ar/R selectivity region (NIP I-NIP III) (Roberts and Routray, 2017). Soybean NOD 26 is the typical example of NIP I type proteins and their physiological role is not well-understood. AtNIP4;1 and AtNIP4;2 are the paralogous pollen-specific proteins belongs to the NIP-I subfamily localized in plasma membrane and intracellular vesicles of pollen tubes (Bock et al. 2006; Di Giorgio et al. 2016). Heterologous functional analysis indicated that AtNIP4;1 is involved in the relatively low permeability of boric acid along with other small molecules (Di Giorgio et al. 2016). However, the participation of the NIP4;1 and NIP4;2 in boric acid transport and pollen physiology under B deficient conditions remains unclear. NIP II proteins are universally present in all the land plants, permeates several metalloid hydroxide substrates in addition to glycerol (Pommerrenig et al. 2020). Boric acid channels of this subgroup regulate the uptake of B (Miwa and Fujiwara 2010; Diehn et al., 2019). NIP III proteins are characterized as silicic acid transporters widely present in monocots and few dicots and they can also transport boric acid (Ma and Yamaji., 2015; Pommerrenig et al., 2015).

1.5.3.1 NIPIIs mediated B transport

AtNIP5;1 was the first characterized boric acid channel with physiological function in B uptake into roots (Takano et al., 2006). Transcription of *AtNIP5;1* has increased immediately after the B starvation. In the plasma membrane of root epidermal, cortical, and endodermal cells, NIP5;1 shows polar localization towards the soil side to transport B from root surface to xylem (Takano et al. 2010; Wang et al. 2017). B uptake and accumulation in roots and shoots of *nip5;1* insertion lines were significantly reduced when plants were cultivated under low B supply compared to the wild type plants. Additionally, the *nip5;1* mutants grown under low B (0.1 µM B) showed severe growth impairments in tap root, lateral root, and rosette leaf expansion (Takano et al., 2006). AtNIP6;1, a closest paralogue of AtNIP5;1, is an extremely boric acid specific water-tight transport channel involved in preferential translocation of B in shoots (Tanaka et al., 2008). Unlike AtNIP5;1, the cell-type specific expression of

AtNIP6;1 was strongly confined in the phloem regions in nodes, including the phloem companion cell, phloem parenchyma cell regions, and sieve elements and is involved in the xylem-phloem transfer of B (Tanaka et al., 2008). The *nip6;1* mutants showed inhibition in rosette leaf expansion and apical dominance under a low B conditions (Tanaka et al., 2006).

AtNIP7;1 is a third member of NIPII subclass protein having a role in pollen development under low B supply (Routray et al., 2018). AtNIP7;1 showed anther-specific expression and primarily localized in the plasma membrane of the tapetum cells (Routray et al., 2018). The loss-of-function NIP7;1 mutants have shown reproductive growth retardation including decreased fertility, petite siliques and increased seed abortion than wild type under limited B conditions (Routray et al., 2018). AtNIP7;1 consisting of identical ar/R regions like AtNIP5;1 and AtNIP6;1 but differs in its intrinsic rate of boric acid transport. Boric acid transport by AtNIP7;1 was proposed to be controlled by a channel gate function of a conserved tyrosine residue in the pore (Li et al. 2011). Substitution of Y81 with cysteine (characteristic of AtNIP6;1) resulted in a significantly higher boric acid transport than wild-type NIP7;1 and NIP5;1 (Li et al, 2011).

1.5.3.2 NIPIIIs and high B tolerance

The NIP III proteins in rice (OsLsi1/OsNIP2;1) are barley (HvLsi1/HvNIP2;1) are silicic acid channels and facilitate Si uptake in plants (Ma et al., 2006; Chiba et al., 2009). The heterologous expression of these proteins in *Xenopus* oocytes showed significant B transport activity along with silicon, germanium, arsenic, and water (Schnurbusch et al., 2010; Mitani-Ueno et al., 2011). The reduced expression of HvNIP2;1 contributes to decreased uptake of B under high soil B condition to provide greater tolerance in a B-tolerant barley genotype and the loss-of-function of OsLsi1 reduced accumulation of B in leaf blades of rice plants (Schnurbusch et al., 2010). Therefore, the abundance of the silicic acid channels is a key factor for high-B tolerance (discussed in detail in the later section on barley).

1.5.4 Role of X Intrinsic Proteins (XIPs) in B transport

Uncharacterized X intrinsic proteins (XIPs) were first identified during the analyses of the whole genome of *Physcomitrella patens* (Danielson and Johanson, 2008). The XIP proteins are present in unicellular eukaryotes to plants, especially in many eudicot plants. However, XIPs are absent in monocots and Brassicaceae family, reasonably due to the functional complementation by other AQP subfamilies in these taxa (Abascal et al. 2014). The variation

in the amino acid residues forming the ar/R filter shows the XIPs closely related to the NIP III group, than any other MIPs, which is known to facilitate the diffusion of urea, glycerol, and metalloids but water (Bienert et al., 2019). Consistent with this prediction, heterologous expression of six Solanaceae XIP's (NtXIP1;1α and NtXIP1;1β, StXIP1;1α and StXIP1;1β, SlXIP1;1α and SlXIP1;1β) resulted in an increased sensitivity to glycerol, urea, boric acid, H_2O_2 and ammonia (Bienert et al., 2011). Water-impermeable XIP channels, VvXIP1 and NbXIP1;1α, involved in facilitated diffusion of boric acid were also reported recently based on yeast growth inhibition experiments (Ampah-Korsah et al., 2016; Noronha et al., 2016). The overexpression of *NtXIP1;1* under the control of *AtNIP5;1* promoter region complemented the B deficiency phenotype of the *Atnip5;1* knockout mutant, showing its ability to act as a boric acid channel *in planta* (Bienert et al., 2019). However, when *NtXIP1;1* is overexpressed in *the Nicotiana tabacum*, and *Arabidopsis* under En2pPMA4 or 35S CaMV promoter, it results in B-deficiency symptoms such as the diminished shoot apical meristem, sterile flowers, and contracted leaves. This may be due to the irregularity in local B gradients, prompted by the universal overexpression of *NtXIP1;1*, caused disturbance in generating the directional flow of B towards the shoot. Further investigation is required on the physiological functions of XIP-mediated B transport.

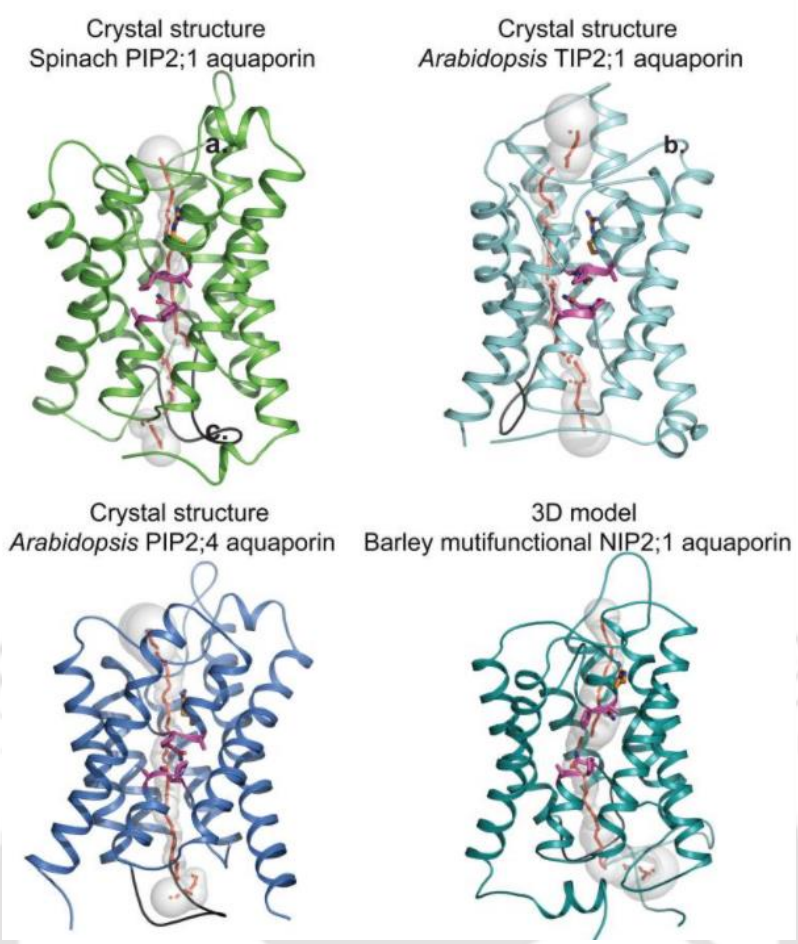

Figure 1.3 Simple representations of monomeric aquaporins enclose pores with morphologies shown by sequences of grey spheres (pore radii are equal to sphere diameters) and red dots. Two conserved NPA motifs (magenta sticks) (cf. panel (a)) and neighbouring Arg222 (one of the selectivity filter residues, orange sticks) line pores in central regions. LD loops (black) show similar dispositions in all aquaporins and are assumed to be essential for pore closure at cytosolic sides of proteins. In barley NIP2;1 the last 20 residues were omitted for clarity (Hrmova et al., 2020).

1.6 B TRANSPORT THROUGH BORATE EFFLUX TRANSPORTERS

When soil B concentration is limited, plants use BOR-type borate exporters for efficient transport of B (Takano et al., 2008). Besides, B exporters are also involved in B exclusion from tissues under excess B conditions (Miwa et al., 2007; Sutton et al., 2007). B transporters have a similar structure to the mammalian Solute Carrier 4 (Slc4) family transporters including anion exchangers (AEs) and sodium-coupled bicarbonate transporters (NCBTs).

The higher pH in the cytoplasm converts boric acid into borate anion which are subsequently transported by the B exporters dependent on the concentration gradient and membrane potential (Yoshinari and Takano., 2017). *Arabidopsis* encodes seven genes of BOR-type borate transporters, BOR1-BOR7 (Takano et al., 2008). BOR-transporters in angiosperms can be classified into two separate clades, clade I and II (Wakuta et al., 2015). It is likely that Clade I BOR-transporters and their homologs are involved in efficient B transport under limited B availability, whereas, clade II BOR-transporters are involved in B exclusion for high B tolerance (Wakuta et al., 2015).

In a medium containing a limited B supply, the *Arabidopsis bor1-1* loss-of-function mutant showed drastically reduced vegetative growth and sterility, whereas the wild type was able to set seeds (Noguchi et al.,1997; Takano et al., 2001; 2002). These defects were due to the defects in root-to-shoot translocation of B and preferential B transport to young leaves and were recovered by higher-B supply. AtBOR1 was localized to the stele-side plasma membrane domain in various cell types in roots and the apical plasma membrane domain in protovascular cells in the root tip (Takano et al. 2010; Yoshinari et al. 2016). The polar localization of BOR1 is assumed to be essential for the efficient transport of B from the root surface to the xylem, in collaboration with boric acid channels (Yoshinari et al., 2019). The cell-type specific expression of AtBOR1 in the epidermal cell layer of the cotyledon suggests their involvement in B uptake at the surface of the cotyledon as uncharged boric acid can theoretically permeate the leaf epidermis via cuticle (Yoshinari et al., 2016).

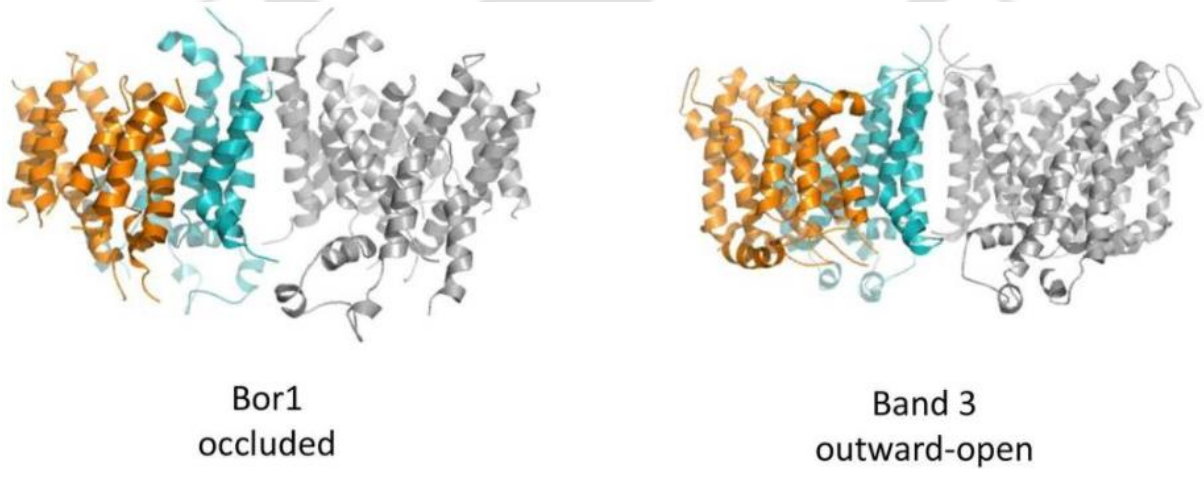

Figure 1.4 Dimeric assemblies for Bor1, Band 3. In each case, one monomer is in gray, whereas the other is displayed with its Gate domain in teal and its Core domain in orange (Thurtle-Schmidta and Stroud., 2016).

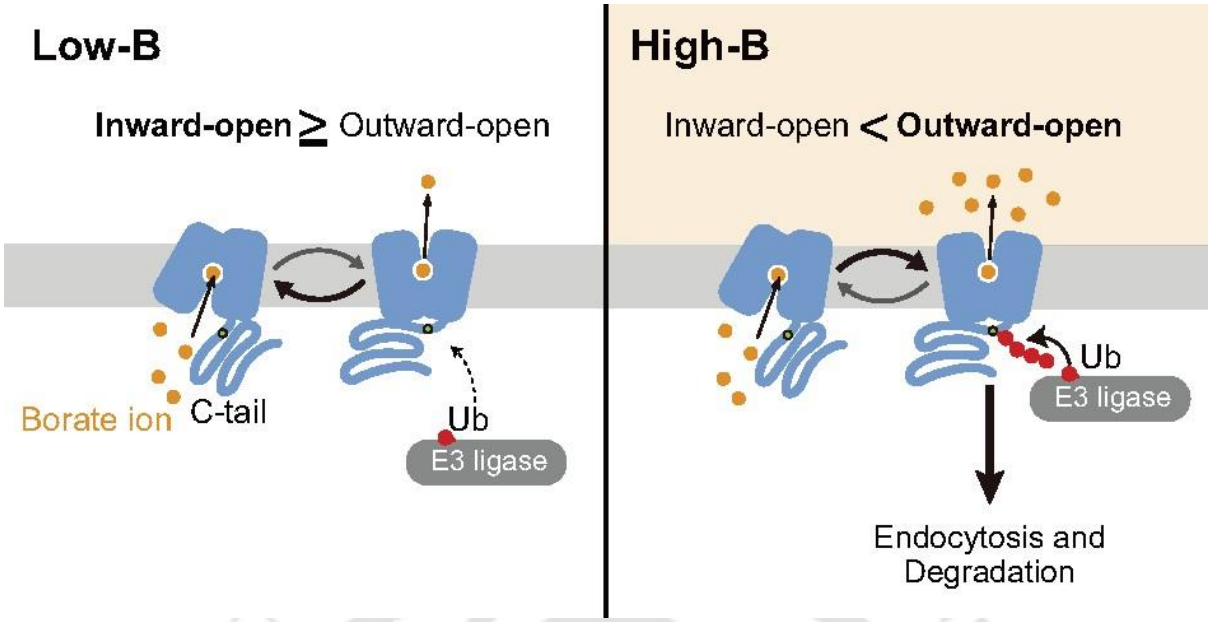

Figure 1.5 A model for B sensing. A transport-ubiquitination coupled model. Under low-B conditions, BOR1 is largely in the inward-open state, with the K590 residue in the C-tail unexposed. Under high-B conditions, BOR1 is more frequently in the outward-open state, with the C-tail exposed, giving access to the K590 residue for E3 ligases. Longer exposure to the E3 ligase results in polyubiquitination and subsequent endocytic degradation of BOR1 (Yoshinari et al., 2016).

AtBOR2, a close paralog of AtBOR1, encodes an efflux B transporter localized in the plasma membrane with stele-side polarity with overlapping but different cell-type specific expression from AtBOR1 in roots (Miwa et al., 2013). BOR2-GFP was not stably localized in the PM but observed also in the endosomal membrane compartments (Miwa et al., 2013). High B induced degradation of BOR2 is consistent with its importance under low B concentration (Miwa et al., 2013). *AtBOR2* T-DNA insertion mutation revealed that no significant differences in the concentrations of total B in the roots of *bor2-1*, *bor2-2*, and wild-type plants, but the formation of RG-II-B dimers to the total RG-II were reduced to 45% in limited B supply (Miwa et al., 2013). This suggests the involvement of BOR2 in the B-RGII crosslinking to enhance the cell elongation for the root growth. The inhibition of *de novo* polysaccharide biosynthesis and the resupply of B to the B-deprived *Rosa* cells indicates that only freshly synthesized RG-II was cross-linked by borate during or just after secretion from the Golgi to the cell wall (Chormova et al., 2014). Since pectin chains are assumed to be synthesized in Golgi and Golgi derived vesicles, it is proposed that BOR2 aids in the RG-II-B dimer formation by transporting boric acid/borate from the cytosol to secretory vesicles (Miwa et al., 2013).

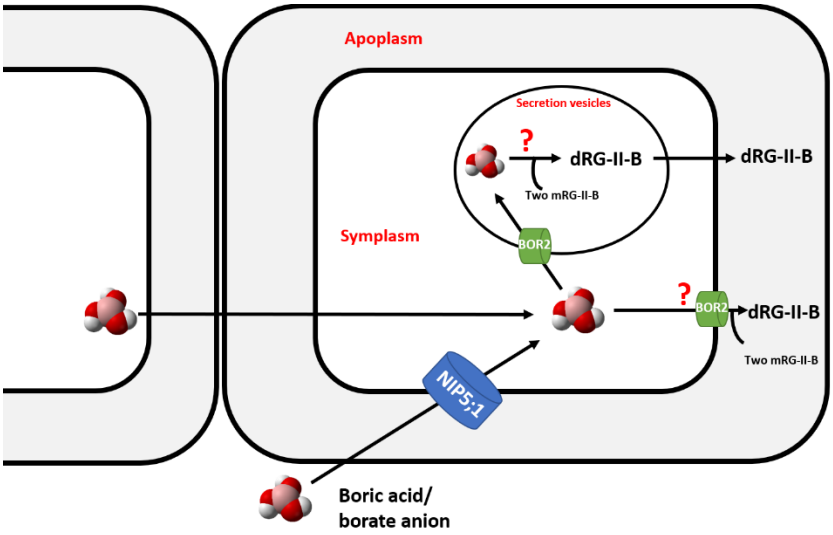

Figure 1.6 A hypothesis of the role of BOR2 in root meristems under deficient B condition. Conceptualized and redrawn based on *Kyoko Miwa, Shinji Wakuta, Shigeki Takada, Koji Ide, Junpei Takano, Satoshi Naito, Hiroyuki Omori, Toshiro Matsunaga, Toru Fujiwara, Roles of BOR2, a Boron Exporter, in Cross Linking of Rhamnogalacturonan II and Root Elongation under Boron Limitation in Arabidopsis, Plant Physiology, Volume 163, Issue 4, December 2013, Pages 1699–1709, https://doi.org/10.1104/pp.113.225995*

AtBOR4, a clade II BOR-transporter, is localized on the distal sides of the epidermal cells for the directional export of B from roots to the soil under toxic B concentration (Miwa et al., 2007). BOR4 T-DNA insertion mutants showed retarded plant growth and accumulated higher B concentration in shoots than the wild-type plants under toxic B supply (Miwa et al., 2014). Whereas, increased B toxicity tolerance has been observed in overexpressed *BOR4 Arabidopsis* lines (Miwa et al., 2014).

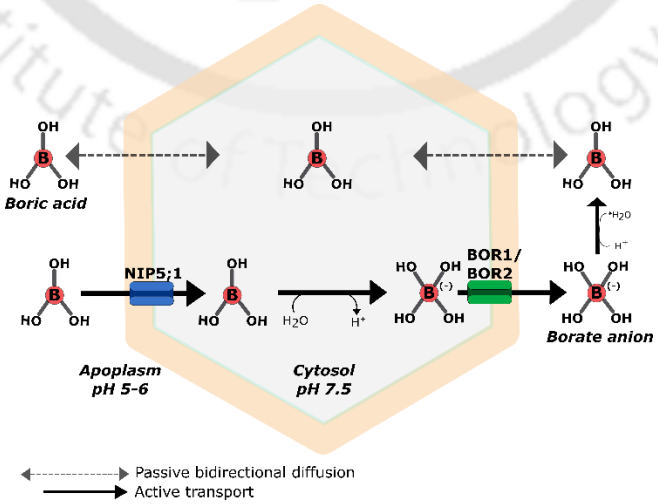

Figure 1.7 Three different mechanisms of B transport across the plasma membrane: 1. simple diffusion of uncharged boric acid 2. facilitated diffusion of boric acid through channel protein

NIP5;1 3. Borate exporters-mediated transport: BOR1 and BOR2. Conceptualized and redrawn based on *Yoshinari, A., & Takano, J. (2017). Insights into the Mechanisms Underlying Boron Homeostasis in Plants. Frontiers in plant science, 8, 1951. https://doi.org/10.3389/fpls.2017.01951*

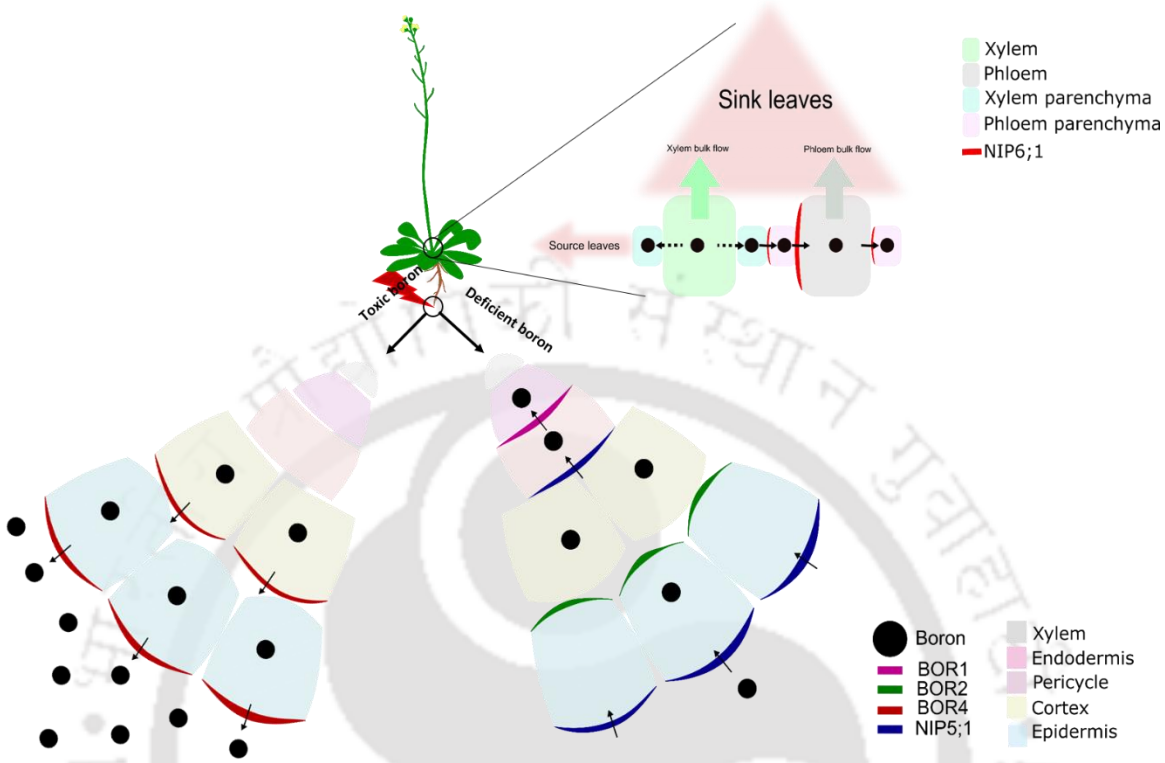

Figure 1.8 Summary of B transport via aquaporins and BOR-transporters under low and toxic B concentration.

1.7 SYSTEMS REGULATING B TRANSPORTERS

The B transport proteins (*NIP5;1*s and *BOR1*s) follows three intriguing mechanisms for the efficient B transport at the cellular level, viz. 1. polar localization of proteins for efficient B transport 2. Endocytic degradation of AtBOR1, and 3. B-dependent post-transcriptional regulation.

1.7.1 Polar localization of proteins for efficient B transport

The polar localization of the transporter proteins is necessary for the directional transport of nutrients in all domains of life. Localization of AtBOR1 in the proximal plasma membrane of endodermal cells suggested a specialized mechanism for polar localization in this cell type. The tyrosine-based motif (YxxΦ) and the dileucine motif (EIDDLL), identified in the cytosolic domain of BOR1, are necessary for the polar localization (Wakuta et al.,

2015). Furthermore, expression of a dominant-negative variant of DRP1A, which has an important role in the pinching off the clahtrin-coated vesicles, and loss-of-function of clathrin adaptor AP2 complex disturbed the polar localization of BOR1 (Yoshinari et al., 2016; 2019). These findings suggested the importance of endocytosis and subsequent recycling for the polar localization.

The polar localization of GFP-NIP5;1 to the outer plasma membrane is consistent with its role in the uptake of B into root cells (Yoshinari and Takano., 2017). The polar localization of AtNIP5;1 is mediated by the phosphorylation of Thr residues in the conserved TPG repeats present in the N-terminal cytosolic region (Wang et al., 2017). Substitution of alanine in place of threonine at these phosphorylation sites (T18A.T21A.T24A) resulted in reduced endocytosis and weak polar localization. The GFP-NIP5;1 localization study in the AP2 mutants indicated that low endocytosis rates coupled with compromised polar localization (Wang et al., 2017). These results indicate that continuous polar cycling between the PM and endosomal compartments through clathrin-mediated endocytosis is required for maintenance of polar localization against the lateral diffusion in the PM. Importantly, expression of the week polar variant (GFP-NIP5;1 T18A.T21A.T24A) only partially rescued the defects of *nip5;1* mutant in B transport and growth under low B conditions. This demonstrated the physiological importance of the polar localization in directional nutrient transport. Consistently, the ap2 mutants, in which polar localization of NIP5;1, BOR1, and BOR2 was compromised, showed limited growth under B limitation (Yoshinari et al. 2019).

1.7.2 Endocytic degradation of AtBOR1

When *Arabidopsis* plants were transferred from a low to high B condition, AtBOR1 is trafficked from the plasma membrane to the endosomes and them into the vacuoles for degradation (Takano et al. 2005). Currently, several other nutrient transporters in plants have been shown to be downregulated via the endocytic degradation under excess concentrations of nutrients in order to avoid nutrient toxicity (Rodriguez-Furlan et al., 2019). For the High B-induced endocytosis and degradation of BOR1, the K63-linked polyubiquitination at the K590 residue is critical and it triggers AP2-independent while DRP1A-dependent endocytosis (Kasai et al., 2011; Yoshinari et al., 2016; 2019; 2021). It was also demonstrated that TOM1-LIKE ubiquitin receptor TOL proteins is involved in the vacuolar transport of BOR1 (Yoshinari et al., 2018). A forward genetic study showed that BOR1 residues involved in borate transport activity were also critical for the high B-induced ubiquitination and degradation (Yoshinari et

al., 2021). Further, targeted mutagenesis studies and comparison to the model of substrate-dependent ubiquitination of yeast amino acid permeases suggested that the conformational transition during the borate transport cycle leads to ubiquitination of BOR1 under high B conditions. Based on these studies, BOR1 was proposed to be a transceptor regulating its own ubiquitination and degradation dependent on its transport activity. It is a different nutrient sensing mechanism from those of known plant transcepters; NRT1 nitrate transceptor and IRT1 metal transceptor (Ho et al., 2009; Dubeaux et al., 2018).

1.7.3 B-dependent post-transcriptional regulation

Accumulation of AtBOR1 protein is regulated by B-dependent translational suppression in addition to the endocytic degradation (Aibara et al. 2018). The 5′-UTR, alone, is sufficient for the B-dependent translational suppression of BOR1 and at least two independent uORFs are responsible for the activity. The transgenic plants defective in translational suppression and protein degradation demonstrated that BOR1 expression was down-regulated mainly by protein degradation under sufficient B conditions and was decreased further by both translational suppression and protein degradation at higher B concentrations (Aibara et al. 2018). Using transgenic *Arabidopsis* lines expressing mutant BOR1 defective for endocytic degradation and translational suppression, it was proved that these two post-transcriptional mechanisms contribute to prevent the overloading of B under high-B conditions.

The post-transcriptional downregulation of *NIP5;1* mRNA level is critical for the acclimation of plants under high B conditions (Tanaka et al., 2011). The upstream region of *NIP5;1* containing 5’ upstream open reading frames (uORF) and AUG-stop sequences play an important role in the B-dependent mRNA decay. High B enhanced ribosome stalling at AUG-stop, accompanied by the suppression of translation and mRNA degradation. However, the reinitiating of translation at the downstream *NIP5;1* ORF is enhanced when plants sense low B conditions (Tanaka et al. 2016). This regulation is primarily based on the cytosolic boric acid concentration. Using *AtNIP5;1* 5’UTR, genetically encoded B sensors were developed to visualize relative B concentrations in various plant cells/tissues (Fukuda et al., 2018).

The clade II BOR transporter protein, AtBOR4, is highly expressed and localized in the distal side of root epidermal cells to exclude B from root to soil under the toxic B conditions (Miwa et al., 2007). Transgenic *Arabidopsis* expressing 3-kb 5' flanking sequence of *BOR4* ORF in the Pro*BOR4*-GUS construct controls the up-regulation of *BOR4* mRNA under the high-B

treatment (Miwa et al., 2014). It has also been reported that promoting the expression of heme oxygenase encoding gene (HY1) in *Arabidopsis* mutant, *sensitive to high-level of boron 1* (*shb1*) decreases B content by inducing the *BOR4* mRNAs to confer excess B tolerance (Lv et al., 2017). Therefore, it is likely that *AtBOR4* expression is regulated at the mRNA level but not at the protein level.

1.8 B TRANSPORT AND REGULATION IN CROP PLANTS

In this section we are describing the mechanisms of B transport and regulation in five well-studied crop plants focusing on the B transport proteins with their physiological function genetically verified or strongly supported by the analysis of orthologs.

1.8.1 *Brassica napus*

Brassica napus, an allotetraploid oilseed crop, is extremely sensitive to B deficiency (Zhang et al., 2014a). B deficiency inhibits the growth and reduce the inflorescence fertility. The genotypic differences among the *B. napus* genotypes have been well-documented (Zhang et al., 2014a). The B-efficient lines have shown better plant growth, and seed yield than B-inefficient lines by accumulating high tissue B under B deficiency (Zhang et al., 2014a). The B-inefficient genotype, Westar 10 (W10), have more B-binding sites in its cell wall and thereby shows a greater B requirement for normal growth and development than B-efficient genotype Qingyou 10 (QY10). In addition, B concentration in pectin and cell wall fractions estimated among the genotypes suggested that the capacity to distribute B to the cell wall pectin was higher in QY10 than W10 (Pan et al. 2012; Pommerrenig et al., 2018).

In *B. napus*, twenty BOR genes were identified that belongs to the six BOR subfamily based on the sequence homology to the *Arabidopsis* family genes (Chen et al., 2018). Compared to other BnaBOR1 transporters, BnaC04.BOR1;1c showed highest similarity to AtBOR1 and exhibited low B-induced expression, at the mRNA level, in root, shoot, and flowers of B-efficient QY10. However, there was no upregulation of *BnaC04.BOR1;1c* under B-deficiency in the European winter-type *B. napus* cv. Darmor-PBY018 (Diehn et al. 2019), indicating the difference among the genotypes. The subcellular localization using GFP fusion revealed that BnaC04.BOR1;1c is localized on the plasma membrane (Zhang et al., 2017). Knockdown of *BnaC04.BOR1;1c* in B-efficient genotype QY 10 reduced B accumulation in flower organs, eventually resulted in flower drooping, severe sterility and seed yield loss. Whereas, the

overexpression of *BnaC04.BOR1;1c* in B-inefficient genotype W10 displayed stronger tolerance to B deficiency (Zhang et al., 2017; Chen et al., 2018). Then, it was discovered that *BnaC04.BOR1;1c* expression is regulated via 5'-UTR-dependent manner (Wang et al., 2021). In the 351 nucleotide 5'-UTR sequence of *BnaC04.BOR1;1c*, two AUG-stop sequences (-24 to 29, and -92 to 97) and three uORFs are present and the first 5' AUG-stop sequence (-24 to 29 nucleotide) contributes to the B-dependent regulation of *BnaC04.BOR1;1c*. This result suggest that a common mechanism of B-dependent mRNA regulation exist in both *AtNIP5;1* and *BnaC04.BOR1;1c* in QY10 (Tanaka et al. 2016; Wang et al., 2021). The difference in the 5'-UTR of *BnaC04.BOR1;1c* in other B-efficient *B. napus* cultivar, ZS11, suggest that there might be different B responses among the *B. napus* lines. While the mRNA regulation varies, the multiple uORF sequences in the 5'-UTR of *BnaC04.BOR1;1c* between the *B. napus* cultivars were highly conserved (Wang et al., 2021). In addition, the results of in-situ PCR, immunohistochemistry staining, and transgenic *Arabidopsis* studies showed that BnaC04.BOR1;1c was polarly localized towards the stele-side of the plasma membrane in root vascular cells, presumably for the efficient xylem loading (Wang et al., 2021). BnaC04.BOR1;1c was also localized in the plasma membrane of cambium cells in the nodes of developing tissues in a polar manner toward the phloem side, presumably for the preferential distribution (Wang et al., 2021).

The involvement of boric acid channels in the low B stress tolerance of *B. napus* was first demonstrated by the identification of a novel QTL, qBEC-A3a, which encodes *BnaA3.NIP5;1* gene (Zhang et al., 2014b; Hua et al., 2016). The BnaA03.NIP5;1b is localized in the plasma membrane in a polar manner toward the soil-side in the lateral root cap (LRC) and is required for the efficient B uptake into the root tip (He et al., 2021). Though there was no difference in amino acid sequence of BnaA03.NIP5;1b between B-efficient (QY10) and B-inefficient (W10) genotypes, they differ in their expression level. The expression of *BnaA03.NIP5;1b* was induced relatively higher in roots and leaves of QY10 under low B condition than W10 (Yuan et al., 2017). Further analysis revealed that a tandem repeat (CTTTC) present in the 5'UTR region is responsible for the differential expression pattern and showed close relationship with plant growth and seed yield under low B conditions in different genotypes (He et al., 2021). Importantly, field tests in a B-deficient plot showed that the varieties with higher expressing *BnaA03.NIP5;1b* allele had significantly improved seed yield. This finding opened the way of marker-assisted breeding of low-B tolerant cultivars.

The involvement of transcription factor WRKY in B stress responses was established in *B. napus* (Feng et al., 2019). A conserved W box (T/CTGACC/T) in the promoter region of the target genes was identified as the typical binding site of WRKY (Eulgem et al., 2000). The *B. napus* B transport genes have been identified to have many W boxes in their 2Kb promoter sequence. The binding of BnaWRKYs to these W boxes of B-responsive *BnaNIP5;1*s and *BnaBOR1*s in Y1H assays suggested that BnaWRKY transcription factors might be involved in low B tolerance by modulating B transporter genes (Feng et al., 2020). Furthermore, the *BnaA9.WRKY47* mutants displayed severe B deficiency phenotypes under B deficiency and the *BnaA9.WRKY47* overexpressing lines showed higher tolerance to low B than wild-type, implying that BnaWRKYs play a vital role in the response of *B. napus* to B deficiency. While *BnaA03.NIP5;1b* was significantly upregulated and down-regulated in the *BnaA9.WRKY47* overexpressing lines and its null mutants, respectively, the expression of other *BnaNIP5;1*s and *BnaBOR1*s was less affected.

BnaA02NIP6;1a is a close homolog of AtNIP6;1 and was reported to have B transport activity in both yeast and oocyte (Diehn et al., 2019). Unlike *AtNIP6;1*, the expression of *BnaA02NIP6;1a* in *B. napus* was identified in roots (matured root zone), stems, leaves, shoot nodal region, buds and floral organs (Song et al., 2021). The B deficiency symptoms of the *BnaA02NIP6;1a* RNAi lines were observed to be prominent in flower buds, indicating that *BnaA02NIP6;1a* is playing an important role in B transport to the developing inflorescence in *B. napus* (Song et al., 2021). The overexpression and knockdown studies revealed that *BnaA02.NIP6;1a* is required for the reproductive organ development by transporting B to the inflorescence organs, which is crucial for fertility.

1.8.2 *Oryza sativa*

As a monocotyledon, rice (*Oryza sativa*) requires almost 10-times lower B for the optimal plant growth than the dicotyledon plants. Though at seedling stage rice showed relative tolerance to the B deficiency than dicots, continual low B supply visibly reduces the seed yield by impairing the vegetative and reproductive growth (Shao et al., 2021). In addition to grain yield, optimal B application (0.21-0.42 mg B/Kg) has increased the straw yield, panicle fertility, and weight of individual kernels of rice on calcareous (pH 7.9-8.8) soil in Pakistan (Rashid and Yasin., 2004). In another study, Uraguchi and Fujiwara., 2011 have demonstrated that the B stored in the seed endosperm have contributed significantly for low B tolerance during the seedling stage in rice. While the rice seedlings without endosperm showed much reduced plant growth in 10

days under low B, plants with endosperm started to show visible low B symptoms after five weeks (Uraguchi and Fujiwara., 2011).

Rice has four BORs and among them, OsBOR1 shows high similarity to AtBOR1. OsBOR1 is a plasma membrane localized B transporter expressed both in roots and nodes of the vegetative and reproductive organs under low B conditions (Shao et al., 2021). In roots, the OsBOR1 cell-type specific expression in the exodermis and endodermis is expected to be important for B to cross these cell-types with Casparian strips. Under sufficient B concentration the OsBOR1 showed cell-type specific expression only in the endodermis. However, it was both in the endodermis and exodermis under B deprived condition (Nakagawa et al., 2007). The existence of exodermis with Casparian strip and OsBOR1 expression in these cell-types would be the reason for high capacity to concentrate B immediately after the uptake in rice roots unlike *Arabidopsis*. OsNIP3;1, a NIP II protein with the highest similarity to AtNIP5;1 and AtNIP6;1, function as boric acid channels and are necessary for the B transport under B deficiency for the vegetative and reproductive growth (Hanaoka et al., 2014). The expression of *OsBOR1* and *OsNIP3;1* was higher in shoot nodes than roots which is involved in preferential distribution of B to the developing tissues (Shao et al., 2018; Shao et al., 2021). This is achieved by the polar localization of OsBOR1 and OsNIP3;1 at the distal side of the bundle sheath and proximal side of the xylem parenchymal cells, respectively (Shao et al., 2021). While high B induced down-regulation of OsBOR1 occurs at protein level, OsNIP3;1 is at both mRNA and protein levels (Shao et al., 2018; Shao et al., 2021). The knockout and localization studies of OsBOR1 and OsNIP3;1 revealed that these proteins cooperatively work in B distribution from the basal node xylem vessels of enlarged vascular bundles, and diffuse vascular bundles, respectively, to the developing tissues (Shao et al., 2021). Similar to the case in the basal node, OsBOR1 and OsNIP3;1 are also involved in intervascular B transport in the node I- the uppermost node responsible for preferential distribution to the panicles.

As we have mentioned earlier, impairment of the reproductive growth such as reduced panicles and grain fertility coupled with poor pollen germination rate were frequent in rice grown under B-deficient conditions (Lordkaew et al. 2012). *OsBOR4* is preferentially expressed in anthers and matured pollen. Disruption of *OsBOR4* led to impaired reproductive competence, as a result of poor pollen germination and reduced growth of pollen tubes. These results showed that *OsBOR4* is involved in B homeostasis in pollen for fertilization (Tanaka et al. 2013).

1.8.3 *Hordeum vulgare* and *Triticum aestivum*

The cereal crops, barley (*Hordeum vulgare* L.) and wheat (*Triticum aestivum* L), are relatively insensitive to low B- conditions during vegetative growth (Wongmo et al., 2004). However, the reproductive growth in barley and wheat is very sensitive to B deficiency causing depressed grain setting (Wongmo et al., 2004). Very recently, a functional boric acid channel of barley (HvNIP2;2/HvLsi6) was identified via boric acid uptake studies using *Xenopus* oocytes (Jia et al., 2021). The variation in mRNA expression levels among the numerous genotypes were identified to be associated with root and shoot B concentrations and root biomass formation under low B conditions (Jia et al., 2021).

Earlier studies on F1 doubled-haploids linkage mapping revealed four (2H, 3H, 4H and 6H) and two (7B and 7D) loci related to B toxicity tolerance in barley and wheat, respectively (Jefferies et al., 1999; Jefferies et al., 2000). The high B tolerant barley genotype, Sahara, maintained low B in roots, xylem and leaves than the high B sensitive genotype, Schooner under excess B conditions (Hayes and Reid., 2004). Barley lines developed by backcrossing tolerant and sensitive cultivars for B toxicity revealed that cultivars with the 4H locus showed high levels of expression of the *Bot1* (*HvBOR2*) gene, encoding an ortholog of *AtBOR4*, and the level of expression was inversely proportional to the concentration of B in roots and shoots. The tolerant cultivar Sahara contains four-times higher gene copies and ~160- and 180-fold higher *Bot1* transcript levels in roots and leaf blades, respectively, as compared to the sensitive cultivar, Clipper (Sutton et al., 2007). Two amino acid residue changes, Leu305→Ser305 and Asp592→ Gly592, between the tolerant and sensitive cultivars, is likely the reason that could affect the B transport (Sutton et al., 2007). Then, a B tolerance QTL region on chromosome 6H was identified and named as *HvNIP2;1* (Schnurbusch et al., 2010). The HvNIP2;1 (also known as HvLsi1) is a close ortholog of OsLsi1/OsNIP2;1 (a NIPIII class protein) and heterologous expression in *Xenopus* oocytes showed significant B transport activity along with silicon, germanium, arsenic, and water (Schnurbusch et al., 2010). The HvNIP2;1/HvLsi1 is localized to the distal-side plasma membrane of the epidermal and cortical cells in the seminal roots and was suggested to be a major silicic acid channel responsible for silicon uptake in barley (Chiba et al., 2009). The Northern and qRT-PCR analysis revealed that the *HvNIP2;1* transcripts were expressed higher in the B-sensitive barley cultivar than tolerant (Schnurbusch et al., 2010). Genetic analysis revealed that reduced expression of HvNIP2;1/HvLsi1 confers tolerance to high B condition in the tolerant cultivar by decreasing the B uptake (Schnurbusch et al., 2010).

The physiological basis for the B toxicity tolerance in wheat is similar to that for barley. The genetic variation for B tolerance in wheat is achieved by a minimum of four genes, namely *Bo1*, *Bo2*, *Bo3*, *Bo4* (Paull et al., 1991; Paull et al., 1992). The locus 7B has been identified to be a crucial factor for the improved yield in wheat genotypes cultivated under excess soil B in southern Australia (Nable et al., 1997). TaBOR2 (otherwise known as, Bot-D2a), an ortholog of OsBOR2 and OsBOR3, was the first B transporter protein reported to be involved in high B-tolerance in wheat (Reid., 2007). The expression analysis revealed that the tolerant wheat cultivar showed higher transcript accumulation of *TaBOR2* than the sensitive cultivar under excess B conditions (Reid., 2007). Pallotta et al., 2014 demonstrated that functional alleles of the B efflux transporter gene *Bot-B5* are essential for the high B tolerance in wheat cultivars. In addition, wheat varieties from various agronomic zones of the world showed loss of *Bot-B5* alleles to adapt low B conditions. This suggests that alleles of *Bot-B5* can have unintended consequences in low B environment.

Three OsBOR1 orthologous B efflux transporters, Bot-A4a (TaBOR1.2), Bot-B4a (TaBOR1.3), and Bot-D4a (TaBOR1.1) were identified in wheat by Leaungthitikanchana et al., 2013. These B efflux transporters have shown plasma membrane localization and B-dependent expressional changes. *TaBOR1.1* and *TaBOR1.3* showed higher mRNA levels under low B conditions, while *TaBOR1.2* showed a higher mRNA level under an excess B condition (Leaungthitikanchana et al., 2013).

1.8.4 Zea mays

Similar to most of the cereals, vegetative growth of maize (*Zea mays* L.) is relatively insensitive to B deficiency. However, the reproductive growth of the maize plants was severely affected with decreased shoot apical meristem, smaller tassels, repressed ear development, dried anthers, and poor pollen vitality when grown under low B conditions (Lordkaew et al., 2011). The studies carried out in two maize mutants, *tassel-less1* (*tsl1)* and *rotten ear* (*rte)* has increased our understanding of B transport in maize reproductive development (Leonard et al., 2014; Durbak et al., 2014; Chatterjee et al., 2014; Chatterjee et al., 2017)**.** The causal gene of the *tsl1* mutant encodes a NIP II protein ZmNIP3;1, an ortholog of AtNIP5;1, AtNIP6;1 and OsNIP3;1. ZmNIP3;1 functions as boric acid channel and is necessary for the B transport under B deficiency for the vegetative and reproductive growth (Leonard et al., 2014; Durbak et al., 2014). The causal gene of *rte* encode an ortholog of AtBOR1. RTE2 is a close ortholog of RTE which encodes a protein that is expressed in roots and shoots. Single (*rte*) and double maize

mutants (*rte;ret2*) showed defects in both vegetative and reproductive development under deficient B condition (Chatterjee et al., 2014; Chatterjee et al., 2017). Whereas, the *ret2* mutants did not show any growth defects except minor decrease in root under low B conditions (Chatterjee et al., 2017). This is clearly suggesting that RTE is the main B transporter protein in maize under deficient B conditions. Since the loss of *RTE2* did not affect the vegetative and reproductive growth, it might be playing a secondary role when the function of *RTE* is lost (Chatterjee et al., 2017). Considering the physiological effects of *rte;ret2* double mutant and *tls1* mutant, it can be assumed that *RTE* and *RTE2* work synergistically with *TLS1* in B uptake and xylem loading in roots (Chatterjee et al., 2017).

1.9 GENERATION OF TRANSGENIC PLANTS TO ALLEVIATE B DEFICIENCY AND TOXICITY

The extensive understanding of the B transport mechanisms provides opportunities to improve crops for better B utilization under varied soil B concentration. For instance, as mentioned earlier, increased production of B complexing sugar alcohol can result in increased B uptake and mobility thus, in turn, increased B deficiency tolerance (Brown et al.,1999; Bellaloui et al., 1999). Additionally, the enhanced expression of *AtBOR1* and *AtNIP5;1* in *Arabidopsis* have shown promising results by increasing root-to-shoot B translocation, shoot growth and the seed yield under limited B concentration (Miwa et al., 2006, Kato et al., 2009). The transgenic tomato (*Solanum lycopersicum* L.) lines overexpressing *AtBOR1* did not show any B-deficient phenotype, and B concentrations in leaves and fruits were observed to be high (Uraguchi et al., 2014). Also, the overexpression of *OsBOR1* under the control of the cauliflower mosaic virus 35S RNA promoter accumulated 1.8-1.9 times higher B concentration in xylem sap and 1.7-1.8 times greater grain yield than the non-transgenic rice under B deficiency (Uraguchi et al., 2009).

The excess concentration of B affects cellular metabolisms, probably through binding to the ribose moieties of ATP, NADH, and/or NADPH in cells (Reid., 2014). The growth enhancement of *BOR4* overexpressed in *A. thaliana* under toxic B concentration can be attributed to the reduced concentration of B in the cells of roots and shoots due to the efficient efflux of B (Miwa et al. 2007). Transgenic rice plants expressing *AtBOR4* showed growth enhancement under excess B (Kajikawa et al., 2011). B transport mechanisms such as active B-RGII complex formation and compartmentation in the cells and tissues, and on B sensing

mechanisms regulating B homeostasis would lead to improvement of crop plants tolerant to low and B conditions.

1.10 IMPORTANCE OF B NUTRITION IN INDIAN MUSTARD

Cruciferous crops including rapeseed-mustard species are extremely sensitive to B deficiency (Diehn et al., 2019). In India, among oilseeds, rapeseed-mustard contributes the most to domestic oilseed production, followed by soybean and groundnut (Rathore et al., 2020). Indian mustard (*Brassica juncea*) shares the major area occupied by this group, and it is the most important winter season (rabi) oilseed crop, which thrives best in light to heavy loam soil in areas having 25-40 cm of rainfall. Mustard yield has been reported to show a positive trend upon B application (Shen et al., 1993; Bora and Hazarika, 1997; Lu et al., 2000; Xue et al., 1998) and the response varies among three species, *B. napus*, *B. campestris* and *B. juncea* (Hossain et al., 2012). *B. juncea* is sensitive to B limiting condition, and the application of B fertilizer in B deficient calcareous soil in India and clay loam soil in Bangladesh significantly increases the yield (Kumararaja et al., 2015; Masum et al., 2019). Severe B deficiency may also result in floral abortion and significant drop in the number of siliquae, seed setting and seed yield of *B. napus* during the field trials in China and Bangladesh (Yang et al. 1989; Zaman et al. 1998; Lei et al. 2009). The uptake and requirement of boron greatly differ among rapeseed-mustard genotypes and species, in different development stages, soil, and plant parts (Xue et al. 1998; Hu et al., 1991; Stangoulis et al., 2000; Pommerrenig et al. 2018), indicating significant differences among Brassica species and cultivars in their response to B deficiency (Hu et al., 1991; Xue et al., 1998; Stangoulis et al., 2000 a, b). Soil B content in major mustard producing states of India, especially in West Bengal and Orissa, is alarmingly low (Das et al., 2017; Prasad et al., 2014), and the B deficiencies ranged from 2% in alluvial soils (Ustipsamments) of Gujarat, to 70% in red soils (Calciorthhents, Haplustalfs) in Orissa, with a mean of 33% for the whole country (Singh, 1999; Singh 2008). Currently, alleviation of B deficiency relies on the application of B fertilizers. The application of B fertilizers can alleviate the problem of B deficiency in soils. However, B being a non-renewable mineral resource, excessive B applications can lead to environmental problems. Breeding mustard cultivars with enhanced B efficiency is rather more sustainable means to address the yield loss due to B deficiency in soils. However, there have been very limited studies in *B. juncea* responses to low B soil and these studies are mostly confined to Bangladesh (Hosain et al., 2012).

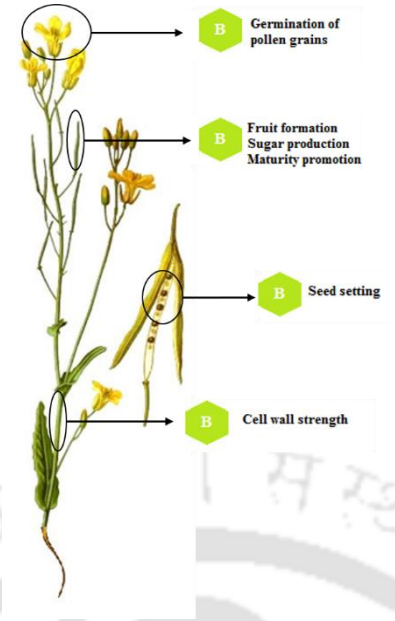

Figure 1.9 Involvement of boron in various plant metabolism

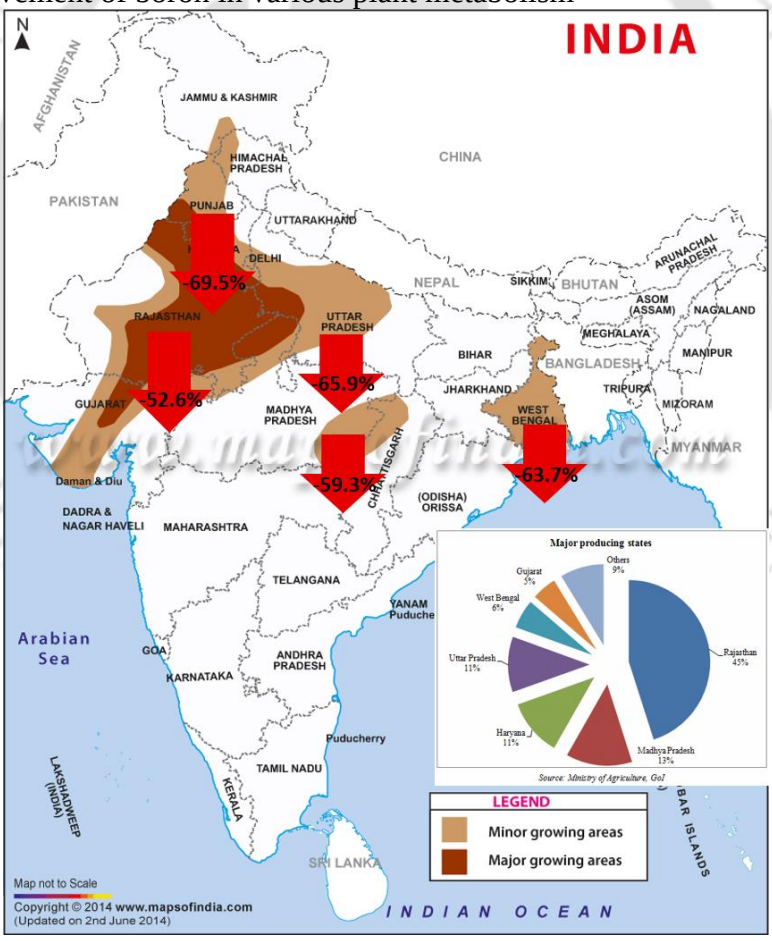

Figure 1.10 Soil B content in major mustard producing states on India. Majority of the high mustard producing states are consisting of low soil B. Inlet picture: percentages of contribution in total rapeseed-mustard production by an individual state of India. (Indian map Copyright to www.mapsofindia.com)

Unlike any other nutrient deficiency, the characteristic visual B deficiency symptoms are not very prominent in *B. juncea* leaves (Kumararaja et al., 2015) and the range between B deficiency and toxicity being quite narrow, this further complicates the understanding of the physiological responses to B deficiency in *B. juncea*. Information on genotypic level variation and B transport networks in *B. juncea* under low B condition is very scarce.

1.11 OBJECTIVES OF THE THESIS

The following objectives were framed in order to study the involvement of AQP and BOR transporters in Indian mustard (*Brassica juncea*):

1. Genome-wide identification and characterization of boron transporter genes in *Brassica juncea*
2. Physiological, biochemical and molecular responses of contrasting Indian mustard genotypes to low boron condition at vegetative stage
3. Generation of B-deficiency tolerant Indian mustard by the manipulation of boron efflux transporter, AtBOR1

Chapter II

Genome-wide identification and characterization of aquaporin and boron transporter genes in Brassica juncea

2.1 BACKGROUND

Brassica juncea is an important oilseed crop around the world and is extremely sensitive to boron (B) deficiency. Therefore, it is crucial to understand the molecular mechanisms governing the uptake and distribution of B in *B. juncea*. In this study, we have carried out genome-wide identification of the genes encoding 104 Aquaporins (AQPs) and 15 BOR-borate efflux transporters in *B. juncea* and characterized in comparison to the homologs in *Arabidopsis thaliana*. Compared to other BjAQP subfamilies, BjNIPs possessed complex selectivity filter compositions that affect permeation of solutes including boric acid. BjNIP5;1s contained ATG-stop sequences in 5'UTR necessary for B dependent post-transcriptional regulation, and both BjNIP5; 1 and BjNIP6;1 homologs possessed N-terminal TPG repeats essential for the polar localization. In clade I BjBOR1s, the characteristic features involved in the endocytic degradation under high-B supply, including tyrosine and acidic di-leucine motifs, and lysine ubiquitination residue, were well conserved. The qRT-PCR analysis in an Indian Mustard cultivar Geeta revealed induced expression of NIP5;1s (BjuA02NIP5_1a, BjuA03NIP5_1b, and BjuA07NIP5_1a) and BOR1 (BjuA03BOR1a) under low B condition, implying their probable role in B uptake and mobilization. These results provide a base to understand the molecular mechanisms of B transport and develop low B tolerant *B. juncea* genotypes.

2.2 MATERIAL AND METHODS

2.2.1 Genome-wide identification of AQP and BOR genes in *B. juncea*

The genomic sequences of *A. thaliana* 35 AQP and 7 BOR genes were retrieved from the TAIR10 database (http://www.arabidopsis.org/index.jsp; Berardini et al., 2015). The genomic sequences of 57 AQP and 7 BOR genes of *B. rapa* (Chiifu V3.5) and 63 AQP, 10 BOR genes of *B. nigra* (NI100 V2.0), and 127 AQP, 20 BOR genes of *B. napus* [18; 51] were retrieved from Brassica database (http://brassicadb.org/brad/index.php; Yang et al., 2016). The AQP and BOR genes were identified in *B. juncea* based on their sequence homology to *A. thaliana* using the BLAST analysis in the Brassica database (BRAD; Braju_tum_ V1.5; http://brassicadb.org/brad/index.php; Yang et al., 2016). An e-value of 10^{-5} was kept as an initial cut-off to identify high-scoring pairs (HSPs). The blast output was tabulated, and the HSPs were showing >100-bit scores were selected. The genomic, cDNA, CDS, and protein sequences of all BjAQPs and BjBORs obtained from the BRAD were verified for their

conserved domains using the Hidden Markov Model of the Pfam database (http://pfam.sanger.ac.uk/search), and NCBI Conserved Domain Search database (https://www.ncbi.nlm.nih.gov/Structure/bwrpsb/bwrpsb.cgi). Full-length sequences were identified after removing the redundant sequences lacking either NPA motifs or ar/R selectivity filters in BjAQPs, and HCO_3^- transporter domain in BjBORs. The BjAQP genes were named according to the standardized gene nomenclature for the Brassica genus proposed by Østergaard and King (2008).

2.2.2 Multiple sequence alignment and phylogenetic tree construction of *B. juncea* AQP and BOR family genes

Multiple sequence alignment of the retrieved AQP and BOR protein sequences from *B. juncea, B. rapa, B. nigra* and *A. thaliana* were accomplished using the ClustalW tool of MEGA 7 software with default parameters (Tamura et al., 2011). An unrooted phylogenetic tree was assembled using the Neighbour-Joining (NJ) method with partial deletion, and the stability of the branch node was measured by 1,000 bootstraps test replicates during the construction. NJ method was selected based on the Bayesian information criterion (BIC) out of six tested models. The phylogenetic tree was illustrated with iTOL (v3.2.317, https://itol.embl.de/; Letunic and Bork, 2016).

2.2.3 Identification of conserved motifs and physicochemical parameters in BjAQP and BjBOR genes

The physicochemical parameters, including the molecular weight (MW), grand average of hydropathicity (GRAVY), and isoelectronic point (pI) for each BjAQP and BjBOR proteins were calculated using ExPASy (http://www.expasy.org/tools/). The transmembrane domains (TMs) and conserved motif structures encoded by BjBOR and BjAQP family proteins/genes were identified using the TMHMM2.0 online server (https://services.healthtech.dtu.dk/service.php?TMHMM-2.0) and MEME motif search tool (http://mem-esuite.org/tools/meme; Bailey et al., 2015), respectively. The parameter settings were default except that the maximum number of motifs was set to 20. The MEME motifs were then annotated using the Pfam (http://pfam.xfam.org/search) and NCBI databases. Additionally, the online tool ProtParam (https://web.expasy.org/protparam/) was used to predict the instability index, atomic composition, and amino acid composition. The subcellular localization of AQP proteins was predicted using the WoLF PSORT tool

(http://www.genscript.com/psort/wolf_psort.html). The physical location of the genes was documented manually on *B. juncea* genomes A and B.

2.2.4 Structural modelling of BjAQPs and BjBORs

The exon-intron structures of the BjAQP and BjBOR family members were investigated based on the coding sequence alignments with corresponding genomic sequences, and the diagram was drawn using the online Gene Structure Display Server (GSDS; http://gsds.cbi.pku.edu.cn/; Hu et al., 2015).

The tertiary protein sequences of the BjAQP and BjBOR genes were created using the Phyre2 protein-modelling server (http://www.sbg.bio.ic.ac.uk/~phyre2; Kelly et al., 2015). The PDB files received are then used to ascribe transmembrane pore, pore-lining residues, pore morphology, and constricts in the 3D protein structures performed using the PoreWalker server (http://www.ebi.ac.uk/thornton-srv/software/PoreWalker/; Pellegrini-Calace et al., 2009).

2.2.5 Prediction of cis-elements in the promoter region of BjAQPs and BjBORs

The 2 kb upstream region relative to the translation start codon of BjAQP and BjBOR genes were extracted from the Brassica database (BRAD; http://brassicadb.org/brad/index.php). The plant cis-element database, PlantCARE, was used to identify the cis-regulatory elements in the promoter regions of the respective genes (Lescot et al., 2002).

2.2.6 Plant material and growth condition

Seeds of the mustard genotype Geeta were surface sterilized in 0.05% mercuric chloride for 10 min, followed by 2-3 times rinsing with sterile deionized water and dried on sterile filter paper. The seeds are then germinated on moistened filter paper for five days in the dark. The germinated seedlings with similar growth were selected and transplanted into Planton boxes (Tarson, Kolkata, India) with Hoagland nutrient solution (Hoagland and Arnon, 1950) at two levels of B concentration: 0.1 µM B (B deficient) and 46 µM B (B sufficient). The pH was maintained at 5.8 using 0.5 M H_2SO_4 or 1 N NaOH. The seedlings were first transplanted to $1/4^{th}$ solution and increasing to ½ strength and finally to full strength as described in Pan et al., 2012. The nutrient solution was aerated continuously and refreshed every five days. The plants were cultured in an illuminated culture room with a temperature of 22^0C, a photoperiod of 16/8 h (day/night), and a light intensity of 300–360 µmol m^{-2} s^{-1}. The experiment was planned in a

completely randomized design with two treatments, and each treatment was replicated three times with one replication contained five seedlings. The plant samples were divided into two groups: the first one to determine B concentration. The second was used for the B transporters gene expression analysis.

2.2.8 RNA isolation and real-time RT-PCR for expression analysis of B transporters

The root tissues of the genotype Geeta grown in hydroponic solution for five days under sufficient (46 µM) and low (0.1 µM) B. Total RNA was isolated using the RNeasy Plant Mini Kit (Qiagen, Netherlands) following the manufacturer's instructions. Two micrograms of total RNA from roots were used as a template for the RT reaction. Total RNA was added to a mixture containing 1 µl of 50 µM oligo(dT) primer, 1 µl of 10 µM dNTPs, 1× Primescript buffer, 20 units of RNase inhibitor, and 200 units of Primescript reverse transcriptase (Takara, Shiga, Japan). The reaction was carried out at 42°C for 60 min, followed by a 10 min step at 70°C and then by cooling to 4°C. Realtime RT-PCR was performed in a Qiagen Rotor-Gene Q (Maryland, USA) using PowerUp™ SYBR™ Green Master mix (Applied Biosystems, USA) according to the manufacturer's protocol 50°C for 2 min 95° C for 2 min, 60° C for 30 s (50 cycles). The *B. juncea* endogenous reference gene (tubulin) was used as an internal control. All the assays were repeated at least three times. The primers used are listed in the section *List of Primers*.

2.2.9 Statistical analysis

All the analyses were performed with a minimum of three samples in triplicates and represented as mean ± SD. Statistical analysis of the data was carried out by unpaired t-test. The statistically significant mean values were denoted by an asterisk ($P \leq 0.05$).

2.3 RESULTS

2.3.1 Genome-wide identification and phylogenetic analysis of BjAQP and BjBOR family genes in *B. juncea*

To identify the *B. juncea* AQP and BOR genes, the BLAST program, available in Brassica database (http://brassicadb.cn/#/), with an annotation search was used based on their sequence homology with *A. thaliana* genes. Phylogenetic analysis of the 104 *BjAQPs* and 15 *BjBORs*, together with 35 *AtAQPs*, 63 *BniAQPs*, 57 *BraAQPs*, 127 *BnaAQPs*, 7 *AtBORs*, 10 *BniBORs*,

7 *BraBORs* and 20 *BnBORs* formed four distinct clusters representing thirty-two subgroups of *BjAQPs* and six subgroups of *BjBORs* (Figure 1 and 2). We have classified and named the AQP candidates according to their respective clusters. The genes *AtPIP1;2, BniPIP1;2, BraPIP1;2, BnaPIP1;2, AtNIP1;1, AtNIP4;2 and BnaNIP4;2* had no orthologous genes in *B. juncea*, whereas all the remaining *AQP* genes had 1-7 corresponding orthologous genes in *B. juncea* (Figure 1). Unlike *B. napus*, *B. juncea* had *PIP2;8* homologous gene family (2 members). Similar to *B. napus*, *B. nigra*, and *B. rapa*, *B. juncea* did not have any homologous gene(s) for *AtNIP1;1*. Interestingly, the homologs of AtPIP2;3, AtPIP2;6, AtPIP2;8, AtNIP2;1, and AtNIP3;1 are present in B. juncea but they are identified to be absent in B. rapa, and B. nigra. Similar to other Brassica crops (B. nigra, B. rapa, and B. napus), we have identified all BOR homologs except for AtBOR5 in B. juncea (Figure 2). Similar to *A. thaliana*, there were no XIP and HIP sub-family genes identified in *B. juncea*.

The *B. juncea* sub-families included 41 PIPs, 32 TIPs, 21 NIPs, and 10 SIP members. The BjPIPs formed two sub-groups, PIP1s and PIP2s, consisting of 15 and 26 members, respectively. The NIPs could be classified into seven sub-groups (NIP1;2 to NIP7;1) (Figure 1). There are four homologous proteins in NIP4;1, and NIP5;1, three in NIP1;2, and two in NIP2;1, NIP6;1 and NIP7;1 sub-groups. The TIP sub-family proteins were categorized into ten sub-groups (TIP1;1 to TIP5;1), with varied members of proteins in each sub-group. There are six members in TIP3;1, five members in TIP2;1, four members in TIP1;2, and TIP3;2. While TIP1;1, TIP2;3, and TIP1;3 subgroup has three members, TIP4;1 and TIP5;1 consist of two homologous proteins. The sub-group TIP2;2 consists of only one homologous protein. The SIPs were divided into two groups, SIP1 and SIP2, containing five numbers of proteins each. Out of them, two proteins were located in contigs (no information of the genome location) (Figure 1).

BjPIP1s showed more sequence similarities at the protein level than the rest of the BjAQPs (Supplementary Figure 1 and 2). In contrast, BjNIPs, BjTIPs, and BjSIPs appeared to have diversified sequences similarity although some similar aminoacid blocks were observed among these subfamily proteins (Supplementary Figure 3). The phylogenetic analysis of BjNIP5_1 and BjNIP6_1 along with their *A. thaliana*, *B. nigra*, *B. rapa* and *B. napus* orthologs revealed that majority of the BjNIP homologs (BjNIP5_1, BjNIP6_1, and BjNIP7_1) are more closely related to the respective *B. napus* NIPs than *A. thaliana*, *B. nigra*, *and B. rapa* counterparts, except BjuB08NIP5_1a, BjuB01NIP7_1a, and BjuB02NIP6_1a (Figure 3). Even

though the B. juncea NIP7;1 proteins, BjuA05NIP7_1a and BjuB01NIP7_1a, are clustered away from each other in the phylogenetic tree, the similarity between them is still identified to be high (97.6%). However, the difference become very evident between the *B. juncea*, *B. nigra*, and *B. napus* orthologs. We did not include BjAQPs, BjuB01NIP4_1a (gene ID: BjuB025800), BjuB08TIP1_1b (gene ID: BjuB016330), and BjuB01SIP1_1a (gene ID: BjuB042435) due to the presence of the stop codons in their coding sequence.

The BjBOR homologs were divided into two primary clusters in the phylogenetic analysis, viz cluster I (BjBOR1, BjBOR2 and BjBOR3) and cluster II (BjBOR 6 and BjBOR7) (Figure 2). In *B. juncea*, cluster I consist of high numbers of BOR proteins (8 members) than cluster II (7 members). Similar to our observation, BOR5 homologs were also previously reported to be absent in *B. napus* (Chen et al., 2018). Also, compared to other BjBOR1s, BjuB08BOR1b and BjuA03BOR1a are more closely related to AtBOR1 (Figure 2). The cluster II in *B. juncea* comprised BOR6 and BOR7 genes which previously had been identified to have restricted pollen-specific expression in *A. thaliana* (Becker et al. 2003; Bock et al. 2006; Figure 2). Each sub-group from the cluster II consisted of a minimum of two homologous proteins. BjBOR1 sub-group marked the highest homologous proteins, five, compared to others. The phylogenetic tree and comparative protein sequence analysis with AtBOR1 revealed that BjuA03BOR1a, BjuB06BOR1a and BjuB08BOR1b share more than 90% amino acid identity with the AtBOR1. Moreover, BjuB06BOR1a and BjuB08BOR1b were highly similar to each other than to BjuA03BOR1a, with an amino acid identity of 96% and these three homologous proteins might possibly function as B efflux transporter similar to AtBORs. The other two BjBOR1 homologs, BjuA04BOR1b and BjuA04BOR1c, were identified to have more than 96% coding nucleotide similarities with AtBOR1 and 98% sequence similarity between themselves. Besides, the BjBOR3, BjBOR6, and BjBOR7 homologs were identified to have more than 80% of identity to their respective *A. thaliana* homologs (Supplementary Figure 6). Since BjuContig917BOR1a (gene ID: BjuO009737), BjuA04BOR2b (gene ID: BjuA014452) did not contain ≥5 TMDs, we did not include them in any of our analysis. Also, we did not include BjuB06BOR4a (gene ID: BjuB046676) due to the presence of stop codon in their coding sequence.

Figure 2.1: Phylogenetic distribution of AQP homologs in *B. juncea*. All the AQP sequences were annotated concerning to its respective homologs of *A. thaliana*, *B. rapa*, *B. nigra* and *B. napus* AQP proteins. Phylogenetic tree was generated using MEGA 7 with Neighbor-Joining (NJ) method, and 1,000 replicates bootstraps, and visualized by iTOL. The names colored with red, green, blue, and yellow represented PIPs, TIPs, NIPs, and SIPs.

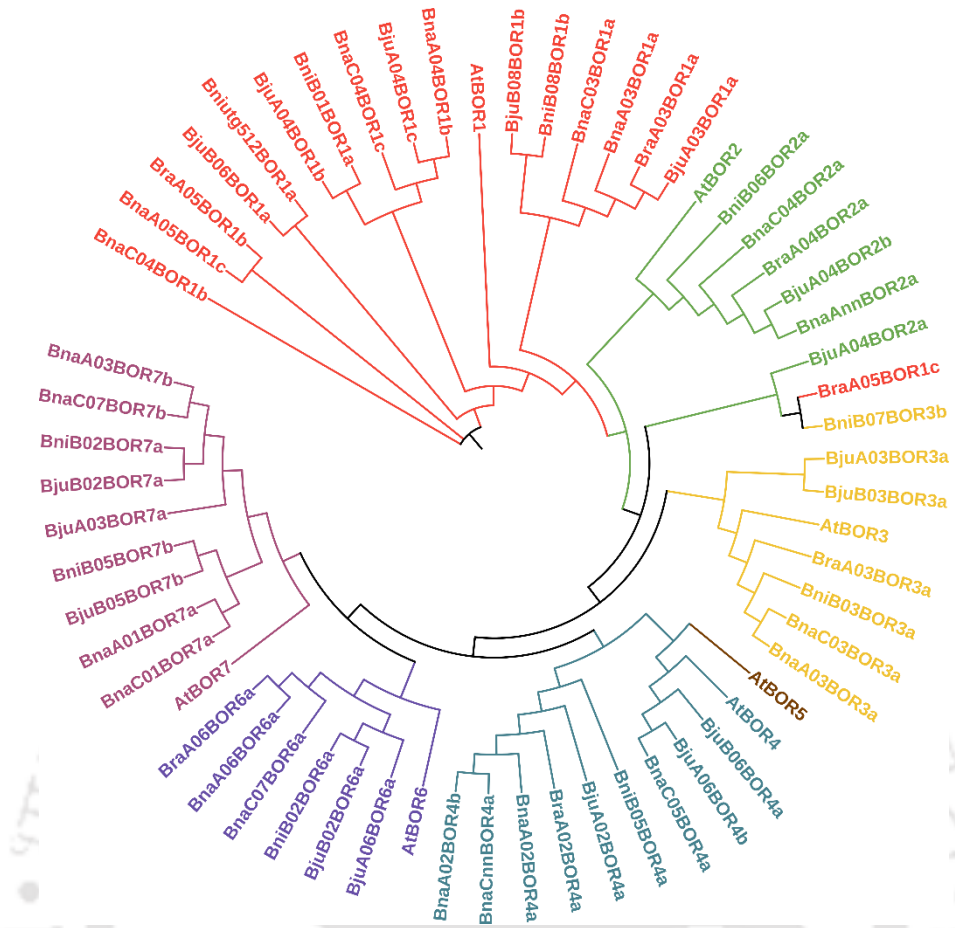

Figure 2.2: Phylogenetic relationship of *B. juncea* BORs. Phylogenetic tree derived from BOR protein sequences of *A. thaliana*, *B. rapa*, *B. nigra*, *B. juncea*, and *B. napus* using MEGA 7 with Neighbor-Joining (NJ) method, and 1,000 replicates bootstraps, and visualized by iTOL. The names colored with red, green, yellow, teal, brown, purple, and red violet represented BOR1s, BOR2s, BOR3s, BOR4s, BOR5s, BOR6s, and BOR7s, respectively.

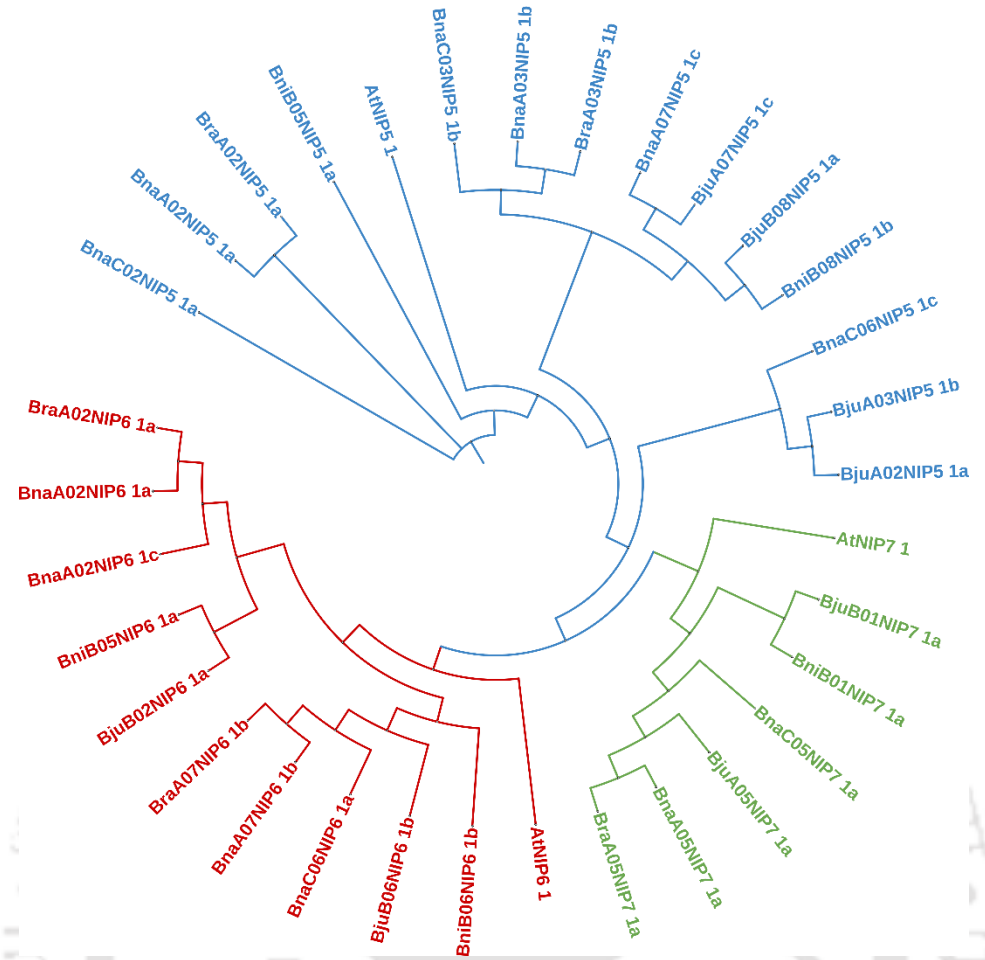

Figure 2.3: Phylogenetic relationship *B. juncea* of NIP5;1, NIP6;1 and NIP7;1 proteins. Phylogenetic tree derived from NIP protein sequences of *A. thaliana*, *B. rapa*, *B. nigra*, *B. juncea*, and *B. napus* using MEGA 7 with Neighbor-Joining (NJ) method, and 1,000 replicates bootstraps, and visualized by iTOL. The names colored with blue, red and green represented NIP5;1s, NIP6;1s and NIP7;1s.

Figure 2.4: Amino acid residues between the BjPIP1 proteins shows highly conserved amino acid residues.

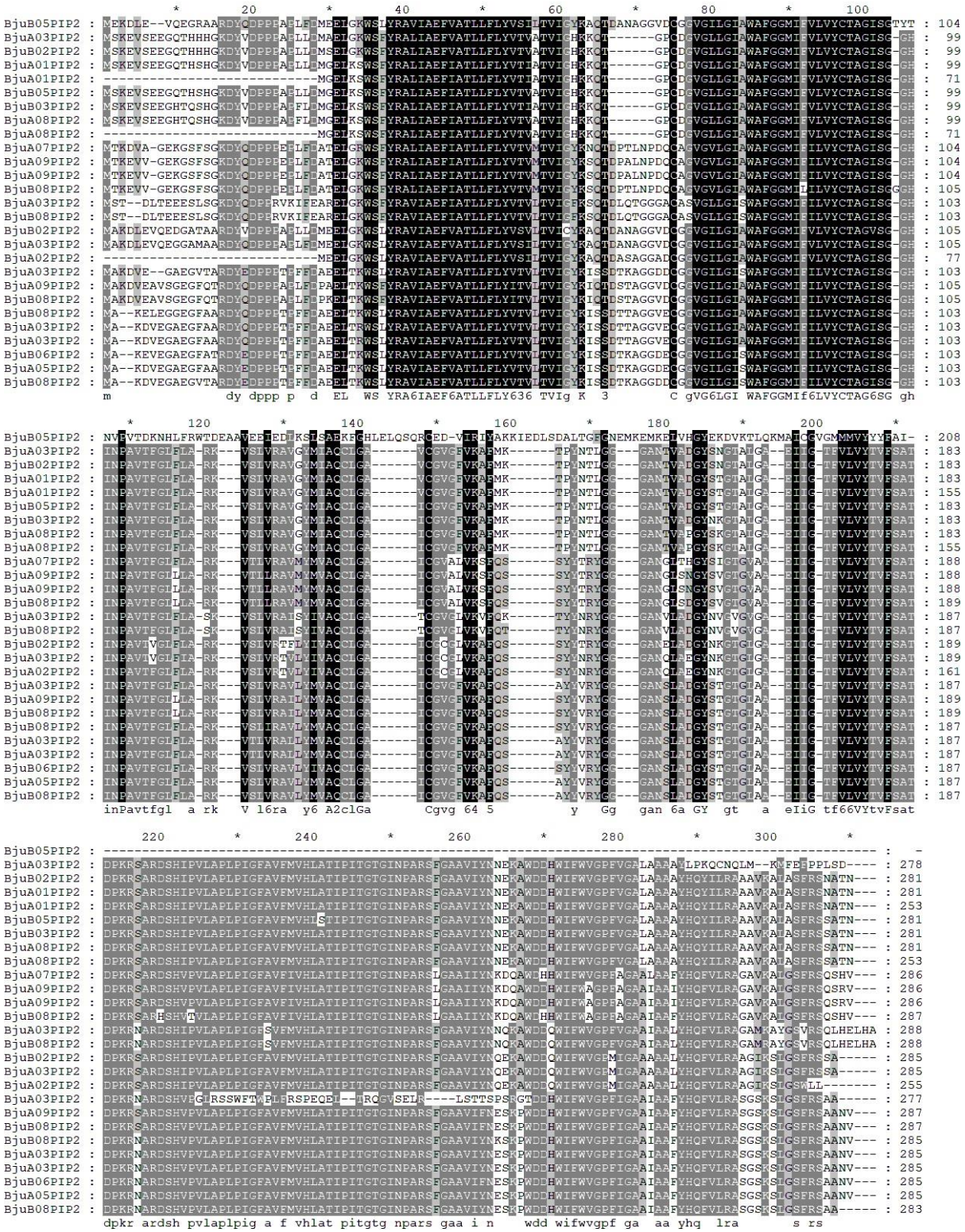

Figure 2.5: Amino acid residues between the BjPIP2 proteins shows highly conserved amino acid residues.

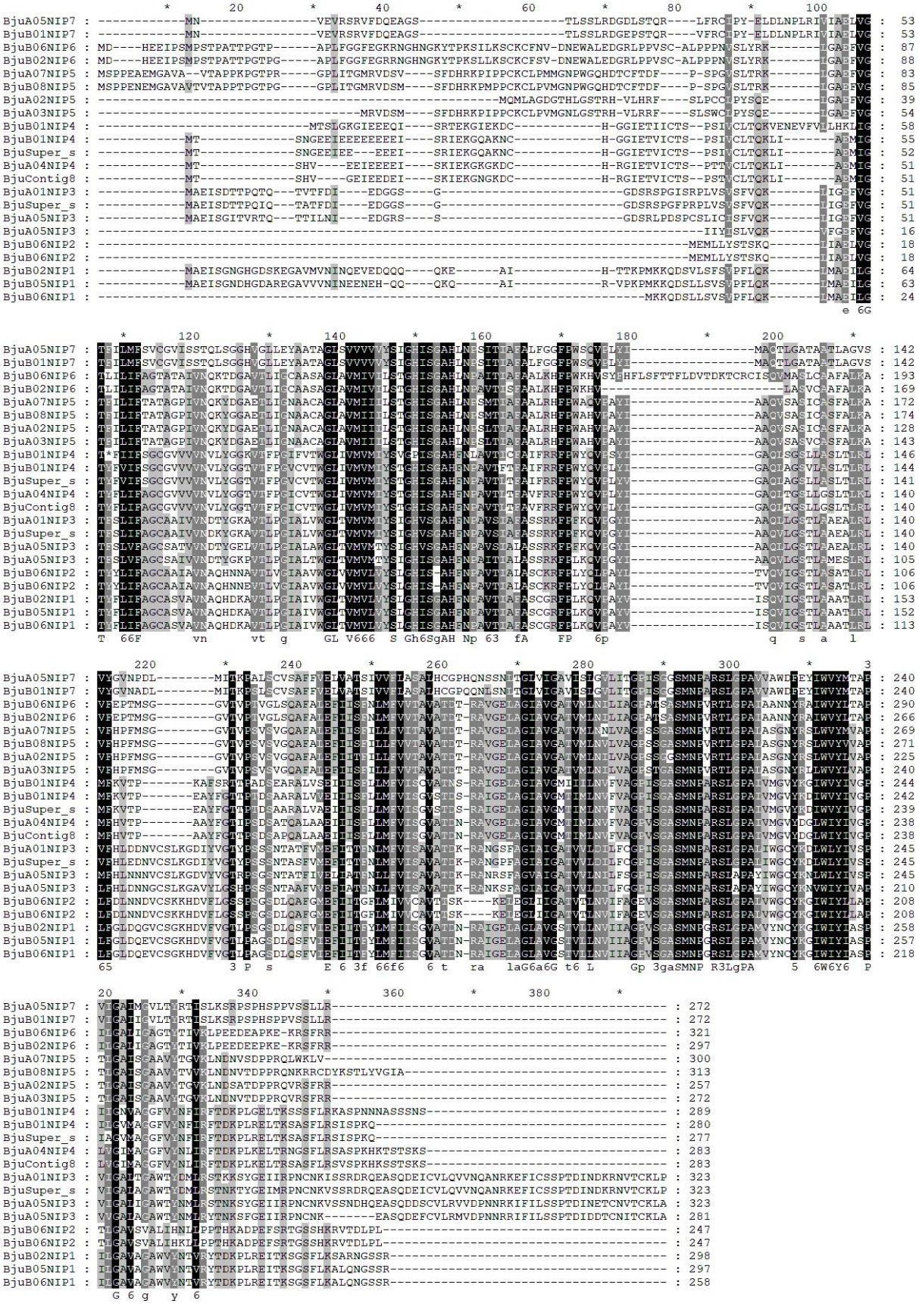

Figure 2.6: Amino acid residues between the BjNIP proteins shows high variation among their amino acid residues.

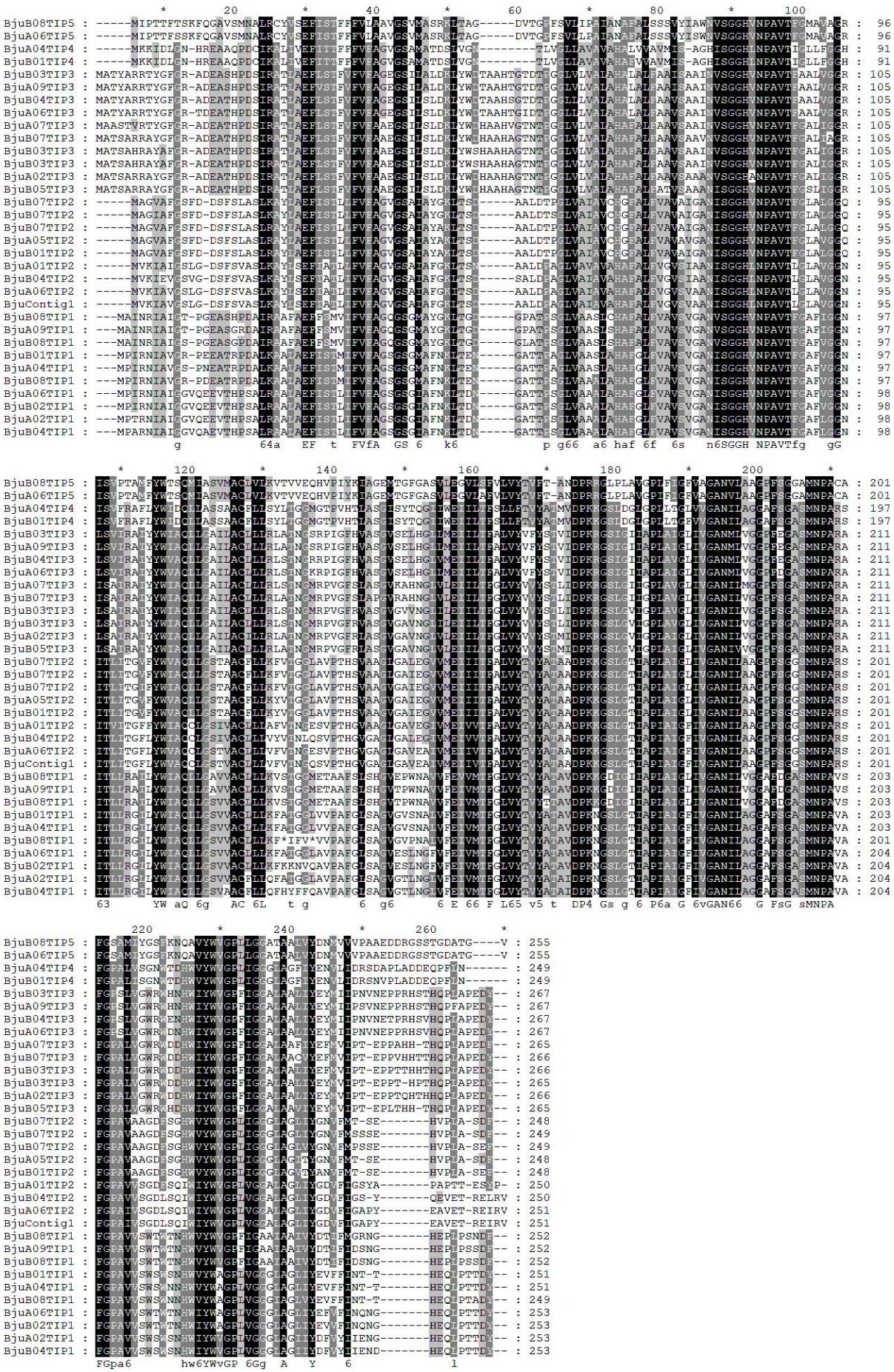

Figure 2.7: Amino acid residues between the BjTIP proteins shows partially conserved amino acid residues.

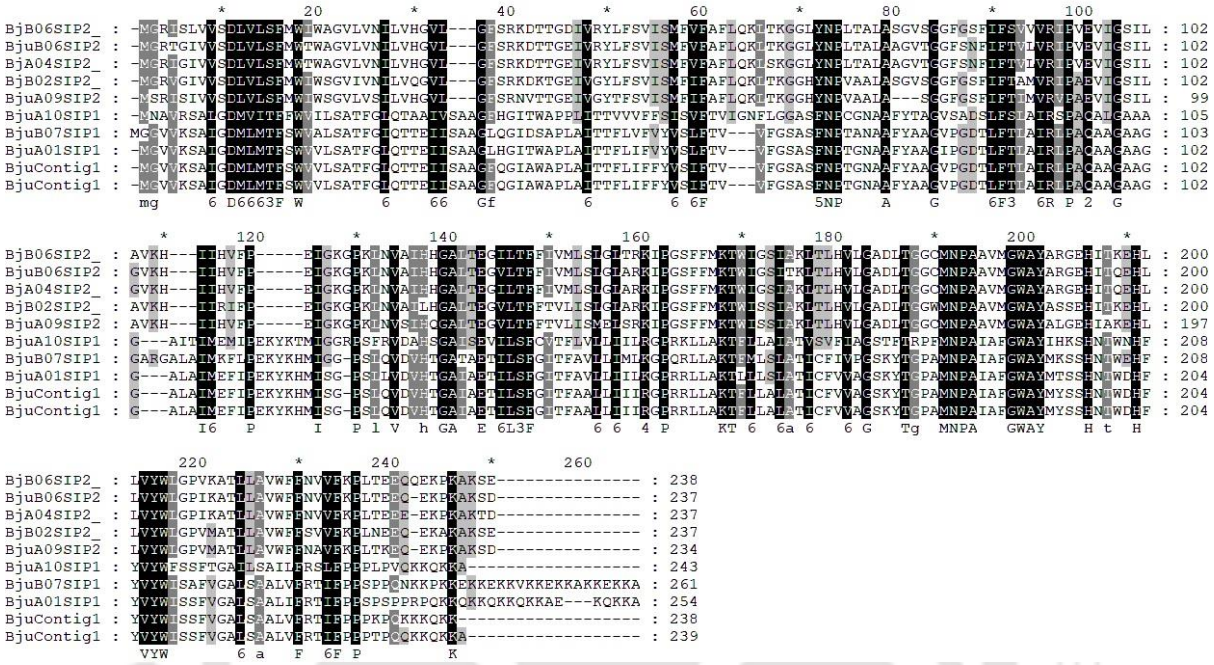

Figure 2.8: Amino acid residues between the BjSIP proteins shows high variation among their amino acid residues.

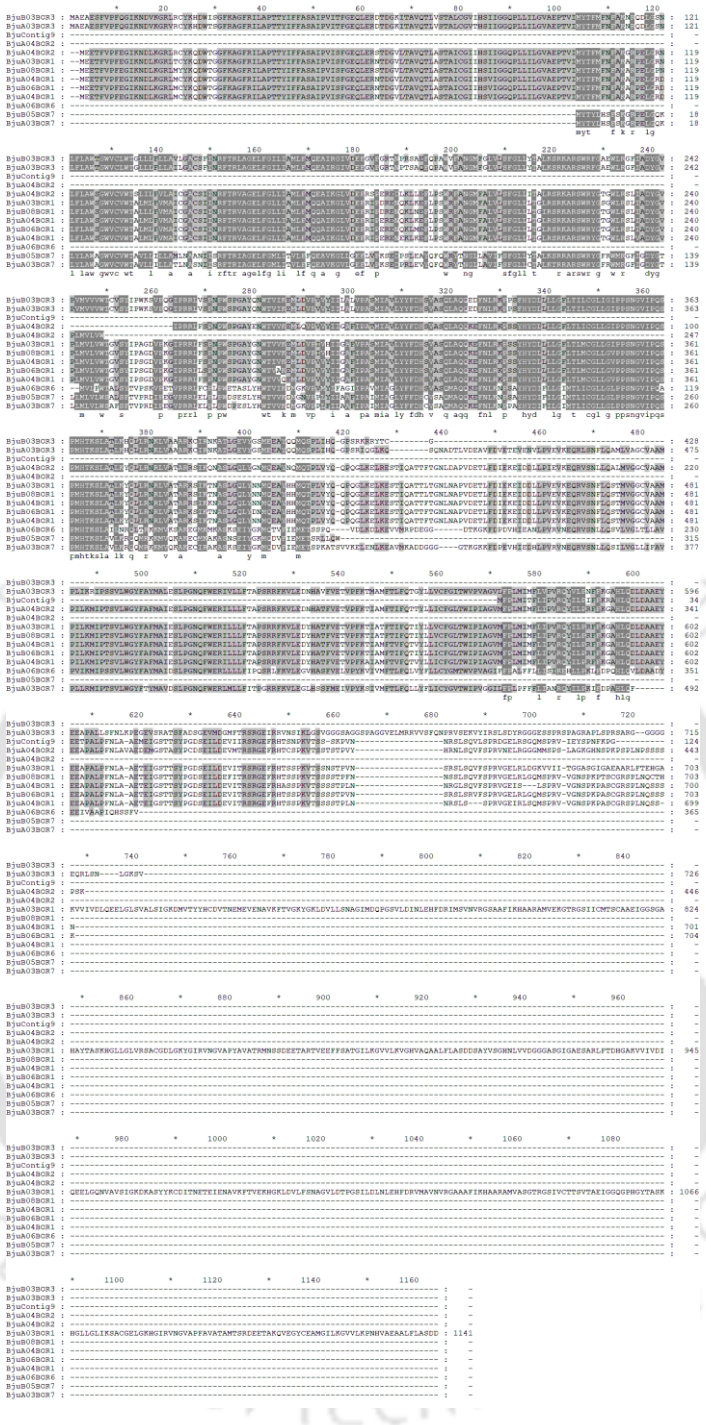

Figure 2.9: Amino acid residues between the BjOR proteins shows conserved amino acid blocks between their subclass proteins.

2.3.2 Structural features of BjAQPs and BjBORs

Gene structure analysis using the Gene Structure Display Server (GSDS) exposed the considerable variation in the number and length of introns and exons in *BjAQPs* and *BjBORs* (Figure 2.10 and 2.11). In *BjPIP*s, the number of exons varied from three (*BjuA09PIP1_3a*, *BjuA10PIP1_3b*, *BjuA03PIP1_5a*, *BjuB02PIP1_5a*, *BjuA01PIP2_8a*, and *BjuA08PIP2_8b*) to 8 (*BjuA09PIP1_1c* and *BjuA02PIP1_1a*), with an overall average of 4 exons (Figure 2.10). Whereas the number of introns varied from 3 (*BjuA09PIP1_3a*, *BjuA10PIP1_3b*, *BjuA03PIP1_5a*, *BjuB02PIP1_5a*, *BjuA01PIP2_8a*, and *BjuA08PIP2_8b*) to 7 (*BjuA09PIP1_1c* and *BjuA02PIP1_1a*) with an overall average of 3 introns. Besides, most of the *BjPIP*s had shorter introns except *BjuA09PIP1_1c* and *BjuA02PIP1_1a*, which comprise the most extended intronic region (3511 and 10115 bp respectively).

The homologous genes belong to the *BjNIP* sub-family comprised greater than or equal to two introns, whereas, *BjNIP4_1s*, *BjuA07NIP5_1c*, *BjuB08NIP5_1a*, *BjNIP6_1s*, *BjNIP7_1s*, *BjuB02NIP1_2a,* and *BjuB05NIP1_2b* each had four, *BjuA02NIP5_1a*, *BjNIP2_1s* consisted three, *BjuA03NIP5_1b*, and *BjuB06NIP1_2c* had two introns (Figure 2.10). Most of the *BjTIP* genes possessed two introns, and interestingly *BjuB08TIP1_3b*, *BjuA09TIP1_3c*, and *BjuB08TIP1_3a* genes lacked any introns. All the *BjSIP* family genes possess 2 introns within their genomic sequence (Figure 2.10).

The *BjBOR* genes had 5-13 introns and 6-14 exons throughout their genomic DNA sequence (Figure 2.11). Among the *BjBOR*s, *BjuA04BOR2a* were predicted to consist of a longest intronic region (2406 bp) (Figure 2.11). Overall, *B. juncea* AQP and BOR genes showed a complex gene structure with varying intron positions and lengths.

Three dimensional structures of the 104 BjAQP and 15 BjBOR proteins were predicted using Phyre2 server (Figure 2.12 and 2.13). All the BjAQPs were predicted to form hourglass like structures and most of the proteins consist 6 transmembrane domains (Figure 2.12). The BjNIP5_1, 6_1 and 7_1 proteins were majorly composed of α-helix (49–60% in each) in their secondary structure, followed by random coils (39-49%). Whereas β-strands were identified as a minor fraction (0–2%) (data not shown). Similarly, BjBOR1 proteins also composed majorly of α-helix (51–59% in each), and random coils (39-41%). A pore runs longitudinally from the extracellular to intracellular opening of the BjAQP and BjBOR proteins were predicted

using PoreWalker software. Also, the pore morphology suggesting that the pore size and constrains that may act as a selectivity barrier (Figure 2.12 and 2.13).

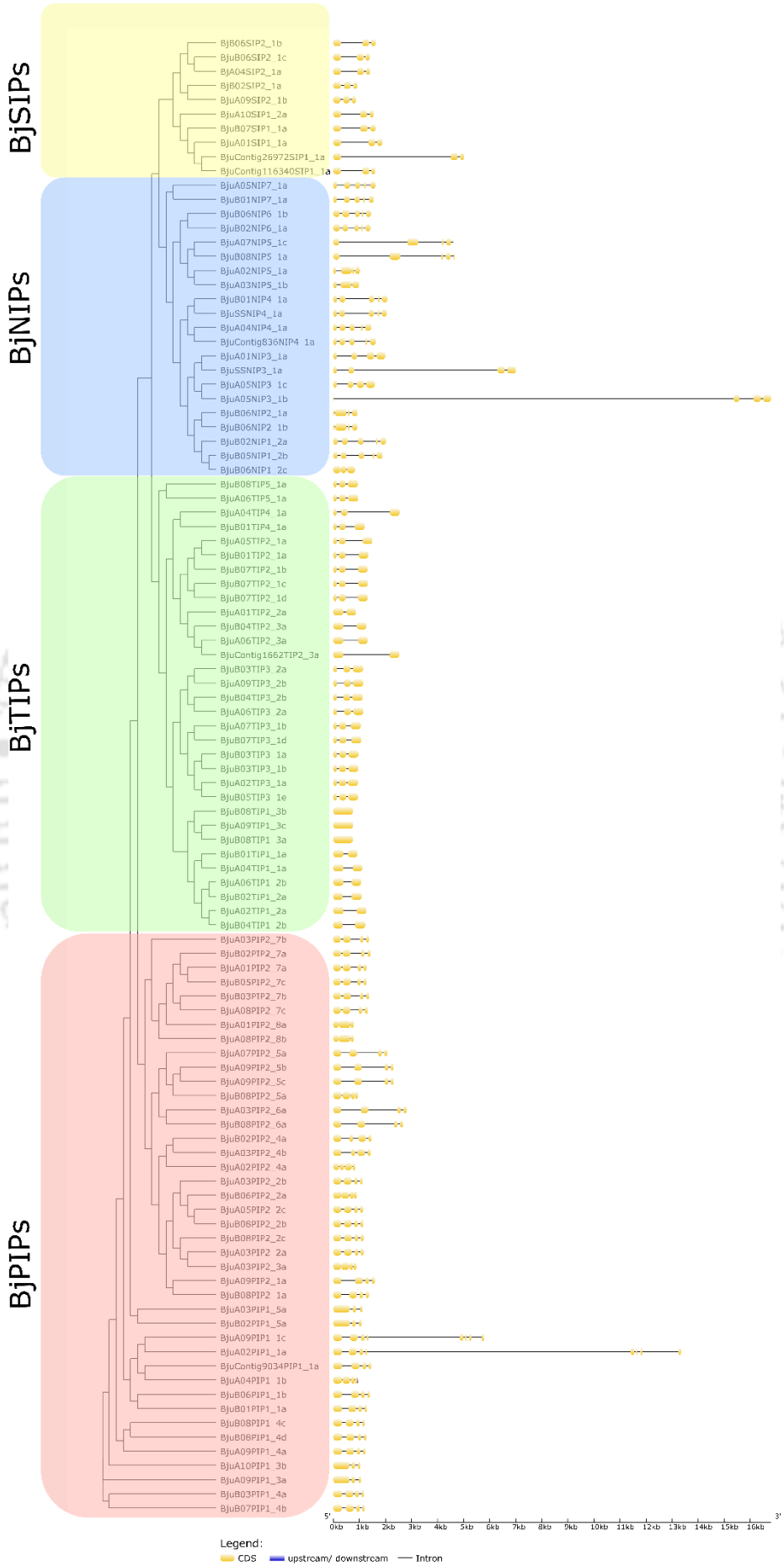

Figure 2.10: Gene structure of BjAQPs. The exon-intron structures of the BjAQPs were determined by the alignments of coding sequences with corresponding genomic sequences, and the diagram was obtained using GSDS (Gene Structure Display Server 2.0) Web server. The purple, yellow, and black line represented the UTR regions, exons and introns, respectively.

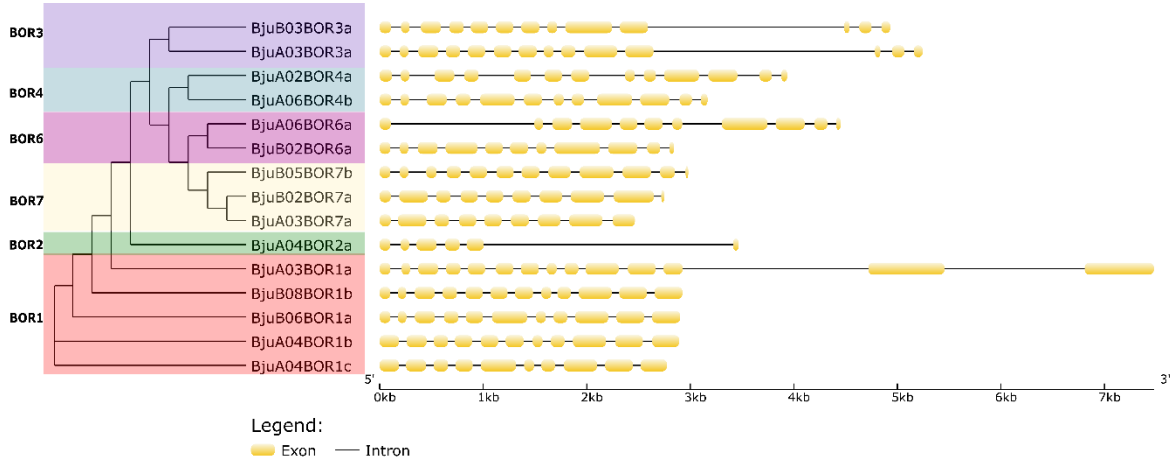

Figure 2.11: Gene structure of BjBORs. The exon-intron structures of the BjBORs were determined by the alignments of coding sequences with corresponding genomic sequences, and the diagram was obtained using GSDS (Gene Structure Display Server 2.0) Web server. The purple, yellow, and black line represented the UTR regions, exons and introns, respectively.

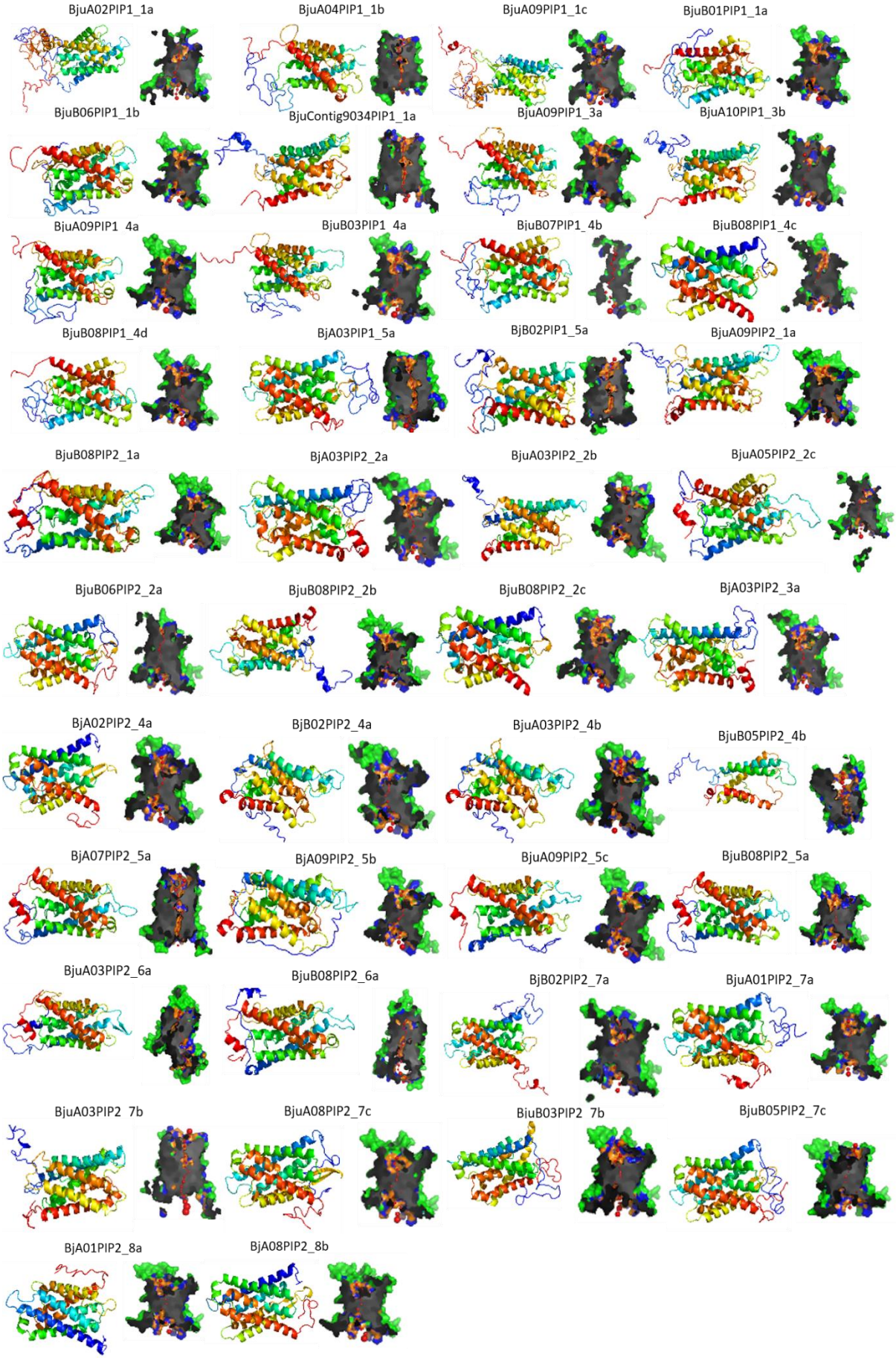

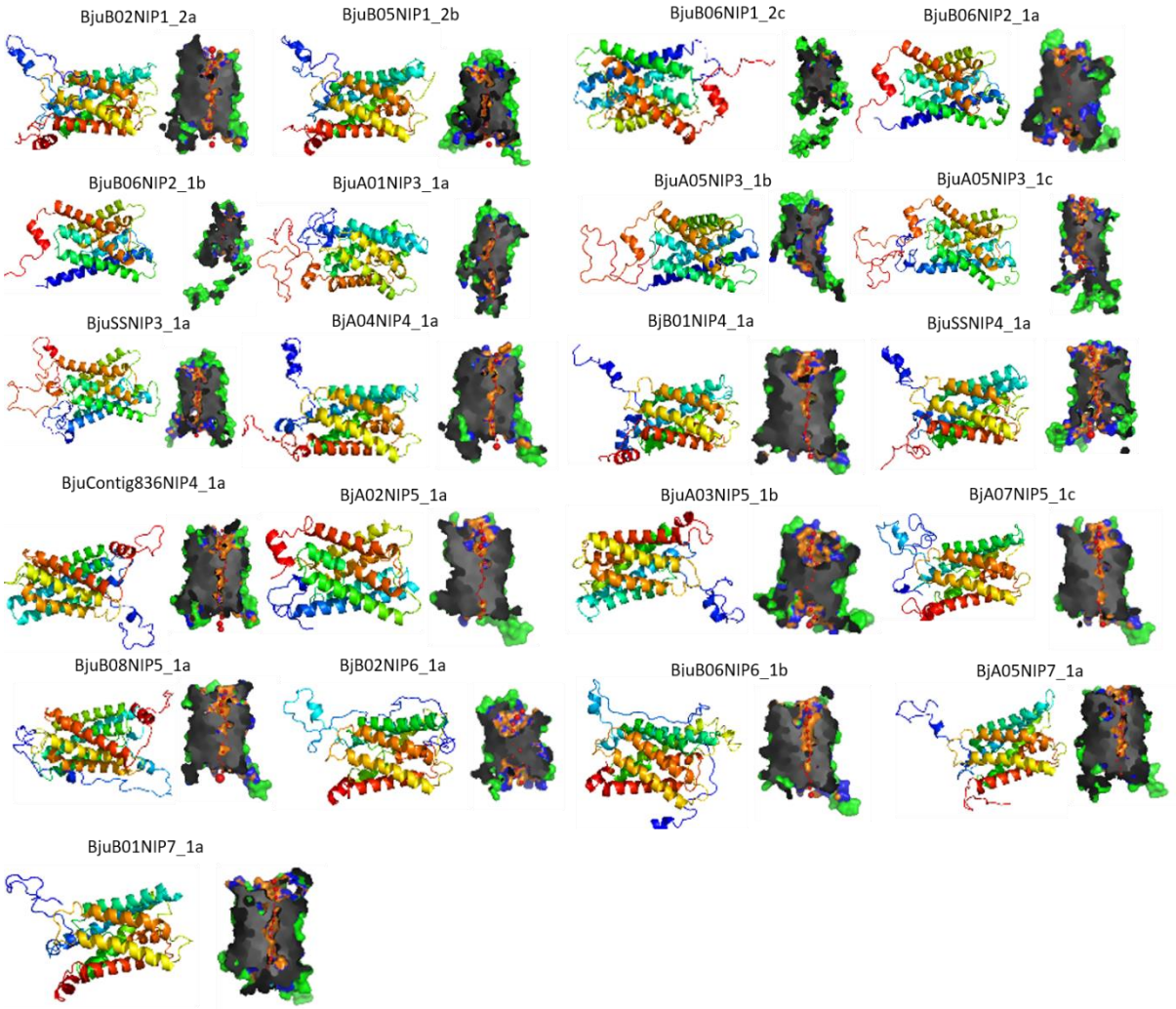


BjA04TIP1_1a
BjB01TIP1_1a
BjA02TIP1_2a
BjA06TIP1_2b
BjB02TIP1_2a
BjB04TIP1_2b
BjA09TIP1_3a
BjB08TIP1_3a
BjB08TIP1_3b
BjA05TIP2_1a
BjB01TIP2_1a
BjB07TIP2_1b
BjB07TIP2_1c
BjB07TIP2_1d
BjA01TIP2_2a
BjA06TIP2_3a
BjB04TIP2_3a
BjContig1662TIP2_3a
BjA02TIP3_1a
BjA07TIP3_1b
BjB03TIP3_1a
BjB03TIP3_1b
BjB05TIP3_1c
BjB07TIP3_1d
BjA06TIP3_2a
BjA09TIP3_2b
BjB03TIP3_2a
BjB04TIP3_2b
BjA04TIP4_1a
BjB01TIP4_1a
BjA06TIP5_1a
BjB08TIP5_1a

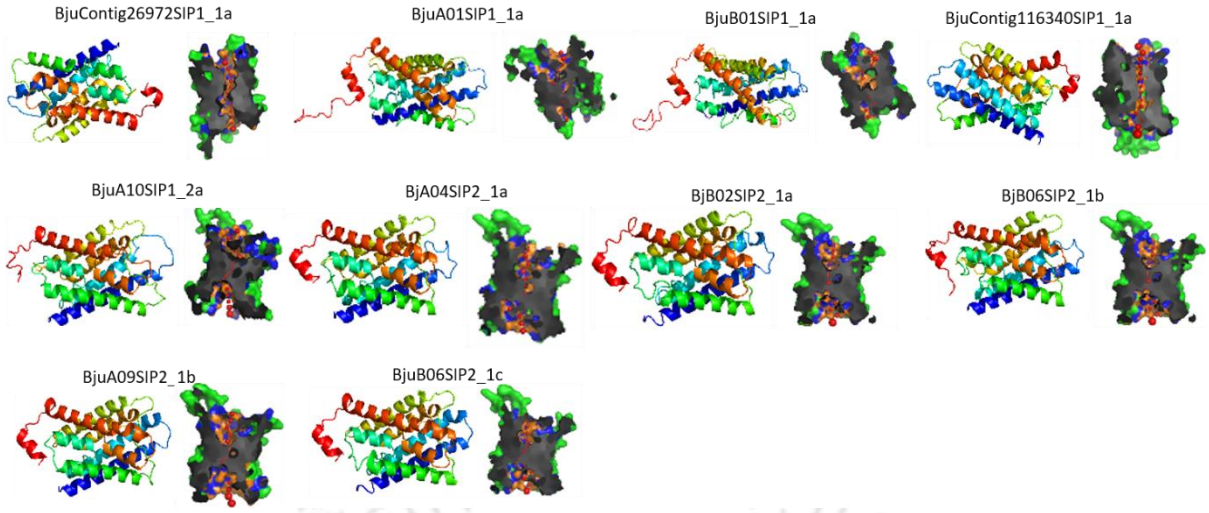

Figure 2.12: Predicted tertiary (3D) proteins structures and pore morphology of 104 BjAQPs.

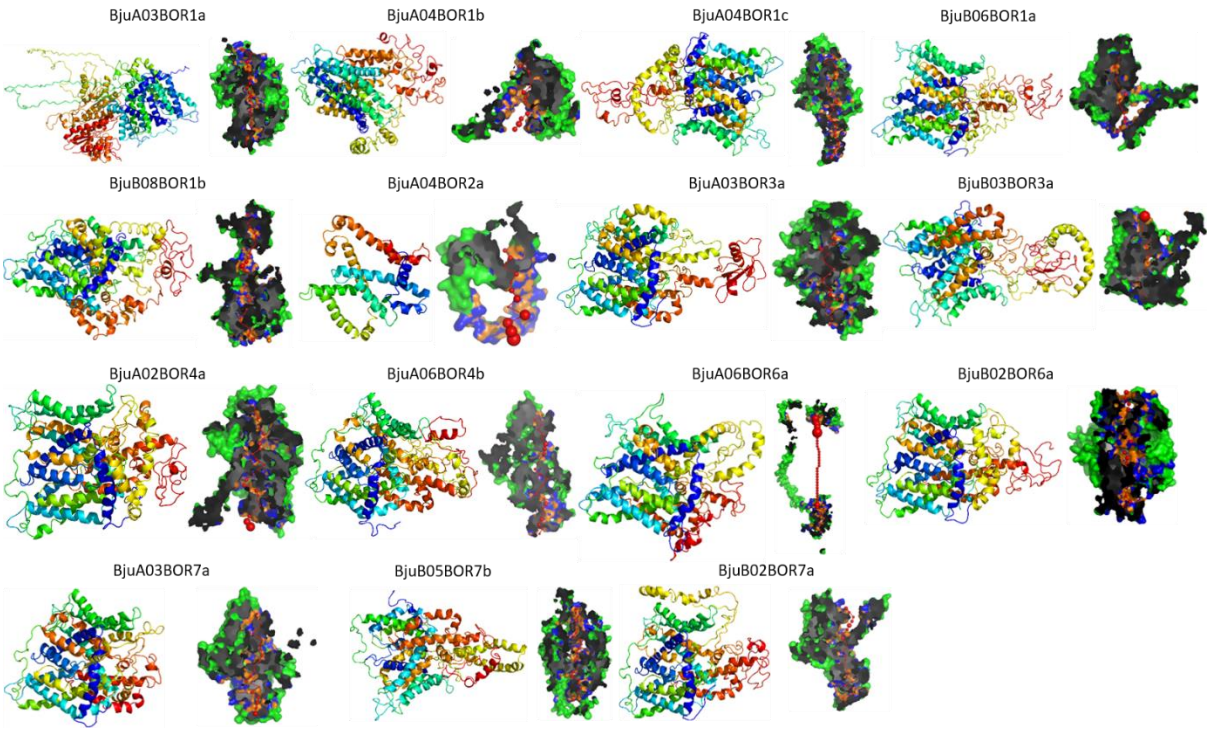

Figure 2.13: Predicted tertiary (3D) proteins structures and pore morphology of 15 BjBORs.

2.3.3 The physicochemical parameters of BjAQPs and BjBORs

The amino acid residues vary from 234 to 395 for BjAQP proteins (Table 2.1). Among the BjAQP proteins, the PIP1;1 proteins BjuA09PIP1_1c and BjuA02PIP1_1a were observed to have the highest MW (42196.43 and 42158.54 Da, respectively) and other BjPIPs comprised of an average molecular weight of 30 KDa, (Table 2.1). Most of the BjNIP proteins, except BjuB06NIP1_2c, BjNIP2_1s, BjuA05NIP3_1b, BjuA02NIP5_1a, BjuA03NIP5_1b, and BjuB06NIP6_1b, possessed relatively longer/shorter amino acid residues to the corresponding *A. thaliana* homologs. Similarly, BjTIPs, BjuA06TIP1_2b, BjuA06TIP1_2c, BjuA02TIP2_3a, and BjuB03TIP3_1c consist of shorter protein length than their *A. thaliana* orthologs. The BjuB07SIP1_1a protein were identified to have 21 longer amino acids than AtSIP1;1. The MW of BjBOR proteins was spanning between 27.6-124 kDa with 247-1141amino acid residues, and BjBOR1 proteins that have relatively higher MW (average MW: 87.49 kDa) (Table 2.2).

The majority of the BjPIP, BjNIP, and BjSIP proteins had higher pI (pI>7), whereas BjuA09PIP1_1c, BjuA02PIP1_1a, BjPIP2_2s (except BjuB08PIP2_2b), BjPIP2_3s, BjuB02PIP2_4a, BjuA01NIP3_1a, BjuSuper_scaffold_128NIP3_1a (here after BjuSSNIP3_1a), BjuB01NIP4_1a, BjuSuper_scaffold_28_1_2326914_1_464645NIP4;1a (hereafter BjuSSNIP4_1a), BjNIP7_1s and BjuB05SIP1_1b sub-family proteins had pI<7 (Table 2.1). In contrast, all BjTIPs identified to have lower pI (pI<7), except BjuB05TIP3_1c. The lowest pI recorded among all the BjTIPs are BjuA06TIP2_3a and BjuB04TIP2_3a (pI=4.98). Unlike BjAQPs, BjBOR most of the proteins have a relatively higher pI range (pI>7) with similar parameters (Table 2.2).

The grand average of hydropathicity (GRAVY) values of most of the BjAQPs were identified to be similar, and most of the proteins that belong to the same sub-family have similar values (Table 2.1). In BjBORs, except BjuA04BOR2b all the remaining proteins have relatively similar GRAVY values (Table 2.2). These differences in GRAVY values can be correlated with the length of N and C-terminal cytosolic amino acids between these proteins. Protein BjuA04BOR2b was consist of shorter N and or C-terminal residues.

The subcellular localization of the BjAQP and BjBOR proteins were predicted using WoLF PSORT tool along with the respective *A. thaliana* homologs. The major fractions, 56.7 and 40.3 percentages, of BjAQP proteins were predicted to be present in plasma and tonoplast membranes, respectively (Table 2.3). While 100% of BjPIPs were predicted to be

localized in the plasma membrane, more than 87.5% and 100% of the BjTIPs and BjSIPs were vacuolar-localized. However, as an exception, two BjTIP proteins were predicted to be localized in the plasma membrane and two in chloroplast. The BjNIP proteins were predicted to be distributed among vacuolar (19%), chloroplast (7%), and plasma membranes (76.1%) (Table 2.3). All the BjBOR proteins were predicted to be located in the plasma membrane suggesting their role in the plasma membrane as reported for homologues in other plant species (Table 2.2). Although the actual localization requires experimental variation, the diverse array of subcellular localization of putative B transporters could reflect need of *B. juncea* plants to control B transport across the membranes for the cell-to-cell transport and compartmentation of B in the cells.

AQP family	At isoform and gene ID	AQP subclass	BjAQP name	Gene ID	Chromosomal location		Gene length (bp)	Protein length (aa)	MW (Da)	pI	GRAVY
					Start	Stop					
PIPs	AtPIP1;1 (At3g61430)	PIP1;1	BjuA09PIP1_1c	BjuA036253	46972955	46978741	5787	395	42196.43	5.6	0.2
			BjuA02PIP1_1a	BjuA007584	15390049	15403391	13343	395	42158.54	5.86	0.238
			BjuB06PIP1_1b	BjuB020023	3271789	3273188	1400	286	30543.60	9.16	0.41
			BjuB01PIP1_1a	BjuB046820	156173	157468	1296	286	30516.57	9.16	0.419
			BjuContig9034PIP1_1a	BjuO009704	60740	62189	1450	286	30627.54	8.86	0.37
			BjuA04PIP1_1b		1860834	1861874	951	286	30614.59	9.01	0.378
	AtPIP1;2 (At2g45960)	PIP1;2	-	-	-	-	-	-	-	-	-
	AtPIP1;3 (At1g01620)	PIP1;3	BjuA09PIP1_3a	BjuA018196	55734982	55736046	1065	286	30554.58	9.03	0.401
			BjuA10PIP1_3b	BjuA038008	3998224	3999263	1040	286	30536.56	9.03	0.395
	AtPIP1;4 (At4g00430)	PIP1;4	BjuB08PIP1_4c	BjuB019317	23838044	23839246	1203	286	30574.62	9.02	0.389
			BjuB08PIP1_4d	BjuB019381	24389051	24390325	1275	286	30532.54	9.02	0.38
			BjuA09PIP1_4a	BjuA031382	307744	308977	1234	286	30560.59	9.02	0.388
			BjuB03PIP1_4a	BjuB030782	23124363	23125538	1176	286	30574.62	9.02	0.385
			BjuB07PIP1_4b	BjuB039281	37012083	37013283	1201	286	30575.61	9.03	0.393
	AtPIP1;5 (At4g23400)	PIP1;5	BjuA03PIP1_5a	BjuA013073	32494528	32495649	1122	287	30614.63	8.99	0.385
			BjuB02PIP1_5a	BjuB044881	63215561	63216640	1080	287	30572.57	9.02	0.396
	AtPIP2;1 (At3g53420)	PIP2;1	BjuA09PIP2_1a	BjuA035536	42774726	42776319	1594	287	30404.19	7.68	0.571
			BjuB08PIP2_1a	BjuB046330	65633417	65634780	1364	287	30475.32	8.3	0.552
	AtPIP2;2 (At2g37170)	PIP2;2	BjuA05PIP2_2b	BjuA018239	4406699	4407839	1141	285	30272.93	6.51	0.518
			BjuA03PIP2_2b	BjuA010365	11249923	11251052	1130	277	29741.00	6.9	0.301
			BjuA03PIP2_2a	BjuA010366	11245096	11246260	1165	285	30268.99	6.95	0.562
			BjuB08PIP2_2a	BjuB016358	20317892	20319041	1150	283	30027.65	6.51	0.515
			BjuB08PIP2_2b	BjuB016359	20323231	20324397	1167	285	30256.03	8.29	0.547
			BjuB06PIP2_2a		4961608	4962808	906	285	30298.95	6.51	0.524
	AtPIP2;3 (At2g37180)	PIP2;3	BjuA03PIP2_3a		11245233	11245953	890	285	30268.99	6.95	0.562
	AtPIP2;4	PIP2;4	BjuB02PIP2_4a	BjuB039047	40479498	40480963	1466	285	30136.96	6.41	0.528

	(At5g60660)		BjuA03PIP2_4b	BjuA009409	5903137	5904564	1428	285	30131.99	7.62	0.507
			BjuA02PIP2_4a		5521487	5522829	847	255	26973.52	8.78	0.66
	AtPIP2;5 (At3g54820)	PIP2;5	BjuA07PIP2_5a	BjuA026543	21147888	21149956	2069	286	30597.47	8.83	0.466
			BjuA09PIP2_5b	BjuA035727	44092414	44094729	2316	286	30418.33	8.82	0.488
			BjuA09PIP2_5c	BjuA035728	44108778	44111093	2316	286	30418.33	8.82	0.488
			BjuB08PIP2_5a		64928576	64930273	942	287	30535.44	8.82	0.484
	AtPIP2;6 (At2g39010)	PIP2;6	BjuA03PIP2_6a	BjuA010446	10511463	10514274	2812	288	30865.76	8.6	0.481
			BjuB08PIP2_6a	BjuB016554	21580944	21583623	2680	288	30866.70	8.3	0.49
	AtPIP2;7 (At4g35100)	PIP2;7	BjuB02PIP2_7a	BjuB038383	65565007	65566433	1427	281	29802.58	8.62	0.459
			BjuA01PIP2_7a	BjuA003036	1748159	1749435	1277	281	29767.57	8.62	0.479
			BjuA03PIP2_7b	BjuA014128	37989656	37991024	1369	278	29650.56	7.07	0.447
			BjuA08PIP2_7c	BjuA043628	15136807	15138132	1326	281	29783.66	8.99	0.481
			BjuB03PIP2_7b	BjuB032090	9172524	9173902	1379	281	29842.68	8.82	0.465
			BjuB05PIP2_7c	BjuB045195	2577820	2579093	1274	281	29756.55	8.62	0.48
	AtPIP2;8 (At2g16850)	PIP2;8	BjuA01PIP2_8a		1748274	1749184	779	253	26721.26	9.32	0.653
			BjuA08PIP2_8b		15136924	15137879	783	253	26703.33	9.51	0.659
TIPs	AtTIP1;1 (At2g36830)	TIP1;1	BjuB01TIP1_1a	BjuB042166	6705696	6706625	930	251	25611.72	6.03	0.813
			BjuA04TIP1_1a	BjuA036493	22031898	22033013	1116	251	25554.63	6.02	0.817
	AtTIP1;2 (At3g26520)	TIP1;2	BjuA02TIP1_2a	BjuA008394	31477407	31478672	1266	253	25792.80	5.32	0.834
			BjuA06TIP1_2b	BjuA024367	25740026	25741100	1075	253	25832.86	5.61	0.816
			BjuB04TIP1_2b	BjuB027347	2842074	2843298	1225	253	26058.07	5.52	0.82
			BjuB02TIP1_2a	BjuB037143	55913207	55914291	1085	253	25983.09	6.17	0.764
	AtTIP1;3 (At4g01470)	TIP1;3	BjuA09TIP1_3c	BjuA031418	1571573	1572328	756	252	25856.93	5.35	0.81
			BjuB08TIP1_3b	BjuB017216	41422472	41423227	756	252	25964.13	5.55	0.787
			BjuB08TIP1_3a	BjuB046056	23303384	23304139	756	252	25831.88	5.1	0.821
	AtTIP2;1 (At3g16240)	TIP2;1	BjuA05TIP2_1b	BjuA020229	23839052	23840545	1494	248	24856.83	5.3	0.967
			BjuB01TIP2_1a	BjuB025600	39985237	39986578	1342	248	24898.91	5.32	0.974
			BjuB07TIP2_1a	BjuB007300	4320025	4321336	1312	249	24992.08	5.32	0.992
			BjuB07TIP2_1b	BjuB008447	23270289	23271615	1327	248	24852.92	5.3	0.99
			BjuB07TIP2_1c	BjuB002374	26932612	26933930	1319	249	24943.99	5.3	0.991
	AtTIP2;2	TIP2;2	BjuA01TIP2_2a	BjuA001118	11628545	11629416	872	250	24993.13	5.1	1.027

	(At4g17340)										
	AtTIP2;3 (At5g47450)	TIP2;3	BjuA06TIP2_3b	BjuA024869	28658153	28659476	1324	251	25205.47	4.98	1.038
			BjuB04TIP2_3a	BjuB027540	4009909	4011181	1273	250	25324.59	4.98	0.992
			BjuContig1662TIP2_3a	BjuO002426	610557	613088	2532	251	25204.48	5.17	1.035
	AtTIP3;1 (At1g73190)	TIP3;1	BjuB03TIP3_1a	BjuB030971	24809855	24810820	966	266	28016.57	6.79	0.658
			BjuB03TIP3_1b	BjuB047355	25170387	25171348	962	265	27849.36	6.74	0.643
			BjuA02TIP3_1a	BjuA007501	13880606	13881551	946	266	27996.47	6.75	0.583
			BjuA07TIP3_1b	BjuA043443	31780595	31781645	1051	265	27981.54	6.54	0.648
			BjuB05TIP3_1d	BjuB025964	58996378	58997334	957	265	27966.49	7.17	0.609
			BjuB07TIP3_1e	BjuB039898	15851421	15852496	1076	266	28057.60	6.79	0.623
	AtTIP3;2 (At1g17810)	TIP3;2	BjuB03TIP3_2a	BjuB032374	15178083	15179222	1140	267	28498.09	6.54	0.572
			BjuA09TIP3_2b	BjuA044283	50705530	50706681	1152	267	28491.06	6.54	0.579
			BjuB04TIP3_2b	BjuB029231	19663140	19664263	1124	267	28551.11	6.49	0.555
			BjuA06TIP3_2a	BjuA022164	6595044	6596200	1157	267	28575.22	6.49	0.564
	AtTIP4;1 (At2g25810)	TIP4;1	BjuA04TIP4_1a	BjuA016231	16816124	16818670	2547	249	26057.27	5.3	0.713
			BjuB01TIP4_1a	BjuB024204	16167170	16168371	1202	249	26166.40	5.5	0.716
	AtTIP5;1 (At3g04090)	TIP5;1	BjuB08TIP5_1a	BjuB019654	54342659	54343600	942	255	26358.67	6.71	0.749
			BjuA06TIP5_1a	BjuA022538	12208202	12209152	951	255	26344.64	6.71	0.748
NIPs	AtNIP1;1 (At4g19030)	-	-	-	-	-	-	-	-	-	-
	AtNIP1;2 (At4g18910)	NIP1;2	BjuB05NIP1_2b	BjuB013594	13507669	13509551	1883	297	31599.75	8.3	0.427
			BjuB06NIP1_2c		30579259	30580787	827	258	27308.07	9.05	0.652
			BjuB02NIP1_2a	BjuB044656	58287198	58289222	2025	298	31619.71	8.61	0.405
	AtNIP2;1 (At2g34390)	NIP2;1	BjuB06NIP2_1a		6176635	6177749	931	247	26280.89	7.68	0.658
			BjuB06NIP2_1b		6231959	6233100	931	247	26353.00	7.68	0.635
	AtNIP3;1 (At1g31885)	NIP3;1	BjuA01NIP3_1a	BjuA005276	20141918	20143910	1993	323	34597.85	6.81	0.292
			BjuSSNIP3_1a	BjuO010478	867264	874272	7009	323	34622.92	6.81	0.282
			BjuA05NIP3_1c	BjuA042762	19272478	19274069	1592	323	34532.83	8.35	0.346
			BjuA05NIP3_1b	BjuA046003	18862186	18878988	16803	281	30180.18	8.81	0.501
	AtNIP4;1 (At5g37810)	NIP4;1	BjuA04NIP4_1a	BjuA015604	7763248	7764705	1458	283	30269.62	8.24	0.58
			BjuB01NIP4_1b	BjuB025802	26973500	26975574	2075	280	30208.44	5.68	0.601

			BjuSSNIP4_1a	BjuO012266	239457	241514	2058	277	29716.94	6.82	0.631
			BjuContig836NIP4_1a	BjuO009541	10401	12036	1636	283	30168.43	8.26	0.593
	AtNIP4;2 (At5g37820)	-	-	-	-	-	-	-	-	-	-
	AtNIP5;1 (At4g10380)	NIP5;1	BjuA02NIP5_1a		20979595	21003720	1021	257	26684.08	8.78	0.661
			BjuA03NIP5_1b		15518069	15523442	990	272	28656.56	9.43	0.61
			BjuA07NIP5_1c	BjuA026523	20998290	21002914	4625	300	31149.39	8.63	0.504
			BjuB08NIP5_1a	BjuB041404	33496653	33501314	4662	313	32459.84	8.76	0.49
	AtNIP6;1 (At1g80760)	NIP6;1	BjuB06NIP6_1b	BjuB046722	32908083	32909527	1445	321	33886.52	8.44	0.404
			BjuB02NIP6_1a	BjuB037862	62584744	62586165	1422	297	31031.14	8.26	0.393
	AtNIP7;1 (At3g06100)	NIP7;1	BjuA05NIP7_1a	BjuA020902	30529118	30530733	1616	272	28595.39	6.57	0.704
			BjuB01NIP7_1a	BjuB042357	44485659	44487212	1554	272	28568.35	6.5	0.714
SIPs	AtSIP1;1 (At3g04090)	SIP1;1	BjuContig26972SIP1_1a	BjuO000969	15127	20141	5015	238	25539.10	9.68	0.676
			BjuContig116340SIP1_1a	BjuO000972	3884	5494	1611	239	25583.06	9.52	0.695
			BjuB07SIP1_1c	BjuB004470	881548	883169	1622	261	27909.01	9.92	0.359
			BjuA01SIP1_1a	BjuA006310	39226169	39228054	1886	254	27250.22	9.93	0.513
	AtSIP1;2 (At5g18290)	SIP1;2	BjuA10SIP1_2a	BjuA039033	13931671	13933220	1550	243	26184.91	10.13	0.746
	AtSIP2;1 (At3g56950)	SIP2;1	BjB06SIP2_1b	BjuB022404	24999741	25001362	1622	238	26012.04	9.68	0.675
			BjuB06SIP2_1c	BjuB028908	30259551	30260944	1394	237	25898.83	9.61	0.643
			BjA04SIP2_1a	BjuA014669	2383497	2384910	1414	237	25895.87	9.49	0.676
			BjB02SIP2_1a	BjuB038410	65722013	65722941	929	237	25744.66	9.66	0.705
			BjuA09SIP2_1b	BjuA035835	45391203	45392074	872	234	25500.36	9.49	0.698

Table 2.1: List of 104 BjAQPs and their protein physicochemical parameters, and functional domains.

Subclass	At isoform and gene ID	Name	Gene ID	Chromosome	Start	Stop	Gene length (bp)	Protein length (aa)	MW (Da)	pI	GRAVY	TMD no.	Sub-cellular localization	Domain family (pfam)	No.of domains
BOR1	AtBOR1 (AT2G47160)	BjuB06BOR1a	BjuB046520	B06	11600410	11603312	2903	704	78591.86	8.85	0.196	11	Plas	HCO_3^- transporter family	2
		BjuB08BOR1b	BjuB017046	B08	32113067	32115990	2924	703	78520.60	8.68	0.197	11	Plas	HCO_3^- transporter family	2
		BjuA03BOR1a	BjuA010783	A03	13819875	13827351	7477	1141	124107.63	6.62	0.196	11	Plas	HCO_3^- transporter family	2
		BjuA04BOR1b	BjuA017612	A04	25497425	25500317	2893	701	78244.37	8.85	0.195	9	Plas	HCO_3^- transporter family	2
		BjuA04BOR1c	BjuA017613	A04	25507480	25510253	2774	699	78032.09	8.67	0.193	11	Plas	HCO_3^- transporter family	2
BOR2	AtBOR2 (AT3G62270)	BjuA04BOR2a	BjuA014451	A04	1555253	1558720	3468	247	27669.74	9.06	0.526	6	Plas	Xan_ur_permease super family	1
BOR3	AtBOR3 (AT3G06450)	BjuB03BOR3a	BjuB031929	B03	13531139	13536069	4931	703	78914.41	8.4	0.273	8	Plas	HCO_3^- transporter family	2
		BjuA03BOR3a	BjuA011823	A03	19073409	19078652	5244	703	78832.32	8.4	0.275	8	Plas	HCO_3^- transporter family	2
BOR4	AtBOR4 (AT1G15460)	BjuA06BOR4b	BjuA022000	A06	5603484	5606650	3167	684	77037.08	8.48	0.093	10	Plas	Xan_ur_permease super family	2
		BjuA02BOR4a	BjuA005569	A02	14304902	14308837	3936	683	76409.21	7.21	0.16	11	Plas	Xan_ur_permease super family	2
BOR5	AtBOR5 (AT1G74810)	-	-	-	-	-	-	-	-	-	-	-	-	-	-
BOR6	AtBOR6 (At5g25430)	BjuA06BOR6a	BjuA023718	A06	22037754	22042205	4452	673	75815.87	6.67	0.271	11	Plas	Xan_ur_permease super family	2
		BjuB02BOR6a	BjuB038006	B02	61728501	61731343	2843	672	75694.77	6.64	0.281	11	Plas	Xan_ur_permease super family	2
BOR7	AtBOR7 (At4g32510)	BjuB02BOR7a	BjuB038275	B02	64949233	64951981	2749	661	74694.77	8.25	0.235	10	Plas	Xan_ur_permease super family	2
		BjuA03BOR7a	BjuA014013	A03	36391995	36394460	2466	594	67238.65	9.26	0.326	10	Plas	Xan_ur_permease super family	2
		BjuB05BOR7b	BjuB045361	B05	4508855	4511835	2981	639	72232.56	8.05	0.195	9	Plas	Xan_ur_permease super family	2

Table 2.2: List of 15 BjBORs and their protein physicochemical parameters, functional domains, and putative sub-cellular localization.

2.3.4 Analysis of conserved motifs of BjAQPs and BjBORs

In total, twenty consensus motifs were identified using MEME motif search tool in both BjAQP and BjBOR proteins as conserved (Figures 2.14 and 2.15). We have observed BjPIP1 and BjPIP2 proteins contains Motif 12 (MEGKEEDVRVGANKFPERQPI), and Motif 14 (HQFVLRAAAVKALGSFRSAAN), respectively, which was unique to the BjPIP sub-groups. Two NPA motifs of all BjAQPs were included in Motif 1 (HLATGPITGASMNPARSFGPA) and Motif 5 (FVLVYCTAGISGGHINPAVTF) and present in all BjAQPs (Supplementary figures 9). The BjNIP and BjSIP proteins were shown high variation in their motif composition among their subfamily. The Motifs 1 (HLATGPITGASMNPARSFGPA), 4 (WDDHWIYWVGPFIGAALAALY), 5 (VYCTAGISGGHINPAVTFGLF), 10 (PDSJRALJAEFISTFIFVFAGC), 11 (AFGKLTHBGALTPGGLVAVALAHAFALFV), and 15 (AVVVVNQKYGGAVTLPGIAATWGLTVMVM) were conserved among all the BjNIP proteins. Besides, the presence of multiple unique motifs in BjNIPs, suggesting the diverse proteins in this sub-family (Supplementary figures 9). BjBOR proteins revealed a total of 5-18 conserved motifs among the fifteen homologs (Supplementary figures 10). All the eighteen motifs were well conserved among BjBOR1s except Motif 18 (QMSPRVVGNSPKPASCGRSPLNQSS). The Motif 18 was absent in BjuA03BOR1a. We have observed all the conserved motifs were present within the bicarbonate (HCO_3^-) (BjBOR1s, and BjBOR3s) and Xan_ur_permease superfamily (BjBOR2s, BjBOR4s, BjBOR6, and BjBOR7s) domains of the BjBOR proteinss (Figures 2.15).

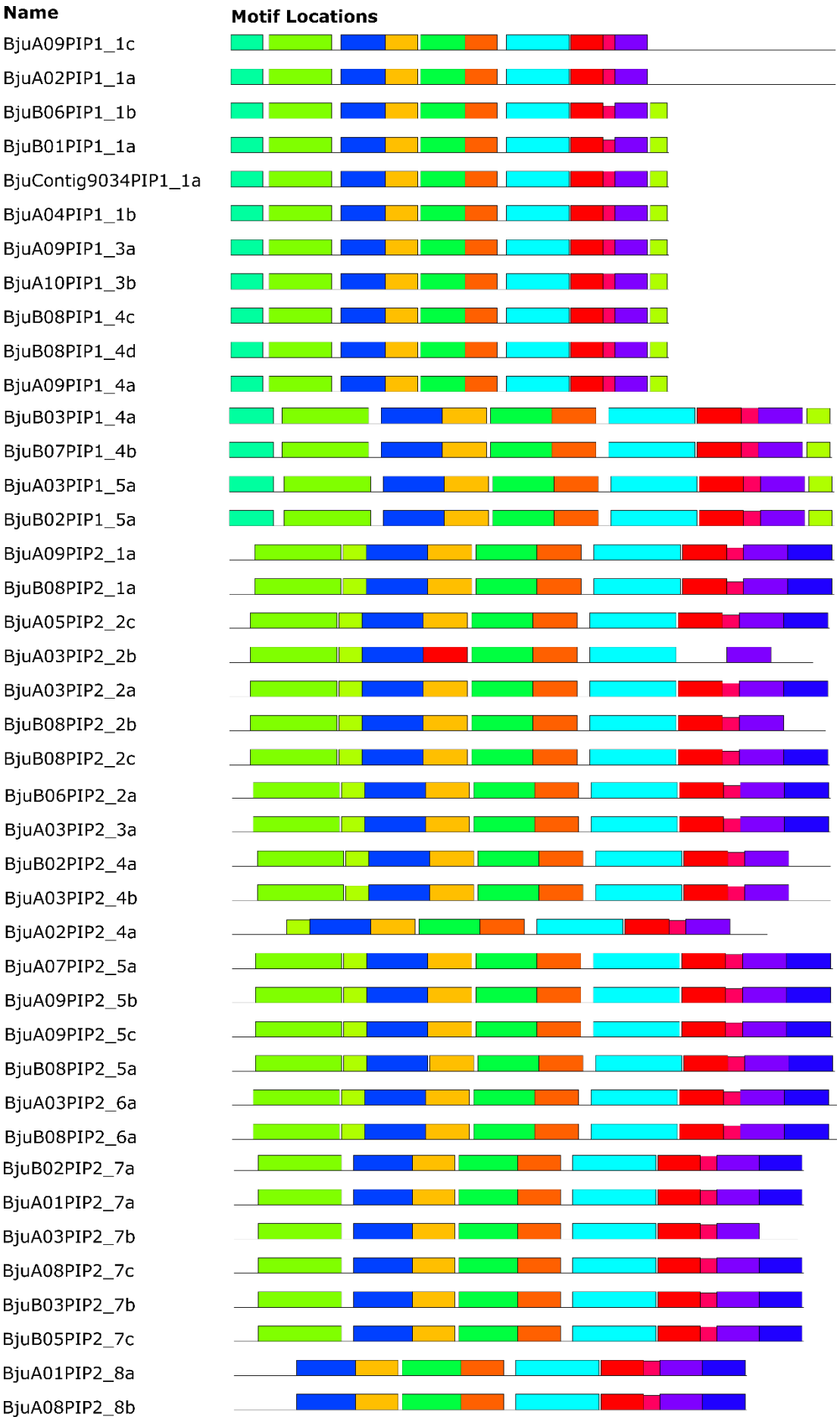

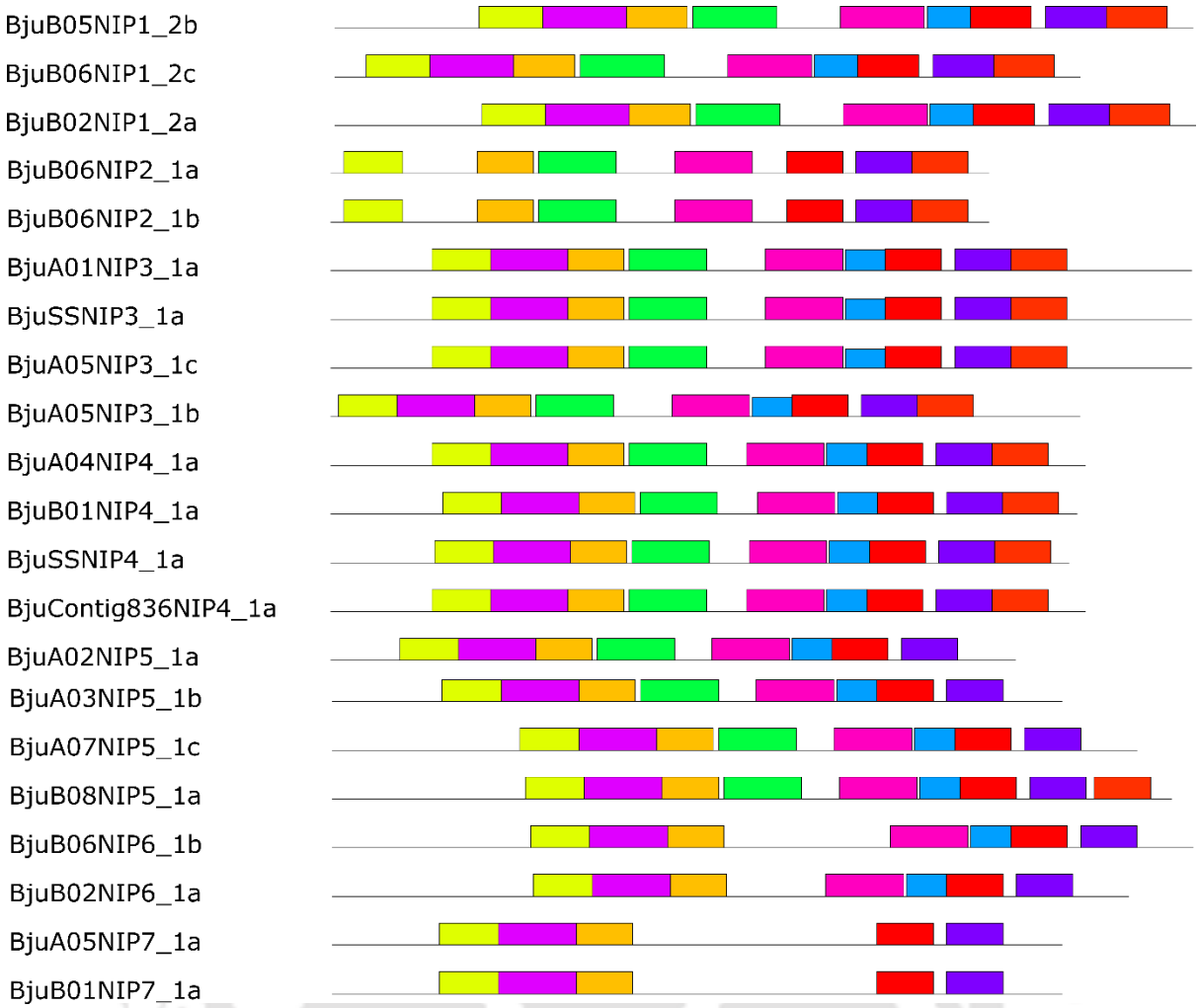

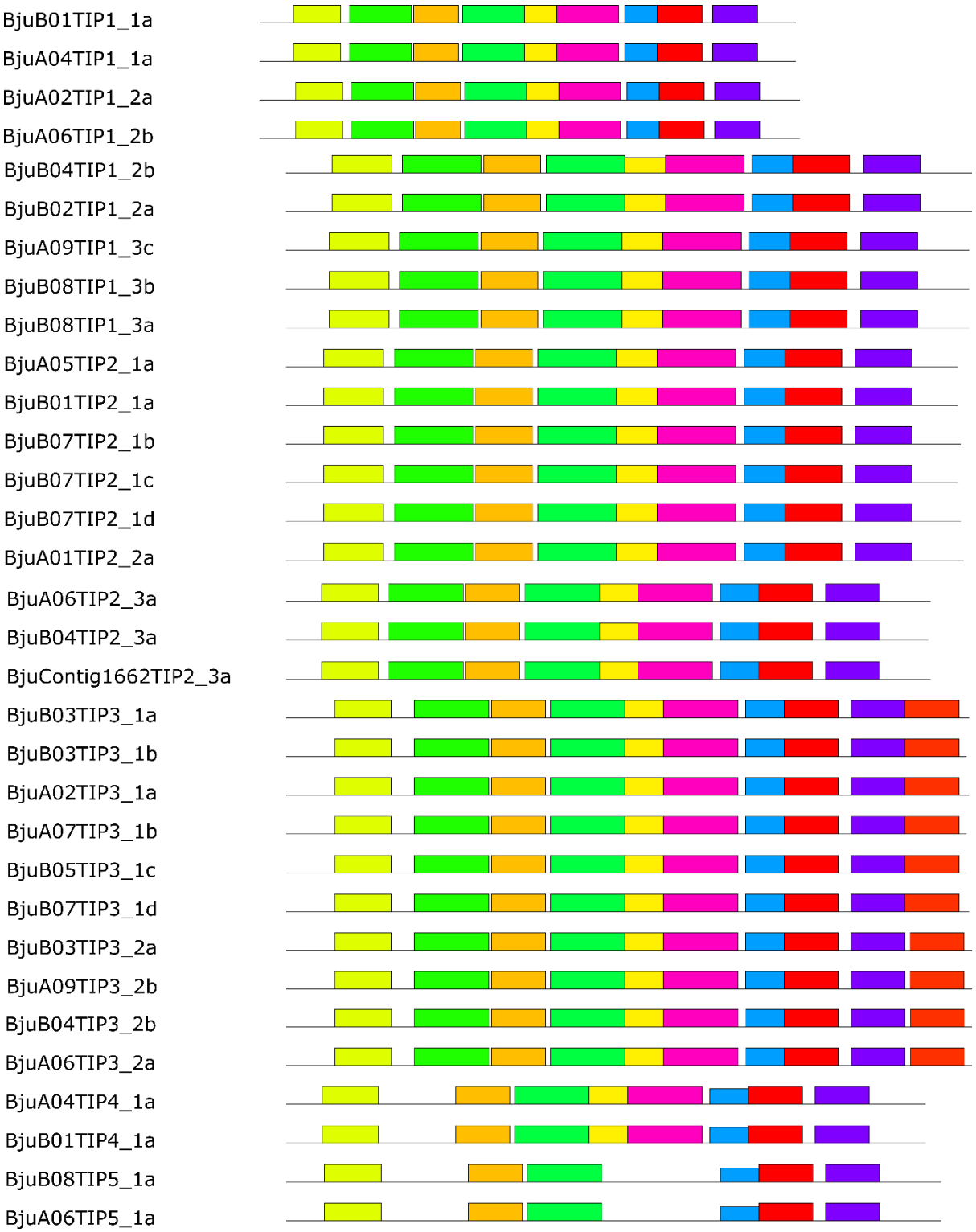

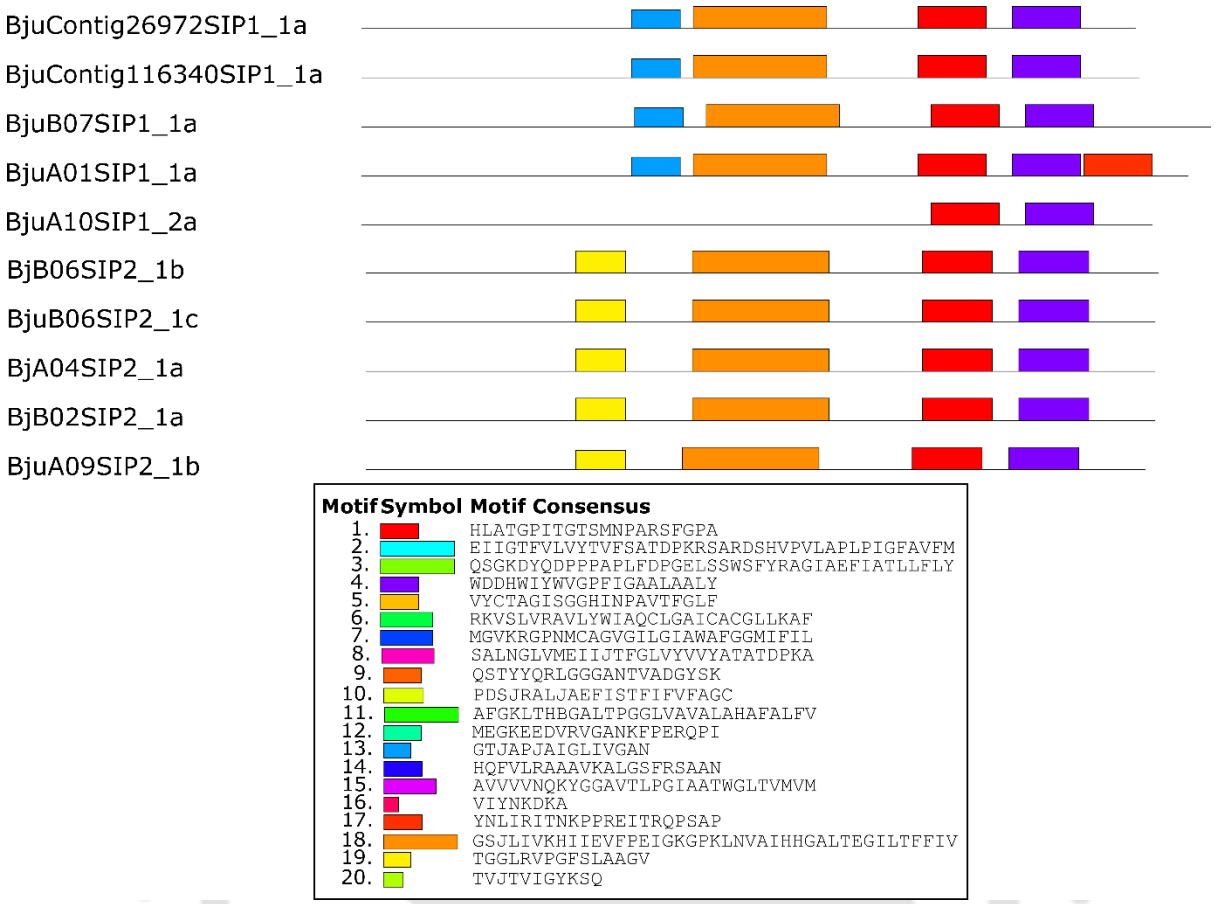

Figure 2.14: Distribution of conserved motifs in BjAQPs. Conserved motifs of BjAQPs were analysed by MEME Web server using the protein sequences of 104 BjAQPs. Maximum twenty conserved motifs were identified, and different motifs were distinguished by different colors.

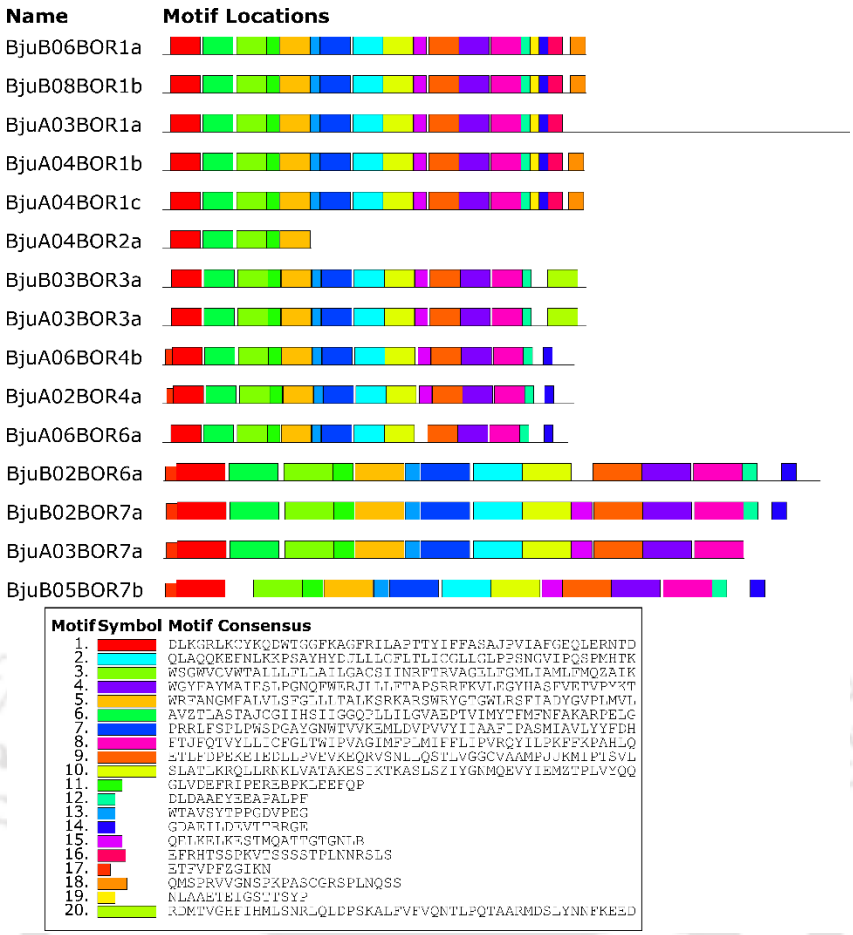

Figure 2.15: Distribution of conserved motifs in BjBORs. Conserved motifs of BjBORs were analysed by MEME Web server using the protein sequences of 15 BjBORs. Maximum twenty conserved motifs were identified, and different motifs were distinguished by different colors.

2.3.5 Signature motifs in BjAQPs

All the BjPIPs (except BjuA03PIP2_2b), BjTIPs, BjNIP2_1s, BjNIP3_1s and BjNIP4_1s displayed dual conserved NPA motifs (NPA/NPA) whereas BjNIP1_2s, BjNIP6_1s, and BjSIPs were identified to contain a single NPA motif (Table 2.3). The NPA motifs of BjNIPs showed extreme variation within their sub-groups (Table 2.3). While the BjNIP5s sub-family proteins have shown a substitution of alanine (A) to serine (S) in the first NPA motif (BjuA02NIP5_1a, BjuA03NIP5_1b, BjuA07NIP5_1c, and BjuB08NIP5_1a), the BjNIP1_2, BjNIP5_1, and BjNIP6_1 proteins showed variation in an alanine (A) to glycine (G) or valine (V) substitution in the second NPA motif. In addition, the dual NPA domains present in BjNIP5_1s are highly conserved to their orthologs in *A. thaliana*, *B. rapa*, and *B. napus* (Figure 2.16). While the second NPA motif was conserved, the first NPA motif in BjSIPs was highly

variable. The first NPA motif was present in two patterns in BjSIP2s (NPL and NPV) and BjSIP1s (NPT and NPC). Furthermore, in the BjSIP1_1a proteins alanine was substituted with threonine (NPT) (Table 2.3).

The amino acid residues in the ar/R positions selectivity filters (SF) are well-conserved among BjPIPs (F/H/T/R), except BjuA03PIP2_2b, than any other BjAQPs; however, these positions showed significant variation in other BjAQP sub-family proteins (Table 2.3). Most of the BjNIP proteins possessed conserved SF residues within their sub-groups. However, except BjNIP5_1s all the remaining NIP proteins showed no variation in SF residues compared to its *A. thaliana* homologs. Among the NIP5;1s, the replacement of non-polar isoleucine (I) with polar asparagine (N) (BjuA07NIP5_1c) and valine (V) (BjuB08NIP5_1a) may be of particular interest as BjNIP5_1 family proteins are strongly correlated to B transport in plants (Table 2.3). The change in H5 SF residue in BjuA07NIP5_1c was also identified to be conserved in *B. napus* homologs, BnaA07NIP5;1c and BnaC06NIP5;1c. The substitution of serine at this position is unique to *B. juncea* since this is position is occupied with glycine in *A. thaliana* and *B. napus*. The reduced pore size due to the replacement of serine at this position may exerts novel transport property to the BjNIP5_1s. In the BjTIP sub-family, the SF is formed by histidine/asparagine in H2; isoleucine/methionine/valine (I/M/V) in H5, alanine/glycine (A/G) in LE1, and valine/arginine/cysteine (V/R/C) in LE2. The BjTIP3_2 sub-family proteins replaced a non-polar methionine (H5) with another non-polar residue isoleucine in AtTIP3;2 (Table 2.3). Unlike the BjSIP1s, BjSIP2s substituted serine/glycine/alanine (S/G/A) in the H2/LE1/LE2 positions (Table 2.3). The H5 position in BjSIP1s was showed high variation between valine/isoleucine/phenylalanine (V/I/F), whereas BjSIP2s contains histidine (H) at this position. In the proteins BjuA03PIP2_2b the proline and glutamine is present in H5 and LE1 positions, respectively (Table 2.3).

The Froger's positions consist of five conserved amino acid residues, P1-P5, which can be used to differentiate between AQPs and GIP-type AQPs (GlpF-like intrinsic proteins) (Froger et al., 1998). More than 78% of BjPIP members exhibited identical amino acids in the Froger's positions (Glutamine/Serine/Alanine/Phenylalanine/Tryptophan; Q/S/A/F/W) except BjuA03PIP2_2b, BjPIP2_7s, and BjPIP2_8 (Table 2.3). Among these proteins BjuA03PIP2_2b, did not have one amino acid residues in P2 Froger's positions. Whereas in the BjPIP2_7 and BjPIP2_8 homologous proteins, glutamine (the polar side chain) was displaced by methionine (the non-polar side chain) at P1 position. BjNIPs consist of F/Y in P1,

S/T in P2, A, Y in P3, and P4, respectively (Table 2.3). The P5 position in Froger's position was highly variable among BjNIP proteins. While in BjNIP1_2, BjNIP3_1, BjNIP4_1 isoleucine present, BjuNIP2_1, BjuA02NIP5_1a, BjuA03NIP5_1b, and BjNIP6_1s possess a leucine. At the same time, the BjNIP7s and BjuA07NIP5_1c, contains methionine and BjuB08NIP5_1a comprised valine in the P5 position. The P1 position of BjTIPs was similar in all subfamily proteins except BjuB04TIP1_2b, BjuB02TIP1_2a, and BjTIP5_1s where threonine (T) was replaced by tyrosine (Y)/lysine (K)/valine (V) residues, respectively (Table 2.3). The P2-P3 positions were alternatively occupied with alanine (A) or serine (S). The P4 and P5 positions were highly conserved with tyrosine (Y)/trytophane (W) and alanine (A)/valine (V)/tryptophan (W) amino acids, respectively. The Froger's positions in BjSIPs, are identical except at P2 (Table 2.3). The P2 position was alternatively shared between alanine (A) and valine (V) in BjSIP1_1s and BjSIP2_1s, respectively. The transmembrane domain (TMD) of all the BjAQPs ranges from a minimum of 5 to a maximum of 7 (Table 2.3).

We also have analyzed the N-terminal conserved TPG repeats, which is necessary for the polar localization, in both BjNIP5_1 and BjNIP6_1 along with their respective Brassica orthologs (Wang et al., 2017). Unlike AtNIP5_1, BniNIP5_1s, BraNIP5_1s and BnaNIP5_1s, we could not identify any conserved TPG repeats in N-terminal region of BjNIP5;1s except in BjuB08NIP5_1a (Figure 2.16). However, unlike three TPG repeats observed in AtNIP5;1, BjuB08NIP5_1a contains two TPG repeats similar to BraNIP5_1s, BniNIP5_1s, BnaA02NIP5_1a, BnaC02NIP5_1a, BnaA03NIP5_1b, and BnaC03NIP5_1b (Figure 2.16). The dual NPA motifs, NPS/NPV, were similar in all except BnaC06NIP5_1c which does not have first NPA motif. While H2 and LE2 SF residues are conserved among the NIP5_1 proteins, whereas H5 and LE1 SF residues are differed between I/N/V (H5) and G/A (LE1). However, BjNIP6_1 protein BjuB02NIP6_1a showed the TPG repeats from 16-21 nucleotides in the N-terminal, suggesting that these sequences may be involved in polar localization (Figure 2.17). In BjuB06NIP6_1b the third residue of the second TPG repeat the glycine residue was replaced by alanine (Figure 2.17).

NIP7;1 is the third member of the NIP II pore subfamily protein which showed anther-specific expression pattern (Li et al., 2011). Loss of function mutants of NIP7;1 showed reduced fertility in *A. thaliana* under limited B condition (Routray et al., 2018). AtNIP7;1 showed water-tight boric acid channel activity in reconstituted proteoliposomes (Routray et al., 2018). However, in *Xenopus* oocyte, AtNIP7;1 showed an extremely low intrinsic boric acid transport activity

unlike AtNIP5;1 and AtNIP6;1 and the substitution of conserved tyrosine residue located in transmembrane helix 2 adjacent to the aromatic arginine (ar/R) pore selectivity region to cysteine (Y81C) conferred higher boric acid channel activity (Li et al., 2011). Together with the homology modelling, the Y81 residue is considered to be a gate of boric acid transport. Analysis of conserved tyrosine residue (Y81) in NIP7;1 orthologs of *A. thaliana*, *B. nigra, B. rapa*, and *B. napus* showed *B. juncea* also possess the Y81 near to ar/R SF. Along with this, residues present in NPA and ar/R SF domains were also conserved among the Brassica species (Figure 2.18). These results suggest that BjNIP7_1 may have similar B transport function as AtNIP7;1.

S No	Class and subclass of BjAQPs	NPA (LB)	NPA (LE)	ar/R selectivity filter				Froger's residue					TMD no	Sub-cellular localization
	PIPs			H2	H5	LE1	LE2	P1	P2	P3	P4	P5		
1	BjuA09PIP1_1c	NPA	NPA	F	H	T	R	Q	S	A	F	W	7	plas
2	BjuA02PIP1_1a	NPA	NPA	F	H	T	R	Q	S	A	F	W	7	plas
3	BjuB06PIP1_1b	NPA	NPA	F	H	T	R	Q	S	A	F	W	6	plas
4	BjuB01PIP1_1a	NPA	NPA	F	H	T	R	Q	S	A	F	W	6	plas
5	BjuContig9034PIP1_1a	NPA	NPA	F	H	T	R	Q	S	A	F	W	6	plas
6	BjuA04PIP1_1b	NPA	NPA	F	H	T	R	Q	S	A	F	W	6	plas
7	BjuA09PIP1_3a	NPA	NPA	F	H	T	R	Q	S	A	F	W	6	plas
8	BjuA10PIP1_3b	NPA	NPA	F	H	T	R	Q	S	A	F	W	6	plas
9	BjuB08PIP1_4c	NPA	NPA	F	H	T	R	Q	S	A	F	W	6	plas
10	BjuB08PIP1_4d	NPA	NPA	F	H	T	R	Q	S	A	F	W	6	plas
11	BjuA09PIP1_4a	NPA	NPA	F	H	T	R	Q	S	A	F	W	6	plas
12	BjuB03PIP1_4a	NPA	NPA	F	H	T	R	Q	S	A	F	W	6	plas
13	BjuB07PIP1_4b	NPA	NPA	F	H	T	R	Q	S	A	F	W	6	plas
14	BjuA03PIP1_5a	NPA	NPA	F	H	T	R	Q	S	A	F	W	6	plas
15	BjuB02PIP1_5a	NPA	NPA	F	H	T	R	Q	S	A	F	W	6	plas
16	BjuA09PIP2_1a	NPA	NPA	F	H	T	R	Q	S	A	F	W	6	plas
17	BjuB08PIP2_1a	NPA	NPA	F	H	T	R	Q	S	A	F	W	6	plas
18	BjuA05PIP2_2c	NPA	NPA	F	H	T	R	Q	S	A	F	W	6	plas
19	BjuA03PIP2_2b	NPA	-	F	P	Q	R	Q	-	L	F	W	5	plas
20	BjuA03PIP2_2a	NPA	NPA	F	H	T	R	Q	S	A	F	W	6	plas
21	BjuB08PIP2_2b	NPA	NPA	F	H	T	R	Q	S	A	F	W	6	plas
22	BjuB08PIP2_2c	NPA	NPA	F	H	T	R	Q	S	A	F	W	6	plas
23	BjuB06PIP2_2a	NPA	NPA	F	H	T	R	Q	S	A	F	W	6	plas
24	BjuA03PIP2_3a	NPA	NPA	F	H	T	R	Q	S	A	F	W	6	plas

25	BjuB02PIP2_4a	NPA	NPA	F	H	T	R	Q	S	A	F	W	6	plas
26	BjuA03PIP2_4b	NPA	NPA	F	H	T	R	Q	S	A	F	W	6	plas
27	BjuA02PIP2_4a	NPA	NPA	F	H	T	R	Q	S	A	F	W	6	plas
28	BjuA07PIP2_5a	NPA	NPA	F	H	T	R	Q	S	A	F	W	6	plas
29	BjuA09PIP2_5b	NPA	NPA	F	H	T	R	Q	S	A	F	W	6	plas
30	BjuA09PIP2_5c	NPA	NPA	F	H	T	R	Q	S	A	F	W	6	plas
31	BjuB08PIP2_5a	NPA	NPA	F	H	T	R	Q	S	A	F	W	6	plas
32	BjuA03PIP2_6a	NPA	NPA	F	H	T	R	Q	S	A	F	W	6	plas
33	BjuB08PIP2_6a	NPA	NPA	F	H	T	R	Q	S	A	F	W	7	Plas
34	BjuB02PIP2_7a	NPA	NPA	F	H	T	R	M	S	A	F	W	6	plas
35	BjuA01PIP2_7a	NPA	NPA	F	H	T	R	M	S	A	F	W	6	plas
36	BjuA03PIP2_7b	NPA	NPA	F	H	T	R	M	S	A	F	W	6	plas
37	BjuA08PIP2_7c	NPA	NPA	F	H	T	R	M	S	A	F	W	6	plas
38	BjuB03PIP2_7b	NPA	NPA	F	H	T	R	M	S	A	F	W	6	plas
39	BjuB05PIP2_7c	NPA	NPA	F	H	T	R	M	S	A	F	W	6	plas
40	BjuA01PIP2_8a	NPA	NPA	F	H	T	R	M	S	A	F	W	6	plas
41	BjuA08PIP2_8b	NPA	NPA	F	H	T	R	M	S	A	F	W	6	plas
	TIPs													
42	BjuB01TIP1_1a	NPA	NPA	H	I	A	V	T	A	A	W	A	7	vacu
43	BjuA04TIP1_1a	NPA	NPA	H	I	A	V	T	A	A	W	A	7	vacu
44	BjuA02TIP1_2a	NPA	NPA	H	I	A	V	T	A	A	W	V	7	vacu
45	BjuA06TIP1_2b	NPA	NPA	H	I	A	V	T	A	A	W	A	7	vacu
46	BjuB04TIP1_2b	NPA	NPA	H	I	A	V	Y	A	A	W	V	6	vacu
47	BjuB02TIP1_2a	NPA	NPA	H	I	A	V	K	A	A	W	A	6	vacu
48	BjuA09TIP1_3c	NPA	NPA	H	I	A	V	T	S	A	Y	W	7	vacu
49	BjuB08TIP1_3b	NPA	NPA	H	I	A	V	T	S	A	Y	W	6	vacu
50	BjuB08TIP1_3a	NPA	NPA	H	I	A	V	T	S	A	Y	W	6	vacu

51	BjuA05TIP2_1a	NPA	NPA	H	I	G	R	T	S	A	Y	W	6	vacu
52	BjuB01TIP2_1a	NPA	NPA	H	I	G	R	T	S	A	Y	W	6	vacu
53	BjuB07TIP2_1b	NPA	NPA	H	I	G	R	T	S	A	Y	W	6	vacu
54	BjuB07TIP2_1c	NPA	NPA	H	I	G	R	T	S	A	Y	W	7	vacu
55	BjuB07TIP2_1d	NPA	NPA	H	I	G	R	T	S	A	Y	W	7	vacu
56	BjuA01TIP2_2a	NPA	NPA	H	I	G	R	T	S	A	Y	W	6	vacu
57	BjuA06TIP2_3a	NPA	NPA	H	I	G	R	T	S	A	Y	W	6	vacu
58	BjuB04TIP2_3a	NPA	NPA	H	I	G	R	T	S	A	Y	W	6	vacu
59	BjuContig1662TIP2_3a	NPA	NPA	H	I	G	R	T	S	A	Y	W	6	vacu
60	BjuB03TIP3_1a	NPA	NPA	H	I	A	R	T	A	A	Y	W	5	vacu
61	BjuB03TIP3_1b	NPA	NPA	H	I	A	R	T	A	A	Y	W	5	vacu
62	BjuA02TIP3_1a	NPA	NPA	H	I	A	R	T	A	A	Y	W	5	vacu
63	BjuA07TIP3_1b	NPA	NPA	H	I	A	R	T	A	A	Y	W	5	vacu
64	BjuB05TIP3_1c	NPA	NPA	H	I	A	R	T	A	A	Y	W	5	vacu
65	BjuB07TIP3_1d	NPA	NPA	H	I	A	R	T	A	A	Y	W	6	vacu
66	BjuB03TIP3_2a	NPA	NPA	H	M	A	R	T	A	S	Y	W	6	vacu
67	BjuA09TIP3_2b	NPA	NPA	H	M	A	R	T	A	S	Y	W	6	vacu
68	BjuB04TIP3_2b	NPA	NPA	H	M	A	R	T	A	S	Y	W	5	vacu
69	BjuA06TIP3_2a	NPA	NPA	H	M	A	R	T	A	S	Y	W	6	vacu
70	BjuA04TIP4_1a	NPA	NPA	H	I	A	R	T	S	A	Y	W	7	plas
71	BjuB01TIP4_1a	NPA	NPA	H	I	A	R	T	S	A	Y	W	7	plas
72	BjuB08TIP5_1a	NPA	NPA	N	V	G	C	V	A	A	Y	W	6	chlo
73	BjuA06TIP5_1a	NPA	NPA	N	V	G	C	V	A	A	Y	W	6	chlo
	NIPs													
74	BjuB05NIP1_2b	NPA	NPG	W	V	A	R	F	S	A	Y	I	5	plas
75	BjuB06NIP1_2c	NPA	NPG	W	V	A	R	F	S	A	Y	I	5	chlo
76	BjuB02NIP1_2a	NPA	NPG	W	V	A	R	F	S	A	Y	I	5	plas

77	BjuB06NIP2_1a	NPA	NPA	W	V	A	R	F	S	A	Y	L	6	vacu
78	BjuB06NIP2_1b	NPA	NPA	W	V	A	R	F	S	A	Y	L	6	vacu
79	BjuA01NIP3_1a	NPA	NPA	W	I	A	R	F	S	A	Y	I	5	plas
80	BjuSSNIP3_1a	NPA	NPA	W	I	A	R	F	S	A	Y	I	5	plas
81	BjuA05NIP3_1c	NPA	NPA	W	I	A	R	F	S	A	Y	I	4	plas
82	BjuA05NIP3_1b	NPA	NPA	W	I	A	R	F	S	A	Y	I	5	plas
83	BjuA04NIP4_1a	NPA	NPA	W	V	A	R	F	S	A	Y	I	6	Plas
84	BjuB01NIP4_1a	NPA	NPA	W	V	A	R	F	S	A	Y	I	6	plas
85	BjuSSNIP4_1a	NPA	NPA	W	V	A	R	F	S	A	Y	I	6	plas
86	BjuContig836NIP4_1a	NPA	NPA	W	V	A	R	F	S	A	Y	I	6	plas
87	BjuA02NIP5_1a	NPS	NPV	A	I	S	R	F	T	A	Y	L	5	vacu
88	BjuA03NIP5_1b	NPS	NPV	A	I	S	R	F	T	A	Y	L	5	vacu
89	BjuA07NIP5_1c	NPS	NPV	A	N	S	R	F	T	A	Y	M	5	plas
90	BjuB08NIP5_1a	NPS	NPV	A	V	S	R	F	T	A	Y	V	5	plas
91	BjuB06NIP6_1b	NPA	NPV	A	I	A	R	F	T	A	Y	L	5	plas
92	BjuB02NIP6_1a	NPA	NPV	A	I	A	R	F	T	A	Y	L	5	plas
93	BjuA05NIP7_1a	NPS	NPA	A	V	G	R	Y	S	A	Y	M	6	plas
94	BjuB01NIP7_1a	NPS	NPA	A	V	G	R	Y	S	A	Y	M	6	plas
	SIPs													
95	BjuContig26972SIP1_1a	NPT	NPA	T	V	P	I	P	A	A	Y	W	5	vacu
96	BjuContig116340SIP1_1a	NPT	NPA	T	V	P	I	P	A	A	Y	W	5	vacu
97	BjuB07SIP1_1a	NPT	NPA	T	I	P	I	P	A	A	Y	W	6	vacu
98	BjuA01SIP1_1a	NPT	NPA	T	V	P	I	P	A	A	Y	W	6	vacu
99	BjuA10SIP1_2a	NPC	NPA	T	F	P	I	P	A	A	Y	W	6	vacu
100	BjuB06SIP2_1b	NPL	NPA	S	H	G	A	P	V	A	Y	W	6	vacu
101	BjuB06SIP2_1c	NPL	NPA	S	H	G	A	P	V	A	Y	W	6	vacu
102	BjA04SIP2_1a	NPL	NPA	S	H	G	A	P	V	A	Y	W	6	vacu

103	BjB02SIP2_1a	NPV	NPA	S	H	G	A	P	V	A	Y	W	6	vacu
104	BjuA09SIP2_1b	NPV	NPA	S	H	G	A	P	V	A	Y	W	5	vacu

Table 2.3: List of 104 BjAQPs and their conserved domains (NPA motifs, ar/R SF, and Froger's residues), number of transmembrane domains and putative sub-cellular localization.

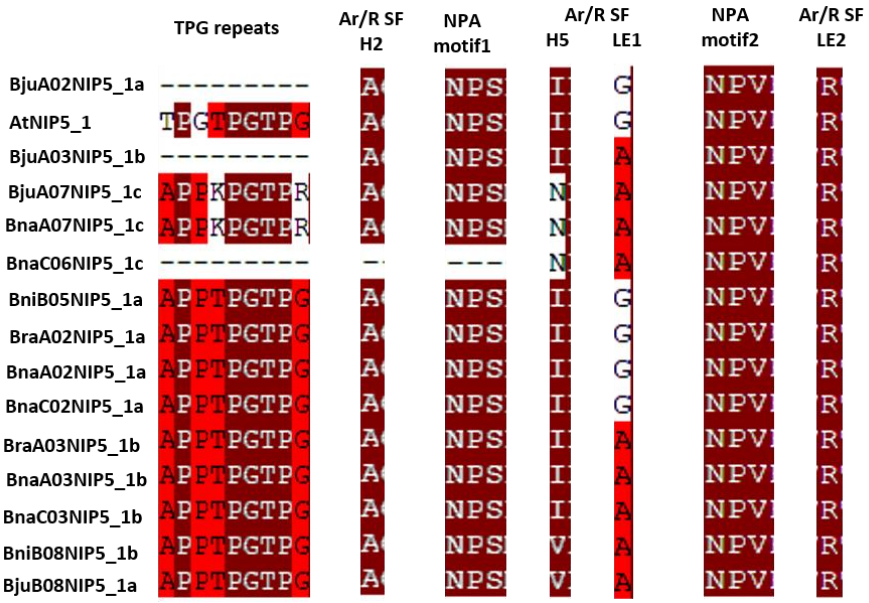

Figure 2.16: Multiple alignments of the amino acid sequences of the motifs required for substrate selectivity and regulation of BjNIP5_1s. The TPG repeats, NPA motifs, the ar/R selectivity filter and corresponding sequences in *A. thaliana*, *B. nigra*, *B. rapa*, and *B. napus* orthologs are shown. The conserved residues in the motifs are highlighted.

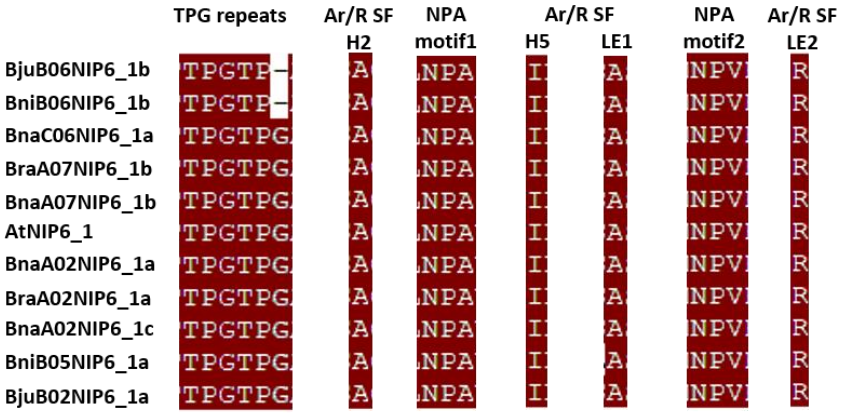

Figure 2.17: Multiple alignments of the amino acid sequences of the motifs required for substrate selectivity and regulation of the BjNIP6_1s. The TPG repeats, NPA motifs, the ar/R selectivity filter and TPG repeats of the corresponding sequences in *A. thaliana*, *B. nigra*, *B. rapa*, and *B. napus* orthologs are shown. The conserved residues in the motifs are highlighted.

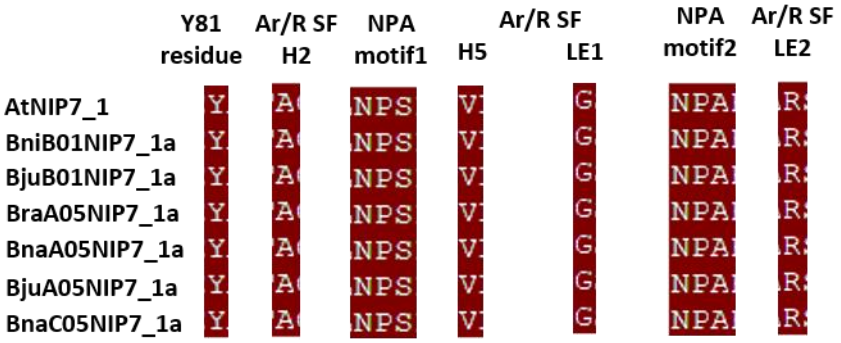

Figure 2.18: Multiple alignments of the amino acid sequences of the motifs required for substrate selectivity of the BjNIP7_1s. The tyrosine-81 residue, NPA motifs, and the ar/R selectivity filter of the corresponding sequences in *A. thaliana*, *B. nigra*, *B. rapa*, and *B. napus* orthologs are shown. The conserved residues in the motifs are highlighted.

2.3.6 Signature motifs in BjBORs

Seven out of fifteen BjBORs (BjBOR1s and BjBOR3s) carried two conserved HCO_3^- transporter domains, a signature B transporter domain (Table 2.2).—The first HCO_3^- transporter domain harbored a minimum of 2 TMDs in all BjBOR1 proteins, and BjuB06BOR1a, BjuB08BOR1b and BjuA03BOR1a had a maximum of three TMDs (Table 2.2). The BjBOR proteins had maximum of 11 TMDs in their sequence (Table 2.2). Proteins belongs to BjBOR2, BjBOR4s, BjBOR6s, and BjBOR7s subfamily is however did not have any HCO_3^- transporter domain, instead they all have Xan_ur_permeases superfamily domain. Information on this domain in BjBOR proteins is still unclear. All the BjBOR proteins comprised their TMDs within their HCO_3^- transporter domain except BjuA03BOR3a (Table 2.2).

In addition, we also have searched previously reported features of AtBOR1 such as tyrosine-based motifs, acidic-di-leucine motifs, and ubiquitination residues in BORs from *A. thaliana*, *B. rapa, B. nigra, B. juncea*, and *B. napus* (Figure 2.19). Tyrosine based motifs, involved in polar localization and B dependent vacuolar sorting, consists of conserved YxxΦ motif, where Y is tyrosine, x is any amino acid and Φ is any bulky hydrophobic residue. AtBOR1 consists of YDNM as a first tyrosine motif whereas, BjBOR1s (except BjuB06BOR1a), BniBOR1s (BniB01BOR1a, Bniutg512BOR1a, and BniB08BOR1b), BraBOR1s (BraA05BOR1b, and BraA03BOR1a), and BnaBOR1s (BnaC03BOR1a, BnaA03BOR1a, BnaA04BOR1b, BnaC04BOR1c, BnaA05BOR1c, and BnaC04BOR1b)

conserved with YNNM. The second amino acid in the first tyrosine motif of BjuB06BOR1a is replaced asparagine (N) by aspartic acid (D) which is similar to AtBOR1 (Figure 2.19). The second tyrosine motif, YHHM, is similar among AtBOR1, BniBOR1s, BraBOR1s, BjuBOR1s, and BnaBOR1s. The rest of the BjBOR proteins (BjBOR3s, BjBOR6s, and BjBOR7) showed high similarity in their dual tyrosine motif composition among the subgroups of *B. rapa, B. nigra, B. napus* and *Aradidopsis*. In clade II BjBORs the second tyrosine motif (YQQM) was replaced by phenylalanine (F)/isoleucine (I)/ glutamic acid (E)/ methionine(M) which is similar to clade II AtBORs, BniBORs, BraBORs, and BnaBORs (Figure 2.19).

The acidic di-leucine motif [D/E]xxxL[L/I], where D is aspartic acid, E is glutamic acid, x is any amino acid, L is leucine and I is isoleucine, is characterized as critical for the polarity and B dependent vacuolar sorting (Wakuta et al., 2015). We have observed the acidic di-leucine motif is present in the same loop regions as the tyrosine-based motifs (Figure 2.19). While L481 is conserved among all the BjBOR proteins, amino acid present in 480th position was differed between clade I and clade II BjBORs. While the BjBOR1s consists of a conserved di-leucine motif, the BjBOR3s and clade II BjBORs (BjBOR4s, BjBOR6s and BjBOR7s) showed variation in these residues (Figure 2.19).

Ubiquitination at the K590 residue is essential for degradation and vacuolar sorting of AtBOR1 in response to high B supply (Kasai et al. 2011). The amino acid residue corresponding to K590 was conserved in clade I BjBORs, while aspartic acid (D)/asparagine (N)/arginine (R)/ leucine(K) was located in clade II (Figure 2.19). We also have observed BniB07BOR3b, BraA05BOR1c, and BjuA04BOR2a BjuB05BOR7a did not have acidic di-leucine and/or ubiquitination site in their sequence.

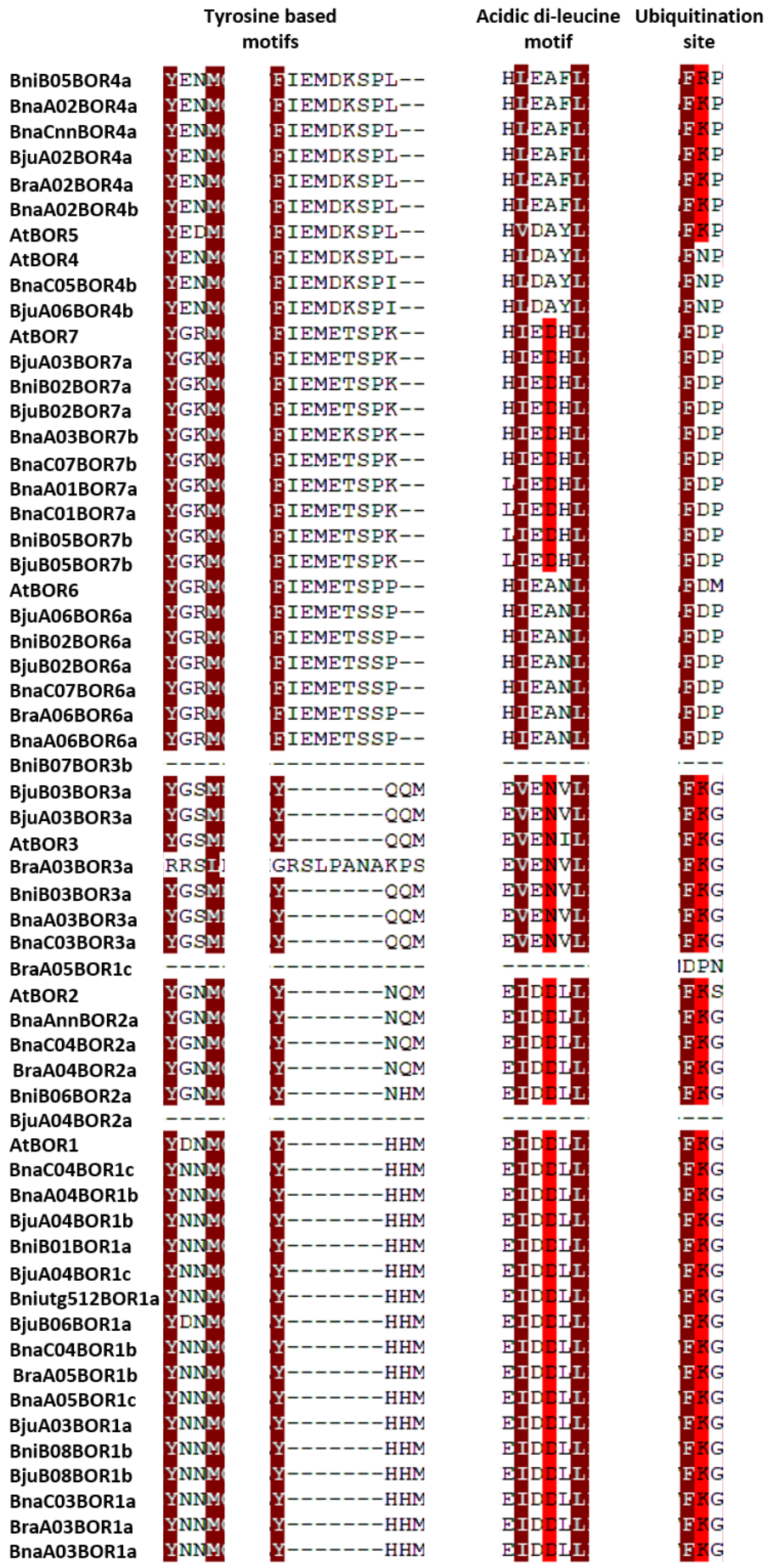

Figure 2.19: Multiple alignments of the amino acid sequences of the motifs required for the polarity and vacuolar sorting. The tyrosine-based motif, the acidic di-leucine motif and the lysine residue in AtBOR1 and corresponding *A. thaliana*, *B. nigra*, and *B. napus* orthologs are shown. The conserved residues in the motifs are highlighted.

2.3.7 Chromosome location of BjAQPs and BjBORs

The higher percentage of the *BjAQP* and *BjBOR* genes were located on the chromosome B08 (11 *BjAQP*s and one *BjBOR*), followed by chromosomes A03 (8 *BjAQP*s, and 3*BjBOR*s), A09 (9 *BjAQP*s), B02 (7 *BjAQP*s, and 2 *BjBOR*s) and B06 (8 *BjAQP*s, and one *BjBOR*) (Figure 2.20). Clustering of four *BjAQP* genes was observed at various positions of chromosomes A03, A09, B02, B06, and B08. Unlike *BjAQP*s, *BjBOR* genes are unevenly distributed throughout the *B. juncea* chromosomes (Figure 2.20). The chromosome A08, and A10 only had two genes, while in each of the A07, and B04 chromosomes three genes were identified. Four genes were identified and mapped in chromosome B05 (*BjuB05PIP2_4b, BjuB05PIP2_7c, BjuB05NIP1_2b*, and *BjuB05TIP3_1c*). The chromosomes A01 (*BjuA01PIP2_8a*, *BjuA01PIP2_7a*, *BjuA01TIP2_2a, BjuA01NIP3_1a*, and *BjuA01SIP1_1a*) and A05 (*BjuA05PIP2_2c, BjuA05NIP3_1c, BjuA05NIP3_1b, BjuA05NIP7_1a*, and *BjuA05TIP2_1a*) consists five genes. The chromosomes A02 (*BjuA02PIP2_4a*, *BjuA02TIP3_1a*, *BjuA02PIP1_1a*, *BjuA02NIP5_1a, BjuA02TIP1_2a,* and *BjuA02BOR4a*) and chromosomes A06 (*BjuA06TIP3_2a, BjuA06TIP5_1a, BjuA06BOR4b, BjuA06BOR6a, BjuA06TIP1_2b, and BjuA06TIP2_3a*), B07 (*BjuB07TIP2_1b, BjuB07SIP1_1c, BjuB07TIP3_1d, BjuB07TIP2_1c, BjuB07TIP2_1d, and BjuB07PIP1_4b*), and B03 (*BjuB03PIP2_7b, BjuB03BOR3a, BjuB03TIP3_2a, BjuB03PIP1_4a, BjuB03TIP3_1a, BjuB03TIP3_1b*), comprises six genes. B01 (*BjuB01PIP1_1a, BjuB01TIP1_1a, BjuB01TIP4_1a, BjuB01NIP4_1a, BjuB01NIP4_1a, BjuB01TIP2_1a, and BjuB01NIP7_1a*) contains seven genes. A total of eight genes were located in chromosome A04 (5 *BjAQP*s and 3 *BjBOR*s) (Figure 2.20).

We also could detect the locus of six *BjAQP* genes on scaffolds and contigs. The majority of *BjBOR* genes are positioned chromosomes A04 (*BjuA04BOR2a, BjuA04BOR1c* and *BjuA04BOR1c*) and A03 (*BjuA03BOR1a, BjuA03BOR3a,* and *BjuA03BOR7a*). All the BjBOR genes are present on the appendages of chromosome A04 which are correlated with high rates of recombination (Figure 2.20). Further

proof on essentiality of the genes in *B. juncea* QTL in B efficiency is needed (Hua et al., 2016). Chromosomes A06 (*BjuA06BOR6a*, and *BjuA06BOR4b*) possess two BjBOR genes., Whereas, B03 (*BjuB03BOR3a*), B05 (*BjuB05BOR7a*), B06 (*BjuB06BOR1a*), and B08 (*BjuB08BOR1b*) each has one BOR gene.

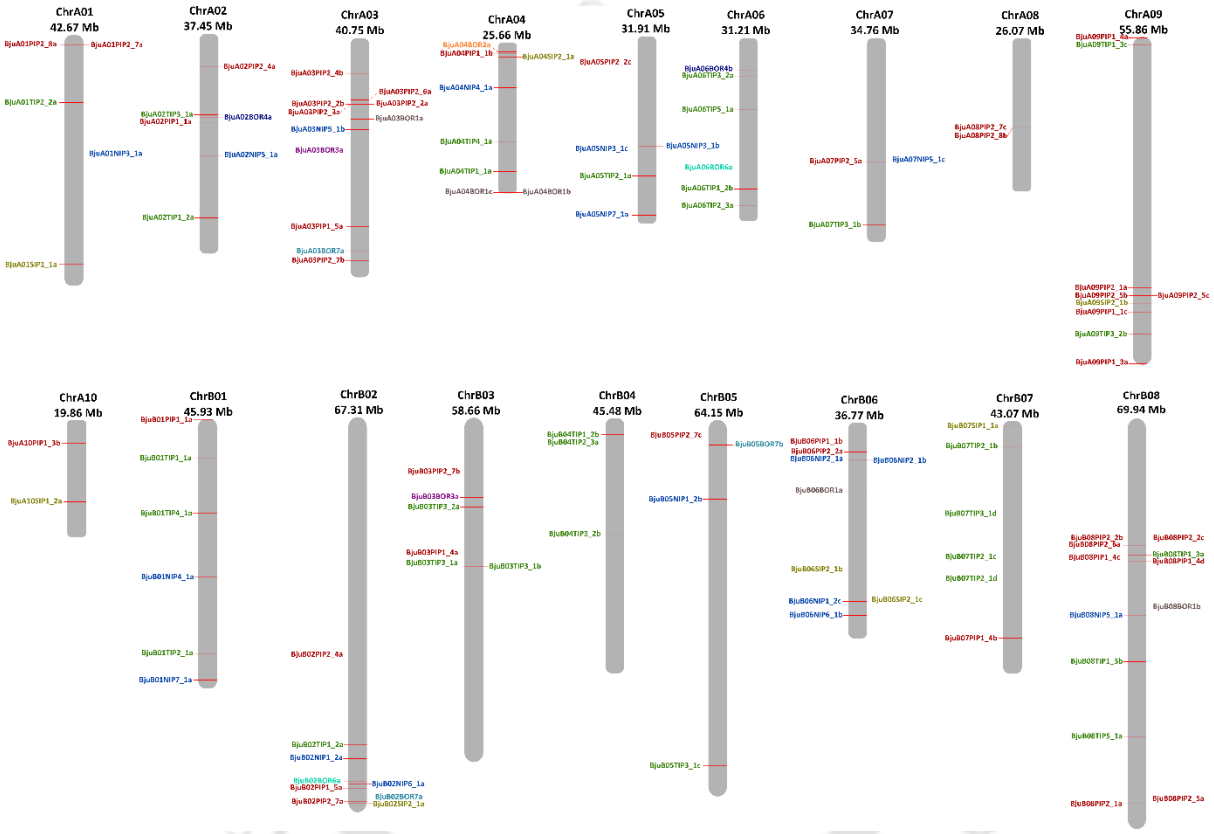

Figure 2.20: Chromosomal location of AQPs and BORs in *B. juncea*. The gene chromosome location diagram was drawn manually. There were 97 BjAQPs and 15 BjBORs located on 18 chromosomes. Seven BjAQPs were located on scaffolds and contigs.

2.3.8 Prediction of cis-acting regulatory elements

The cis-acting regulatory elements are the specific motifs that bind to an appropriate transcription factor to regulate gene transcription in plants (Wittkopp and Kalay, 2012). Scanning of 2000 bp upstream promoter regions before the translational start site (ATG) were used to identify the cis-acting elements of *BjAQP* and *BjBOR* genes (Figure 2.21 and 2.22).

Stress-related cis-regulatory elements that were identified in most of the *BjAQP* and *BjBOR* genes included low-temperature responsive element (LTR; 77 *BjAQP*s and 11 *BjBOR*s), light-responsive element (G-box; 234 *BjAQP*s and 31 *BjBOR*s), salicylic acid-responsive element (TCA-element; 88 *BjAQP*s and 16 *BjBOR*s), anaerobic induction regulatory element (ARE; 248 *BjAQP*s and 39 *BjBOR*s), defense and stress-responsive element (TC-rich repeats; 67 *BjAQP* and 11 *BjBOR*s), ABA-responsive element (ABRE; 227 *BjAQP*s and 29 *BjBOR*s), MYB binding site involved in drought-inducibility (MBS; 58 *BjAQP*s and 11 *BjBOR*s), auxin-responsive element (TGA-element; 49 *BjAQP*s and 19 *BjBOR*s), and MeJA-responsive element (CGTCA-motif; 147 *BjAQP*s and 32 *BjBOR*s). This result suggested that the AQP and BOR members in *B. juncea* may be regulated by various drought and ABA-induced transcription factors (Figure 2.21 and 2.22).

The involvement of transcription factor WRKY in B stress responses was established in *A. thaliana* and *B. napus* (Kasajima et al., 2010; Feng et al., 2019). Recently, the contribution of *BnaA9.WRKY47* gene in upregulating *BnaA3.NIP5;1* expression to facilitate efficient B uptake in *B. napus* was discovered. The 2 Kb 5'-UTR were retrieved for *BjNIP5_1*, *BjNIP6_1*, *BjNIP7_1* and *BjBOR1* genes and analyzed for the conserved W-box (T/CTGACC/T) domain which is the binding site of WRKY (Eulgem et al., 2000). The W box domain was observed at various positions in the *BjuA02NIP5_1a, BjuB08NIP5_1a, BjuB02NIP6_1a, BjuB06NIP6_1b, BjuA05NIP7_1a, BjuB01NIP7_1a, BjuA03BOR1a, BjuB06BOR1a, BjuB08BOR1b, BjuA04BOR1b,* and *BjuA04BOR1c* promoter region (Table 2.4). Unlike others *BjuB06BOR1a* and *BjuA04BOR1c* consist of four W box domains at various position in their promoter region (Table 2.4).

AtNIP5;1 possess two minimum upstream open reading frames (uORFs), AUGUAA (AUG-stop), located at -122 and -312 which is critical for B dependent posttranscriptional regulation (Tanaka et al., 2016). It was demonstrated that either one of the two AUG-stop 5'UTR is sufficient for the B-dependent ribosome stalling and mRNA degradation. Analysis of the 500 bp 5'UTR regions of the *BjNIP5_1, BjNIP6_1, BjBOR1,* and *BjBOR2* revealed that these genes also consist minimum one to maximum five AUG-stop sequence in their respective 5'UTR positions (Table 2.5). This result suggests that these homologs may regulate their expression via B-dependent manner. However, further studies will be needed to confirm this hypothesis.

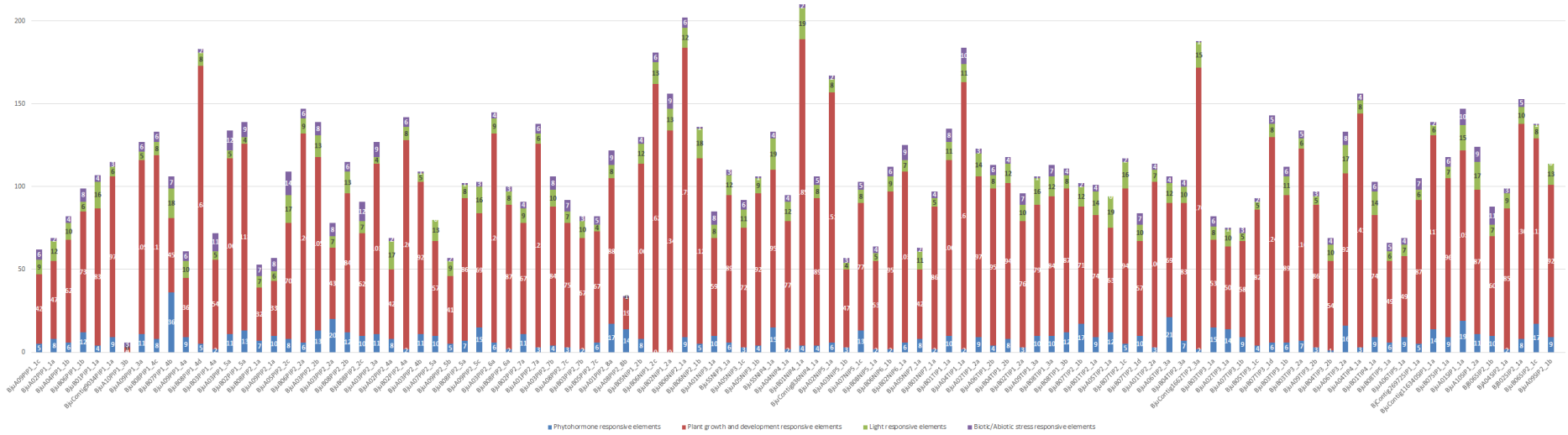

Figure 2.21: Analysis of cis-acting elements in *B. juncea* aquaporin genes. The bars colored with blue, red, light green, and purple represented phytohormone-responsive, plant growth and developmental-responsive, light-responsive and biotic/abiotic-responsive elements, respectively. The number of cis-elements are mentioned in their respective bars.

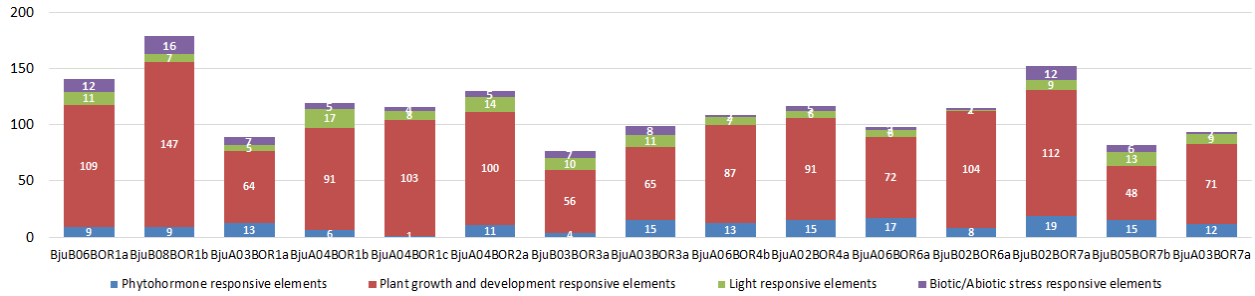

Figure 2.22: Analysis of cis-acting elements in *B. juncea* BOR genes. The bars colored with blue, red, light green, and purple represented phytohormone-responsive, plant growth and developmental-responsive, light-responsive and biotic/abiotic-responsive elements, respectively. The number of cis-elements are mentioned in their respective bars.

Gene	W-box motif (TTGACC)		
	No.	Position	Strand
BjuA02NIP5_1a	1	-1303	+
BjuB08NIP5_1a	1	-1029	-
BjuB02NIP6_1a	1	-941	+
BjuB06NIP6_1b	1	-319	+
BjuA05NIP7_1a	1	-703	+
BjuB01NIP7_1a	1	-808	+
BjuA03BOR1a	2	-480	-
		-859	+
BjuB06BOR1a	2	-580	-
		-964	+
BjuB08BOR1b	1	-1272	+
BjuA04BOR1b	1	-1283	+
BjuA04BOR1c	2	-192	-
		-625	+

Table 2.4: The presence of W box domain in the promoter region of the BjNIP5;1, BjNIP6;1, BjNIP7;1 and BjBOR1 genes.

Gene	ATG-Stop sequence	
	No.	Position
BjuA03NIP5_1b	1	-1939
BjuA07NIP5_1c	1	-550
BjuB08NIP5_1a	3	-102, -284, -1430
BjuB02NIP6_1a	3	-1791, -865, -742
BjuB06NIP6_1b	1	-954
BjuA03BOR1a	3	-260, -346, -1964
BjuB06BOR1a	3	-625, -1861, -1925
BjuB08BOR1b	3	-278, -347, -1117
BjuA04BOR1b	5	-285, -349, -1113, -1468, -1822
BjuA04BOR1c	3	-269, -344, -753
BjuA04BOR2a	1	-891

Table 2.5: Multiple alignments of the 5'-UTR sequences of NIP5;1, NIP6;1, BjBOR1, and BjBOR2 required for the B-dependent ribosome stalling and mRNA degradation. The number and the positions of the AUG-stop sequences have been mentioned.

2.3.9 Expression profiles of B transporter genes correlated with B concentration

The gene expression of *NIP5;1s* and *BOR1s* in high-yielding Indian mustard genotype, Geeta, were analyzed in the root samples under sufficient (46 µM B) and low (0.1 µM B) B concentration (Figure 2.23 A and B). The root biomass, taproot length and leaf biomass was observed to be better in plants grown under sufficient (46 µM) B than low (0.1 µM) B media. Interestingly, all three *BjNIP5_1* genes tested in our study showed increased expression in root tissues under low B concentration (Figure 2.23A). While *BjuA02NIP5_1a* and *BjuA03NIP5_1b* genes were markedly increased to 7-folds in roots under low B concentration, *BjuA07NIP5_1c* had shown 17-folds higher expression (Figure 2.23A). Interestingly, while the expression of the BOR-transporter gene *BjuB08BOR1b* was unaltered, the *BjuA03BOR1a* was up-regulated to 3-folds in roots under low-B conditions (Figure 2.23A).

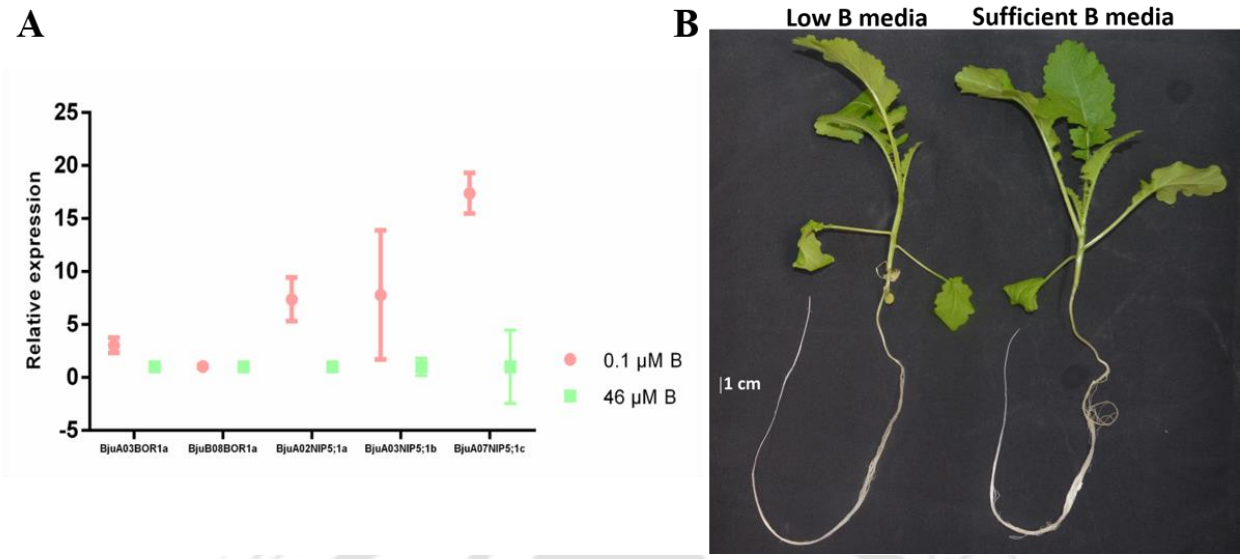

Figure 2.23: A. The expression analysis of three BjNIP5;1s (BjuA02NIP5_1a, BjuA03NIP5_1b, and BjuA07NIP5_1c) and two BjBOR1s (BjuA03BOR1a and BjuB08BOR1a) in roots of mustard genotype Geeta. Total RNA was extracted after a week under low and sufficient B treatment. The relative expression was determined by qRT-PCR. Values are mean ± SD of three replications. *Bj*tubulin primers were used as internal control. **B.** Difference in physiological growth of Indian mustard genotype Geeta grown under low B (0.1 µM B) and sufficient B media (46 µM B).

2.4 DISCUSSION

AQPs are highly diversified proteins in plants that facilitate the transport of water and other small uncharged molecules, including boric acid (Hove and Bhave., 2011). The 104AQP genes are identified and categorized into four established sub-families (41 *PIPs*, 32 *TIPs*, 21 *NIPs*, and 10 *SIPs*) in *B. juncea* genome. Consistent with other Brassicaceae species such as *A. thaliana*, *B. rapa*, *B. nigra*, *B. oleracea*, and *B. napus*, there were no XIP family proteins observed in the *B. juncea* genome (Johanson et al., 2001; Tao et al., 2014; Diehn et al., 2015; Yuvan et al., 2017). The number of full-length AQPs identified in *B. juncea* is relative to that in *B. napus* (127 members) than other Brassica species (Yuan et al. 2017). In addition, the genome of *B. juncea* consists of higher numbers of AQPs than its diploid predecessors *B. rapa* (57 members) and *B. nigra* (63 members). The higher numbers of homologous AQP proteins

in *B. juncea* might have been created via whole-genome duplication events during evolution, unlike in *A. thaliana*, in which duplication events did not occur (Diehn et al., 2015).

The maximum number of homologous proteins was found in sub-families BjTIP3_1, BjPIP1_1, BjPIP2_2, BjPIP2_7, and (six proteins). Phylogenetic analysis revealed that AtPIP1;2, AtNIP1;1, and AtNIP4;2 had no orthologs in *B. juncea* (Figure 2.1). We also have observed the loss and uneven gene(s) distribution on the A and B chromosomes of *B. juncea*. While there were six *SIP* genes observed in *B. rapa*, twelve *SIP* family genes were identified in the genome of *B. juncea*. The high numbers of *BjAQP* were observed in B08 and high numbers of *BjBOR* genes were observed in chromosomes A03 and A04 (Figure 2.20). Gene replication and chromosome rearrangement in *B. rapa* and *B. nigra* is therefore expected to result in the loss and uneven distribution of AQP genes in the respective A and B chromosomes of *B. juncea*.

2.4.1 PIPs and TIPs

The PIP and TIP proteins are extensively studied for their water transport activity, and the conserved NPA motifs and ar/R residues between them strongly support their role in the water transport (Fox et al., 2017). All 12 PIP and 10 TIP sub-family proteins are well-conserved with dual NPA motifs (NPA/NPA). While all the PIP subfamily proteins have conserved ar/R residues (F/H/T/R), the TIPs comprise different sets of ar/R residues specific to their sub-family proteins (Table 2.3). These similar signature motifs of BjPIPs are in accordance with the other plants, including *A. thaliana*, *B. rapa*, *B. oleracea*, *B. napus*, *H. vulgare*, and *P. vulgaris*, suggesting that the PIPs have been subjected to strong selection in different plant taxonomic lineages. Suga and Maeshima., 2004 have identified key valine/isoleucine residues located next to the P3 Froger's position, which is critical for the water transport activity of PIPs. While valine increases the water transport, substitution of isoleucine at this position significantly reduces the water transport. In addition, similar to *B. napus*, we could classify the PIPs into PIP1s and PIP2s based on the residues at these positions (Yuvan et al., 2017). All the BjPIP1s and BjPIP2_5s are consisting Ile/Ile residues in these regions, whereas BjPIP2s are occupied with Val/Ile residues. The B transport activity of PIP members in barley (*Hordeum vulgare;* HvPIP1;3 and HvPIP1;4) and maize (*Zea maize*; ZmPIP1) has been demonstrated through transport assay in yeast, and B permeability assay in oocytes, respectively, showed channel activity for B (Fitzpatrick and Reid

2009; Zangi and Filella 2012; Dordas et al., 2000). However, the role of the *HvPIP1* genes in B transport was considered as uncertain since their expression was not regulated by the B (Zangi and Filella 2012). In addition, transgenic *A. thaliana* lines overexpressed *OsPIP2;4, OsPIP2;7, OsPIP1;3* and *OsPIP2;6* having influx and efflux activity and enhanced tolerance for B toxicity (Kumar et al. 2014; Mosa et al. 2016). Besides, many PIPs in rice were proposed to work as a bidirectional boric acid channel to avoid the accumulation of B inside the plant cells. The sequence analysis of these PIP proteins and their respective orthologs in *B. juncea* revealed the amino acid residues in the key motifs including NPA domains and ar/R SF were highly conserved (data not shown) and hence they may involve in the boric acid efflux activity.

The TIP family proteins are the second-largest MIP subfamily in *B. juncea*, comprising 32 genes. The sequence homology analysis of BjTIPs with AtTIPs showed greater diversity within the ar/R selectivity filter region. TIPs showed the most diversity within putative pore regions with four different ar/R subgroups: TIP Group I-III, with group II consisting of group IIA and group IIB (Wallace and Roberts, 2004). The SF residues of the respective groups are given in Table 2.3. Similar to the *B. rapa*, *B. oleracea*, and *B. napus*, the BjTIP3_2 proteins (BjuB03TIP3_2a, BjuA09TIP3_2b, BjuB04TIP3_2b, and BjuA06TIP3_2a) also had novel SF residues (H, M, A, R) (Table 2.3) (Tao et al., 2014; Diehn et al., 2015; Yuvan et al., 2017). Of all, group III proteins BjuB08TIP5_1a, and BjuA06TIP5_1a had considerably distinct SF residue composition, N/V/G/C, indicating the unique transport function. The maximum number of homologous proteins was identified in group IIA (9 proteins), whereas group III is the lowest (two proteins). The heterologous expression of maize (ZmTIP1;1 and ZmTIP1;2) and grape (VvTnTIP1;1, VvTnTIP2;1, VvTnTIP2;2 and VvTnTIP 4;1) TIPs showed a high capacity to transport boric acid in the presence of H_3BO_3 in the growth medium (Bárzana et al. 2014; Sabir et al. 2014). The expression of pollen-specific *AtTIP5;1* is induced under high B and *AtTIP5;1* overexpression *in planta* conferred B toxicity tolerance with an increased silique production (Pang et al., 2010). In addition, transcript profiling of B-efficient citrus rootstock has demonstrated the upregulation of *TIP2;2* and *TIP4;1*, under boron deficiency with different temporal expressions (Zhou et al. 2015). Similar to PIPs, the protein sequence analysis of the TIPs mentioned-above to their respective *B. juncea* orthologs showed highly similar conserved amino acid residues (data not shown) in the NPA motifs and ar/R SF residues, which suggesting their possible role in B transport.

2.4.2 NIPs

The NIP subfamily represents the highest sequence diversity among all the four AQP subfamilies (Bansal and Sankararamakrishnan, 2007). Phylogenetic analysis in *A. thaliana* and *B. juncea* revealed that NIPs possess nine and twenty-one subgroups, respectively. The NPA motifs in all the BjNIPs are similar to the *A. thaliana, B. rapa, B. nigra* and *B. napus* NIPs. The NPA domains are the characteristic features of the AQPs involved in the pore formation and solute transport (Pommerrenig et al., 2017). The presence of amino acid residues in these regions renders solute selectivity for the specific sub-group of AQPs. All the BjNIP5_1 and BjNIP6_1 proteins consist of NPS-NPV or NPA-NPV in place of NPA-NPA in pore forming region, respectively (Table 2.3). The substitution of these amino acids allows the respective proteins to form reduced constriction regions with polar residues for the substrate specificity. Also, these NPA domains were well conserved among the other Brassica species including *A. thaliana*, *B. rapa, B. nigra* and *B. napus*.

The ar/R selectivity filter serves as a selectivity filter by forming the second most narrower pore constriction which is acting as a size exclusion barrier for the transport of water and small solutes (Fu et al., 2000; Sui et al., 2001). Based on the modelled ar/R regions in *A. thaliana*, NIPs are classified into two ar/R subgroups: NIP I and II proteins, with unique transport properties conserved within each subgroup (Wallace and Roberts, 2004). The ar/R region of NIP subgroup I have a conserved tetrad of residues with a Trp at H2, Val/Ile at H5, Ala at LE1, and Arg at LE2 (Wallace and Roberts, 2004). All the *A. thaliana, B. rapa, B. nigra* and *B. napus* orthologs of NIP subgroup I family proteins in *B. juncea* possess similar ar/R selectivity filter, W/V/A/R. The NIP subgroup II in *B. juncea* contains a conserved amino acid substitution of alanine at H2 for tryptophan in subgroup I. Interestingly, the functional characterization of NIP subgroup II shows that this H2 substitution is responsible for a distinct transport selectivity compared to NIP subgroup I transporters (Wallace and Roberts., 2004; Wallace and Roberts., 2005). Out of the eight NIP subgroup II members, the *B. juncea* orthologs of AtNIP6;1 and AtNIP7;1 having identical conserved amino acids in the ar/R selectivity regions (A/I/A/R, and A/V/G/R, respectively) (Table 2.3). However, the BjNIP5_1 homologs have been highly variable at H5 position compared to AtNIP5;1. While isoleucine is present in BjuA02NIP5_1a and BjuA03NIP5_1b proteins, BjuB08NIP5_1a possesses valine at this position. The change of amino acid valine in place of

isoleucine may increase the pore size in the ar/R region since the residue size of valine is smaller than isoleucine. Also, we have observed the BjuA07NIP5_1c protein comprised a polar neutral side-chain amino acid asparagine at this position indicating that they may have acquired a more specialized function for substrate transport than the latter. The point mutation study of the AtNIP5;1 revealed that H5 position is critical for the B transport (Mitani-Ueno et al., 2011). The H5 amino acid residue in most of the BjNIP5_1 is conserved among the *A. thaliana*, *B. nigra*, *B. rapa*, and *B. napus*. Therefore, studying the function of BjNIP5_1s in B transport will be of particular interest in the future. The NIP III subfamily was observed to be completely absent in *B. juncea*. NIP III proteins are an essential component of silicon transport. Thus, the absence of the Si transporter protein family precisely confirms that *B. juncea* is a weak Si accumulator like any other Brassica plant (Montpetit et al., 2012; Vivancos et al., 2015).

The NIP5;1 and NIP6;1 proteins are well-established for their role in boric acid transport in *A. thaliana*. Recently, the boric acid transport activity of *B. napus* NIP genes including A02.NIP5;1a, A03.NIP5;1b, A02.NIP6;1a in *Xenopus* oocytes and *in planta* characterization analysis revealed their involvement in B transport under low B condition (Diehn et al., 2019; He et al., 2021; Song et al., 2021). Since these orthologous BjNIP5_1 and 6_1 encoded in sub-genome A are very similar to BnaNIP5;1 and 6;1s in terms of the NPA and ar/R SF motifs composition, they are likely involved in the B transport.

The polar localization of the channel proteins towards the soil/stele side in the plasma membrane contributes in the efficient uptake and the radial transport of the nutrients (Yoshinari and Takano 2017). The analysis of TPG repeats in both BjNIP5_1s and BjNIP6_1s revealed their presence in BjuB08NIP5_1a and BjuB02NIP6_1a. Also, the BjNIP5_1 proteins consist of different amino acid composition in their N-terminal region in comparison to their orthologs from *A. thaliana*, *B. nigra, B. rapa*, and *B. napus* and further studies related to their polar localization will be needed.

BjNIPs are highly responsive to B deficiency as their expression is upregulated under the deficient B in root tissues. The expression of *BjuA07NIP5_1c* and *BjuA02NIP5_1a* and *BjuA03NIP5_1b* transcripts was upregulated to 14- and 7-folds, respectively, in roots under low B conditions (Figure 2.23A). Out of three highly

expressing *BjNIP5_1s*, *BjuA02NIP5_1a* gene contains WRKY binding site in their upstream region (Table 2.4). Recently, the positive regulation by *A9.WRKY47* gene in *A3.NIP5;1* expression under low B condition was revealed in *B. napus* (Feng et al., 2019). Since the upregulated *BjNIP5_1* genes also contains WRKY binding sites we can assume the involvement of *BjWRKY* genes in their regulation under low B concentration. Besides, we also have identified dual ATG-stop sequences located at various positions in *BjNIP5_1*, *BjNIP6_1*, *BjBOR1s* and *BjBOR2s* upstream region (Table 2.5) which is important for B dependent posttranscriptional regulation (Tanaka et al., 2016). The presence of these minimal uORFs suggests that the expression of BjNIP5_1 homologs might be controlled by B-dependent ribosome stalling and mRNA degradation.

2.4.3 SIPs

BjSIPs comprise only 9.6% of total BjAQPs. The dual NPA motif analysis exhibited the variation in the third amino acid residue of the first NPA motif of the BjSIPs. This residue was tyrosine and cysteine in BjSIP1_1s, BjSIP1_2s, respectively. Whereas, BjSIP2_1s showed variation between lysine (BjuB06SIP2_1b, BjuB06SIP2_1c, and BjuA04SIP2_1a) and valine (BjuB02SIP2_1a, and BjuA09SIP2_1b). While BjSIP2_1s contain similar ar/R SF composition, BjSIP1_1s showed variation in H5 position between valine, isoleucine and phenylalanine. Among the BjSIPs, BjSIP2_1 have the highest homologous proteins (five members). The AtSIPs fused with GFP were majorly detected in ER and the heterologous expression of AtSIP1;1 and AtSIP1;2 in yeast were characterized as AQPs (Ishikawa et al., 2005). Also, the expression analysis revealed that AtSIP1;1 is constitutively expressed under drought stress in roots (Alexandersson et al., 2005). However, the role of SIP family members is unclear to date.

2.4.4 BORs

In our present study, we have identified and characterized the BOR transporter family proteins for the first time in *B. juncea*, a second-most important oilseed crop in India. The phylogenetic tree of all BjBORs, BnaBORs, and AtBORs clustered the proteins into two groups, i.e., AtBOR1-like and AtBOR4-like (Figure 2.3). We could identify 15 BOR genes categorized into six subfamilies (*BOR1*, *BOR2*, *BOR3*, *BOR4*, *BOR6*, and *BOR7*). Seven out of fifteen BjBOR proteins carried two conserved HCO_3^- transporter domains essential for B transport functions (Table 2.2). The anion

exchanger bicarbonate (HCO_3^-) domain has been reported in many plant families as a conserved domain of BOR transporters. TMDs are essential for transporters anchored to the membrane; thus, the functions of these proteins in B transport require further validation. The first domain of all the HCO_3^- transporter comprised a minimum of two and a maximum of four TMDs in all BjBOR proteins. There are seven BOR genes identified in *A. thaliana*, and *B. juncea* has comprised almost two folds higher BOR genes due to spontaneous gene duplication created from their diploid progenitors *B. rapa* and *B. nigra*. The *BjBOR* genes are randomly distributed on seven out of 18 chromosomes of *B. juncea*, and the chromosomal locations in the A genome are not completely homologous in the B genome. Also, we observed *BjBOR* genes at the chromosomal arms (A04), which are prone to high recombination. This may be due to the evolutionary advantage of adapting to a challenging B environment (Hua et al., 2016). The BOR genes can also be grouped as BOR1-like (Group 1) and BOR4-like (Group 2) based on the protein structure, and as mentioned earlier, the physicochemical properties of these two groups are substantially distinct, possibly due to the different response to the environmental stimuli. The amino acid length of all the BjBORs varied from 247 to 1141.

The tyrosine-based motifs are recognized by the adaptor protein (AP) complexes and function as sorting signal into clathrin-coated vesicles (Bonifacino and Traub 2003). It was previously demonstrated that the tyrosine-based motifs of AtBOR1 are involved in the polar localization and vacuolar sorting (Takano et al. 2010). The single and double amino acid substitution of tyrosine residue resulted in weak polarity and no B dependent vacuolar sorting (Takano et al. 2010). These tyrosine motifs were shown to be required for interaction with the adaptor protein (AP) complex 3 and 4, which are involved in selective sorting in vacuolar pathway (Yoshinari et al. 2019). The YxxΦ motif is conserved in the clade I BjBORs and the bulky hydrophobic Φ residue was always methionine. Unlike clade I BORs, clade II BORs comprise F/ I/E/M in place of Y/Q/Q/M and is well conserved in *B. juncea* similar to *A. thaliana*, *B. nigra*, *B. rapa*, and *B. napus*. The involvement of FxxM motif in AP complex mediated regulation was also previously have been demonstrated in glucose transporter, GLUT4, of mammal adipocytes (Al-Hasani et al. 2002, Schmidt et al. 2006). Considering all together, our observation suggests that similar to other BORs, the tyrosine-based motifs are common in BjBOR proteins and thus they may also be involved in the polar localization and/or B dependent vacuolar sorting.

The acidic di-leucine motif, which is present in the same loop region as the tyrosine-based motifs, is a characteristic signal recognized by the AP2 complex in mammals (Schmidt et al. 2006). The acidic di-leucine motif was identified to be conserved in all BjBOR1s except, BjuA04BOR2b, BjBOR3s and clade II BjBORs. The amino acid residue corresponding to K590 was also identified to be conserved only in clade I BjBORs (BjBOR1, and BjBOR3) (Figure 2.19). Since acidic di-leucine motif was demonstrated to be involved in polarity, rapid degradation of AtBOR1, their presence in BjBOR1s suggests similar functions in *B. juncea*. These results suggest that BjuA03BOR1a, BjuB06BOR1a and BjuB08BOR1b, which are the close orthologs of BnaC03BOR1b, BnaC04BOR1b, BnaA05BOR1c and BnaA03BOR1a, might also share the characteristic of B-dependent vacuolar sorting dependent on the acidic di-leucine motif, the tyrosine-based signals and the ubiquitination lysine residue similar to AtBOR1.

AtBOR1 is preferentially expressed in roots, and the polar localization of BOR1 is likely essential for the efficient transport of boron from the root surface to the xylem, in collaboration with boric acid channels (Yoshinari et al., 2017; 2019). *AtBOR1* is constitutively expressed at the mRNA level and is regulated by post-translational degradation when boron supply becomes adequate (Takano et al. 2005). However, in *B. napus*, *BnBOR1;1c* expression both in roots and shoots were upregulated under low B conditions (Chen et al., 2018). Similarly, the low B condition strongly induces the expression of *BjuA03BOR1a* in root tissues. On the contrary, the expression of *BjuB08BOR1b* was unaltered in roots under the low of B (Figure 2.23A). Like *BjNIP5_1s*, *BjuA03BOR1* gene also contains a WRKY binding domain in the upstream region. The analysis of the upstream region of *BnBOR1;1c* between low B efficient (QY10) and sensitive (W10) *B. napus* genotypes revealed the presence of *WRKY* genes and the enhanced expression of both in roots and shoots of the low B efficient QY10 (Chen et al., 2018). The presence of similar WRKY binding domain in the upstream region of *BjuA03BOR1*, and its increased expression suggests that the expression of *BjuA03BOR1a* may be regulated in a similar way to the *BnBOR1;1c*.

AtBOR4, a clade II BOR-transporter, is localized on the distal plasma membrane domain of the epidermal cells for the directional export of B from roots to the soil under toxic B concentration (Miwa et al., 2007). BOR4 T-DNA insertion mutants showed retarded plant growth and accumulated higher B concentration in tissues than the wild-type plants under toxic B supply

(Miwa et al., 2014). Interestingly we have identified two homologs of AtBOR4 in *B. juncea*. The sub-genome A orthologue which was present in *B. napus* was present in two copies in chromosomes A02, and A06 in *B. juncea*. Since B transport by BOR4 is required for the effective B toxicity tolerance in *A. thaliana*, the exploration of these two homologs in *B. juncea* may be crucial to unveil its function under B toxicity. However, further research is necessary to ascribe which *B. juncea* BOR transporter is involved in the B toxicity tolerance.

Chapter III

Contrasting responses of Indian mustard genotypes to low boron condition at vegetative stage

3.1 BACKGROUND

Boron (B) is an essential micronutrient required for the optimal growth and development of plants. Often, seed yield and quality are compromised in plants grown under limited soil B availability. Indian mustard (*Brassica juncea* L.) has a relatively high demand for internal B and is, therefore, one of the most susceptible plants to B deficiency. However, genetic improvement studies are currently limited because the bioavailability of B is challenging to control in addition to the complex genome architecture of *B. juncea*. Thus, identifying new cultivars of *B. juncea* for low B soil requires a more comprehensive understanding of B deficiency responses. Hydroponic media experiments were conducted to screen twenty-seven Indian mustard genotypes under different B concentrations, and performances of the genotypes were evaluated based on the taproot length. Significant alterations of physiological responses, conditioned to low B levels, have been observed at the early vegetative stages of several *B. juncea* genotypes. B-efficient cultivar Geeta was more tolerant to low B, with very mild symptoms and a higher growth rate. Also, root meristem cells in B-efficient cultivar were more viable, and less reactive oxygen species (ROS) activity has been observed than B-inefficient cultivar, Maya. FTIR data have demonstrated the modified composition of pectin, cellulose, and callose among contrasting genotypes under different B levels. Furthermore, the low B condition has altered the expression profile of the major B transporters among the genotypes.

3.2 MATERIALS AND METHODS

3.2.1 Plant material and treatment

Twenty-seven genotypes of mustard procured from Directorate of Rapeseed/Mustard Research (DRMR), Rajasthan, India were used in this study. Seeds were surface sterilized using 0.05% (w/v) mercuric chloride for 10 min and washed 3 times in sterile deionized water and dried on sterile filter paper. The seeds were then germinated on moistened filter paper for five days in the dark. The germinated seedlings with uniform root length were selected and grown in Hoagland solution (Hoagland and Arnon, 1950) at two varying B concentration: 0.46 µM B (B deficient); 46 µM B (B sufficient; control treatment). Previously, we determined 1/100th of the B sufficient concentration, i.e., 0.46 µM B induced B deficiency symptoms in *B. juncea* genotypes. The

seedlings were first transplanted into planton boxes (Tarson, Kolkata, India) with 1/4th strength Hoagland solution with respective B concentration as described in previous literature (Pan et al., 2012). The plants were cultivated for 5 days in an illuminated culture room at 22^0C under a 16/8 h day/night photoperiod with a photon flux density of 300–360 μmol m^{-2} s^{-1}. Then, the roots were carefully rinsed with deionised water, and the plant were transferred to ½ strength Hoagland solution with respective B concentration for 5 days. Finally, the plants were shifted to full strength Hoagland solution with respective B concentration and the nutrient solution was replaced every five days. The shoots and roots were harvested separately after the plants had grown with 3-4 leaves for about 20 days. The experiment was designed in a completely randomized block with three treatments, and each treatment was replicated three times with each replication containing five seedlings. The pH was maintained at 5.8 every day using 0.5 M H_2SO_4 or 1 M NaOH.

The plant samples were divided into three groups, first one to determine biomass and B concentration, the second was immediately frozen in liquid nitrogen for cell wall extraction and component analysis, and the third was used for the B transporters gene expression analysis.

3.2.2 Plant Sampling and B Analysis

Individually separated youngest opened leaves (YOL) and root samples were dried in an oven at 65° C until it reaches a constant weight. Dried plant samples were then dry ashed at 550° C for 4 h and dissolved in 0.1 M HCl. The suspension was centrifuged to avoid any insoluble matters, and the supernatant was used to determine the B concentration spectrophotometrically by azomethine-H at 420 nm (Wolf, 1971). The pectin (CDTA and Na_2CO_3-soluble) fraction was directly used to determine the B concentration.

3.2.3 Preparation of the cell wall materials

The YOL and roots were separated from the rest of the plant parts and washed thoroughly with deionized water. Samples from each treatment were pooled, frozen in liquid nitrogen, and ground into a fine powder with a mortar pestle. The cell wall materials (CWM) from the homogenized samples were extracted using the previously described method (Hu and Brown, 1994). Briefly, 1 g of homogenized samples were washed with 10 ml ice-cold HEPES buffer (pH 7.0) containing 2 mM potassium metabisulfite. The suspension was then ultrasonicated at 0.5 cycles with 50%

amplitude in the Hielscher ultrasonic device (model UP200S, Hielscher Ultrasound Technology, Brandenburg, Germany), by immersing in an ice bath. After ten cycles of sonication for 5 min each, the suspensions were centrifuged at 5,000 ×g for 10 min. The insoluble pellet was then washed twice with 10 ml of ultrapure water and centrifuged again at 5,000 ×g for 10 min. Finally, the residue was sequentially washed with ice-cold 80%, 95%, 100% (v/v) ethanol, chloroform: methanol (1:1, v/v), and acetone (80% v/v). The air-dried pellet, designated as an alcohol insoluble residue (AIR), was used for further analysis. All the procedures were carried out in the polyethylene vessels. The CWM was divided into three portions: the first portion was used for estimation of B by drying to ashes at 550°C for 4 h. The second and third portions were used for fractionation and determination of cell wall pectin and FTIR analysis, respectively.

3.2.4 Sequential chemical extraction of cell wall pectin

Chemical fractionation of cell wall pectin from AIR was conducted by using trans-1,2-diaminocyclohexane-N,N,N′,N′-tetraacetic acid (CDTA), and Na_2CO_3, as described by Wu et al (2017). The AIR was sequentially extracted with sodium acetate buffer (50 mM, pH 6.5) containing 0.05 M CDTA for 12 h at 24°C in a horizontal shaker. The suspension was then centrifuged (5000 × g, 5 min), and the collected supernatant was designated as a CDTA-soluble pectin fraction. The CDTA-insoluble residue was washed twice with an extraction solution (sodium acetate buffer, 50 mM, pH 6.5) and transferred into the new tube. The chelated pectin was estimated from the CDTA fraction, and the residue was used to extract alkali-soluble pectin. The CDTA-insoluble pellet was then resuspended in 100 mL Na_2CO_3 (50 mM) and incubated for 12 h at 24°C. The Na_2CO_3-soluble pectin fraction was collected after centrifugation at 5,000 ×g for 20 min at 4°C. Both CDTA and Na_2CO_3-soluble fractions are used to determine the concentrations of pectin and B.

3.2.5 Determination of Uronic Acid (UA) and the Degree of Methylation (DM) of pectin

Galacturonic acid, one of the major uronic acids, is a principal component of pectic polysaccharide rhamnogalacturonan, and the pectin content can therefore be presented as GalA equivalents. The uronic acid (UA) contents in the cell walls were determined by dissolving the CWM in concentrated sulphuric acid (Hu et al., 1996). The aliquotes were then assayed using the m-hydroxy

diphenyl colorimetric method as per the procedure described by Blumenkrantz and Asboe-Hansen (1973). A standard curve was plotted with galacturonic acid and the UA content was estimated by comparison with the standard curve of GalA.

Colorimetric quantification of methanol is used to determine the degree of methylation (DM) of pectins. The DM in CDTA and Na_2CO_3-soluble pectin fractions was determined by saponification of AIR and enzymatic oxidation of methanol released by alcohol oxidase as per the alcohol oxidase/N-methylbenzothiazolinone-2-hydrazone (MBTH) method described by Anthon and Barrett (2004). Briefly, 100 µl of pectin fractions were saponified by 50 µl of 1.5 M NaOH solution for 30 min at 25°C in order to release the methanol from pectins, followed by the addition of 55 µl of 0.75 M H_2SO_4 to neutralize the excess alkaline, 200 µl of 0.2 M Tris base (pH 7.5), 80 µl of MBTH (3 mg/ml), 20 µl of alcohol oxidase (AO, 0.01 U/µl), and then the mixture was incubated for 20 min at 30°C. The reaction was terminated by adding 400 µl of ammonium ferric sulphate (5 mg/ml) and sulfaminic acid, and incubating for 20 min at room temperature. Finally, the reaction mixture was diluted with water to 2 ml, and the absorbance was measured at 620 nm by using a Spectrophotometer.

3.2.6 Cell viability and localization of Reactive Oxygen Species (ROS) in root tips

Cell viability of mustard root tips has been earlier demonstrated by dual staining of fluorescein diacetate–propidium iodide (FDA–PI) using the methods described by Ishikawa and Wagatsuma (1998). The FDA (Sigma) stock solution was prepared by dissolving 5 mg/ml in acetone, and the working solution was freshly prepared by adding 4 µl of stock to 1 ml of Dulbecco's phosphate-buffered saline (DPBS). 0.1 mg of PI (Sigma) was dissolved in 5 ml of DPBS and used as a stock solution. Taproots were excised from the respective mustard genotypes, washed well in deionized water, and stained for 10 min with the FDA (20 µg/ml) and PI (5 µg/ml). The stained roots were then rinsed with deionized water thrice and observed under confocal microscopy (JSM-7610F) under excitation filter, 450-490 nm, and barrier filter, 520 nm.

H_2O_2 was detected in mustard root tips by incubation with 25 µM 2,7-dichlorofluorescein diacetate (DCF-DA) (Sigma) for 30 min and then washed in distilled water (Rodríguez-Serrano et al., 2006). DCF-DA is commonly used as a marker of oxidants and has increased sensitivity for H_2O_2 over

the free radicals (Rodríguez-Serrano et al., 2006). After three consecutive washes with double-distilled water, the specimens were examined under a confocal laser scanning microscope (JSM-7610F; 485 nm excitation, 530 nm emission). The fluorescence intensity was quantified using ImageJ software (Shihan et al., 2021).

3.2.7 Cell wall composition analysis by Fourier-Transform Infrared Spectroscopy-Attenuated Total Reflectance (FTIR-ATR)

FTIR-ATR spectra obtained from dried root powders of the contrasting mustard genotypes, grown in different B concentrations, were compared for the difference in cell wall composition. The spectral range (400-4000 cm^{-1}) was recorded with a resolution of 4 cm^{-1} and 32 scans per sample. Each sample was subjected to background scanning before analysis. FTIR spectral baseline was corrected to determine the peak value and absorbance with a PerkinElmer Spectrum two (PerkinElmer, Singapore). The spectra of cell walls with different B treatments were normalized, and graphical data were processed with PerkinElmer Spectrum Analyst version 10.4.3 software.

3.2.8 RNA isolation and Real-time RT-PCR for B transporters expression analysis

The relationships between the B efficiency of *B. juncea* genotypes and B transporter expression were examined using the qRT-PCR experiment. The *B. juncea* genotypes cultivated for 30 days in hydroponic solution with varying B concentrations were included in this experiment. Total RNA was isolated from contrasting mustard genotypes using the RNeasy Plant Mini Kit (Qiagen, Netherlands) following the manufacturer's instructions. Two micrograms of total RNA from roots were used as a template for the RT reaction. Total RNA was added to a mixture containing 1 µl of 50 µM oligo(dT) primer, 1 µl of 10 µM dNTPs, 1× Primescript buffer, 20 units of RNase inhibitor, and 200 units of Primescript reverse transcriptase (Takara, Shiga, Japan). The reaction was carried out at 42°C for 60 min, followed by a 10 min step at 70°C and then by cooling to 4°C. Realtime RT-PCR was performed in a Qiagen Rotor-Gene Q (Maryland, USA) using PowerUp™ SYBR™ Green Master mix (Applied Biosystems, USA) according to the manufacturer's protocol 50°C for 2 min 95° C for 2 min, 60° C for 30 s (50 cycles). The *B. juncea* endogenous reference gene (tubulin) was used as an internal control. All the assays were repeated at least three times. (The primers used is listed in the section *List of primers*).

3.2.9 Statistical analysis

All the results are represented as mean ± SD. Statistical analyses of data were carried out by unpaired t-test at $P < 0.05$ level.

3.3 RESULTS

3.3.1 Plant growth, biomass and B concentration

In this chapter, we established a hydroponic based growth cultivation system in which Indian mustard genotypes can be grown in Hoagland's medium in hydroponic system with clearly defined B concentrations. Based on the preliminary screening of effect of varying B concentrations on plant growth, we selected 0.46 µM B to serve as B deficient concentration based on the criteria that it has B levels 1/100th that of the B sufficient concentration (46 µM B) and it induced B deficiency symptoms in *B. juncea* genotypes. *B. juncea* seedlings grown on B deficient (0.46 µM B) medium showed strong B deficiency symptoms across the 27 genotypes except that in Geeta, with apparent impaired leaf elongation, reduced shoot and root growth, and retarded biomass (Figure 3.1). These low B sensitive genotypes exhibited reduced leaf area, retarded root growth, and arrested emergence of new leaves. The deficiency symptoms were markedly more severe in the sensitive genotype, Maya (Figure 3.1). The relative plant growth in five B-efficient genotypes viz., Geeta, DRMRIJ31, Kranti, Laxmi, and PJ, in B deficient condition was significantly higher than that of low B-sensitive genotypes. On the contrary, the plant growth was normal in B-sufficient condition, in all the tested genotypes.

Root length of all the twenty-seven mustard genotypes was negatively influenced by the low B condition (Figure 3.2). The five B-efficient genotypes (Geeta, DRMRIJ31, Kranti, Laxmi, and PJ) however, maintained better root growth as compared to low B-sensitive genotypes, under low B condition (Figure 3.2). Significantly reduced root length and fewer lateral roots were noted in the genotype, Maya under low B condition. Based on the root growth response to low B condition, we classified the genotypes into six groups, the genotypes with root growth inhibition (RGI) <0% as very efficient, 0-19% RGI as efficient, 20-49% RGI as moderately sensitive, 50-69% RGI as sensitive, and >70% RGI as very sensitive (Table 3.1). The genotypes with <0% RGI was classified as tolerant (Geeta), 20-49% RGI as moderately sensitive (RH406), and >70% RGI as

sensitive (Maya) (Table 3.1). These contrasting genotypes identified in our studies are different from those described in previous screenings (Stangoulis et al., 2000 a, b).

Significant variation in root and shoot dry weight was observed when *B. juncea* genotypes were grown in low B concentration (Figure 3.3). The root and shoot dry weight, and the shoot length at low B condition were significantly higher in the genotype, Geeta, compared to other two contrasting genotypes, Maya and RH406 (Figure 3.3). The low B inefficient genotype, Maya showed 52.42% less root growth and 24.57% less shoot growth than the low B efficient genotype, Geeta (Figure 3.3).

Under low B condition, the tissue (root or leaf) B concentration declined than those grown under B sufficient condition (Figure 3.4). However, the tissue B content decreased under low B condition in other two contrasting genotypes, Maya and RH406 (Figure 3.4). In Geeta, the B content in root CWM, its pectin fractions and root biomass were significantly higher than low B inefficient genotype Maya (Figure 3.4). The B content in leaf CWM and its pectin fraction in low B-efficient genotype Geeta was however significantly higher under low B condition, as compared to low B-inefficient genotype Maya (Figure 3.5).

Figure 3.1: Growth variations of Indian mustard genotypes. Physiological growth three contrasting genotypes Geeta (B-deficiency tolerant), RH406 (B-deficiency moderative sensitive) and Maya (B-deficient sensitive) under two different B concentration: B deficient (0.46µM) and B sufficient (46µM). Scale bar 1cm.

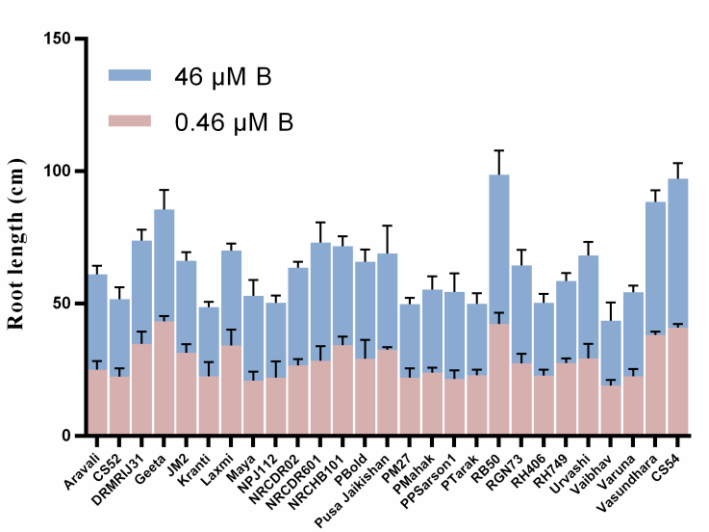

Figure 3.2: Root length variations of Indian mustard genotypes under different B concentrations. Taproot length of the 27 Indian mustard genotypes under two different B concentration: B deficient (0.46 µM) and B sufficient (46 µM).

Genotype	Percentage of root inhibition	Rank	Genotype	Percentage of root inhibition	Rank
Aravali	-30.05	3	PM27	-20.30	3
CS52	-23.39	3	PMahak	-23.34	3
DRMRIJ31	-10.76	2	PPSarson1	-34.34	3
Geeta	2.43	1	PTarak	-14.85	2
JM2	-9.66	3	RB50	-24.95	3
Kranti	-14.09	2	RGN73	-26.02	3
Laxmi	-4.41	2	RH406	-29.44	3
Maya	-47.27	4	RH749	-10.88	2
NPJ112	-21.71	3	Urvashi	-24.61	3
NRCDR02	-27.72	3	Vaibhav	-22.35	3
NRCDR601	-36.30	3	Varuna	-28.65	3
NRCHB101	-8.31	2	Vasundhara	-23.98	3
PBold	-20.19	3	CS54	-27.09	3
PJ	-10.56	2			

Table 3.1: Root growth inhibition of Indian mustard genotypes. Effect of B concentrations on tap root length of 27 *B. juncea* genotypes hydroponic culture. Root growth inhibition percentage between 46µM B and 0.46µM B. Rank for boron use efficiency is arbitrarily divided into six as follows: <0% (1, very efficient), 0 to -19% (2, moderately sensitive), -20 to -49% (3, very sensitive).

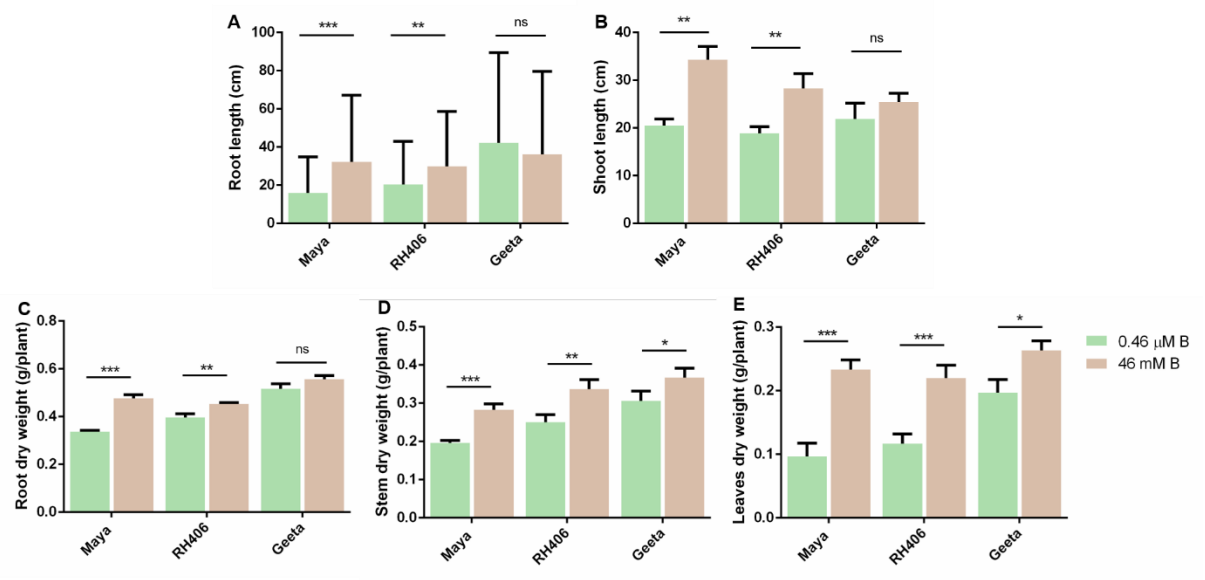

Figure 3.3: Growth rate of Indian mustard genotypes. Root, shoot length and dry weight differences depicted for the three contrasting genotypes. Root (A), shoot length (B) and dry weight (C-E) differences demonstrated that the B-deficient tolerant cv. Geeta can perform better under B-deprived media than others. Data represents mean values (n = 3) ± SD, where n is the number of times experiment repeated and SD denotes Standard Deviation. An asterisk indicates significant differences from non-transgenic plants (Student's t-test, $p < 0.05$).

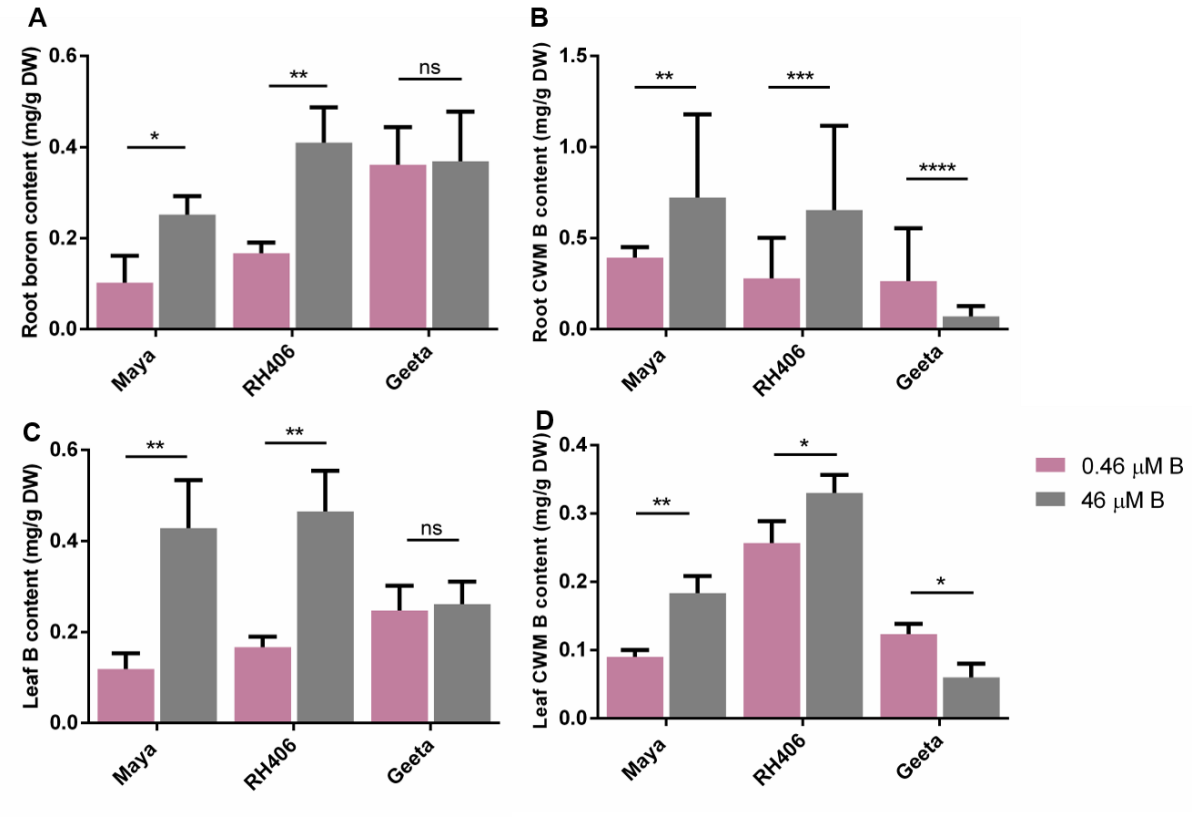

Figure 3.4: Difference in B content among the Indian mustard genotypes grown under varied B conditions.

The differences in B concentration in root (A), leaf (C), root (B) and leaf CWM (D) of low B inefficient (Maya), moderately efficient (RH406) and low B efficient (Geeta) genotypes demonstrated that the B-deficient tolerant cv. Geeta can perform better under B-deficient media than others. Data represents mean values (n = 3) ± SD, where n is the number of times experiment repeated and SD denotes Standard Deviation. An asterisk indicates significant differences from non-transgenic plants (Student's t-test, $p < 0.05$).

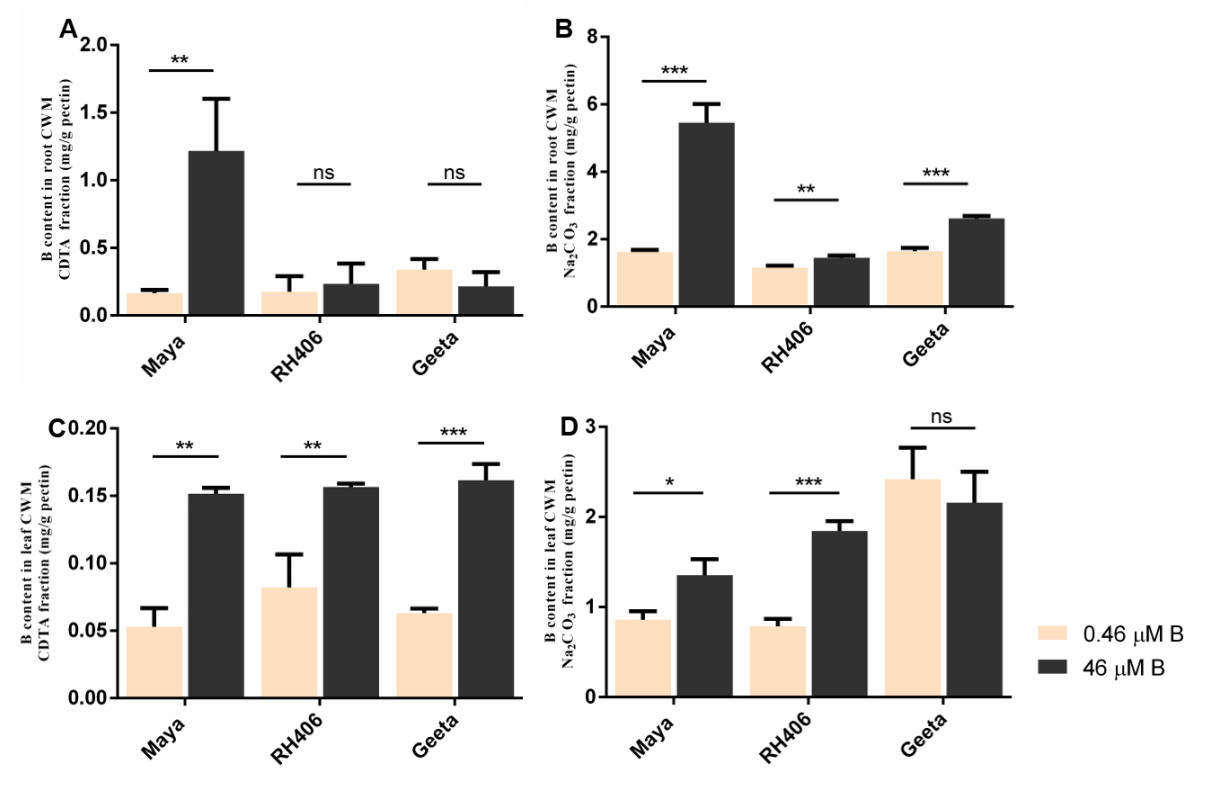

Figure 3.5: Difference in B content in the pectin fractions among the Indian mustard genotypes grown under varied B conditions.
The differences in B concentration in root (A, B) and leaf (C, D) pectin fractions of low B inefficient (Maya), moderately efficient (RH406) and low B efficient (Geeta) genotypes demonstrated that the B-deficient tolerant cv. Geeta can perform better under B-deficient media than others. Data represents mean values (n = 3) ± SD, where n is the number of times experiment repeated and SD denotes Standard Deviation. An asterisk indicates significant differences from non-transgenic plants (Student's t-test, $p < 0.05$).

3.3.2 Changes in Uronic Acid (UA) and Degree of Methylation (DM)

The percentages of uronic acid (UA) in CDTA and Na_2CO_3 soluble pectin from the root cell walls decreased under low B condition, in both the contrasting genotypes (Geeta and Maya), suggesting the inhibition of the synthesis of the two different kinds of pectin and the decrease in the binding sites of B in cell walls under B deficiency. The decrease in the UA is relatively similar in both of the pectin fractions (Figure 3.6). However as evident from the bar graph (Figure 3.6), the UA

increased to 17.18% in the low B-efficient genotype, Geeta under low B condition. The degree of methylation (DM) in CDTA pectin fractions of all the genotypes, increased possibly due to loss of cell wall integrity induced by the B deficiency (Figure 3.7). Compared to the low B-efficient genotype, Geeta, the DM was significantly higher in Maya.

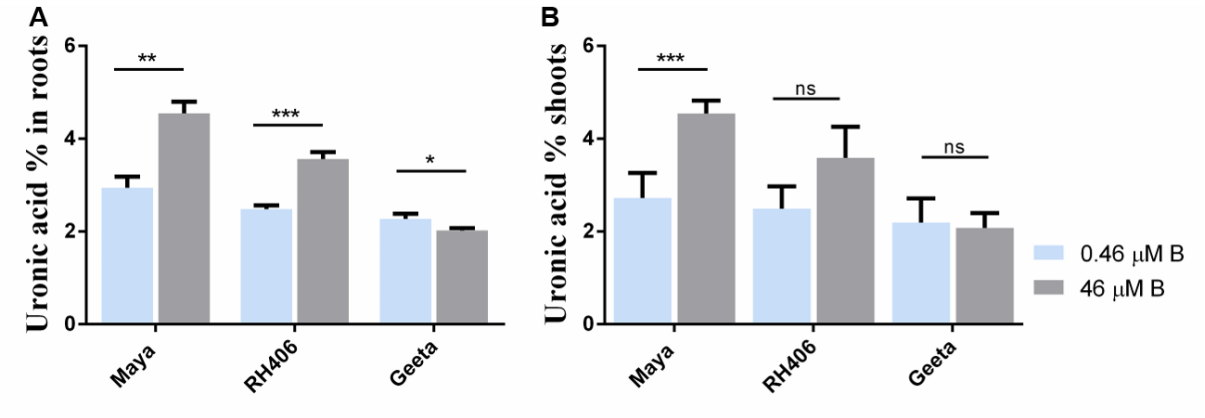

Figure 3.6: Difference in uronic acid (UA) percentages in root and shoot tissues among the Indian mustard genotypes grown under varied B conditions.

The differences in UA% in root (A) and leaf (C) pectin fractions of low B inefficient (Maya), moderately efficient (RH406) and low B efficient (Geeta) genotypes demonstrated that the B-deficient tolerant cv. Geeta can perform better under B-deficient media than others. Data represents mean values (n = 3) ± SD, where n is the number of times experiment repeated and SD denotes Standard Deviation. An asterisk indicates significant differences from non-transgenic plants (Student's t-test, $p < 0.05$).

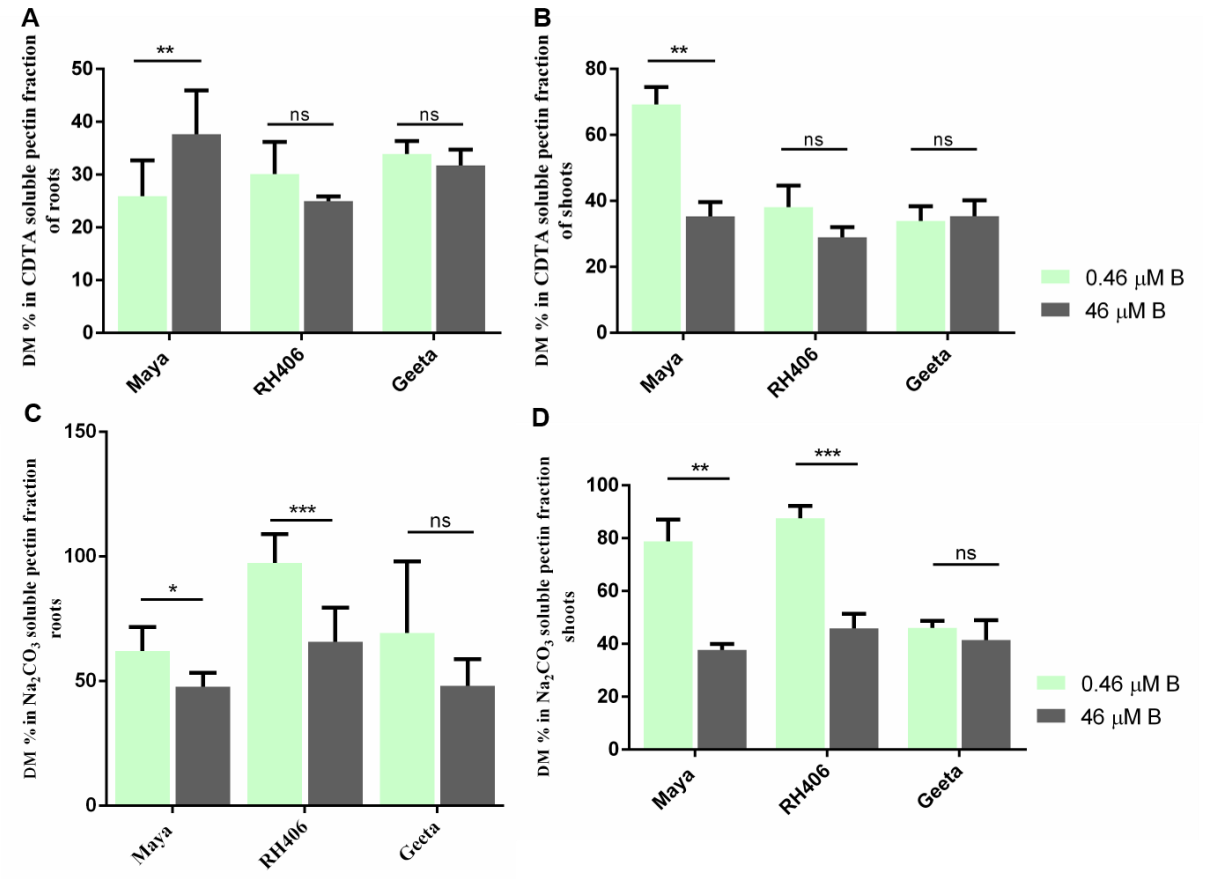

Figure 3.7: Difference in degree of methylation (DM) percentages in root and shoot tissues among the Indian mustard genotypes grown under varied B conditions.

The differences in DM% in CDTA and Na_2CO_3 pectin fractions of root (A, B) and leaf (C, D) pectin fractions of low B inefficient (Maya), moderately efficient (RH406) and low B efficient (Geeta) genotypes demonstrated that the B-deficient sensitive cv. Maya have more cell wall damage under B-deficient media than others. Data represents mean values (n = 3) ± SD, where n is the number of times experiment repeated and SD denotes Standard Deviation. An asterisk indicates significant differences from non-transgenic plants (Student's t-test, $p < 0.05$).

3.3.3 Histochemical observation of cell viability and ROS accumulation

Exposure to low B condition resulted in cell death in all three contrasting genotypes, as evident from increased red fluorescence and across the root length (Figure 3.8 and 3.9). Similarly, low B condition compared to the control treatment, induced enhanced ROS accumulation in all the three contrasting genotypes, exhibiting strong fluorescence in the root tips (Figure 3.10 and 3.11).

Among the contrasting genotypes, the low B efficient genotype Geeta showed minimal cell death and lower ROS accumulation in the root tips whereas the oxidative damage was much higher in low B inefficient genotype Maya.

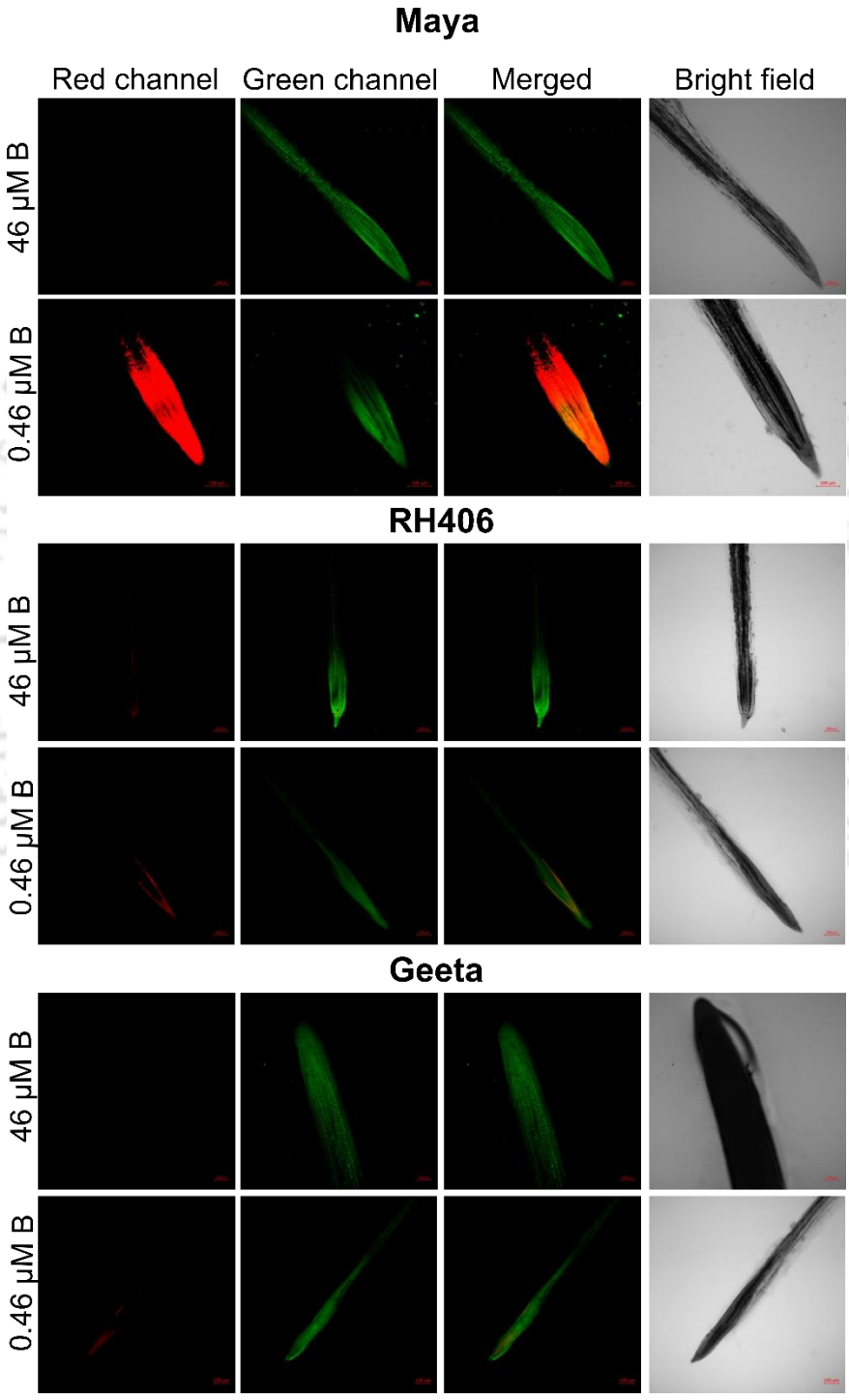

Figure 3.8: Effects of different B concentration on viability of root tips visualized by confocal microscopy of contrasting Indian mustard genotypes. The roots were stained with FDA-PI. Green and red fluorescence shows viable and dead cells respectively. (Scale bar 100 µm). The live and dead cell fluorescence clearly demonstrates that the B-deficient sensitive cv. Maya have more dead cells under B-deficient media than others.

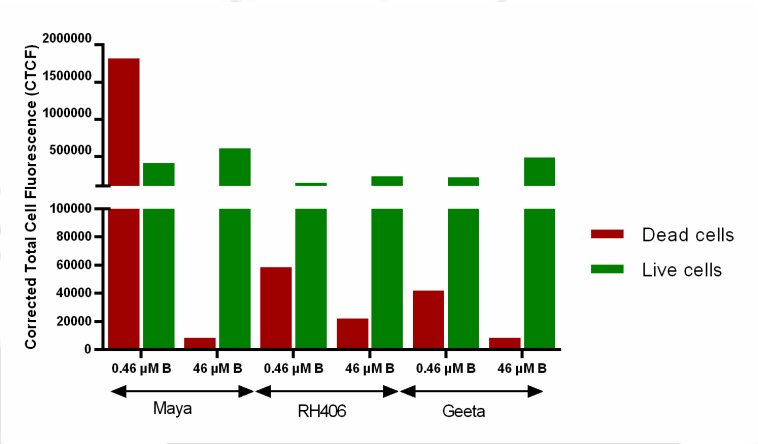

Figure 3.9: Effects of different B concentration on the corrected total cell fluorescence (CTCF) obtained using ImageJ software. Green and red bar diagram shows live and dead cells respectively.

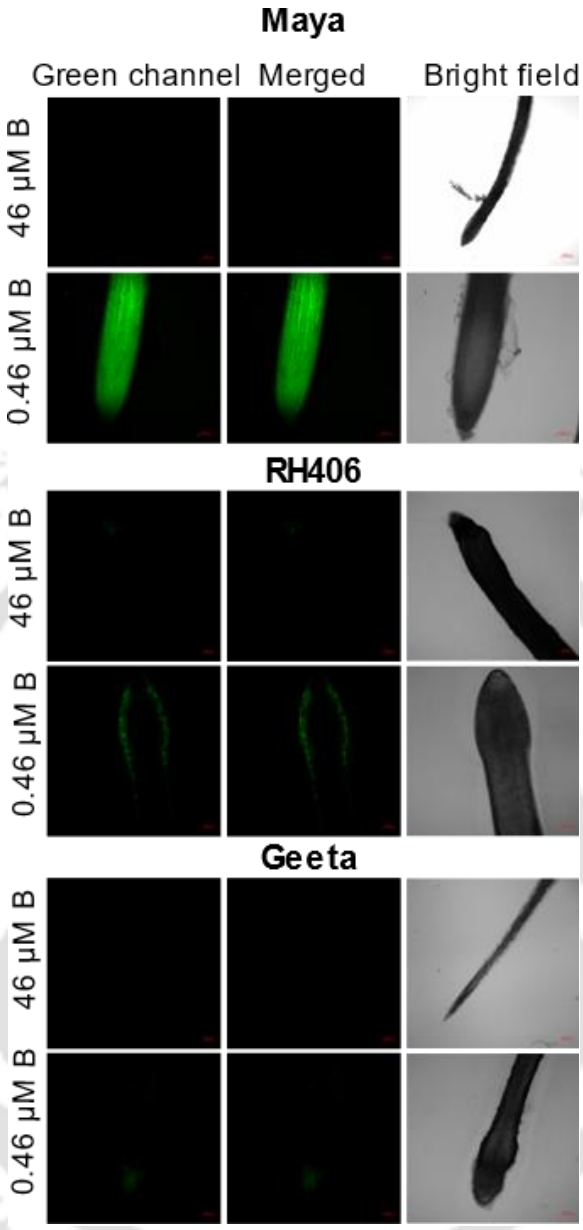

Figure 3.10: Localization of ROS in roots of contrasting Indian mustard genotypes in different B levels visualized by confocal microscopy. The roots were stained with DHFDA. Intensity of green fluorescence can be directly related to the ROS accumulation. Fluorescence indicates the presence of ROS. (Scale bar 100 µm).

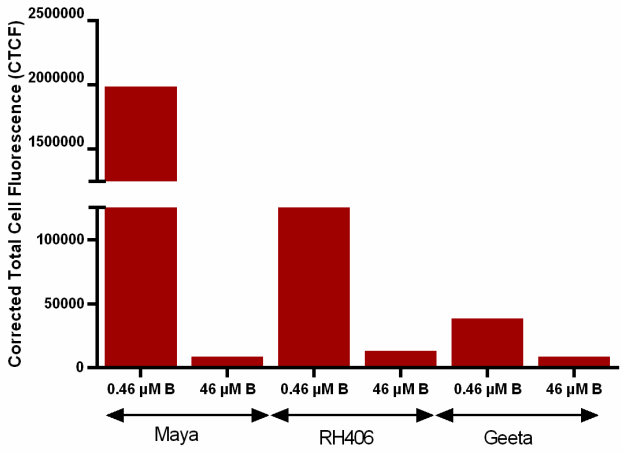

Figure 3.11: Effects of different B concentration on the corrected total cell fluorescence (CTCF) obtained using ImageJ software. Red bar diagram shows the intensity of ROS accumulation.

3.3.4 FTIR analysis of root cell wall composition

FTIR analysis was carried out to see the effect of low B concentration on the root cell wall composition. The difference in the FTIR spectrum of the root cell wall of contrasting genotypes under different B concentrations, between 4000 and 400 cm^{-1} as the vibration of chemical bonds absorbs radiation in the IR region and each functional group in a molecule has its characteristic absorption frequencies in the IR spectrum. After chemical extraction of root cell walls, components and possible cross-links of each fraction were identified by FTIR microspectroscopy. The result showed that the relative absorbance corresponding to characteristic peaks of cell wall in B-deficient roots was higher than that in control roots. The characteristic absorption peaks significantly changed in the FTIR spectrum of the root cell wall under low B condition, which were indicative of differences in the structure and composition of the root cell walls between B sufficient and B deficient conditions in contrasting genotypes. Absorption bands located around 3400 cm^{-1} correspond to O-H and N-H stretching vibrations, this characteristic band value indicated the hydrogen bonding in hydroxyl groups predominantly occurring in carbohydrates (Yang and Yen, 2002). In low B condition, the intensities of absorbance particularly in carbohydrate fingerprint region (900-1200 cm^{-1}) were altered among all the genotypes as compared to B sufficient condition in root cell walls indicating carbohydrate content was relatively

modified in the B-deficient root cell walls (Figure 3.12). The stretching of vibration peaks near 3342 cm^{-1} typical of OH- stretching vibration due to callose, in root cell wall under low B condition suggested the accumulation of callose in root cell walls of low B inefficient genotype (Figure 3.12). The positions of the most characteristic bands for lignin in the fingerprint regions ~1600 cm^{-1} (for aromatic skeletal vibrations), indicated a clear connection between absorbance differences in B-deficiency induced lignin contents (Figure 3.12). In B-deficient plant root cell walls, the spectra had enhanced relative absorbance at ~1,740 cm^{-1} (Figure 3.12), typical characteristic of the C=O stretching vibration of alkyl-esters in pectin, in low B efficient genotype Geeta (Abidi et al., 2008). Low B condition significantly increased the relative concentration of cellulose as indicated by the enhanced absorption peaks in the characteristic polysachharide fingerprints in the root cell wall (Figure 3.12). B deficiency significantly increased the relative concentration of cellulose as evident from enhanced characteristic peak at 1,032 cm^{-1} (Abidi et al., 2008) in all the contrasting mustard genotypes (Figure 3.12). The spectra of the cell walls from B-deficient roots of low B efficient Geeta showed higher absorbance peaks in the characteristic lignin fingerprint regions (~1600 cm^{-1} for aromatic skeletal vibrations) (Figure 3.12). These results imply that cell wall composition was altered in roots under low B condition with changes more significant in the low B efficient genotype Geeta.

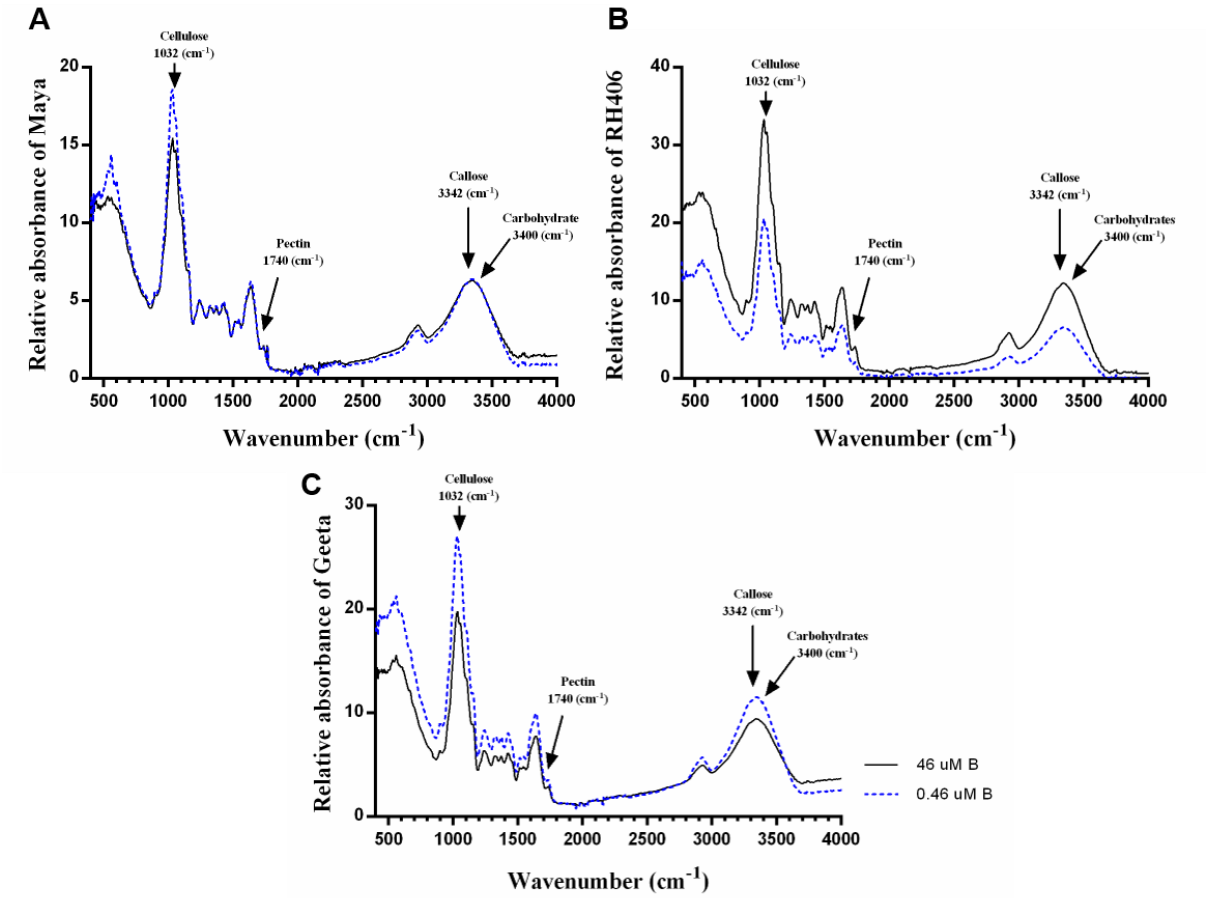

Figure 3.12: Changes in infrared absorption spectra of contrasting mustard genotypes roots under different B concentration. Low B-efficient genotype Geeta showed increased amounts of carbohydrates, pectin, callose and cellulose than other two genotypes.

3.3.5 Expression analysis of B transporters

The most rapid response to B deficiency in vascular plants, is the growth inhibition of roots (Dell and Huang, 1997). Furthermore, B deficiency elicits a decrease in the cell elongation of the primary root (Camacho-Cristóbal et al., 2015). These subtle changes in root architecture seriously affect the ability of plants to take up water and nutrients. The differential B uptake and translocation by plant roots in different species and genotypes are mostly attributed to expression and regulation of B transporters, AQPs and BORs (Matthes et al., 2020). In order to understand the molecular basis of effect of low B condition on B uptake and translocation in roots of contrasting genotypes, we examined the relative expression of major B transporters of *B. juncea* (BjNIP5:1, BjNIP6:1 and

BjBOR1) by quantitative RT-PCR. The expression of these B transporters was detected in the roots of all the three contrasting genotypes under low B as well B-sufficient conditions. However, the expressions of both BjuA03BOR1a and BjuB08BOR1a were downregulated in the roots of both, Geeta and Maya (Figure 3.13). In low B inefficient genotype Maya, the relative expression of all the three BjNIP5;1s tested (BjuA02NIP5_1a, BjuA03NIP5_1b, and BjuA07NIP5_1c) were increased to more than 4-fold (Figure 3.13). Under low B condition, the expression of BjuA07NIP5_1c showed upregulation in Geeta (1.9-folds). Also, the relative expression of BjuB02NIP6_1b gene were downregulated both in Maya and Geeta (Figure 3.13). Since AtNIP5;1, AtNIP6;1, and their orthologs are known to mediate the transport of boric acid (Takano et al., 2006; Tanaka et al, 2008; Yoshinari and Takano, 2017; Onuh and Miwa, 2021), we therefore checked the relative expression of three NIP5;1 genes and a NIP6;1 gene in contrasting genotypes to determine the effect of low B condition. The expression levels of the one gene (BjuA07NIP5_1c) in the genotype Geeta was enhanced under low B condition, whereas in Maya three genes (BjuA02NIP5_1a, BjuA03NIP5_1b, and BjuA07NIP5_1c) were upregulated (Figure 3.13).

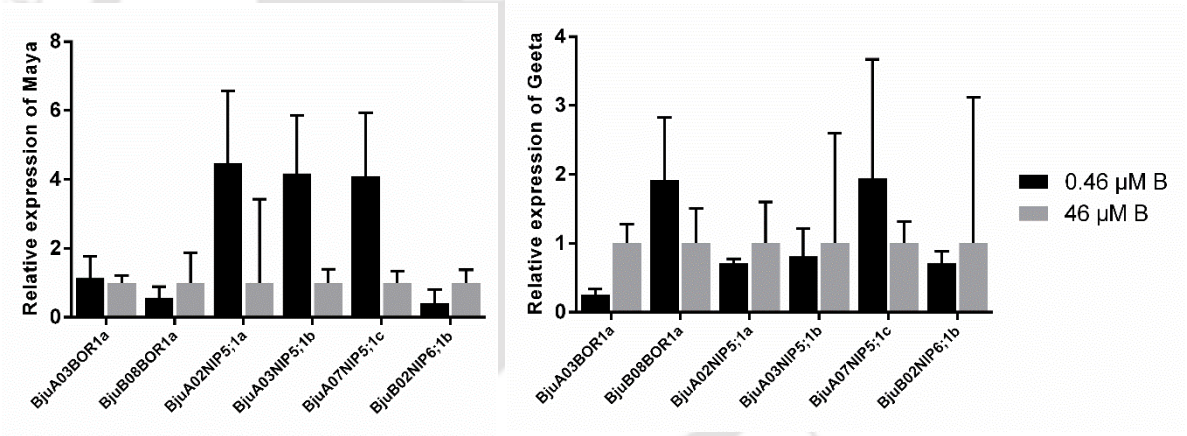

Figure 3.13: Expression analysis by real-time RT-PCR. Total RNA was extracted from the roots of the low B efficient Geeta and Maya genotype and real-time RT-PCR performed by BjuA03BOR1a, BjuB08BOR1a, BjuA02NIP5_1a, BjuA03NIP5_1b, BjuA07NIP5_1c, and BjuB02NIP6_1b gene specific primers. Bjtubulin primers were used as internal control.

3.4 DISCUSSION

B deficiency causes a negative impact on plant growth, development, and performance. The earliest response to B deficiency is the arrest of growth in the meristem regions of the plants rather than mature tissues. The B deficiency thus leads to rapid cessation of cell elongation and cell division (Dell and Huang, 1997; Poza-viejo et al. 2018), in roots and shoots, eventually leading to a decrease in shoot and root biomass. The present study revealed a substantial variation in response to low B condition in 27 *B. juncea* genotypes. B deficiency affected the root growth more than shoot growth which is consistent with observations in other plant species (Dell and Huang, 1997, Camacho-Cristóbal and González-Fontes, 2007). The low B-inefficient genotypes showed significant reduction of root elongation and number of lateral roots, and the symptoms were more severe in the genotype Maya. The genotype Geeta showed obvious higher relative root growth as compared to other low B-efficient genotypes. We found root length as a good indicator of selection in screening genotype response to B deficiency, and this study indicates that B efficiency in *B. juncea* depends primarily on the roots. Our results are in accordance with similar observations in wheat (Chantachume et al., 1995; Jamjod et al., 2004; Campbell et al., 1998). The low B-efficient genotypes identified in our study have not yet been described earlier. B deficiency possibly modifies the dynamic root architecture, by increasing root length due to root meristematic cell elongation and division, and lateral root formation in low B-efficient genotypes, which influences their adaptation to low B availability (Zhang et al. 2009; Hodge et al. 2009). Increased root length and dense lateral roots provide low B-efficient genotypes a competitive advantage for B uptake deeper in the root zone under limiting B condition. Both root and shoot growth were severely restrained by low B, accompanied by a concomitant reduction in dry weight in low B-inefficient genotype Maya (Figure 3.3). The effects of B on root and shoot dry weights were the reflection of B effects on their growth.

Plant B is primarily involved in the structural function in the primary cell wall by cross-linking the apiosyl residues of two rhamnogalacturonan II (RG-II) pectic subunits and thus physiologically important for the stability of the cell wall (Ishii and Matsunaga, 1996; Kobayashi et al. 1996). Both cell wall biosynthesis and stability being essential for proper plant development therefore, B has to be continuously transported from the soil through the root and vascular tissues to growing tissues by directional cell to cell transport. In our study, we found that B concentrations were higher in leaves than roots in genotypes Maya and RH406, under both B deficient and B sufficient conditions

implicating an elevated B demand in leaves of low B-sensitive genotypes of *B. juncea* (Figure 3.4). These results also indicated that under low B condition, the B was preferentially distributed to leaves of B-sensitive genotypes. However, the B-efficient Geeta accumulated more B in root tissues than shoots under low B condition. These results suggested that the B uptake and transport mechanisms in low B contrasting genotypes, are not main factors for B efficiency.

The B and pectin content of the root- and shoot cell wall decreased significantly under low B condition. The comparison of the cell wall compositions of the two low B contrasting *B. juncea* genotypes revealed that low B inefficient Maya had significantly higher proportion of root cell wall B and pectin than that of low B efficient Geeta (Figure 3.4). This suggests low B inefficient Maya preferentially fixes root B to cell walls under B starvation and thus possibly has high physiological B requirements for optimal root growth and development. Significantly higher pectin content in shoot cell wall of low B efficient Geeta under low B condition was found compared to low B inefficient Maya (Figure 3.5).

Pectins are an important group of polymers in the primary plant cell wall which act as a gel, forming an amorphous substrate into which cellulose and hemicelluloses structural network are embedded. The three domains of pectin molecules are homogalacturonan (HG), rhamnogalacturonan I (RG-I), and rhamnogalacturonan II (RG-II) that are covalently linked to each other. HG pectin is the most abundant form representing more than 60% of cell wall pectins (Caffall and Mohnen, 2009). RG-I pectins are very complex and highly versatile, which act as a scaffold to covalently bind the two other pectic polysaccharides of HG and RG-II, forming the pectin matrix (Vincken et al., 2003). RG-II is the highly branched domain of pectin polysaccharides with a very complex structure, the borate cross-links RG-II monomers of pectic polysaccharides, and this forms a network which increases the stiffness of the wall and decreases its porosity (Dumont et al., 2014; Funakawa and Miwa, 2015). The CDTA- and Na_2CO_3-soluble fractions represents the ionically and covalently bound pectic polysaccharides, respectively. Low B condition increased the UA content in CDTA-soluble fractions in low B inefficient Maya while increased UA content was observed in the Na_2CO_3-soluble fractions of low B efficient Geeta (Figure 3.6). Overall water insoluble pectic polysaccharides content was more in Geeta under low B condition. In plants insoluble B is the functional form which are found predominantly bound to the cell wall while the soluble B represents the surplus and the mobile form. The insoluble B

molecular entity is the borate diester with RG-II regions of pectic polysaccharides. Our results suggest that low B condition increased the pectin concentration under low B condition and proportion of B cross-linking with RG-II (Ishii et al., 2001).

Plant cell walls are composed of diverse polymers (polysaccharides and proteins) with unique molecular confirmation (Séné et al., 1994). The specific interactions of these cell wall macro molecules and the bonding pattern are important for performance of cell wall. Fourier transform infrared spectroscopy is a reliable method to study the changes in the root cell wall components grown under different media (Yang et al. 2002). Hydrogen bonding is the most predominant type of bonding between the macromolecules (Burgert and Dunlop, 2011), that revolves at about 3430 cm^{-1} in the FTIR spectra (Liu et al., 2014). The FTIR spectra of roots of contrasting genotypes grown under low B condition showed increase in absorption peaks at 3400 cm^{-1} suggesting alteration of the hydrogen bonding pattern associated with mainly protein and carbohydrates. A corresponding decrease in absorbance peaks in low B inefficient Maya indicates the inhibition of the protein synthesis in cell wall under low B condition. As the cell wall proteins contributes mechanical strength, the inhibition of protein synthesis inevitably affected the function and integrity of the cell wall in low B inefficient genotype (Jamet et al., 2006). B deficiency induces subtle changes in the overall carbohydrate metabolism (Chen et al., 2012; Hajiboland et al., 2012). The relative absorbance peaks in the carbohydrate fingerprint region, i.e., 900–1200 cm^{-1}, increased under B deficiency in low B efficient genotype Geeta (Figure 3.12). Low B efficient Geeta showed higher absorbance peaks, especially in the cellulose fingerprint region, than the low B inefficient Maya indicating increase in the root carbohydrates in Geeta primarily to avail more B binding sites in the cell wall whereas corresponding reduction of root carbohydrates in Maya possibly rendered it sensitive to low B condition. With agreement to our results, previous studies have also demonstrated that the B deficiency triggers carbohydrate accumulation in cotton and tobacco (Li et al., 2017; Camacho-Cristóbal et al., 2004). Lignin and callose are complex macromolecules that play an essential role in linking cell wall polysaccharides (Tzin and Galili, 2010). We found B deficiency increased lignin, and callose in cell wall. The B efficient Geeta accumulated higher lignin and callose compared to B inefficient Maya. Two clearly defined absorption peaks were observed at 1593 and 1506 cm^{-1} for aromatic skeleton in lignin. In B efficient Geeta, the absorption peaks at these locations were identified to be higher than Maya. The

participation of B in lignin metabolism in B-deprived roots has been recently reported (Bellaloui, 2012; Dong et al., 2016). Increase in lignin content has been reported in leaf cell walls of a navel orange and roots of rape indicating, their accumulation is critical for the optimal plant growth under B deficiency (Liu et al., 2014; Yang and Yen, 2002). Pectins are the predominant plant polysaccharides made up of (1→4) linked and partially methyl esterified α-d-galacturonic acid. The characteristic peak of pectin is at 1740 cm^{-1}, arising from the ester carbonyl (C=O) stretching of pectin. The relative intensity of the absorption band in this region increased, under low B conditions in B efficient Geeta indicating the strengthening of the C=O stretching vibration of alkyl-esters in pectin, and a significantly positive correlation between B content and pectin in cell walls. The low B condition has increased the pectin content drastically in the cell walls of low B efficient genotypes of maize and wheat (Yu et al., 2002). This increased cell wall pectins improve the mechanical strength by influencing the expansion, thickness and porosity of the cell walls and B-RG-II compounds (O'Neill et al., 2001). The FTIR absorption peak at 1032 cm^{-1} is attributed to C-O-C stretching of cellulose and represented cellulose in the cell walls. B deficiency exhibited significant increase in the intensity in the peak, in low B efficient Geeta. suggesting that B deficiency influenced the accumulation of cellulose in root cell walls of low B efficient genotype. Due to the complexity of the chemical composition in root tissues, FTIR data are usually considered qualitative rather than quantitative, allowing the establishment of a pattern trend for compositional changes in plant cell wall under B deficiency or sufficiency. These results suggested that changes in both cell wall structure and components due to B deficiency were more significant in low B efficient Geeta than low B inefficient Maya.

Plants ensure continuous supply of B for its growth and development through B uptake from the soil, as this element is poorly remobilized in most plant species (Diehn et al., 2019). Efficient delivery of B to tissues with high B demand such as young sink leaves, meristems, or the inflorescences that are mostly low transpiring, becomes a formidable challenge (Brown and Shelp, 1997) as long-distance B transport is mostly through transpiration stream. Its long-distance transport is highly connected to the transpiration stream leading to a quantitatively significant B flow towards fully developed and photosynthetically active source leaves. However, organs and tissues with a high demand for B are in fact mostly low transpiring such as young sink leaves, meristems, or the inflorescences. In order to ensure that irreversible tissue damages not caused by

spatiotemporal B deficiency even under sufficient soil B condition, plants efficiently regulate B fluxes through an elaborate B uptake and translocation mechanisms involving two rapidly regulated transmembrane transporter protein families, namely Boric acids channels of the major intrinsic protein (MIPs) and borate transporters of the BOR family. Under low soil B concentrations, boric acids are taken up into the root cells at soil physiological pH (5-6) with the help of nodulin 26-like Intrinsic proteins (NIPs) subfamily of MIPs, and exported from the cell at cytosolic pH (7.5) by borate exporters of the BOR family. The NIP5;1 belonging to subclass II of NIPs transports boric acid into the root from the soil across the membranes, while BOR1 is involved in the transport toward root stele for translocation to leaves under low B conditions. Both of these transporter families display polar localization, NIP5;1 showing polar localization towards the soil side in root epidermal, endodermal and root cap cells (Takano et al., 2010; Wang et al., 2016) and BOR1 displays polar localization towards the inner/stele side in various cell types in the roots, hypocotyl, and cotyledons (Takano et al., 2010; Yoshinari et al., 2019). The other membrane boric acid channel protein, NIP6;1 is shown to participate in transfer of B from xylem to the phloem in growing shoot tissues in *Arabidopsis* (Tanaka et al. 2008). The synergistic action of NIP5;1 and BOR1 and their homologs ensures uptake, root-to-shoot translocation, and preferential translocation to young portions of shoot in model *Arabidopsis* and other crop plant species (Takano et al., 2006; Miwa et al., 2007; Tanaka et al., 2008; Kajikawa et al.,2011; Miwa et al., 2013; Routray et al., 2018; Shao et al., 2018). The borate exporter BOR4 and its homologs are additionally involved in B exclusion in conditions of excessive B (Miwa et al. 2007; Sutton et al. 2007). In the light of the above knowledge, B transporters BOR1, NIP5;1 and NIP6;1 emerge as the key candidates regulating B uptake and translocation and ion homeostasis under B deficiency (Takano et al., 2006; Tanaka et al., 2008; Hanaoka et al., 2014). In order to understand the molecular basis underlying low B efficiency in *B. juncea*, we investigated differential expression of B transporters. We found alterations in expression profiles of BjBOR1, BjNIP5;1 and BjNIP6;1 in root tissues of *B. juncea* genotypes under both low B and under sufficient B conditions, suggesting that these B transporters were transcriptionally regulated in *B. juncea*. However, negative regulation in the transcription level of these B transporter genes between the two low B contrasting genotypes (Maya and Geeta) were observed. Under low B condition, the transcript abundances of BjBOR1 decreased by 0.37-fold (BjuA03BOR1a) and 0.002-fold (BjuB08BOR1a), in low B efficient genotype Geeta (Figure 3.13). Among the three NIP5;1, the

expression of BjuA02NIP5_1a, BjuA03NIP5_1b and BjuA07NIP5_1c increased by 4-fold respectively in genotype Maya (Figure 3.13). Under low B condition, the A03NIP5_1b downregulated by merely 0.8-fold in genotype Geeta indicating no significant differences between low B inefficient Maya and low B efficient Geeta. However, the further corroboration with the fact that physiological high root tissue B content to the low expression of B transporter genes under low B condition in genotype Geeta need to be explored. On the other hand, the transcript accumulation of BjuB02NIP6_1a downregulated by 0.4 and 0.7-fold in the genotype, Maya and Geeta respectively. AtNIP6;1, is a close homolog to AtNIP5;1, preferentially transport boric acid young developing shoot tissues (Tanaka et al., 2008). However, recently it was identified that BnNIP6;1 is ubiquitously expressed in all the tissues and having diverse function compared to *Arabidopsis* (Song et al., 2021). Whether these differential expressions of key B transporters are involved in the regulation of efficient soil B uptake, tissue accumulation, translocation of B to the growing tissues and homeostasis in low B efficient genotype Geeta, should be investigated further.

Chapter IV

Generation of Indian mustard tolerant to B deficiency by the manipulation of B efflux transporter, AtBOR1

4.1 BACKGROUND

Boron (B) is a plant micronutrient crucial for plants throughout their existence. B deficiency is a widespread agricultural problem worldwide, and it affects the crop yield severely. Indian mustard (*Brassica juncea* L.) is highly sensitive to B deficiency, especially during reproductive growth, as required in enormous quantities for proper fertilization. AtBOR1 encodes an efflux B transporter, involved in xylem loading of B. Earlier researches suggest overexpression of AtBOR1 improved the growth of crop plants under B-deficient conditions. In our current study, we overexpressed AtBOR1 in mustard and attempt to validate its growth under B deficient conditions. Three independent transgenic mustard lines were generated using *Agrobacterium*-mediated transformation. The presence and expression of AtBOR1 in successive generations of transgenic mustard plants were confirmed by polymerase chain reaction (PCR), qualitative, and quantitative PCR analysis. However, in line T_2.3.1, AtBOR1 expressed more than the other two lines: T_2.1.1 and T_2.2.1. Physiological and molecular changes were analyzed by growing transgenic mustard in hydroponic media along with the non-transgenics under B deficiency. As expected, the transgenic plants showed a better relative growth rate than non-transgenics without any typical B deficiency symptoms in deficient B concentration. Cell wall B, uronic acid percentages were relatively higher in transgenic roots and leaves with a low degree of methylation (DM) under B-deficiency. The present study demonstrates that stable expression of AtBOR1 improved growth in mustard under B-deficient conditions.

4.2 MATERIALS AND METHODS

4.2.1 Plant material and plasmid construct preparation

Seeds of Indian mustard (*Brassica juncea L.*) cultivar Maya, obtained from the Indian Agriculture Research Institute, New Delhi, were used. Seeds were surface sterilized with 0.05% $HgCl_2$ (w/v) for 10 min and subsequently rinsed three times with sterile distilled water before being cultured on basal half-strength MS medium (Murashige and Skoog 1962). Explant preparation, transformation, and regeneration were followed as described in Saha et al., 2016. A plasmid carrying the CaMV35S RNA promoter (P35S): AtBOR1 was constructed to transform mustard explants. The AtBOR1 fragment of pAT69 (kindly provided by Prof. Junpei Takano, Osaka Prefecture University, Japan) was amplified by polymerase chain reaction (PCR) using the primers

forward 5`-ATGGAAGAGACTTTTGTGCCGTT-3` and reverse 5`-TCAGTTCGATGACGACTGGTTCAAGG -3`. The amplified fragment was subcloned into pRT101 between PstI and XbaI restriction sites. P35S:AtBOR1: PolyA was then subcloned into pCAMBIA2301 (CAMBIA, Australia). The T-DNA of pCAMBIA2301 (CAMBIA, Australia) contains neomycin phosphotransferase (npt II) gene as a selectable marker driven by cauliflower mosaic virus (CaMV) 35S promoter and polyA terminator. We also have cloned CaMV35S promoter and hygromycin phosphotransferase (hpt II) gene from pCAMBIA1301 using the primers CaMV35S forward: 5'-CTATTTCTTTGCCCTCGGACGAGT-3' hpt II reverse 5'-ACGTCGCGCACTCAAGTCCGAAAAAGTA-3' and PolyA (NOS) gene using forward: 5'-GATCTGGATTTTAGTACTGGATT-3' and reverse: 5'-CTTGATGAGTGTGTAATAATACCTCTTT-3' from the pCAMBIA1301 and cloned into pCAMBIA2301 between HindIII and PstI restriction sites. pCAMBIA2301::CaMV35S:hptII:PolyA:CaMV35S:AtBOR1:PolyA was confirmed with restriction digestion and then mobilized into Agrobacterium tumefaciens EHA105 by triparental mating (Bevan, 1984). The *Agrabacterium tumefaciens* harbouring the construct was maintained on solid LB medium supplemented with 10 mg/L rifampicin, and 50 mg/L kanamycin.

4.2.2 Molecular evaluation of transgenic events

4.2.2.1 Confirmation of T-DNA integration based on PCR analysis

Genomic DNA was isolated from the leaf (100 mg) of both non-transformed, and T_0 transformed putative AtBOR1 overexpression lines using the CTAB (cetyltrimethylammonium bromide) method (Rogers and Bendich 1994). Obtained DNA was used as a template to confirm T-DNA integration into the genome of Indian mustard by PCR. The presence of nptII, gus and AtBOR1 was detected by polymerase chain reaction (PCR) in T_0 transformed putative plants. Gene-specific primers (forward primer 5`-CCACCATGATATTCGGCAAC-3` and reverse primer 5`-GTGGAGAGGCTATTCGGCTA-3`) were used to amplify a 0.54 kb fragment of nptII. The PCR condition was 95 ºC for 10 min; 35 cycles of 95 ºC for 1 min, 58 ºC for 30 s and 72 ºC for 30 s; and a final extension of 72 ºC for 10 min. Similarly, primers specific to a 2.8 kb fragment, AtBOR1, and NOS-terminator in the T-DNA were designed as 5`-ATGGAAGAGACTTTTGTGCCGTT-3` and 5`- CGCGCCACAGTAGATACAATGATCTAG-3` and were used to amplify the T-DNA

fragment. The PCR condition was set as 95 ºC for 10 min; 35 cycles of 95 ºC for 1 min, 52 ºC for 30 sec, and 72 ºC for 3 min; and a final extension of 72 ºC for 10 min. 1.6 kb of gus gene was also amplified using the primers (forward: 5'-GGTGGAGAGGCTATTCGGCTA-3' and reverse: 5'-GGTAGCCAACGCTATGTCCTGA-3') with the PCR conditions of 95 ºC for 10 min; 35 cycles of 95 ºC for 1 min, 52 ºC for 30 sec, and 72 ºC for 2 min; and a final extension of 72 ºC for 10 min. The PCR fragments were analysed on 1 % agarose gel.

4.2.2.2 Plant growth conditions

Seeds of non-transgenic and transgenic plants (T_2) were germinated on germination media (see above section) supplemented with 110 mg/l kanamycin + 10 mg/l hygromycin and grown for ten days (22 ^{0}C, 16h light/8 h dark) to screen positive TDNA insertion lines (Saha et al., 2016). The surviving seedlings were selected for AtBOR1 PCR analysis, as mentioned above. PCR-positive transgenic plants and non-transgenic plants were transferred to full-strength Hoagland solution (Hoagland and Arnon, 1950) at two levels of B concentration: 0.46 µM B (B deficient); 46 µM B (B sufficient). The nutrient solution was refreshed and aerated continuously throughout the experiments every four days. The plants were cultured in a bright culture room with a temperature of 22 ^{0}C, a photoperiod of 16/8 h (day/night), and a light intensity of 300–360 µmol m^{-2} s^{-1}. Fourteen days after transfer, roots of the plants were harvested for RNA extraction. The RNA extraction and cDNA synthesis was followed as described in the Section 3.2.9.

4.2.2.3 Real-time PCR

Total RNA has been isolated from three independent transgenic PCR positive lines in successive (T1, T2, T3) using RNeasy Plant Mini Kit (Qiagen, Venlo, Limburg, Netherlands) following the manufacturer's instructions, and cDNA was prepared. Real-time was performed using a set of gene-specific primers (AtBOR1 forward primer 5'-GATGAGGTTATGACCCGAAGCAGAGGAGAG-3' and AtBOR1 reverse primer 5'-CTGACCCAACCTGATTCCACTCACTCTTGG-3') for amplifying a 141 bp fragment. Housekeeping *Bj*tubulin primers (forward primer 5`-CACCAACGGGTTTGAAAATG-3` and reverse primer 5` - TGCTCACTCACACGCCTAAA-3`) were used as an internal control to amplify a fragment of 100 bp. Realtime RT-PCR was performed in a Qiagen Rotor-Gene Q (Maryland, USA) using PowerUp™ SYBR™ Green Master mix (Applied Biosystems, USA)

according to the manufacturer's protocol 50°C for 2 min 95° C for 2 min, 60° C for 30 s (50 cycles). The experiment was repeated twice independently, with three replicates each time. The expression values relative to the standard curve was calculated for each sample. The relative expression of AtBOR1 in wild-type (WT) and transgenic *B. juncea* lines was estimated by normalizing expression values of AtBOR1 with that of housekeeping *Bj*tubulin.

4.2.2.4 Cell wall preparation

Plants were harvested at the four-leaf stage, and the leaves from the same relative positions on each plant were separated from stems and roots. The alcohol insoluble residue (AIR), was prepared accordingly as mentioned in Section 3.2.3.

4.2.2.5 Sequential chemical extraction of cell wall pectin

CDTA and Na_2CO_3 soluble pectin were extracted as described by Section 3.2.4. Both CDTA and Na_2CO_3-soluble fractions are used to determine the concentrations of pectin and B.

4.2.2.6 Determination of Uronic Acid (UA) and the Degree of Methylation (DM) of Pectin

The colorimetric estimation of UA and DM percentages were performed as per the protocol given Section 3.2.5.

4.2.2.7 Plant Sampling and Boron Analysis

Plant samples were harvested at the end of the experiments, rinsed in deionized water, divided into individual parts of roots, stems, and leaves. The B in the dried plants samples, CWM, and the pectin (CDTA and Na_2CO_3-soluble) fractions were determined according to the method described in Section 3.2.2.

4.2.2.8 Statistical analysis

To verify the statistical significance of differences among the lines, the data were analysed using the Student's t-test ($p < 0.05$).

4.3 RESULTS

4.3.1 Generation of AtBOR1 overexpressing mustard plants

TDNA region of pCAMBIA2301 harbouring pCAMBIA2301::CaMV35S:hptII:PolyA:CaMV35S:AtBOR1:PolyA was confirmed using restriction digestion, and then used for transformation (Figure 4.1A, B). Regenerated shoots from the *Agrobacterium* infected hypocotyl explants are subjected to kanamycin (10 mg/l) and hygromycin (10 mg/l) selection, and individual shoots are then cultured in rooting media until the emergence of roots. The transient GUS assay was performed randomly after the cocultivation (Figure 4.2 D-G). The well-rooted plants are then acclimatized to the soil and maintained in the greenhouse at 22^0C, 300–360 µmol m^{-2} s^{-1} and 16/8 PP.

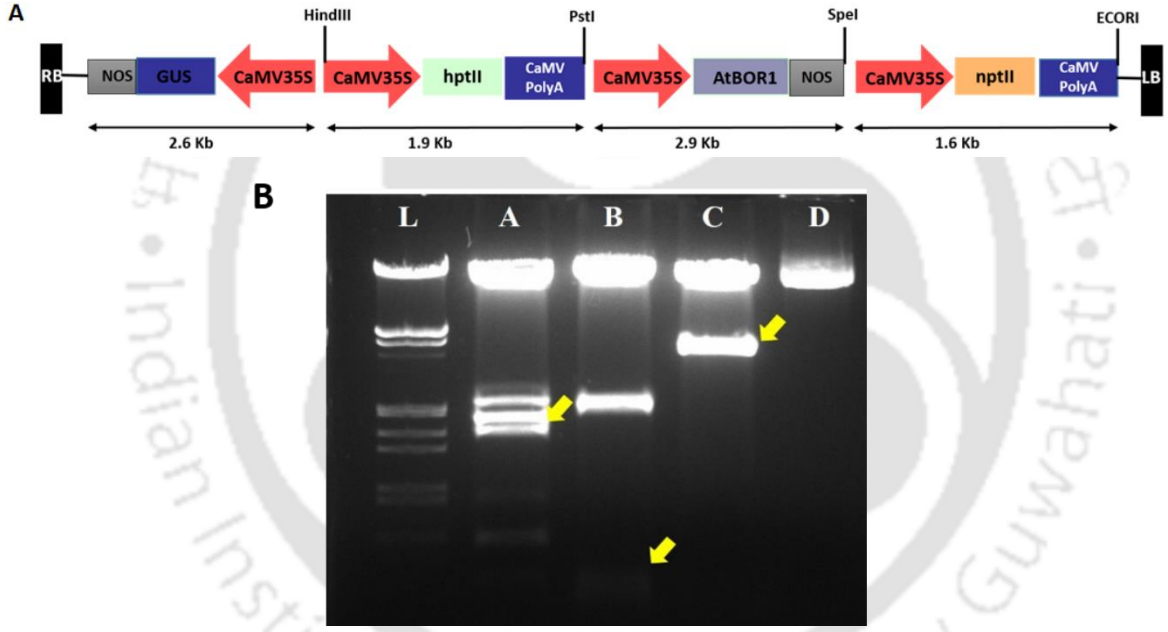

Figure 4.1: T-DNA construct preparation and confirmation A) TDNA region of pCAMBIA2301 harboring *CaMV35S:hptII:PolyA:CaMV35S:AtBOR1:PolyA*. **B)** Confirmation of AtBOR1 clone by restriction digestion. A. Doubled digested plasmid with HindIII and PstI for the confirmation of hptII (1.8kb) B. SpeI and ECORI digested plasmid for the confirmation of NOS (173bp) C. PstI and SpeI digested

plasmid for the confirmation of AtBOR1 (2.8kb) D. undigested plasmid L. DNA ladder.

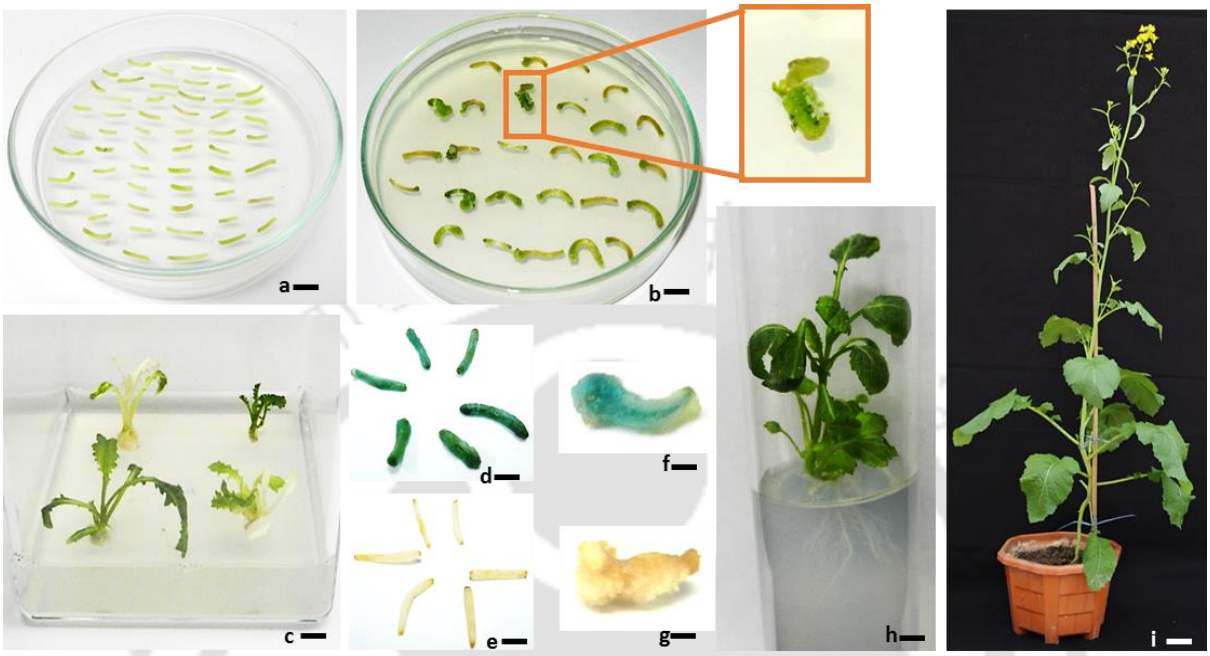

Figure 4.2: Stages in course of recovery of transgenic mustard plants. (a). hypocotyl explants in preculture (bar 8mm); (c). selection (bar 8mm) inset explant showing regeneration; (c). shoots in selection (bar 6mm);Transient gus assay (d), (f) transformed explants after 1 day in co-cultivation (bar 5mm) and after 7 days in selection medium (bar 3mm) showing gus activity respectively; (e), (g) untransformed controls showing no gus activity; (h). rooted shoots (bar 6mm); (i). fully grown acclimatised transgenic plant (bar 5 cm).

4.3.2 Gene integration and expression analysis through PCR and real-time PCR

Genomic DNA isolated from the leaves of the T_0 plants and their T-DNA integration was examined by PCR analysis using TDNA specific primers (Figure 4.3A). We have observed the expected amplicon size for kanamycin, GUS and AtBOR1 in three transgenics but not in non-transgenic

plants. Among them we only have advanced three T_0 seeds to successive generation (T_0.1, T_0.2, and T_0.3). The successive progenies were first screened on kanamycin containing ½MS media (100 mg/l) for ten days, followed by de-rooting and sub-cultured on to ½MS media without any selection till rooting emerges. Healthy seedlings are chosen for the further hydroponic growth evaluation and expressional analysis under different B concentration (46 µM and 0.46 µM B).

Real-time PCR analysis was carried out to evaluate the expression levels of AtBOR1 in transgenic lines (Figure 4.3B). The increase in the AtBOR1 transcripts in T_2 transgenic lines, T_2.1.1, T_2.2.1, and T_2.3.1 were confirmed by qRT-PCR (Figure 4.3B). AtBOR1 expression showed a significant increase in the transcript level of transgenic plants concerning non-transgenic. In particular, the T_2.3.1 plant's expression level is significantly higher than the other two transgenic lines (T_0.1.1 and T_0.2.1). These results suggest that introduced AtBOR1 is expressed relatively strongly in T_0.3.1 followed by T_0.1.1 and T_0.2.1 (Figure 4.3B).

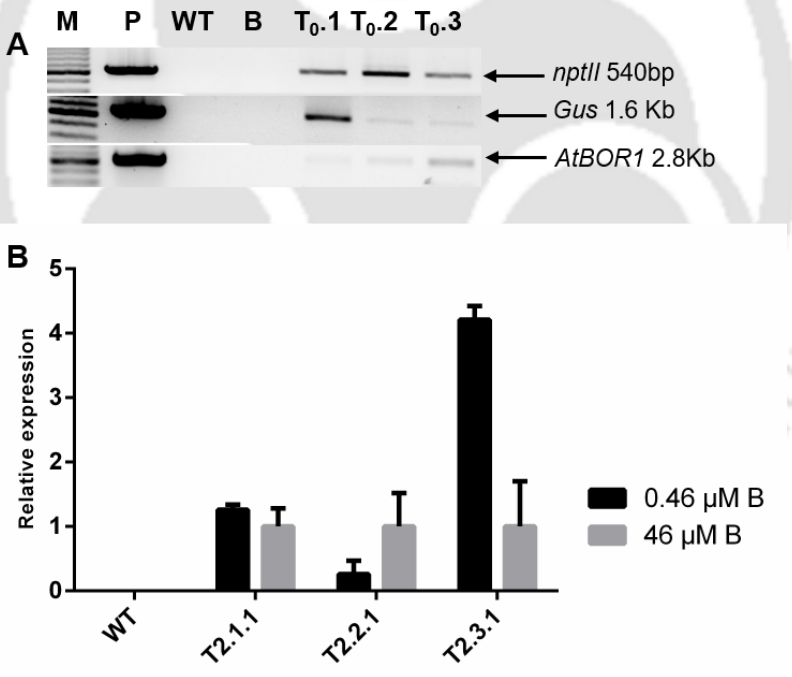

Figure 4.3: Establishment of transgenic mustard expressing AtBOR1. A, PCR was performed using genomic DNA as a template with primers specific to 540 bp with nptII primers, 1.6 Kb with gus primers, C. 2.8 Kb with

AtBOR1. **B, Total RNA was extracted from the roots of non-transgenic plants (NT) and transgenic T2 plants (T_2.1.1, T_2.2.1, and T_2.3.1). RT-PCR was performed using primers specific to AtBOR1 or the tubulin like gene.** M: ladder; WT: wild type; B: blank; P: plasmid.

4.3.3 Overexpression of AtBOR1 in Indian mustard confers better plant growth and cell wall composition under low B

The T_2 lines of transgenic and non-transgenic plants of Indian mustard are hydroponically grown in the presence of boric acid (0.46 or 46 µM) to examine the heterologous expression of AtBOR1. T_2 transgenic seeds are screened in germination media supplemented with kanamycin 100 mg/l+ 10 mg/l hygromycin, and the surviving seedlings (data not shown) were selected for the hydroponic assay and cell wall composition analysis. To investigate the effect of heterologous AtBOR1 expression on growth of mustard plants under B-deficiency, non-transgenic plants and three transgenic T_2 lines were grown hydroponically in the presence of 0.46 or 46 µM boric acid. Experiments were performed with at least four replications and representative individuals are shown in Figure 4.4. The phenotypic differences among the non-transgenics and transgenic plants were merely indifferent under sufficient B concentration (46 µM), though the T_2.3.1 line showed relatively low shoot compared to others (Figure 4.4). However, the phenotypic differences between transgenic and non-transgenic plants were prominent under low B concentration (0.46 µM), and non-transgenic plants appeared to have B inefficient under low B concentration (Figure 4.4). Under deficient B concentration, the shoot and root growth were severely retarded in non-transgenic plants (63.6% and 62.3% decreased root and shoot growth, respectively) compared to transgenics (Figure 4.5A, B). They also showed the lowest growth rate (77.1 %, 71.4% and 56.6% reduced root, stem, and leaf dry weight, respectively, concerned 46 µM B) (Figure 4.5C-E). In non-transgenics, the newly forming leaves were often inhibited along with the lower leaf expansion rate by the B deficient treatment. However, none of these phenotypic deformities have been observed in transgenic plants under low B concentration. The plant growth and the development of new leaves were healthy in low B concentration. Besides, the T_2.3.1 line accumulated an immense amount of biomass under low B concentration with the most extended taproot length and bigger leaf blades (38.2%, 100%, and 55.5% increase root, stem, and leaf dry weight respectively

in low B concentration) (Figure 4.5C-E). Significant ($p < 0.05$) variation in plant dry weight was present at two different B supply, between transgenics and non-transgenics (Figure 4.5). B deficiency has also increased the taproot length in transgenics, and the highest dry weight of root, stem, and leaf has been observed in comparison to the non-transgenics. These results indicated that heterologous expression of AtBOR1 increases the tolerance of Indian mustard plants to B-deficiency stress. These results indicated that heterologous expression of AtBOR1 increases tolerance of mustard plants to B-deficiency stress.

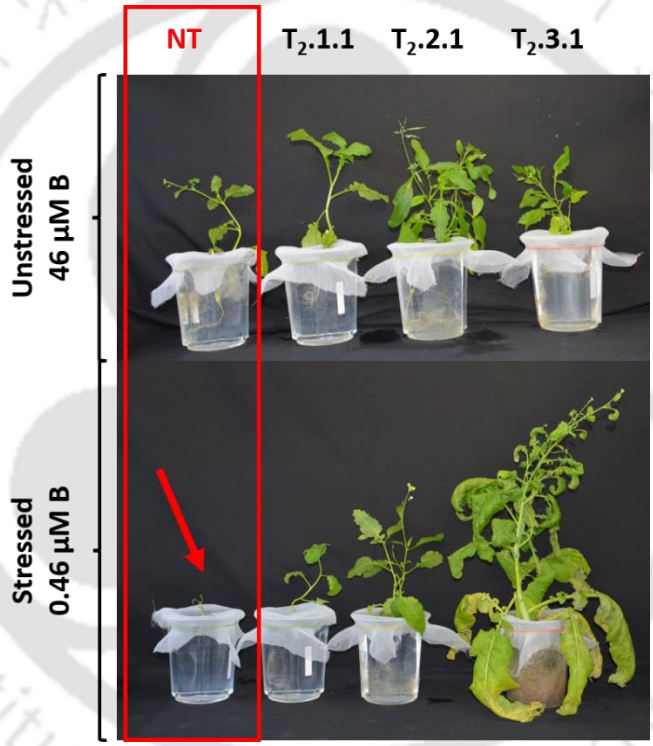

Figure 4.4: Overexpression of AtBOR1 in Indian mustard confers better plant growth. Low B tolerance of mustard plants overexpressing AtBOR1. 40 days old T_2 plants (T_2.1.1, T_2.2.1, and T_2.3.1) and non-transgenic (NT) were subjected to low B stress (0.46 µM B). Low B stress was given by avoiding the boron during hydroponic media preparation.

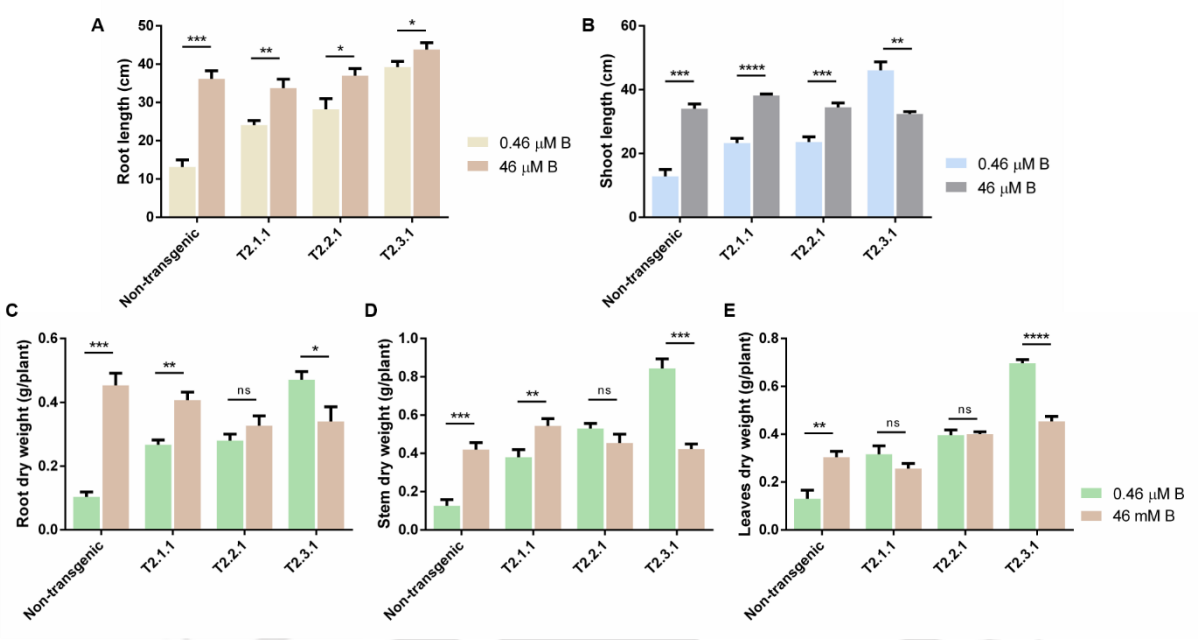

Figure 4.5: Root and shoot length, dry weights and B concentrations in transgenic mustard plants expressing AtBOR1 under B-deficiency and sufficiency. Non-transgenic (NT) and transgenic (T_2.1.1, T_2.2.1, and T_2.3.1) plants were grown for 40 days in a hydroponic solution containing 0.46 or 46 µM boric acid. Root **(A)**, shoot length **(B)** and dry weight **(C-E)** differences demonstrated that the transgenic mustard performs better under B-deprived media than non-transgenics. Data represents mean values (n = 3) ± SD, where n is the number of times experiment repeated and SD denotes Standard Deviation. An asterisk indicates significant differences from non-transgenic plants (Student's t-test, $p < 0.05$).

4.3.4 Changes in Uronic Acid (UA) and Degree of Methylation (DM) of two different pectin fractions

The percentages of UA in the cell wall of roots and shoots have decreased under low B concentration, suggesting the inhibition of the synthesis of the two different kinds of pectin and the decrease of the binding sites of B in cell walls under B deficiency. The decrease in the UA in

both roots (59.6%) and shoots (52.2%) is very evident in non-transgenic plants under low B conditions (Figure 4.6). While the transgenic plants T_2.1.1, and T_2.2.1 showed reduced UA% in roots (22.9%, and 38.4%, respectively) and shoots (23.4%, and 5.57%, respectively), T_2.3.1 showed increased UA% in roots (9.65%) and shoots (3.15%) (Figure 4.6). Similarly, DM in both the pectin fractions has decreased in non-transgenics, but not in transgenics, under low B condition due to cell wall integrity loss induced by the B deficiency (Figure 4.7).

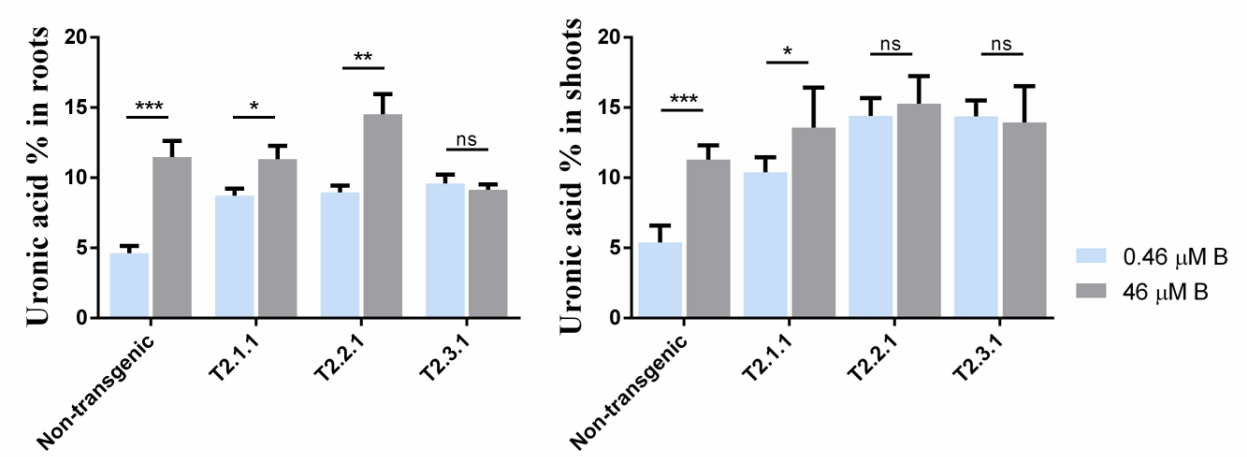

Figure 4.6 Difference in uronic acid (UA) percentages in root and shoot tissues of the transgenic Indian mustard genotypes grown under varied B conditions shows that transgenic mustard performs better under B-deprived media than non-transgenics (Figure A and B).
Data represents mean values (n = 3) ± SD, where n is the number of times experiment repeated and SD denotes Standard Deviation. An asterisk indicates significant differences from non-transgenic plants (Student's t-test, $p < 0.05$).

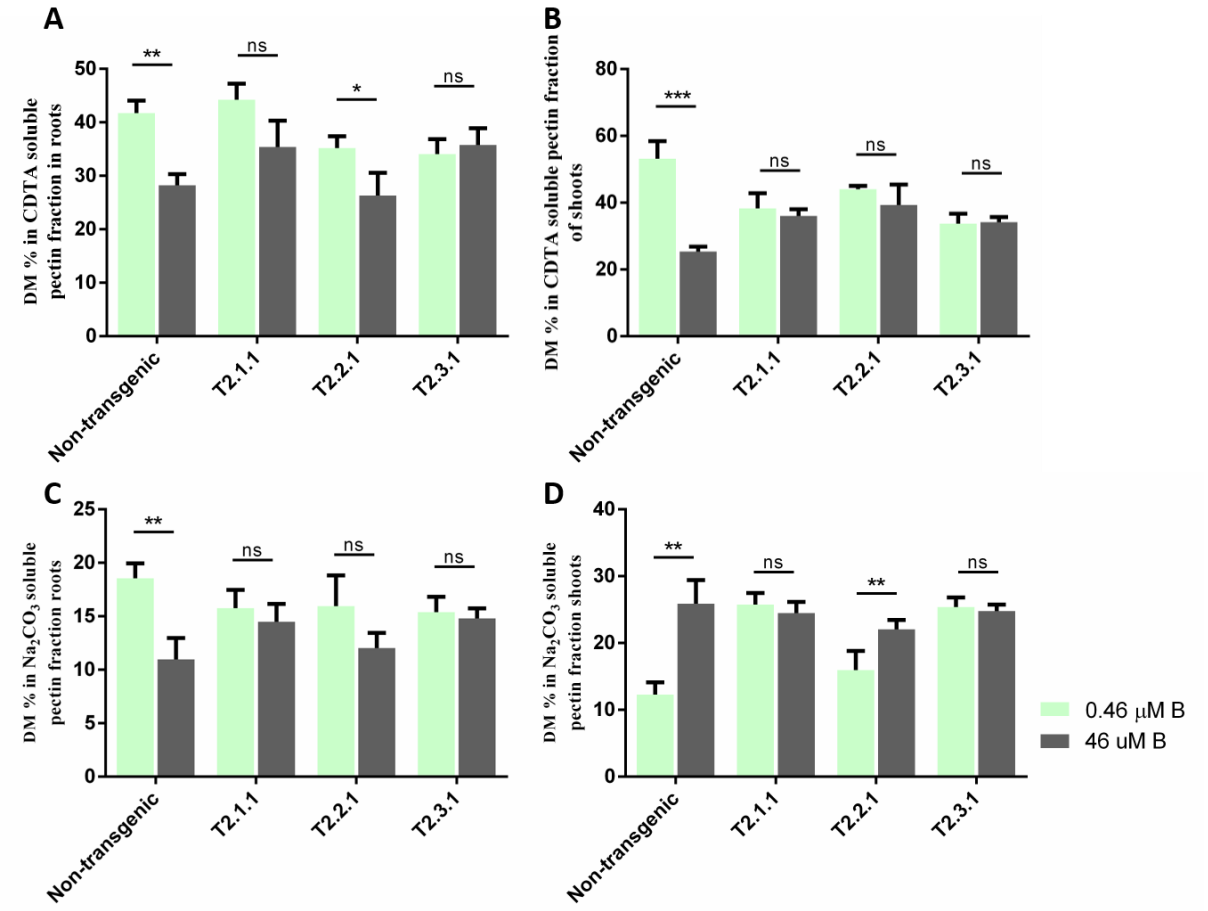

Figure 4.7: Difference in degree of methylation (DM) percentages in root and shoot tissues among the transgenic and non-transgenic Indian mustard lines grown under varied B conditions.

The differences in DM% in CDTA and Na_2CO_3 pectin fractions of root (A, C) and leaf (B, D) pectin fractions of transgenic mustard lines demonstrated that the nontransgenics have more cell wall damage under B-deficient media than others. Data represents mean values (n = 3) ± SD, where n is the number of times experiment repeated and SD denotes Standard Deviation. An asterisk indicates significant differences from non-transgenic plants (Student's t-test, $p < 0.05$).

4.3.5 Improved B accumulation in AtBOR1 overexpressed mustard plants under the B deficient condition

The B concentration in plant tissues was compared among the transgenic and non-transgenic mustard lines grown under two different B concentration (0.46 and 46 uM B) (Figure 4.7 and 4.8). In non-transgenic mustard lines net B uptake drastically declined under B deficiency (Figure 4.7 and 4.8). In B-deficient transgenic plants, the proportion of cell wall B in root and leaf B were much higher than that of the non-transgenics (3.0-6.1% and 4.0-8.3% increased B in root and leaf CWM, respectively than non-transgenic) (Figure 4.7). Whereas, the B content of the non-transgenic plants were decreased to 77.9% and 65.7% in the root and leaf CWM, respectively (Figure 4.7).

Additionally, in CDTA and Na_2CO_3 soluble pectin fraction, the transgenic plants had accumulated similar B content under both sufficient and low B conditions (Figure 4.8). Whereas, the non-transgenic plants grown under low B condition accumulated drastically low B content in both the pectin fractions (more than 60% lesser B in CDTA and Na_2CO_3 pectin fractions of both roots and leaves). The B content in both the cell wall fractions of roots was decreased in T_2.1.1, whereas it has increased in other two transgenics (T_2.2.1and T_2.3.1). In particular, transgenic line T_2.3.1 showed 15.2% and 44.5% increased B in CDTA and Na_2CO_3 cell wall fractions, respectively (Figure 4.8). Unlike roots, the B content in the leaf cell wall fraction has decreased in all the transgenic plants (6.2%- 12.5% and 3.4%- 36.3% in CDTA and Na_2CO_3 cell wall fractions, respectively). These results suggested that B in transgenic plant's roots was assigned preferentially to cell walls than non-transgenics under B starvation.

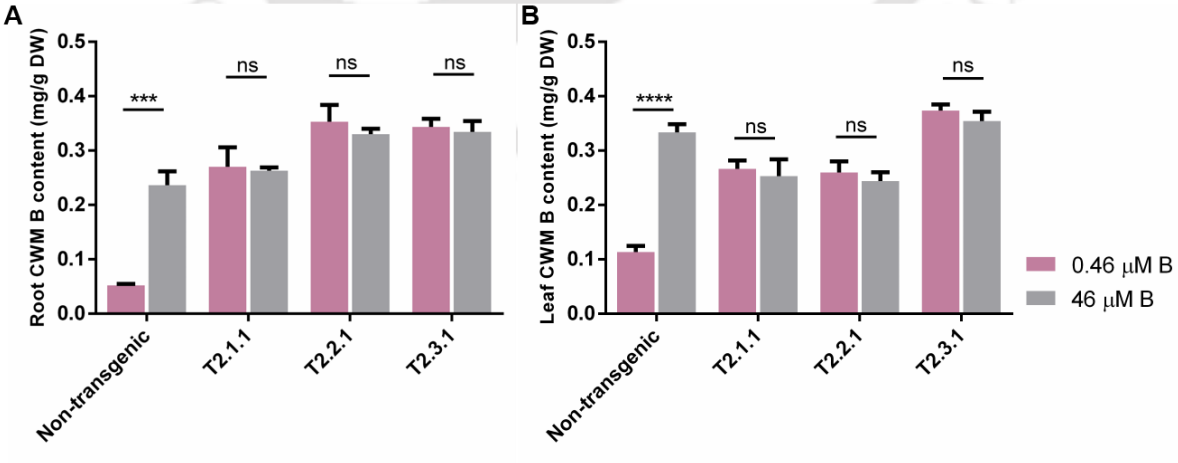

Figure 4.8: AtBOR1 overexpressed mustard lines accumulates more B in the cell wall than non-transgenics. The concentration of B in cell wall material (CWM) of root (A), and leaf (B) of transgenic and non-transgenic mustards. Data represents mean values (n = 3) ± SD, where n is the number of times experiment repeated and SD denotes Standard Deviation. Statistically significant values at $P < 0.05$ using Student's t-test analysis are indicated by asterisks. ns: nonsignificant

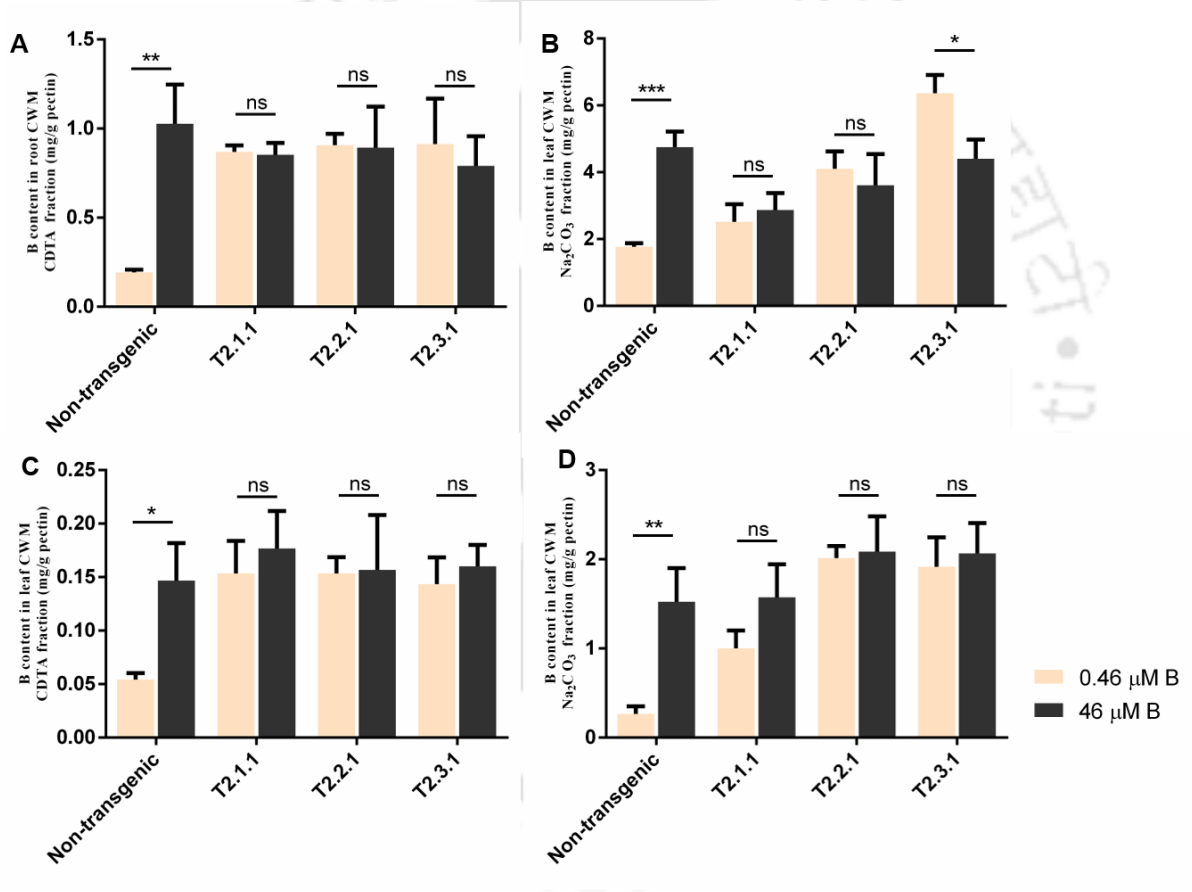

Figure 4.9: AtBOR1 overexpressed mustard lines accumulates more B in the CDTA cell wall fractions than non-transgenics. The concentration of B in cell wall fractions (CDTA and Na_2CO_3) of root (A and B), and leaf (C and D) of transgenic and non-transgenic mustards. Data represents mean values (n = 3)

± SD, where n is the number of times experiment repeated and SD denotes Standard Deviation. Statistically significant values at $P < 0.05$ using Student's t-test analysis are indicated by asterisks. ns: nonsignificant

4.4 DISCUSSION

When soil B concentration is limited, plants additionally use borate transporters, which in turn effectively alleviates boron deficiency. The majority of these B transporters are effluxers concentrating B in the apoplast for xylem loading (Takano et al., 2002). Besides, B transporters are also involved in B exclusion from tissues under excess B conditions (Miwa et al., 2007; Sutton et al., 2007). Takano et al., 2002 reported the first B transporter, AtBOR1, as an efflux pump, which preferentially transports B to the younger leaves under limited B concentration. The polar localization of BOR1 to the stele-side plasma membrane is likely essential for the efficient transport of B from the root surface to the xylem, in collaboration with boric acid channels (Yoshinari and Takano., 2017). Homologous BOR-type transporters required for B transport under limited B, have been identified and some of them are characterized in crop plants (Nakagawa et al., 2007; Pérez-Castro et al., 2012; Cañon et al., 2013; Leaungthitikanchana et al., 2013; Chatterjee et al., 2014; Zhang et al., 2017). Additionally, increased expression of AtNIP5;1 and/or AtBOR1 significantly improved the vegetative and reproductive growth of *A. thaliana* with limited B supply.

Indian mustard is an important oilseed crop in India. Globally, India ranks third in Rapeseed-Mustard production, with 16.6% (Kumararaja et al., 2015). In India, Rapeseed-Mustard group of species account for 3% of the gross cropped area. Among the seven annual edible oilseeds cultivated in India, rapeseed-mustard contributes nearly 30 percent in the total production of oilseeds. Indian Mustard belongs to the Brassica family and thus very sensitive to B deficiency (Shorrocks., 1997). Boron deficiency may also cause floral abortion and sterility of seed, which ultimately affects the reduction of seed yields tremendously in mustard (Hossain et al., 2012). There are copious records available on the positive response of yield and yield attributing characters of mustard to B fertilization (Islam, 2005; Hossain et al., 2012 and Saha et al., 2003). The seed yield increases significantly in the range of 16-47%, with the average response from 21-31%. The yield increase was 27% and 10% increase, respectively, in seed/siliqua and 1000 seed

weight, indicating the critical role in seed formation (Islam, 2005; Hossain et al., 1995 and Saha et al., 2003). In a recent field experiment conducted by Kumararajaa et al., 2015, the application of 16 kg Borax/ ha improves the yield by 35-39% over the control consistently for two years.

As far as to our knowledge, this is the first research work carried out on heterologous expression of B transporter in Indian mustard to alleviate B deficiency. In our current study, the non-transgenic mustard plants showed typical B deficient symptoms, including retarded growth, reduced leaf elongation rates, and diminished taproot length under deficient B concentration (0.46 μM B). Besides, our hydroponic screening condition was suitable for accessing the physiological contortions and effects of AtBOR1 overexpression in mustard plants concerning non-transgenics under limited B concentration. Expressional analysis AtBOR1 lines have revealed that T_2.3.1 was the highest expressing line followed by T_2.1.1 and T_2.2.1. The highly expressing T_2.3.1 line did not show any typical B deficiency symptoms, unlike non-transgenic mustard plants under low B concentration. The T_2.3.1 plant has produced an extraordinary amount of biomass under low B concentration, which is positively correlated with AtBOR1 expression. The trend of positive correlation between the increased biomass with AtBOR1 expression was also observed in the remaining transgenic lines under B deficiency. The B concentration in roots and leaves CWM, were considerably lower in non-transgenic than transgenic plants. B forms dimers with RGII to maintain cell wall integrity (Funakawa and Miwa., 2015). B deprivation in the media immediately arrests the mechanical strength and elasticity of the root cell wall, possibly due to insufficient B to form dimerization with RGII (Onuh et al., 2021). It can be hypothesized that this unique trend in transgenics states B redistribution pattern might be the reason for its B deficient-tolerance. The B content, in CDTA and Na_2CO_3 soluble pectin fractions, is also in accordance with this hypothesis. The highest B accumulation is directly proportional to the AtBOR1 expression in transgenic plants, which ultimately maintains the cell wall integrity and optimal plant growth. Moreover, improved AtBOR1 expression enhanced the root-to-shoot translocation of B in mustards as the shoot B accumulation was increased in all three transgenics.

Chapter V

Conclusion and Future Prospects

Considering the importance of B in growth and development of *B. juncea*, exploring the B transport mechanisms in the species could be an exciting option, as it lacks any preliminary studies. Hence, in the current study we have focused on B transport mechanisms by exploiting the various B transporting AQP and BOR proteins and their relevance in B transport. The salient conclusions of the work have been categorized under three major subheadings and delineated below:

Genome-wide identification and characterization of aquaporin and boron transporter genes in mustard (*Brassica juncea*)

- The 110 and 13 AQP and BOR genes, respectively, in *B. juncea* have been identified and classified into their respective *Arabidopsis* and *B. napus* subfamilies.
- The characteristic features of phylogenetic relationship, gene structure, conserved motifs/domains, and cis-regulatory elements, of all the BjAQPs and BjBORs were evaluated to recognize the variation among the proteins.
- The examination of the differential expression pattern of NIP5;1s (BjuA02NIP5_1a, BjuA03NIP5_1b, BjuA07NIP5_1c) and BOR1s (BjuA03BOR1a, and BjuB08BOR1b) along with the different B accumulation in roots revealed that the B transporter proteins were upregulated for the B transport.
- All these results provide better insights into the B transporting family members in *B. juncea* and highlight the diversity, which could be valuable for further biological functional studies focused on these genes.

Contrasting responses of Indian mustard genotypes to low boron condition at vegetative stage

- Contrasting responses to low B condition among the twenty-seven *B. juncea* genotypes and performances of the genotypes were evaluated based on the taproot length.
- Significant alterations of physiological responses, conditioned to low B levels, have been observed at the early vegetative stages of several *B. juncea* genotypes.
- B-efficient cultivar Geeta was more tolerant to low B, with very mild symptoms and a higher growth rate. Also, root meristem cells in B-efficient cultivar were more viable, and less reactive oxygen (ROS) activity has been observed than B-inefficient cultivar, Maya.

- FTIR data have demonstrated the modified composition of pectin, cellulose, and callose among contrasting genotypes under different B levels. Furthermore, the low B condition has altered the expression profile of the major B transporters among the genotypes.
- In summary, we have provided comprehensive experimental evidences of substantial differences among *B. juncea* genotypes in terms of plant growth and biomass, tissue B content, differential pectin content and expressional profile of major B transporter genes in response to an inadequate supply. Existence of diversity in plant responses to low B in *B. juncea* is fundamental for molecular breeding to improve efficiency of *B. juncea* cultivars under low B condition and meet future agricultural challenges.

Generation of Indian mustard tolerant to B deficiency by the manipulation of B efflux transporter, AtBOR1

- Transgenic mustard overexpressed with AtBOR1, encodes an efflux B transporter involved in xylem loading of B, and attempt to validate its growth under B deficient conditions.
- The B deficiency tolerance of the transgenics was evaluated with the gene integration and expression level of AtBOR1 concerning B content and cell wall composition analysis in tissues.
- Also, the overexpression resulted in enhanced B transport to the leaves and improved plant growth under B-deficient conditions. It is also observed that no adverse side effects associated with AtBOR1 overexpression on the plant's growth and performance under low B concentration concerning non-transgenics.
- B deficiency is a global agricultural problem, and thus our findings offer a basis for the improvement of crop production in B-deficient soils in parallel to the application of AtBOR1 to crop breeding in mustard.

Future prospects of the current work

- Insights in to the expressional changes, via transcriptomics study, of the AQP and BOR genes among the contrasting mustard genotypes under low B condition.
- Heterologous expression and transport assays of the proteins upregulated by low B condition to ascertain their function related to B transport.

- Functional characterization of the major B transporting genes via gene complementation in *Arabidopsis mutants*, gene knock-out and overexpression in *B. juncea*.
- This work provides a future scope of understanding the B transport network and development of novel mustard genotype for low soil B conditions.

REFERENCES

1) Abascal, F., Irisarri, I., & Zardoya, R. (2014). Diversity and evolution of membrane intrinsic proteins. Biochimica et Biophysica Acta (BBA)-General Subjects, 1840(5), 1468-1481.
2) Abidi, N., Hequet, E., Cabrales, L., Gannaway, J., Wilkins, T., & Wells, L. W. (2008). Evaluating cell wall structure and composition of developing cotton fibers using Fourier transform infrared spectroscopy and thermogravimetric analysis. Journal of applied polymer science, 107(1), 476-486.
3) Ahmad, W., Zia, M. H., Malhi, S. S., Niaz, A., & Ullah, S. (2012). Boron Deficiency in soils and crops: a review. Crop plant, 2012, 65-97.
4) Aibara, Izumi, Tatsuya Hirai, Koji Kasai, Junpei Takano, Hitoshi Onouchi, Satoshi Naito, Toru Fujiwara, and Kyoko Miwa (2018). "Boron-dependent translational suppression of the borate exporter BOR1 contributes to the avoidance of boron toxicity." Plant Physiology 177, no. 2: 759-774.
5) Alexandersson, E., Fraysse, L., Sjövall-Larsen, S., Gustavsson, S., Fellert, M., Karlsson, M., ... & Kjellbom, P. (2005). Whole gene family expression and drought stress regulation of aquaporins. Plant molecular biology, 59(3), 469-484.
6) Al-Hasani, H., Kunamneni, R. K., Dawson, K., Hinck, C. S., Muller-Wieland, D., & Cushman, S. W. (2002). Roles of the N-and C-termini of GLUT4 in endocytosis. Journal of cell science, 115(1), 131-140.
7) Ampah-Korsah, Henry, Hanna I. Anderberg, Angelica Engfors, Andreas Kirscht, Kristina Nordén, Sven Kjellstrom, Per Kjellbom, and Urban Johanson (2016). "The aquaporin splice variant NbXIP1; 1α is permeable to boric acid and is phosphorylated in the N-terminal domain." Frontiers in plant science 7: 862.
8) Anthon, G. E., & Barrett, D. M. (2004). Comparison of three colorimetric reagents in the determination of methanol with alcohol oxidase. Application to the assay of pectin methylesterase. Journal of agricultural and food chemistry, 52(12), 3749-3753.
9) Bailey, T. L., Johnson, J., Grant, C. E., & Noble, W. S. (2015). The MEME suite. Nucleic acids research, 43(W1), W39-W49.
10) Bansal, A., & Sankararamakrishnan, R. (2007). Homology modeling of major intrinsic proteins in rice, maize and Arabidopsis: comparative analysis of transmembrane helix association and aromatic/arginine selectivity filters. BMC structural biology, 7(1), 1-17.

11) Bańuelos, G. S., Cardon, G. E., Phene, C. J., Wu, L., Akohoue, S., & Zambrzuski, S. (1993). Soil boron and selenium removal by three plant species. Plant and Soil, 148(2), 253-263.
12) Bárzana, G., Aroca, R., Bienert, G. P., Chaumont, F., & Ruiz-Lozano, J. M. (2014). New insights into the regulation of aquaporins by the arbuscular mycorrhizal symbiosis in maize plants under drought stress and possible implications for plant performance. Molecular Plant-Microbe Interactions, 27(4), 349-363.
13) Becker, J. D., Boavida, L. C., Carneiro, J., Haury, M., & Feijó, J. A. (2003). Transcriptional profiling of Arabidopsis tissues reveals the unique characteristics of the pollen transcriptome. Plant physiology, 133(2), 713-725.
14) Bellaloui, N., Brown, P. H., & Dandekar, A. M. (1999). Manipulation of in vivo sorbitol production alters boron uptake and transport in tobacco. Plant Physiology, 119(2), 735-742.
15) Bellaloui, N., Mengistu, A., & Zobiole, L. H. (2012). Phomopsis seed infection effects on soybean seed phenol, lignin, and isoflavones in maturity group V genotypes differing in phomopsis resistance. Journal of Crop Improvement, 26(5), 693-710.
16) Bellaloui, N., Yadavc, R.C., Chern, M.-S., Hu, H., Gillen, A.M., Greve, C., Dandekar, A.M., Ronald, P.C. and Brown, P.H. (2003), Transgenically enhanced sorbitol synthesis facilitates phloem-boron mobility in rice. Physiologia Plantarum, 117: 79-84. https://doi.org/10.1034/j.1399-3054.2003.1170110.x
17) Berardini, T.Z., Reiser, L., Li, D., Mezheritsky, Y., Muller, R., Strait, E. and Huala, E. (2015), The arabidopsis information resource: Making and mining the "gold standard" annotated reference plant genome. genesis, 53: 474-485. https://doi.org/10.1002/dvg.22877
18) Bevan, M. (1984). Binary Agrobacterium vectors for plant transformation. Nucleic acids research, 12(22), 8711-8721.
19) Bienert M.D., Bienert G.P. (2017) Plant Aquaporins and Metalloids. In: Chaumont F., Tyerman S. (eds) Plant Aquaporins. Signaling and Communication in Plants. Springer, Cham. https://doi.org/10.1007/978-3-319-49395-4_14
20) Bienert, G. P., & Chaumont, F. (2014). Aquaporin-facilitated transmembrane diffusion of hydrogen peroxide. Biochimica et Biophysica Acta (BBA)-General Subjects, 1840(5), 1596-1604.
21) Bienert, G. P., & Jahn, T. P. (2010). Major intrinsic proteins and arsenic transport in plants: new players and their potential role. MIPs and their role in the exchange of metalloids, 111-125.
22) Bienert, G. P., Bienert, M. D., Jahn, T. P., Boutry, M., & Chaumont, F. (2011). Solanaceae XIPs are plasma membrane aquaporins that facilitate the transport of many uncharged substrates. The Plant Journal, 66(2), 306-317.

23) Bienert, M. D., Muries, B., Crappe, D., Chaumont, F., & Bienert, G. P. (2019). Overexpression of X Intrinsic Protein 1; 1 in Nicotiana tabacum and Arabidopsis reduces boron allocation to shoot sink tissues. Plant direct, 3(6), e00143.
24) Blevins, D. G., & Lukaszewski, K. M. (1998). Boron in plant structure and function. Annual review of plant biology, 49(1), 481-500.
25) Blumenkrantz, N., & Asboe-Hansen, G. (1973). New method for quantitative determination of uronic acids. Analytical biochemistry, 54(2), 484-489.
26) Bock, Kevin W., David Honys, John M. Ward, Senthil kumar Padmanaban, Eric P. Nawrocki, Kendal D. Hirschi, David Twell, and Heven Sze (2006). "Integrating membrane transport with male gametophyte development and function through transcriptomics." Plant Physiology 140, no. 4: 1151-1168.
27) Bogacki, P., Peck, D. M., Nair, R. M., Howie, J., & Oldach, K. H. (2013). Genetic analysis of tolerance to Boron toxicity in the legume Medicago truncatula. BMC plant biology, 13(1), 1-11.
28) Bonifacino, J. S., & Traub, L. M. (2003). Signals for sorting of transmembrane proteins to endosomes and lysosomes. Annual review of biochemistry, 72(1), 395-447.
29) Bora, P. C. and Hazarika, U. (1997). Effect of lime and boron on rainfed toria (Brassica campestris subsp. Oleifera var. Toria). Indian Journal of Agronomy, 42, 361-364.
30) Brdar-Jokanović, M. (2020). Boron toxicity and deficiency in agricultural plants. International Journal of Molecular Sciences, 21(4), 1424.
31) Brown, P. H., & Shelp, B. J. (1997). Boron mobility in plants. Plant and soil, 193(1), 85-101.
32) Brown, P. H., Bellaloui, N., Hu, H., & Dandekar, A. (1999). Transgenically enhanced sorbitol synthesis facilitates phloem boron transport and increases tolerance of tobacco to boron deficiency. Plant Physiology, 119(1), 17-20.
33) Brown, P.H.; Bellaloui, N.; Wimmer, M.A.; Bassil, E.S.; Ruiz, J.; Hu, H.; Pfeffer, H.; Dannel, F.; Romheld, V. Boron in plant biology. Plant Biol. 2002, 4, 205–223.
34) Burgert, I., and Dunlop, J. W. C. (2011). Micromechanics of Cell Walls, Mechanical Integration of Plant Cells and Plants. Berlin: Springer, 27–52. doi: 10.1007/978-3-642-19091-9_2
35) Caffall, K. H., & Mohnen, D. (2009). The structure, function, and biosynthesis of plant cell wall pectic polysaccharides. Carbohydrate research, 344(14), 1879-1900.
36) Camacho-Cristóbal, J. J., & González-Fontes, A. (2007). Boron deficiency decreases plasmalemma H+-ATPase expression and nitrate uptake, and promotes ammonium assimilation into asparagine in tobacco roots. Planta, 226(2), 443-451.

37) Camacho-Cristóbal, J. J., Anzellotti, D., & González-Fontes, A. (2002). Changes in phenolic metabolism of tobacco plants during short-term boron deficiency. Plant Physiology and Biochemistry, 40(12), 997-1002.
38) Camacho-Cristóbal, J. J., Lunar, L., Lafont, F., Baumert, A., & González-Fontes, A. (2004). Boron deficiency causes accumulation of chlorogenic acid and caffeoyl polyamine conjugates in tobacco leaves. Journal of Plant Physiology, 161(7), 879-881.
39) Camacho-Cristóbal, J. J., Martín-Rejano, E. M., Herrera-Rodríguez, M. B., Navarro-Gochicoa, M. T., Rexach, J., and González-Fontes, A. (2015). Boron deficiency inhibits root cell elongation via an ethylene/auxin/ROS-dependent pathway in Arabidopsis seedlings. J. Exp. Bot. 66, 3831–3840.
40) Campbell, T. A., Rathjen, A. J., Paull, J. G., & Islam, A. K. M. R. (1998). Method for screening bread wheat for tolerance to boron. Euphytica, 100(1), 131-135.
41) Cañon, P., Aquea, F., Rodríguez-Hoces de la Guardia, A., & Arce-Johnson, P. (2013). Functional characterization of Citrus macrophylla BOR1 as a boron transporter. Physiologia plantarum, 149(3), 329-339.
42) Chantachume, Y. (1995). Genetic studies on the tolerance of wheat to high concentrations of boron. University of Adelaide, Department of Plant Science.
43) Chatterjee, M., Liu, Q., Menello, C., Galli, M., & Gallavotti, A. (2017). The combined action of duplicated boron transporters is required for maize growth in boron-deficient conditions. Genetics, 206(4), 2041-2051.
44) Chatterjee, M., Tabi, Z., Galli, M., Malcomber, S., Buck, A., Muszynski, M., & Gallavotti, A. (2014). The boron efflux transporter ROTTEN EAR is required for maize inflorescence development and fertility. The Plant Cell, 26(7), 2962-2977.
45) Chaumont, F., Barrieu, F., Wojcik, E., Chrispeels, M. J., & Jung, R. (2001). Aquaporins constitute a large and highly divergent protein family in maize. Plant physiology, 125(3), 1206-1215.
46) Chen, H., Zhang, Q., He, M., Wang, S., Shi, L., & Xu, F. (2018). Molecular characterization of the genome-wide BOR transporter gene family and genetic analysis of BnaC04. BOR1; 1c in *Brassica napus*. BMC plant biology, 18(1), 1-14.
47) Chen, Z., Pan, Y., Wang, S., Ding, Y., Yang, W., & Zhu, C. (2012). Overexpression of a protein disulfide isomerase-like protein from Methanothermobacter thermoautotrophicum enhances mercury tolerance in transgenic rice. Plant science, 197, 10-20.
48) Chiba, Y., Mitani, N., Yamaji, N., & Ma, J. F. (2009). HvLsi1 is a silicon influx transporter in barley. The Plant Journal, 57(5), 810-818.
49) Chormova, D., Messenger, D. J., & Fry, S. C. (2014). Boron bridging of rhamnogalacturonan-II, monitored by gel electrophoresis, occurs during polysaccharide synthesis and secretion but not post-secretion. The Plant Journal, 77(4), 534-546.

50) Danielson, J. Å., & Johanson, U. (2008). Unexpected complexity of the aquaporin gene family in the moss Physcomitrella patens. BMC plant biology, 8(1), 1-15.
51) Das, R., Mandal, B., Sarkar, D., Pradhan, A. K., Datta, A., Padhan, D., ... & Narkhede, W. N. (2019). Boron availability in soils and its nutrition of crops under long-term fertility experiments in India. Geoderma, 351, 116-129.
52) Das, S. K., Avasthe, R. K., & Yadav, A. (2017). Secondary and micronutrients: deficiency symptoms and management in organic farming. Innov Farm, 2(4), 209-211.
53) Dean, R. M., Rivers, R. L., Zeidel, M. L., & Roberts, D. M. (1999). Purification and functional reconstitution of soybean nodulin 26. An aquaporin with water and glycerol transport properties. Biochemistry, 38(1), 347-353.
54) Dell, B., & Huang, L. (1997). Physiological response of plants to low boron. Plant and soil, 193(1), 103-120.
55) Di Giorgio, Juliana Andrea Pérez, Gerd Patrick Bienert, Nicolás Daniel Ayub, Agustín Yaneff, María Laura Barberini, Martín Alejandro Mecchia, Gabriela Amodeo, Gabriela Cynthia Soto, and Jorge Prometeo Muschietti (2016). "Pollen-specific aquaporins NIP4; 1 and NIP4; 2 are required for pollen development and pollination in Arabidopsis thaliana." The Plant Cell 28, no. 5: 1053-1077.
56) Diehn, T. A., Pommerrenig, B., Bernhardt, N., Hartmann, A., & Bienert, G. P. (2015). Genome-wide identification of aquaporin encoding genes in Brassica oleracea and their phylogenetic sequence comparison to Brassica crops and Arabidopsis. Frontiers in plant science, 6, 166.
57) Diehn, Till Arvid, Manuela Désirée Bienert, Benjamin Pommerrenig, Zhaojun Liu, Christoph Spitzer, Nadine Bernhardt, Jacqueline (2019). "Boron demanding tissues of Brassica napus express specific sets of functional Nodulin26-like Intrinsic Proteins and BOR 1 transporters." The Plant Journal 100, no. 1: 68-82.
58) Dong, X., Liu, G., Wu, X., Lu, X., Yan, L., Muhammad, R., ... & Jiang, C. (2016). Different metabolite profile and metabolic pathway with leaves and roots in response to boron deficiency at the initial stage of citrus rootstock growth. Plant Physiology and Biochemistry, 108, 121-131.
59) Dordas, C., Chrispeels, M. J., & Brown, P. H. (2000). Permeability and channel-mediated transport of boric acid across membrane vesicles isolated from squash roots. Plant physiology, 124(3), 1349-1362.
60) Du, W., Pan, Z. Y., Hussain, S. B., Han, Z. X., Peng, S. A., & Liu, Y. Z. (2020). Foliar supplied boron can be transported to roots as a boron-sucrose complex via phloem in citrus trees. Frontiers in plant science, 11, 250.

61) Dubeaux, G., Neveu, J., Zelazny, E., & Vert, G. (2018). Metal sensing by the IRT1 transporter-receptor orchestrates its own degradation and plant metal nutrition. Molecular cell, 69(6), 953-964.
62) Dumont, M., Lehner, A., Bouton, S., Kiefer-Meyer, M. C., Voxeur, A., Pelloux, J., ... & Mollet, J. C. (2014). The cell wall pectic polymer rhamnogalacturonan-II is required for proper pollen tube elongation: implications of a putative sialyltransferase-like protein. Annals of botany, 114(6), 1177-1188.
63) Durbak, Amanda R., Kimberly A. Phillips, Sharon Pike, Malcolm A. O'Neill, Jonathan Mares, Andrea Gallavotti, Simon T. Malcomber, Walter Gassmann, and Paula McSteen (2014). "Transport of boron by the tassel-less1 aquaporin is critical for vegetative and reproductive development in maize." The Plant Cell 26, no. 7: 2978-2995.
64) Eulgem, T., Rushton, P. J., Robatzek, S., & Somssich, I. E. (2000). The WRKY superfamily of plant transcription factors. Trends in plant science, 5(5), 199-206.
65) Feng, Yingna, Rui Cui, Sheliang Wang, Mingliang He, Yingpeng Hua, Lei Shi, Xiangsheng Ye, and Fangsen Xu. "Transcription factor BnaA9. WRKY47 contributes to the adaptation of Brassica napus to low boron stress by up-regulating the boric acid channel gene BnaA3. NIP5; 1." Plant biotechnology journal 18, no. 5 (2020): 1241-1254.
66) Finn, R. N., Chauvigné, F., Hlidberg, J. B., Cutler, C. P., & Cerdà, J. (2014). The lineage-specific evolution of aquaporin gene clusters facilitated tetrapod terrestrial adaptation. PloS one, 9(11), e113686.
67) Fitzpatrick, K. L., & Reid, R. J. (2009). The involvement of aquaglyceroporins in transport of boron in barley roots. Plant, cell & environment, 32(10), 1357-1365.
68) Fortin, M. G., Morrison, N. A., & Verma, D. P. S. (1987). Nodulin-26, a peribacteroid membrane nodulin is expressed independently of the development of the peribacteroid compartment. Nucleic acids research, 15(2), 813-824.
69) Fox, A. R., Maistriaux, L. C., & Chaumont, F. (2017). Toward understanding of the high number of plant aquaporin isoforms and multiple regulation mechanisms. Plant Science, 264, 179-187.
70) Froger, A., Thomas, D., Delamarche, C., & Tallur, B. (1998). Prediction of functional residues in water channels and related proteins. Protein Science, 7(6), 1458-1468.
71) Fu, D., Libson, A., Miercke, L. J., Weitzman, C., Nollert, P., Krucinski, J., & Stroud, R. M. (2000). Structure of a glycerol-conducting channel and the basis for its selectivity. science, 290(5491), 481-486.
72) Fukuda, M., Wakuta, S., Kamiyo, J., Fujiwara, T., & Takano, J. (2018). Establishment of genetically encoded biosensors for cytosolic boric acid in plant cells. The Plant Journal, 95(5), 763-774.

73) Funakawa H and Miwa K (2015) Synthesis of borate cross-linked rhamnogalacturonan II. Front. Plant Sci. 6:223. doi: 10.3389/fpls.2015.00223
74) Goldbach, H. E., & Wimmer, M. A. (2007). Boron in plants and animals: Is there a role beyond cell-wall structure?. Journal of Plant Nutrition and Soil Science, 170(1), 39-48.
75) Goldbach, H. E., Yu, Q., Wingender, R., Schulz, M., Wimmer, M., Findeklee, P., & Baluška, F. (2001). Rapid response reactions of roots to boron deprivation. Journal of Plant Nutrition and Soil Science, 164(2), 173-181.
76) González-Fontes, A., Rexach, J., Quiles-Pando, C., Herrera-Rodríguez, M. B., Camacho-Cristóbal, J. J., & Navarro-Gochicoa, M. T. (2013). Transcription factors as potential participants in the signal transduction pathway of boron deficiency. Plant signaling & behavior, 8(11), e26114.
77) González-Fontes, A., Rexach, J., Quiles-Pando, C., Herrera-Rodríguez, M. B., Camacho-Cristóbal, J. J., & Navarro-Gochicoa, M. T. (2013). Transcription factors as potential participants in the signal transduction pathway of boron deficiency. Plant signaling & behavior, 8(11), e26114.
78) Guan, X. G., Su, W. H., Yi, F., Zhang, D., Hao, F., Zhang, H. G., ... & Ma, T. H. (2010). NPA motifs play a key role in plasma membrane targeting of aquaporin-4. IUBMB life, 62(3), 222-226.
79) Gupta, A. B., & Sankararamakrishnan, R. (2009). Genome-wide analysis of major intrinsic proteins in the tree plant Populus trichocarpa: characterization of XIP subfamily of aquaporins from evolutionary perspective. BMC plant biology, 9(1), 1-28.
80) Gupta, U. C. (1993). Boron and its role in crop production. CRC press.
81) Hajiboland, R., Farhanghi, F., & Aliasgharpour, M. (2012). Morphological and anatomical modifications in leaf, stem and roots of four plant species under boron deficiency conditions. In Anales de Biología (No. 34, pp. 15-29). Servicio de Publicaciones de la Universidad de Murcia.
82) Hanaoka, H., Uraguchi, S., Takano, J., Tanaka, M., & Fujiwara, T. (2014). O s NIP 3; 1, a rice boric acid channel, regulates boron distribution and is essential for growth under boron-deficient conditions. The Plant Journal, 78(5), 890-902.
83) Hayes, J. E., & Reid, R. J. (2004). Boron tolerance in barley is mediated by efflux of boron from the roots. Plant Physiology, 136(2), 3376-3382.
84) He, Mingliang, Sheliang Wang, Cheng Zhang, Liu Liu, Jinyao Zhang, Shou Qiu, Hong Wang et al. "Genetic variation of BnaA3. NIP5; 1 expressing in the lateral root cap contributes to boron deficiency tolerance in Brassica napus." PLoS genetics 17, no. 7 (2021): e1009661.
85) Henzler, T., & Steudle, E. (2000). Transport and metabolic degradation of hydrogen peroxide in Chara corallina: model calculations and measurements with

the pressure probe suggest transport of H2O2 across water channels. Journal of experimental botany, 51(353), 2053-2066.

86) Ho, C. H., Lin, S. H., Hu, H. C., & Tsay, Y. F. (2009). CHL1 functions as a nitrate sensor in plants. Cell, 138(6), 1184-1194.

87) Hoagland, D. R., & Arnon, D. I. (1950). The water-culture method for growing plants without soil. Circular. California agricultural experiment station, 347(2nd edit).

88) Hodge, A., Berta, G., Doussan, C., Merchan, F., & Crespi, M. (2009). Plant root growth, architecture and function. Plant and soil, 321(1), 153-187.

89) Hossain, M. A., Jahiruddin, M., & Khatun, F. (1995). Response of wheat and mustard to manganese, zinc and boron in calcareous soil. Bangladesh J. Crop Sci, 6(1&2), 51-56.

90) Hossain, M. A., Jahiruddin, M., & Khatun, F. (2012). Response of mustard (Brassica) varieties to boron application. Bangladesh Journal of Agricultural Research, 37(1), 137-148.

91) Hove, R. M., & Bhave, M. (2011). Plant aquaporins with non-aqua functions: deciphering the signature sequences. Plant molecular biology, 75(4-5), 413-430.

92) Hu, B., Jin, J., Guo, A. Y., Zhang, H., Luo, J., & Gao, G. (2015). GSDS 2.0: an upgraded gene feature visualization server. Bioinformatics, 31(8), 1296-1297.

93) Hu, B., Z. Jiang and Y. Zeng. 1991. Slurry sample introduction with fluorinating electrothermal vaporization for the direct ICP-AES determination of boron in plant leaves (Brassica napus L.). Oil Crops (China) 16(3): 43-46.

94) Hu, H., & Brown, P. H. (1994). Localization of boron in cell walls of squash and tobacco and its association with pectin (evidence for a structural role of boron in the cell wall). Plant Physiology, 105(2), 681-689.

95) Hu, H., Brown, P. H., & Labavitch, J. M. (1996). Species variability in boron requirement is correlated with cell wall pectin. Journal of Experimental Botany, 47(2), 227-232.

96) Hu, H., Penn, S. G., Lebrilla, C. B., & Brown, P. H. (1997). Isolation and characterization of soluble boron complexes in higher plants (the mechanism of phloem mobility of boron). Plant Physiology, 113(2), 649-655.

97) Hua Y., Zhang D., Zhou T., He M., Ding G., Shi L. et al. Transcriptomics-assisted quantitative trait locus fine mapping for the rapid identification of a nodulin 26-like intrinsic protein gene regulating boron efficiency in allotetraploid rapeseed. Plant Cell Environ. 2016; 39, 1601–1618. https://doi.org/10.1111/pce.12731 PMID: 26934080

98) Hua, Yingpeng, Yingna Feng, Ting Zhou, and Fangsen Xu. "Genome-scale mRNA transcriptomic insights into the responses of oilseed rape (Brassica napus L.) to varying boron availabilities." Plant and Soil 416, no. 1 (2017): 205-225.

99) Ishii, T., & Matsunaga, T. (1996). Isolation and characterization of a boron-rhamnogalacturonan-II complex from cell walls of sugar beet pulp. Carbohydrate Research, 284(1), 1-9.

100) Ishii, T., Matsunaga, T., & Hayashi, N. (2001). Formation of rhamnogalacturonan II-borate dimer in pectin determines cell wall thickness of pumpkin tissue. Plant Physiology, 126(4), 1698-1705.

101) Ishikawa, F., Suga, S., Uemura, T., Sato, M. H., & Maeshima, M. (2005). Novel type aquaporin SIPs are mainly localized to the ER membrane and show cell-specific expression in Arabidopsis thaliana. FEBS letters, 579(25), 5814-5820.

102) Ishikawa, S., & Wagatsuma, T. (1998). Plasma membrane permeability of root-tip cells following temporary exposure to Al ions is a rapid measure of Al tolerance among plant species. Plant and cell physiology, 39(5), 516-525.

103) Islam, M. B. (2005). Requirement of boron for mustard, wheat and chickpea based rice cropping patterns. PhD diss., Department Soil Science, Bangladesh Agricultural University, Mymensingh, Bangladesh.

104) Jahn, T. P., Møller, A. L., Zeuthen, T., Holm, L. M., Klærke, D. A., Mohsin, B., ... & Schjoerring, J. K. (2004). Aquaporin homologues in plants and mammals transport ammonia. FEBS letters, 574(1-3), 31-36.

105) Jamet, E., Canut, H., Boudart, G., & Pont-Lezica, R. F. (2006). Cell wall proteins: a new insight through proteomics. Trends in plant science, 11(1), 33-39.

106) Jamjod, S., Niruntrayagul, S., & Rerkasem, B. (2004). Genetic control of boron efficiency in wheat (Triticum aestivum L.). Euphytica, 135(1), 21-27.

107) Javot H, Maurel C (2002) The role of aquaporins in root water uptake. Annals of Botany. 90: 301–313

108) Jefferies, S. P., A. R. Barr, A. Karakousis, J. M. Kretschmer, S. Manning, K. J. Chalmers, J. C. Nelson, A. K. M. R. Islam, and P. Langridge. "Mapping of chromosome regions conferring boron toxicity tolerance in barley (Hordeum vulgare L.)." Theoretical and applied Genetics 98, no. 8 (1999): 1293-1303.

109) Jefferies, S. P., Pallotta, M. A., Paull, J. G., Karakousis, A., Kretschmer, J. M., Manning, S., ... & Chalmers, K. J. (2000). Mapping and validation of chromosome regions conferring boron toxicity tolerance in wheat (Triticum aestivum). Theoretical and applied Genetics, 101(5-6), 767-777.

110) Jia, Z., Bienert, M. D., von Wirén, N., & Bienert, G. P. (2021). Genome-wide association mapping identifies HvNIP2; 2/HvLsi6 accounting for efficient boron transport in barley. Physiologia Plantarum, 171(4), 809-822.

111) Johanson, U., Karlsson, M., Johansson, I., Gustavsson, S., Sjövall, S., Fraysse, L., ... & Kjellbom, P. (2001). The complete set of genes encoding major intrinsic proteins in Arabidopsis provides a framework for a new nomenclature for major intrinsic proteins in plants. Plant physiology, 126(4), 1358-1369.

112) Johnson, K. D., & Chrispeels, M. J. (1987). Substrate specificities of N-acetylglucosaminyl-, fucosyl-, and xylosyltransferases that modify glycoproteins in the Golgi apparatus of bean cotyledons. Plant Physiology, 84(4), 1301-1308.

113) Kasai, K., Takano, J., Miwa, K., Toyoda, A., & Fujiwara, T. (2011). High boron-induced ubiquitination regulates vacuolar sorting of the BOR1 borate transporter in Arabidopsis thaliana. Journal of Biological Chemistry, 286(8), 6175-6183.

114) Kasajima, I., Ide, Y., Yokota Hirai, M., & Fujiwara, T. (2010). WRKY6 is involved in the response to boron deficiency in Arabidopsis thaliana. Physiologia plantarum, 139(1), 80-92.

115) Kato, Y., Miwa, K., Takano, J., Wada, M., and Fujiwara, T. (2009). Highly boron deficiency-tolerant plants generated by enhanced expression of NIP5;1, a boric acid channel. Plant Cell Physiol.50, 58–66. doi: 10.1093/Pcp/Pcn168

116) Kelley, L., Mezulis, S., Yates, C. et al. The Phyre2 web portal for protein modeling, prediction and analysis. Nat Protoc 10, 845–858 (2015). https://doi.org/10.1038/nprot.2015.053

117) Kobayashi, M. (2000) Studies on the Boron-Polysaccharide Complex of Higher Plant. Plant Physiol, 105, 681-689.

118) Kobayashi, M., Matoh, T., & Azuma, J. I. (1996). Two chains of rhamnogalacturonan II are cross-linked by borate-diol ester bonds in higher plant cell walls. Plant Physiology, 110(3), 1017-1020.

119) Kong, W., Yang, S., Wang, Y., Bendahmane, M., & Fu, X. (2017). Genome-wide identification and characterization of aquaporin gene family in Beta vulgaris. PeerJ, 5, e3747.

120) Kumar, K., Mosa, K. A., Chhikara, S., Musante, C., White, J. C., & Dhankher, O. P. (2014). Two rice plasma membrane intrinsic proteins, OsPIP2; 4 and OsPIP2; 7, are involved in transport and providing tolerance to boron toxicity. Planta, 239(1), 187-198.

121) Kumar, K., Mosa, K. A., Meselhy, A. G., & Dhankher, O. P. (2018). Molecular insights into the plasma membrane intrinsic proteins roles for abiotic stress and metalloids tolerance and transport in plants. Indian Journal of Plant Physiology, 23(4), 721-730.

122) Kumararaja, P., Premi, O. P., & Kandpal, B. K. (2015). Application of boron enhances Indian mustard (Brassica juncea) productivity and quality under boron deficient calcareous soil in semi-arid environment.

123) Kyoko Miwa, Toru Fujiwara, Boron transport in plants: co-ordinated regulation of transporters, Annals of Botany, Volume 105, Issue 7, June 2010, Pages 1103–1108, https://doi.org/10.1093/aob/mcq044

124) Laloux, T., Junqueira, B., Maistriaux, L. C., Ahmed, J., Jurkiewicz, A., & Chaumont, F. (2018). Plant and mammal aquaporins: same but different. International journal of molecular sciences, 19(2), 521.

125) Landi, M., Margaritopoulou, T., Papadakis, I. E., & Araniti, F. (2019). Boron toxicity in higher plants: an update. Planta, 250(4), 1011-1032.

126) Leaungthitikanchana, S., Fujibe, T., Tanaka, M., Wang, S., Sotta, N., Takano, J., & Fujiwara, T. (2013). Differential expression of three BOR1 genes corresponding to different genomes in response to boron conditions in hexaploid wheat (Triticum aestivum L.). Plant and cell physiology, 54(7), 1056-1063.

127) Lei, S. H. I., Yun-Hua, W. A. N. G., Fu-Zhao, N. I. A. N., Jian-Wei, L. U., Jin-Ling, M. E. N. G., & Fang-Sen, X. U. (2009). Inheritance of boron efficiency in oilseed rape. Pedosphere, 19(3), 403-408.

128) Leonard, April, Beth Holloway, Mei Guo, Mary Rupe, GongXin Yu, Mary Beatty, Gina Zastrow-Hayes (2014). "tassel-less1 encodes a boron channel protein required for inflorescence development in maize." Plant and Cell Physiology 55, no. 6: 1044-1054.

129) Lescot, M. (2002). Dé hais P, Thijs G, Marchal K, Moreau Y, Van de Peer Y, et al. PlantCARE, a database of plant cis-acting regulatory elements and a portal to tools for in silico analysis of promoter sequences. Nucleic acids res, 30(1), 325-327.

130) Letunic, I., & Bork, P. (2016). Interactive tree of life (iTOL) v3: an online tool for the display and annotation of phylogenetic and other trees. Nucleic acids research, 44(W1), W242-W245.

131) Li, M., Zhao, Z., Zhang, Z., Zhang, W., Zhou, J., Xu, F., & Liu, X. (2017). Effect of boron deficiency on anatomical structure and chemical composition of petioles and photosynthesis of leaves in cotton (Gossypium hirsutum L.). Scientific reports, 7(1), 1-9.

132) Li, T., Choi, W. G., Wallace, I. S., Baudry, J., & Roberts, D. M. (2011). Arabidopsis thaliana NIP7; 1: an anther-specific boric acid transporter of the aquaporin superfamily regulated by an unusual tyrosine in helix 2 of the transport pore. Biochemistry, 50(31), 6633-6641.

133) Liu, G., Dong, X., Liu, L., Wu, L., & Jiang, C. (2014). Boron deficiency is correlated with changes in cell wall structure that lead to growth defects in the leaves of navel orange plants. Scientia Horticulturae, 176, 54-62.

134) Liu, Q., Wang, H., Zhang, Z., Wu, J., Feng, Y., & Zhu, Z. (2009). Divergence in function and expression of the NOD26-like intrinsic proteins in plants. BMC genomics, 10(1), 1-13.

135) Loomis, W. D., & Durst, R. W. (1992). Chemistry and biology of boron. BioFactors (Oxford, England), 3(4), 229-239.

136) Loqué, D., Ludewig, U., Yuan, L., & von Wirén, N. (2005). Tonoplast intrinsic proteins AtTIP2; 1 and AtTIP2; 3 facilitate NH3 transport into the vacuole. Plant physiology, 137(2), 671-680.

137) Lordkaew, S., Dell, B., Jamjod, S., & Rerkasem, B. (2011). Boron deficiency in maize. Plant and Soil, 342(1), 207-220.

138) Lordkaew, S., Konsaeng, S., Jongjaidee, J., Dell, B., Rerkasem, B. and Jamjod, S. (2012) Variation in responses to boron in rice. Plant Soil 363: 287–295.

139) Lu, X., Y. Lu, D. Mao, Y.F. Lu. and D.M. Mao. 2000. The levels of available boron in red earth in Central Zhejiang Provice and boron nutrition of rape. Institute of Soils and Fertilizers, Beijing. 5(1): 30-31

140) Lung-Jiun Shin, Jing-Chi Lo, Guan-Hong Chen, Judy Callis, Hongyong Fu, Kuo-Chen Yeh, IRT1 DEGRADATION FACTOR1, a RING E3 Ubiquitin Ligase, Regulates the Degradation of IRON-REGULATED TRANSPORTER1 in Arabidopsis, The Plant Cell, Volume 25, Issue 8, August 2013, Pages 3039–3051, https://doi.org/10.1105/tpc.113.115212

141) Luo, J., Liang, Z., Wu, M., & Mei, L. (2019). Genome-wide identification of BOR genes in poplar and their roles in response to various environmental stimuli. Environmental and Experimental Botany, 164, 101-113.

142) Lv, Qiang, Lei Wang, Jin-Zheng Wang, Peng Li, Yu-Li Chen, Jing Du, Yi-Kun He, and Fang Bao (2017). "SHB1/HY1 alleviates excess boron stress by increasing BOR4 expression level and maintaining boron homeostasis in Arabidopsis roots." Frontiers in plant science 8: 790.

143) Ma, J. F., & Yamaji, N. (2006). Silicon uptake and accumulation in higher plants. Trends in plant science, 11(8), 392-397.

144) Ma, J. F., & Tsay, Y. F. (2021). Transport systems of mineral elements in plants: transporters, regulation and utilization. Plant and Cell Physiology.

145) Ma, J. F., & Yamaji, N. (2015). A cooperative system of silicon transport in plants. Trends in Plant Science, 20(7), 435-442.

146) Marschner, H. (2011). Marschner's mineral nutrition of higher plants. Academic press

147) Masataka KAJIKAWA, Takahiro FUJIBE, Shimpei URAGUCHI, Kyoko MIWA & Toru FUJIWARA (2011) Expression of the Arabidopsis Borate Efflux Transporter Gene, AtBOR4, in Rice Affects the Xylem Loading of Boron and Tolerance to Excess Boron, Bioscience, Biotechnology, and Biochemistry, 75:12, 2421-2423, DOI: 10.1271/bbb.110629

148) Masum, M. A., Miah, M. N. H., Islam, M. N., Hossain, M. S., Mandal, P., & Chowdhury, A. P. (2019). Effect of boron fertilization on yield and yield attributes of mustard var. BARI Sarisha-14. Journal of Bioscience and Agriculture Research, 20(02), 1717-1723.

149) Matoh, T. (1997). Boron in plant cell walls. Plant and Soil, 193(1), 59-70.
150) Matoh, T. (2013). Boron in plant nutrition and cell wall. Plant Nutr. Acquis, 227-250.
151) Matoh, T., Ishigaki, K. I., Ohno, K., & Azuma, J. I. (1993). Isolation and characterization of a boron-polysaccharide complex from radish roots. Plant and cell physiology, 34(4), 639-642.
152) Matthes, M. S., Robil, J. M., & McSteen, P. (2020). From element to development: the power of the essential micronutrient boron to shape morphological processes in plants. Journal of experimental botany, 71(5), 1681-1693.
153) Maurel, C., Verdoucq, L., & Rodrigues, O. (2016). Aquaporins and plant transpiration. Plant, cell & environment, 39(11), 2580-2587.
154) Mitani-Ueno, N., Yamaji, N., & Ma, J. F. (2011). Silicon efflux transporters isolated from two pumpkin cultivars contrasting in Si uptake. Plant Signaling & Behavior, 6(7), 991-994.
155) Miwa, K., & Fujiwara, T. (2010). Boron transport in plants: co-ordinated regulation of transporters. Annals of Botany, 105(7), 1103-1108.
156) Miwa, K., Takano, J., and Fujiwara, T. (2006). Improvement of seed yields under boron-limiting conditions through overexpression of BOR1, a boron transporter for xylem loading, in Arabidopsis thaliana. Plant J. 46, 1084–1091. doi: 10.1111/J.1365-313x.2006.02763.X
157) Miwa, K., Takano, J., Omori, H., Seki, M., Shinozaki, K., & Fujiwara, T. (2007). Plants tolerant of high boron levels. Science, 318(5855), 1417-1417.
158) Miwa, K., Aibara, I., & Fujiwara, T. (2014). Arabidopsis thaliana BOR4 is upregulated under high boron conditions and confers tolerance to high boron. Soil Science and Plant Nutrition, 60(3), 349-355.
159) Miwa, Kyoko, Shinji Wakuta, Shigeki Takada, Koji Ide, Junpei Takano, Satoshi Naito, Hiroyuki Omori, Toshiro Matsunaga, and Toru Fujiwara (2013). "Roles of BOR2, a boron exporter, in cross linking of rhamnogalacturonan II and root elongation under boron limitation in Arabidopsis." Plant physiology 163, no. 4: 1699-1709.
160) Montpetit, J., Vivancos, J., Mitani-Ueno, N., Yamaji, N., Rémus-Borel, W., Belzile, F., ... & Bélanger, R. R. (2012). Cloning, functional characterization and heterologous expression of TaLsi1, a wheat silicon transporter gene. Plant molecular biology, 79(1-2), 35-46.
161) Mosa, K. A., Kumar, K., Chhikara, S., Musante, C., White, J. C., & Dhankher, O. P. (2016). Enhanced boron tolerance in plants mediated by bidirectional transport through plasma membrane intrinsic proteins. Scientific reports, 6(1), 1-14.

162) Murashige, T., & Skoog, F. (1962). A revised medium for rapid growth and bio assays with tobacco tissue cultures. Physiologia plantarum, 15(3), 473-497.
163) Nable, R. O., Bañuelos, G. S., & Paull, J. G. (1997). Boron toxicity. Plant and soil, 193(1), 181-198.
164) Nagaharu, U. (1935). Genome analysis in Brassica with special reference to the experimental formation of B. napus and peculiar mode of fertilization. Jpn. J. Bot, 7(7), 389-452.
165) Nakagawa, Y., Hanaoka, H., Kobayashi, M., Miyoshi, K., Miwa, K., & Fujiwara, T. (2007). Cell-type specificity of the expression of Os BOR1, a rice efflux boron transporter gene, is regulated in response to boron availability for efficient boron uptake and xylem loading. The Plant Cell, 19(8), 2624-2635.
166) Noguchi, Kyotaro, Miho Yasumori, Takahiro Imai, Satoshi Naito, Toshiro Matsunaga, Hisao Oda, Hiroaki Hayashi, Mitsuo Chino, and Toru Fujiwara (1997). "bor1-1, an Arabidopsis thaliana mutant that requires a high level of boron." Plant Physiology 115, no. 3: 901-906.
167) Noronha, Henrique, Diogo Araújo, Carlos Conde, Ana P. Martins, Graca Soveral, François Chaumont, Serge Delrot, and Hernâni Gerós (2016). "The grapevine uncharacterized intrinsic protein 1 (VvXIP1) is regulated by drought stress and transports glycerol, hydrogen peroxide, heavy metals but not water." PloS one 11, no. 8: e0160976.
168) O'Neill, M. A., Eberhard, S., Albersheim, P., & Darvill, A. G. (2001). Requirement of borate cross-linking of cell wall rhamnogalacturonan II for Arabidopsis growth. Science, 294(5543), 846-849.
169) O'Neill, M. A., Ishii, T., Albersheim, P., & Darvill, A. G. (2004). Rhamnogalacturonan II: structure and function of a borate cross-linked cell wall pectic polysaccharide. Annu. Rev. Plant Biol., 55, 109-139.
170) O'Neill, M. A., Warrenfeltz, D., Kates, K., Pellerin, P., Doco, T., Darvill, A. G., & Albersheim, P. (1996). Rhamnogalacturonan-II, a pectic polysaccharide in the walls of growing plant cell, forms a dimer that is covalently cross-linked by a borate ester: in vitro conditions for the formation and hydrolysis of the dimer. Journal of Biological chemistry, 271(37), 22923-22930.
171) Onuh, A. F., & Miwa, K. (2021). Regulation, Diversity and Evolution of Boron Transporters in Plants. Plant and Cell Physiology.
172) Østergaard, L., & King, G. J. (2008). Standardized gene nomenclature for the Brassica genus. Plant methods, 4(1), 1-4.
173) Pallotta, M., Schnurbusch, T., Hayes, J., Hay, A., Baumann, U., Paull, J., ... & Sutton, T. (2014). Molecular basis of adaptation to high soil boron in wheat landraces and elite cultivars. Nature, 514(7520), 88-91.
174) Pan Y, Wang ZH, Yang L, Wang ZF, Shi L, Naran R, Azadi P, Xu FS 2012: Differences in cell wall components and allocation of boron to cell walls confer

variations in sensitivities of Brassica napus cultivars to boron deficiency. Plant Soil, 354, 383–394. doi:10.1007/s11104-011-1074-6

175) Pang, Yongqi, Lijuan Li, Fei Ren, Pingli Lu, Pengcheng Wei, Jinghui Cai, Lingguo Xin, Juan Zhang, Jia Chen, and Xuechen Wang (2010). Overexpression of the tonoplast aquaporin AtTIP5; 1 conferred tolerance to boron toxicity in Arabidopsis. Journal of Genetics and Genomics 37, no. 6: 389-397.

176) Park, W., Scheffler, B. E., Bauer, P. J., & Campbell, B. T. (2010). Identification of the family of aquaporin genes and their expression in upland cotton (Gossypium hirsutum L.). BMC plant biology, 10(1), 1-17.

177) Parker, M. D., & Boron, W. F. (2013). The divergence, actions, roles, and relatives of sodium-coupled bicarbonate transporters. Physiological reviews, 93(2), 803-959.

178) Pasković, I., Soldo, B., Talhaoui, N., Palčić, I., Brkljača, M., Koprivnjak, O., ... & Ban, S. G. (2019). Boron foliar application enhances oleuropein level and modulates volatile compound composition in olive leaves. Scientia Horticulturae, 257, 108688.

179) Paull, J. G., Nable, R. O., & Rathjen, A. J. (1992). Physiological and genetic control of the tolerance of wheat to high concentrations of boron and implications for plant breeding. Plant and Soil, 146(1), 251-260.

180) Paull, J. G., Rathjen, A. J., & Cartwright, B. (1991). Major gene control of tolerance of bread wheat (Triticum aestivum L.) to high concentrations of soil boron. Euphytica, 55(3), 217-228.

181) Pellegrini-Calace, M., Maiwald, T., & Thornton, J. M. (2009). PoreWalker: a novel tool for the identification and characterization of channels in transmembrane proteins from their three-dimensional structure. PLoS Comput Biol, 5(7), e1000440.

182) Pérez-Castro, R., Kasai, K., Gainza-Cortés, F., Ruiz-Lara, S., Casaretto, J. A., Peña-Cortés, H., ... & González, E. (2012). VvBOR1, the grapevine ortholog of AtBOR1, encodes an efflux boron transporter that is differentially expressed throughout reproductive development of Vitis vinifera L. Plant and Cell Physiology, 53(2), 485-494.

183) Pommerrenig, B., Diehn, T. A., & Bienert, G. P. (2015). Metalloido-porins: Essentiality of Nodulin 26-like intrinsic proteins in metalloid transport. Plant Science, 238, 212-227.

184) Pommerrenig, B., Junker, A., Abreu, I., Bieber, A., Fuge, J., Willner, E., ... & Bienert, G. P. (2018). Identification of rapeseed (Brassica napus) cultivars with a high tolerance to boron-deficient conditions. Frontiers in plant science, 9, 1142.

185) Pommerrenig, Benjamin, Till A. Diehn, Nadine Bernhardt, Manuela D. Bienert, Namiki Mitani-Ueno, Jacqueline Fuge, Annett Bieber (2020).

"Functional evolution of nodulin 26-like intrinsic proteins: from bacterial arsenic detoxification to plant nutrient transport." New Phytologist 225, no. 3: 1383-1396.

186) Poza-Viejo, L., Abreu, I., González-García, M. P., Allauca, P., Bonilla, I., Bolaños, L., & Reguera, M. (2018). Boron deficiency inhibits root growth by controlling meristem activity under cytokinin regulation. Plant Science, 270, 176-189.

187) Prasad, R., Kumar, D., Shivay, Y. S., & Rana, D. S. (2014). Boron in Indian agriculture–A review. Indian Journal of Agronomy, 59(4), 511-17.

188) Quigley, F., Rosenberg, J. M., Shachar-Hill, Y., & Bohnert, H. J. (2001). From genome to function: the Arabidopsis aquaporins. Genome biology, 3(1), 1-17.

189) Rashid A, Yasin M (2004) Boron deficiency in calcareous soil reduces rice yield and impairs grain quality. Int Rice Res Notes 29:57–59

190) Rashid, A., Yasin, M., Ali, M. A., Ahmad, Z., & Ullah, R. (2009). Boron deficiency in rice in Pakistan: A serious constraint to productivity and grain quality. In Salinity and water stress (pp. 213-219). Springer, Dordrecht.

191) Rathore SS, Shekhawat K, Babu S, Singh VK (2020) Mitigating moisture stress in Brassica juncea through deficit irrigation scheduling and hydrogel in ustocherpts soils of semi-arid India. Heliyon, 6(12) e05786

192) Redondo-Nieto, M., Wilmot, A. R., El-Hamdaoui, A., Bonilla, I., & Bolaños, L. (2003). Relationship between boron and calcium in the N2-fixing legume–rhizobia symbiosis. Plant, cell & environment, 26(11), 1905-1915.

193) Reid, R. (2007). Identification of boron transporter genes likely to be responsible for tolerance to boron toxicity in wheat and barley. Plant and cell physiology, 48(12), 1673-1678.

194) Reid, R. (2014). Understanding the boron transport network in plants. Plant and soil, 385(1), 1-13.

195) Rerkasem, B., Jamjod, S., & Pusadee, T. (2020). Productivity limiting impacts of boron deficiency, a review. Plant and Soil, 1-18.

196) Rivers, R. L., Dean, R. M., Chandy, G., Hall, J. E., Roberts, D. M., & Zeidel, M. L. (1997). Functional analysis of nodulin 26, an aquaporin in soybean root nodule symbiosomes. Journal of Biological Chemistry, 272(26), 16256-16261.

197) Roberts, D. M., & Routray, P. (2017). The nodulin 26 intrinsic protein subfamily. In Plant Aquaporins (pp. 267-296). Springer, Cham.

198) Rodriguez-Furlan, C., Minina, E. A., & Hicks, G. R. (2019). Remove, recycle, degrade: regulating plasma membrane protein accumulation. The Plant Cell, 31(12), 2833-2854.

199) Rodríguez-Serrano, M. A. R. Í. A., ROMERO-PUERTAS, M. C., Zabalza, A. N. A., Corpas, F. J., Gomez, M., Del Rio, L. A., & Sandalio, L. M. (2006). Cadmium effect on oxidative metabolism of pea (Pisum sativum L.) roots. Imaging of

reactive oxygen species and nitric oxide accumulation in vivo. Plant, Cell & Environment, 29(8), 1532-1544.

200) Rogers, S. O., & Bendich, A. J. (1994). Extraction of total cellular DNA from plants, algae and fungi. In Plant molecular biology manual (pp. 183-190). Springer, Dordrecht.

201) Routray, Pratyush, Tian Li, Arisa Yamasaki, Akira Yoshinari, Junpei Takano, Won Gyu Choi, Carl E. Sams, and Daniel M. Roberts (2018). "Nodulin intrinsic protein 7; 1 is a tapetal boric acid channel involved in pollen cell wall formation." Plant physiology 178, no. 3: 1269-1283.

202) Sabir, F., Leandro, M. J., Martins, A. P., Loureiro-Dias, M. C., Moura, T. F., Soveral, G., & Prista, C. (2014). Exploring three PIPs and three TIPs of grapevine for transport of water and atypical substrates through heterologous expression in aqy-null yeast. PloS one, 9(8), e102087.

203) Saha, B., Mishra, S., Awasthi, J. P., Sahoo, L., & Panda, S. K. (2016). Enhanced drought and salinity tolerance in transgenic mustard [Brassica juncea (L.) Czern & Coss.] overexpressing Arabidopsis group 4 late embryogenesis abundant gene (AtLEA4-1). Environmental and Experimental Botany, 128, 99-111.

204) Saha, P. K., Saleque, M. A., Zaman, S. K., & Bhuiyan, N. J. (2003). Response of mustard to S, Zn and B in calcareous soil. Bangladesh J. Agril. Res, 28(4), 633-636.

205) Sakurai, J., Ishikawa, F., Yamaguchi, T., Uemura, M., & Maeshima, M. (2005). Identification of 33 rice aquaporin genes and analysis of their expression and function. Plant and Cell Physiology, 46(9), 1568-1577.

206) Schmidt, U., Briese, S., Leicht, K., Schuïrmann, A., Joost, H. G., & Al-Hasani, H. (2006). Endocytosis of the glucose transporter GLUT8 is mediated by interaction of a dileucine motif with the β2-adaptin subunit of the AP-2 adaptor complex. Journal of cell science, 119(11), 2321-2331.

207) Schnurbusch, Thorsten, Julie Hayes, Maria Hrmova, Ute Baumann, Sunita A. Ramesh, Stephen D. Tyerman, Peter Langridge, and Tim Sutton. "Boron toxicity tolerance in barley through reduced expression of the multifunctional aquaporin HvNIP2; 1." Plant Physiology 153, no. 4 (2010): 1706-1715.

208) Secchi, F., Pagliarani, C., & Zwieniecki, M. A. (2017). The functional role of xylem parenchyma cells and aquaporins during recovery from severe water stress. Plant, cell & environment, 40(6), 858-871.

209) Séné, C. F., McCann, M. C., Wilson, R. H., & Grinter, R. (1994). Fourier-transform Raman and Fourier-transform infrared spectroscopy (an investigation of five higher plant cell walls and their components). Plant Physiology, 106(4), 1623-1631.

210) Shao JF, Yamaji N, Liu XW, Yokosho K, Shen RF, Ma JF. 2018. Preferential distribution of boron to developing tissues is mediated by the intrinsic protein OsNIP3. Plant Physiology 176: 1739–1750.

211) Shao, J. F., Yamaji, N., Huang, S., & Ma, J. F. (2021). Fine regulation system for distribution of boron to different tissues in rice. New Phytologist, 230(2), 656-668.

212) Shen ZG, Liang YC, Shen K (1993) Effect of boron on the nitrate reductase-activity in oilseed rape plants. J Plant Nutr. 16 (7):1229–1239

213) Shihan, M. H., Novo, S. G., Le Marchand, S. J., Wang, Y., & Duncan, M. K. (2021). A simple method for quantitating confocal fluorescent images. Biochemistry and Biophysics Reports, 25, 100916.

214) Shorrocks, V. M. (1997). The occurrence and correction of boron deficiency. Plant and soil, 193(1), 121-148.

215) Sillanpää, M. (1982). Micronutrients and the nutrient status of soils: a global study (Vol. 48). Food & Agriculture Org..

216) Singh, M. V. (1999). Current status of micro and secondary nutrients deficiencies and crop response in different agroecological regions. Experiments of AICRP on micro and secondary nutrients and pollutant elements in soil and plants. Fertilizer News, GCI, 63-82.

217) Singh, M. V. (2008). Micronutrient deficiencies in crops and soils in India. In Micronutrient deficiencies in global crop production (pp. 93-125). Springer, Dordrecht.

218) Song, G., Li, X., Munir, R., Khan, A. R., Azhar, W., Khan, S., & Gan, Y. (2021). BnaA02. NIP6; 1a encodes a boron transporter required for plant development under boron deficiency in Brassica napus. Plant Physiology and Biochemistry, 161, 36-45.

219) Stangoulis, J. C., Reid, R. J., Brown, P. H., & Graham, R. D. (2001). Kinetic analysis of boron transport in Chara. Planta, 213(1), 142-146.

220) Stangoulis, J. C., Webb, M. J., & Graham, R. D. (2000a). Boron efficiency in oilseed rape: II. Development of a rapid lab-based screening technique. Plant and soil, 225(1), 253-261.

221) Stangoulis, J., Tate, M., Graham, R., Bucknall, M., Palmer, L., Boughton, B., & Reid, R. (2010). The mechanism of boron mobility in wheat and canola phloem. Plant physiology, 153(2), 876-881.

222) Stangoulis, J.C.R., Grewal, H.S., Bell, R.W. et al. Boron efficiency in oilseed rape: I. Genotypic variation demonstrated in field and pot grown Brassica napus L. and Brassica juncea L.. Plant and Soil 225, 243–251 (2000b). https://doi.org/10.1023/A:1026593528256

223) Sudhakaran, Sreeja, Vandana Thakral, Gunashri Padalkar, Nitika Rajora, Pallavi Dhiman, Gaurav Raturi, Yogesh Sharma (2021) "Significance of solute

specificity, expression, and gating mechanism of tonoplast intrinsic protein during development and stress response in plants." Physiologia Plantarum 172, no. 1: 258-274.

224) Suga, S., & Maeshima, M. (2004). Water channel activity of radish plasma membrane aquaporins heterologously expressed in yeast and their modification by site-directed mutagenesis. Plant and cell physiology, 45(7), 823-830.

225) Sui, H., Han, B. G., Lee, J. K., Walian, P., & Jap, B. K. (2001). Structural basis of water-specific transport through the AQP1 water channel. Nature, 414(6866), 872-878.

226) Sutton, Tim, Ute Baumann, Julie Hayes, Nicholas C. Collins, Bu-Jun Shi, Thorsten Schnurbusch, Alison Hay (2007). "Boron-toxicity tolerance in barley arising from efflux transporter amplification." Science 318, no. 5855: 1446-1449.

227) Takano, J., Miwa, K., & Fujiwara, T. (2008). Boron transport mechanisms: collaboration of channels and transporters. Trends in plant science, 13(8), 451-457.

228) Takano, J., Noguchi, K., Yasumori, M., Kobayashi, M., Gajdos, Z., Miwa, K., ... & Fujiwara, T. (2002). Arabidopsis boron transporter for xylem loading. Nature, 420(6913), 337-340.

229) Takano, J., Tanaka, M., Toyoda, A., Miwa, K., Kasai, K., Fuji, K., ... & Fujiwara, T. (2010). Polar localization and degradation of Arabidopsis boron transporters through distinct trafficking pathways. Proceedings of the National Academy of Sciences, 107(11), 5220-5225.

230) Takano, J., Wada, M., Ludewig, U., Schaaf, G., Von Wirén, N., & Fujiwara, T. (2006). The Arabidopsis major intrinsic protein NIP5; 1 is essential for efficient boron uptake and plant development under boron limitation. The Plant Cell, 18(6), 1498-1509.

231) Takano, J., Yamagami, M., Noguchi, K., Hayashi, H., & Fujiwara, T. (2001). Preferential translocation of boron to young leaves in Arabidopsis thaliana regulated by the BOR1 gene. Soil science and plant nutrition, 47(2), 345-357.

232) Takano, Junpei, Kyotaro Noguchi, Miho Yasumori, Masaharu Kobayashi, Zofia Gajdos, Kyoko Miwa, Hiroaki Hayashi, Tadakatsu Yoneyama, and Toru Fujiwara (2002). "Arabidopsis boron transporter for xylem loading." Nature 420, no. 6913: 337-340.

233) Tamura, K., Peterson, D., Peterson, N., Stecher, G., Nei, M., & Kumar, S. (2011). MEGA5: molecular evolutionary genetics analysis using maximum likelihood, evolutionary distance, and maximum parsimony methods. Molecular biology and evolution, 28(10), 2731-2739.

234) Tanaka, M., & Fujiwara, T. (2008). Physiological roles and transport mechanisms of boron: perspectives from plants. Pflügers Archiv-European Journal of Physiology, 456(4), 671-677.

235) Tanaka, M., Wallace, I. S., Takano, J., Roberts, D. M., & Fujiwara, T. (2008). NIP6; 1 is a boric acid channel for preferential transport of boron to growing shoot tissues in Arabidopsis. The Plant Cell, 20(10), 2860-2875.

236) Tanaka, N., Uraguchi, S., Saito, A., Kajikawa, M., Kasai, K., Sato, Y., Nagamura, Y. and Fujiwara, T., 2013. Roles of pollen-specific boron efflux transporter, OsBOR4, in the rice fertilization process. Plant and cell physiology, 54(12), pp.2011-2019.

237) Tanaka, Mayuki, Junpei Takano, Yukako Chiba, Fabien Lombardo, Yuki Ogasawara, Hitoshi Onouchi, Satoshi Naito, and Toru Fujiwara (2011). "Boron-dependent degradation of NIP5; 1 mRNA for acclimation to excess boron conditions in Arabidopsis." The Plant Cell 23, no. 9: 3547-3559.

238) Tanaka, Mayuki, Naoyuki Sotta, Yusuke Yamazumi, Yui Yamashita, Kyoko Miwa, Katsunori Murota, Yukako Chiba (2016). "The minimum open reading frame, AUG-stop, induces boron-dependent ribosome stalling and mRNA degradation." The Plant Cell 28, no. 11: 2830-2849.

239) Tao, P., Zhong, X., Li, B., Wang, W., Yue, Z., Lei, J., ... & Huang, X. (2014). Genome-wide identification and characterization of aquaporin genes (AQP s) in Chinese cabbage (Brassica rapa ssp. pekinensis). Molecular Genetics and Genomics, 289(6), 1131-1145.

240) Thurtle-Schmidt, B. H., & Stroud, R. M. (2016). Structure of Bor1 supports an elevator transport mechanism for SLC4 anion exchangers. Proceedings of the National Academy of Sciences, 113(38), 10542-10546.

241) Tzin, V., & Galili, G. (2010). New insights into the shikimate and aromatic amino acids biosynthesis pathways in plants. Molecular plant, 3(6), 956-972.

242) Uehlein, N., Lovisolo, C., Siefritz, F., & Kaldenhoff, R. (2003). The tobacco aquaporin NtAQP1 is a membrane CO 2 pore with physiological functions. Nature, 425(6959), 734-737.

243) Uraguchi, S., & Fujiwara, T. (2011). Significant contribution of boron stored in seeds to initial growth of rice seedlings. Plant and soil, 340(1), 435-442.

244) Uraguchi, S., Hanaoka, H., Aizawa, K., Kato, Y., Nakagawa, Y., & Fujiwara, T. (2009). Boron deficiency in rice and the potential of up-regulated rice boron transporter in improving boron deficient symptoms.

245) Uraguchi, S., Kato, Y., Hanaoka, H., Miwa, K., & Fujiwara, T. (2014). Generation of boron-deficiency-tolerant tomato by overexpressing an Arabidopsis thaliana borate transporter AtBOR1. Frontiers in plant science, 5, 125.

246) Vincken, J. P., Schols, H. A., Oomen, R. J., Beldman, G., Visser, R. G., & Voragen, A. G. (2003). Pectin—the hairy thing. In Advances in pectin and pectinase research (pp. 47-59). Springer, Dordrecht.

247) Vivancos, J., Labbé, C., Menzies, J.G. & Bélanger, R.R. (2015) Silicon-mediated resistance of Arabidopsis against powdery mildew involves

mechanisms other than the salicylic acid (SA)-dependent defence pathway. Molecular Plant Pathology, 16, 572–582.

248) Wakuta, S., Mineta, K., Amano, T., Toyoda, A., Fujiwara, T., Naito, S., & Takano, J. (2015). Evolutionary divergence of plant borate exporters and critical amino acid residues for the polar localization and boron-dependent vacuolar sorting of AtBOR1. Plant and Cell Physiology, 56(5), 852-862.

249) Wallace, I. S., & Roberts, D. M. (2004). Homology modeling of representative subfamilies of Arabidopsis major intrinsic proteins. Classification based on the aromatic/arginine selectivity filter. Plant Physiology, 135(2), 1059-1068.

250) Wallace, I. S., & Roberts, D. M. (2005). Distinct transport selectivity of two structural subclasses of the nodulin-like intrinsic protein family of plant aquaglyceroporin channels. Biochemistry, 44(51), 16826-16834.

251) Wang, N.; Yang, C.; Pan, Z.; Liu, Y.; Peng, S. Boron deficiency in woody plants: Various responses and tolerance mechanism. Front. Plant Sci. 2015.

252) Wang, Y., Shi, L., Cao, X., & Xu, F. (2007). Plant boron nutrition and boron fertilization in China. Advances in plant and animal boron nutrition, 93-101.

253) Wang, Sheliang, Akira Yoshinari, Tomoo Shimada, Ikuko Hara-Nishimura, Namiki Mitani-Ueno, Jian Feng Ma, Satoshi Naito, and Junpei Takano (2017). "Polar localization of the NIP5; 1 boric acid channel is maintained by endocytosis and facilitates boron transport in Arabidopsis roots." The Plant Cell 29, no. 4: 824-842.

254) Wang, Sheliang, Ling Liu, Dan Zou, Yupu Huang, Zhe Zhao, Guangda Ding, Hongmei Cai, Chuang Wang, Lei Shi, and Fangsen Xu. "Vascular tissue-specific expression of BnaC4. BOR1; 1c, an efflux boron transporter gene, is regulated in response to boron availability for efficient boron acquisition in Brassica napus." Plant and Soil (2021): 1-14.

255) Wimmer, M.A., Abreu, I., Bell, R.W., Bienert, M.D., Brown, P.H., Dell, B., Fujiwara, T., Goldbach, H.E., Lehto, T., Mock, H.-P., von Wirén, N., Bassil, E. and Bienert, G.P. (2020), Boron: an essential element for vascular plants. New Phytol, 226: 1232-1237. https://doi.org/10.1111/nph.16127

256) Wittkopp, P. J., & Kalay, G. (2012). Cis-regulatory elements: molecular mechanisms and evolutionary processes underlying divergence. Nature Reviews Genetics, 13(1), 59-69.

257) Wolf, B. (1971). The determination of boron in soil extracts, plant materials, composts, manures, water and nutrient solutions. Communications in Soil Science and Plant Analysis, 2(5), 363-374.

258) Wong, M. (2003). Monitor crops closely for signs of low boron. *Farming Ahead*, Xiao-Dong, Y. A. N. G., Su-Qin, S. U. N., & Yi-Qin, L. I. (1999). Boron

deficiency causes changes in the distribution of major polysaccharides of pollen tube wall. Journal of Integrative Plant Biology, 41(11).

259) Wongmo, J., Jamjod, S., & Rerkasem, B. (2004). Contrasting responses to boron deficiency in barley and wheat. Plant and soil, 259(1), 103-110.

260) Wu, X., Riaz, M., Yan, L., Du, C., Liu, Y., & Jiang, C. (2017). Boron deficiency in trifoliate orange induces changes in pectin composition and architecture of components in root cell walls. Frontiers in plant science, 8, 1882.

261) Xue, J., L. Minshu, W. Richard, R.D. Bell, X.Y. Graham and Y. Yuai. 1998. Deferential response of oilseed rape (Brassica napus L.) cultivars to low boron supply. Plant and Soil. 204(2): 155-163.

262) Yaneff, A., Vitali, V., & Amodeo, G. (2015). PIP1 aquaporins: Intrinsic water channels or PIP2 aquaporin modulators?. FEBS letters, 589(23), 3508-3515.

263) Yang YA, Xu HK, Jie ZQ, Wang BY (1989) Influences of B, N and K nutritional level on B uptake, quality and yield of rapeseed. Scientia Agricultura Sinica, 22, 44-45.

264) Yang, J., & Yen, H. E. (2002). Early salt stress effects on the changes in chemical composition in leaves of ice plant and Arabidopsis. A Fourier transform infrared spectroscopy study. Plant physiology, 130(2), 1032-1042. (135).

265) Yang, J., Liu, D., Wang, X. et al. The genome sequence of allopolyploid Brassica juncea and analysis of differential homoeolog gene expression influencing selection. Nat Genet 48, 1225–1232 (2016). https://doi.org/10.1038/ng.3657

266) Yoshinari, A., & Takano, J. (2017). Insights into the mechanisms underlying boron homeostasis in plants. Frontiers in Plant Science, 8, 1951.

267) Yoshinari, A., Fujimoto, M., Ueda, T., Inada, N., Naito, S., & Takano, J. (2016). DRP1-dependent endocytosis is essential for polar localization and boron-induced degradation of the borate transporter BOR1 in Arabidopsis thaliana. Plant and Cell Physiology, 57(9), 1985-2000.

268) Yoshinari, A., Korbei, B., & Takano, J. (2018). TOL proteins mediate vacuolar sorting of the borate transporter BOR1 in Arabidopsis thaliana. Soil Science and Plant Nutrition, 64(5), 598-605.

269) Yoshinari, Akira, Takuya Hosokawa, Marcel Pascal Beier, Keishi Oshima, Yuka Ogino, Chiaki Hori, Taichi E. Takasuka, Yoichiro Fukao, Toru Fujiwara, and Junpei Takano (2021). "Transport-coupled ubiquitination of the borate transporter BOR1 for its boron-dependent degradation." The Plant Cell 33, no. 2: 420-438.

270) Yoshinari, Akira, Takuya Hosokawa, Taro Amano, Marcel Pascal Beier, Tadashi Kunieda, Tomoo Shimada, Ikuko Hara-Nishimura, Satoshi Naito, and Junpei Takano (2019). "Polar localization of the borate exporter BOR1 requires AP2-dependent endocytosis." Plant Physiology 179, no. 4: 1569-1580.

271) Yu, Q., Hlavacka, A., Matoh, T., Volkmann, D., Menzel, D., Goldbach, H. E., & Baluška, F. (2002). Short-term boron deprivation inhibits endocytosis of cell wall pectins in meristematic cells of maize and wheat root apices. Plant Physiology, 130(1), 415-421.

272) Yuan D, Li W, Hua Y, King GJ, Xu F and Shi L (2017) Genome-Wide Identification and Characterization of the Aquaporin Gene Family and Transcriptional Responses to Boron Deficiency in Brassica napus. Front. Plant Sci. 8:1336. doi: 10.3389/fpls.2017.01336

273) Yuan, D., Li, W., Hua, Y., King, G. J., Xu, F., & Shi, L. (2017). Genome-wide identification and characterization of the aquaporin gene family and transcriptional responses to boron deficiency in Brassica napus. Frontiers in plant science, 8, 1336.

274) Yuan, D., Li, W., Hua, Y., King, G. J., Xu, F., & Shi, L. (2017). Genome-wide identification and characterization of the aquaporin gene family and transcriptional responses to boron deficiency in Brassica napus. Frontiers in plant science, 8, 1336.

275) Zaman, N. W. Farid, A. T. M. Rahman, A. F. M. Talukder, M. Z. I. and Sarker, R. H. (1998). Yield and fertility of Brassica napus as affected by boron deficiency in soil. Thailand Journal of Agricultural Science.

276) Zangi, R., & Filella, M. (2012). Transport routes of metalloids into and out of the cell: a review of the current knowledge. Chemico-Biological Interactions, 197(1), 47-57.

277) Zhang D., Hua Y., Wang X., Zhao H., Shi L. and Xu F. A high-density genetic map identifies a novel major QTL for boron efficiency in oilseed rape (Brassica napus L.). Plos One. 2014b; 9, e112089. https://doi.org/10.1371/journal.pone.0112089 PMID: 25375356

278) Zhang, D., Zhao, H., Shi, L., & Xu, F. (2014a). Physiological and genetic responses to boron deficiency in Brassica napus: a review. Soil Science and Plant Nutrition, 60(3), 304-313.

279) Zhang, Q., Chen, H., He, M., Zhao, Z., Cai, H., Ding, G., ... & Xu, F. (2017). The boron transporter BnaC4. BOR1; 1c is critical for inflorescence development and fertility under boron limitation in Brassica napus. Plant, cell & environment, 40(9), 1819-1833.

280) Zhang, S., Wei, Y., Lu, Y., & Wang, X. (2009). Mechanisms of brassinosteroids interacting with multiple hormones. Plant signaling & behavior, 4(12), 1117-1120.

281) Zhou, G. F., Liu, Y. Z., Sheng, O., Wei, Q. J., Yang, C. Q., & Peng, S. A. (2015). Transcription profiles of boron-deficiency-responsive genes in citrus rootstock root by suppression subtractive hybridization and cDNA microarray. Frontiers in plant science, 5, 795.

Publications and Conferences

PUBLICATIONS

1. Muthuvel J., Saharia M., Kumar S., Abiala M.A., Rao G.J.N., Sahoo L. (2021) Progress in Genetic Engineering of Cowpea for Insect Pest and Virus Resistance. In: Kavi Kishor P.B., Rajam M.V., Pullaiah T. (eds) Genetically Modified Crops. Springer, Singapore. https://doi.org/10.1007/978-981-15-5897-9_7

2. Muthuvel J, Junpei Takano, Lingaraj Sahoo (2021) Genome-wide identification and characterization of boron transporter genes in Indian mustard (*Brassica juncea*) (Manuscript communicated to MDPI Plants).

3. Muthuvel J, Takuya Hosokawa, Junpei Takano, Lingaraj Sahoo (2021) Contrasting responses of Indian mustard genotypes to low boron condition at vegetative stage (Manuscript under communication).

4. Muthuvel J, Junpei Takano, Lingaraj Sahoo (2021) Boron transport in plants (Manuscript communicated to Soil Science and Plant Nutrition).

5. Muthuvel J, Sanjeev Kumar, Lingaraj Sahoo (2021) Transgenic cowpea expressing a sequence-modified cry1Ab gene of *Bacillus thuringiensis* for improved resistance to legume pod borer insect *Maruca vitrata* (Manuscript under communication).

6. Sanjeev Kumar, Muthuvel J, Lingaraj Sahoo (2021) A cowpea transcription factor, VuDREB2A confers drought and heat tolerance in transgenic cowpea by activating the stress-responsive genes (Manuscript prepared).

WORKSHOPS, CONFERENCES AND SEMINARS

1. Muthuvel J, Richa Srivastava, Sanjeev Kumar, Lingaraj Sahoo, (2016). Overexpression of Arabidopsis PYL9 in Indian mustard enhances drought and salinity tolerance by modulating ABA signalling, At National Seminar on Plant Genomics and Biotechnology: Challenges and Opportunities in 21st Century, (pp 54), OUAT, Bhubaneswar

2. Muthuvel J, Angana Kalita, Sweta Kumari, Sanjeev Kumar, Vinay Kalia, Manikatlavenkat Rajam, Lingaraj Sahoo (2017) Bt- and RNAi- mediated protection in

cowpea to legume pod borer (Maruca vitrata) At National Symposium on Pulses for Nutritional Security and Agricultural Sustainability, (PP 117), IIPR, Kanpur

3. Muthuvel J, Junpei Takano Lingaraj Sahoo (2019) Physiological and molecular responses to boron deficiency influenced by genotypic variation in Indian mustard at International Conference on Trends in Plant Sciences and Agrobiotechnology, IIT Guwahati, Assam

4. Muthuvel J, Takuya Hosokawa, Junpei Takano, Lingaraj Sahoo (2021) Physiological and Molecular responses to boron deficiency influenced by genotypic and expressional variation in Indian mustard regulated by NIPs and BOR-transporters at International Symposium on "Advances in Plant Biotechnology and Genome Editing", Virtual mode

List of Primers

Gene	Primer
BjuA03BOR1a	Fw: 5′-GGAGATTGGATCGACAACTT-3'
	Rv: 5′-AGGACTACTCGTGTGTCTAA-3'
BjuB08BOR1a	Fw: 5′-GGTAACAAGGTCACGAGTTC-3'
	Rv: 5′-TCATCTGACCCAACCTGAGT-3'
BjuA02NIP5_1a	Fw: 5'- GAGTGAGAGACTTGTCGACA -3'
	Rv: 5'-CGTGGACTTATAGTCACATCTCC-3'
BjuA03NIP5_1b	Fw: 5'- GCTATAAATCCGATGCGACCTCGTCTC -3'
	Rv: 5'-AGCCTTGTCACCGAGGTTGC-3'
BjuA07NIP5_1c	Fw: 5'- CACAAGTCTTCTGCTTGTTACTGTTACTGTATG-3'
	Rv: 5'-CGCAGCGTGGACTTGTAGTCACAT-3'
BjuB02NIP6_1a	Fw: 5′- ATGGACCATGAGGAGATTCCA -3′
	Rv: 5′- TGACTTTGGCGTGTATTTACC -3′
Bjtubulin	Fw: 5′-CACCAACGGGTTTGAAAATG-3′
	Rv: 5′-TGCTCACTCACACGCCTAAA-3′